Distribution Agreement

In presenting this thesis or dissertation as a partial fulfillment of the requirements for an advanced degree from Emory University, I hereby grant to Emory University and its agents the non-exclusive license to archive, make accessible, and display my thesis or dissertation in whole or in part in all forms of media, now or hereafter known, including display on the world wide web. I understand that I may select some access restrictions as part of the online submission of this thesis or dissertation. I retain all ownership rights to the copyright of the thesis or dissertation. I also retain the right to use in future works (such as articles or books) all or part of this thesis or dissertation.

Signature:

_____ _____

Ashley R. Cross Date

Regulation of *Pseudomonas aeruginosa* Chronic Infection Phenotypes

By

Ashley R. Cross
Doctor of Philosophy

Graduate Division of Biological and Biomedical Science
Microbiology and Molecular Genetics

Joanna B. Goldberg, PhD
Advisor

Charles P. Moran, PhD
Committee Member

David S. Weiss, PhD
Committee Member

Philip N. Rather, PhD
Committee Member

William M. Shafer, PhD
Committee Member

Accepted:

Lisa A. Tedesco, Ph.D.
Dean of the James T. Laney School of Graduate Studies

Date

Regulation of *Pseudomonas aeruginosa* Chronic Infection Phenotypes

By

Ashley R. Cross
B.S., Young Harris College, 2013

Advisor: Joanna B. Goldberg, Ph.D.

An abstract of
A dissertation submitted to the Faculty of the
James T. Laney School of Graduate Studies of Emory University
in partial fulfillment of the requirements for the degree of
Doctor of Philosophy
Graduate Division of Biological and Biomedical Sciences
in Microbiology and Molecular Genetics
2020

ABSTRACT

Regulation of *Pseudomonas aeruginosa* Chronic Infection Phenotypes

By Ashley Cross

Pseudomonas aeruginosa is an opportunistic bacterial pathogen with the ability to persist in many complex environments. The resilient nature of *P. aeruginosa* supports rapid adaption and long-term survival of this bacterium in stressful niches. This is especially true when it comes to the establishment of chronic lung infections in people with cystic fibrosis (CF). The most significant manifestation of CF disease occurs in the lungs where there is increased inflammation, thick mucus accumulation, and reduced clearance of inhaled bacteria. As a result, lung damage and persistent bacterial infections are the leading cause of morbidity and mortality in this population. Up to 50% of people with CF in the United States culture positive for *P. aeruginosa*, making it one of the most predominant pathogens.

The persistence, survival, and adaption to this unique lung ecosystem is reflected by the expression of unique phenotypes. These phenotypes are collectively termed the "chronic infection phenotype" and distinguishes chronic CF isolates from most other types of infections and environmental sources. This is because CF isolates are often mucoid, due to the overproduction of the exopolysaccharide alginate, and have defective lipopolysaccharide O antigen production. The studies presented here contribute to our understanding of the regulation of chronic infection phenotypes in *P. aeruginosa*. This includes the discovery of a novel feedback mechanism linking alginate biosynthesis to alginate promoter expression as well as the characterization of the regulon of a histone-like protein once thought to be involved in regulating alginate production.

Control of alginate production is regulated primarily by the sigma factor AlgT. Experiments performed here also reveal that overproduction of AlgT is lethal to mucoid strains of *P. aeruginosa* and that very long O antigen production is regulated at the genetic level by the AlgT-dependent transcription factor AmrZ. Understanding the regulation of these chronic phenotypes will elucidate mechanisms that are important for the establishment of a long-term *P. aeruginosa* lung infection and ultimately provide an opportunity for intervention. Preventing *P. aeruginosa* from chronically adapting to the CF lung environment could provide a better outcome for people who are infected.

Regulation of *Pseudomonas aeruginosa* Chronic Infection Phenotypes

By

Ashley R. Cross
B.S., Young Harris College, 2013

Advisor: Joanna B. Goldberg, Ph.D.

A dissertation submitted to the Faculty of the
James T. Laney School of Graduate Studies of Emory University
in partial fulfillment of the requirements for the degree of
Doctor of Philosophy
Graduate Division of Biological and Biomedical Sciences
in Microbiology and Molecular Genetics
2020

TABLE OF CONTENTS

DISTRIBUTION AGREEMENT i

APPROVAL SHEET ii

ABSTRACT COVER PAGE iii

ABSTRACT iv

COVER PAGE v

TABLE OF CONTENTS vi

LIST OF FIGURES VII

LIST OF TABLES XI

Chapter 1. An introduction to *Pseudomonas aeruginosa*, an adaptable bacterium 1

Chapter 2. The AlgP histone-like protein regulon is distinct in nonmucoid and mucoid *Pseudomonas aeruginosa* and does not include alginate biosynthesis genes 27

Chapter 3. Remodeling of O antigen in mucoid *Pseudomonas aeruginosa* via transcriptional repression of *wzz2* 58

Chapter 4. Overexpression of the AlgT sigma factor is lethal to mucoid *Pseudomonas aeruginosa* 99

Chapter 5. The alginate biosynthesis operon is autoregulated in *Pseudomonas aeruginosa* through a positive-feedback loop involving the AlgT sigma factor 117

Chapter 6. Discussion and future directions for the studies of chronic phenotypes in *Pseudomonas aeruginosa* 141

Appendix 1. Construction of reporters to test the temperature regulation and single cell dynamics of *wzz1* and *wzz2* in *Pseudomonas aeruginosa* 148

Appendix 2. Generation and phenotypic analysis of *Pseudomonas aeruginosa wzz* mutants 173

Appendix 3. Nucleotide duplications in *algT* cause nonmucoid reversion 195

REFERENCES 206

LIST OF FIGURES

Chapter 1.

Figure 1.1. Genetic maps of *P. aeruginosa* strains PAO1.....17

Figure 1.2. Prevalence of respiratory microorganisms in people with CF.....18

Figure 1.3. *P. aeruginosa* phenotypic changes that occur during the transition from an acute to chronic infection.....19

Figure 1.4. Model for alginate biosynthesis.....20

Figure 1.5. Structure of lipopolysaccharide.....22

Figure 1.6. Organization of genes within the O antigen biosynthesis clusters in each *P. aeruginosa* serotype.....23

Figure 1.7. Model for O antigen biosynthesis.....24

Chapter 2.

Figure 2.1. Deletion of *algP* from mucoid strains does not decrease alginate levels.....49

Figure 2.2. *algP* promoter expression is reduced in PDO300 compared to PAO1.....50

Figure 2.3. Deletion of *algP* increases survival of PAO1 in nitric oxide.....51

Figure 2.4. *algP* promoter activity is increased in stationary phase independent of RpoS.....52

Figure S2.1. Deletion of *algP* does not significantly alter alginate production in LB.....53

Figure S2.2. Growth of PAO1 and PDO300 is unaltered when *algP* is deleted.....54

Chapter 3.

Figure 3.1. Mucoid strains produce less Wzz2 compared to nonmucoid strains resulting in less very long O antigen.....84

Figure 3.2. Overexpression of *wzz2* in PDO300 increases very long O antigen production...85

Figure 3.3. The *wzz2* steady-state mRNA levels and promoter activity are repressed in PDO300.....86

Figure 3.4. Nonmucoid isolates of mucoid strains express more Wzz2 and very long O antigen.....87

Figure 3.5. Overexpression of *algT* results in less very long O antigen and decreased *wzz2* promoter activity.....88

Figure 3.6. Overexpression of *amrZ* represses *wzz2* promoter activity.....89

Figure 3.7. Disruption of *amrZ* restores Wzz2 production in mucoid strains.....90

Figure 3.8. Model for the inverse regulation of alginate and very long O antigen in mucoid *P. aeruginosa*.....91

Figure S3.1. Mucoid PA14 has reduced levels of Wzz2 and fewer very long O antigen chain-lengths compared to nonmucoid PA14.....92

Figure S3.2. Disruption of *amrZ* in PAO1 does not alter Wzz2 or O antigen production.....93

Chapter 4.

Figure 4.1. Overproduction of *algT* is lethal in *mucA22* strains.....110

Figure 4.2. Complementation with wild type *mucA* partially rescues *algT* lethality.....111

Figure 4.3. Identification of suppressors.....112

Figure 4.4. Mutations identified in *mucP*.....113

Figure 4.5. Complementation of *mucP* suppressor mutants restores *algT* sensitivity.....114

Chapter 5.

Figure 5.1. Deletion of alginate biosynthesis genes alters activity of the *algT* promoter.....132

Figure 5.2. Deletion of alginate biosynthesis genes alter expression of the alginate operon promoter.....133

Figure 5.3. PDO300 Δ*algD* and Δ*algA* complementation increases alginate production, but not *algT* promoter activity.....134

Figure 5.4. Alginate production of PDO300 and PAO1 strains.....135

Figure 5.5. Replacing the alginate operon promoter disrupts *algT* promoter activity, independent of alginate production.....136

Figure 5.6. Complementation of *algT* activity is not restored when the alginate operon promoter and the *algD* gene are both provided in trans.....137

Figure 5.7. Model for the regulation of AlgT by the alginate biosynthesis operon.....138

Appendix 1.

Figure A1.1. Promoter activity of different sized fragments from upstream of *wzz2*.....165

Figure A1.2. PA0937 and *wzz2* can be co-transcribed on the same mRNA.....166

Figure A1.3. Identification of the *wzz2* transcription start site in PAO1 and PDO300.....167

Figure A1.4. Temperature alters promoter activity of *wzz1* or *wzz2* in PAO1 at stationary phase.....168

Figure A1.5. The *wzz1* and *wzz2* promoters are both expressed at the single cell level.....169

Figure A1.6. Flow cytometry analysis of single PAO1 cells expressing fluorescent reporters for *wzz1* and *wzz2*.....170

Figure A1.7. Single cell images of PAO1 using interferometry.....171

Appendix 2.

Figure A2.1. Pro-Q staining of all serotype strains.....185

Figure A2.2. O antigen immunoblot of all serotype strains.....186

Figure A2.3. Deletion of *wzz2* decreases very long O antigen production in serotype O5 and O1.....187

Figure A2.4. Deletion of *wzz2* decreases resistance of serotype O1 to normal human serum, does not alter resistance of serotype O5 PAO1.....188

Figure A2.5. Disruption of *wzz1* or *wzz2* does not alter resistance to polymyxin B.....189

Figure A2.6. A PDO300 *wzz2* transposon mutant is more resistant to subinhibitory concentration of gentamicin compared to parent strains and *wzz1* mutants.....190

Figure A2.7. PDO300 *wzz2::tet* has increased survival after growth in increasing concentrations of gentamicin.....191

Figure A2.8. PDO300 *wzz2::tet* grows better in 2 μg/ml concentrations of gentamicin than wild type PDO300 or PAO1 strains.....192

Appendix 3.

Figure A3.1. AlgT sequence alignment of PDO300 and two nonmucoid revertants.....200

Figure A3.2. Nonmucoid reversion by duplications in AlgT does not result in a growth advantage.....201

Figure A3.3. Predicted model of AlgT based on *E. coli* RpoE.....202

Figure A3.4. Amino acid duplications in AlgT do not dramatically alter predicted protein shape.....203

LIST OF TABLES

Chapter 1.

Table 1.1. Functional class of predicted open reading frames in PAO1.....25

Table 1.2. Summary of PAO1 genomes from different sources.....26

Chapter 2.

Table 2.1. PAO1 v. PAO1 Δ*algP* significant expression differences. 55

Table 2.2. PDO300 v. PDO300 Δ*algP* significant expression differences.....56

Table S2.1. Strains, plasmids, and primers used in this study.....57

Chapter 3.

Table 3.1. Alginate produced by strains overexpressing *wzz2*.....94

Table 3.2. Alginate produced by strains overexpressing *amrZ*.....95

Table S3.1. Alginate produced by strains overexpressing *algT*.....96

Table S3.2. Strains and plasmids used in this study.....97

Table S3.3. Primers used in this study.....98

Chapter 4.

Table 4.1. Suppressor mutations.....115

Table 4.2. Strains, plasmids, and primers used in this study.....116

Chapter 5.

Table S5.1. Strains and plasmids used in this study.....139

Table S5.2. Primers used in this study.....140

Appendix 1.

Table A1.1. Strains, plasmids, and primers used in this study.....172

Appendix 2.

Table A2.1. Polyvalent and primary antibodies to detect serotype O antigen.....193

Table A2.2. Strains, plasmids, and primers used in this study.....194

Appendix 3.

Table A3.1. Summary of nonmucoid revertants.....204

Table 3.2. Strains and primers used in this study.....205

Chapter 1

An introduction to *Pseudomonas aeruginosa*, a versatile bacterium

***Pseudomonas aeruginosa*, an adaptable bacterium.**

Originally detected by the distinctive blue-green pigment found on the bandages of infected wounds, *Pseudomonas aeruginosa* was first isolated by Carle Gessard in 1882 (1). "*Pseudomonas*" is derived from the Greek words *pseudo*, meaning false, and *monas*, meaning a single unit. "*Aeruginosa*" is derived from the Latin word *aerugo*, meaning rusted copper. Since Gessard's discovery, over 65,000 research papers have been published describing various aspects of *P. aeruginosa* basic biology and pathogenesis (PubMed, Jan 2020). The first fully sequenced genome of *P. aeruginosa* was made available 20 years ago further expanding our view on the full complexity of this bacterium (2). Today, *P. aeruginosa* is a model organism for studying quorum sensing, biofilm formation, gene regulation, antibiotic resistance, and pathogenesis.

The first *P. aeruginosa* sequenced, strain PAO1, was isolated from a wound in Australia around 1954 and the first report describing this strain was published in 1955 (3). Subsequently, PAO1 became the most common reference strain for *P. aeruginosa* experiments. At the time of whole genome sequencing, PAO1 was the largest bacterial genome reported at 6,264,403 base pairs, 5,570 predicted open reading frames, and a G+C content of 66.6% (2). Almost 10% of the genome encodes transcriptional regulators, two-component systems, and environmental sensors shedding light on how this organism is so versatility and resourceful (Table 1.1). Comparing this genetic map to a previous genetic map of PAO1, constructed just 14 years prior (Fig. 1.1), it is remarkable how far *P. aeruginosa* research has advanced and reveals how much is still waiting to be discovered (4).

Due to the popularity of PAO1 as a laboratory strain, many labs worldwide have obtained and successively shared their PAO1s. Consequently, researchers began to notice that an experiment in one lab using PAO1 would not necessarily yield the same results as another lab

using a different PAO1 (5, 6). As a result, a recent study investigated the genotypic and phenotype variation among 9 different PAO1 sublines from 10 different locations (Table 1.2) (7). While 95.63% of the genes across all 9 strains were identical, there were a number of phenotypic differences observed in motility, small molecule secretion, and exopolysaccharide production. Interestingly, because of the similarity between genomes, the authors attributed these differences to likely post-transcriptional modifications and not genetic mutations.

The second *P. aeruginosa* genome sequenced was that of strain PA14 (8). PA14 is the second most commonly used lab strain and exhibits a higher virulence profile than that of PAO1. This is mostly due to the presence of two pathogenicity islands. Recently, in conjunction with the 17th International Conference on *Pseudomonas* held in her home country, Dr. Kalai Mathee published an editorial describing her search for the original publication in which PA14 was first described (9). After speaking with Dr. Milton Schroth at the University of California Berkeley, he sent Dr. Mathee a photocopy of the lost original PA14 publication and shared that PA14 was originally acquired from Mercy Hospital in Pennsylvania where it was isolated from a burn wound (10). Since then, PA14 has been used extensively to study plant, insect, and animal pathogenesis.

The PAO1 and PA14 strains, however, do not represent all *P. aeruginosa* strains. Strains can greatly vary depending on the presence or absence of prophages, plasmids, transposons, and genomic islands. More recently, the pangenome of *P. aeruginosa* was described and found to be vastly greater than just what is known of PAO1 or PA14. Of 1,311 genomes analyzed from many different clinical and environment sources, the *P. aeruginosa* pangenome contains 54,272 genes with only 1% of those genes shared among all strains tested, designated the core genome (11). This number is likely to increase as more *P. aeruginosa* strains are sequenced.

While the pangenome is important for studying the adaptability and the evolution of *P. aeruginosa* to different niches, it is also imperative to understand the *P. aeruginosa* core essential genome to aid in the development of targeted antibiotics and therapies. The core essential genome is composed of necessary processes such as DNA replication, RNA processing, metabolism, transcription, translation, and cell division. What is defined as the core essential genome, however, can change depending on the environment in which the bacteria are growing. Using transposon mutagenesis of 10 *P. aeruginosa* strains from 5 different infections sites grown in 5 different media, Poulsen et al. sought to address this disparity (12). The authors identified 321 genes (6.6% of the total genome) they deemed the core essential genome. This number is similar to the number of core genes found in the 1,311 strain pangenome described above and by others (11, 13). What is exciting is that in each study there were a number of uncharacterized core essential genes discovered meaning there are still novel opportunities for intervention waiting to be discovered.

Nevertheless, these 5 growth conditions are far from exhaustive. Furthermore, it is vital to know which, if not all, of these genes are expressed *in vivo*. To this end, the transcriptome of *P. aeruginosa* from human sputum obtained from people with cystic fibrosis (CF), from chronic wounds, and from burn wounds was assessed (13, 14). It was found that genes for the biosynthesis of amino acids, carbohydrates, and nucleotides as well as the TCA cycle and quorum sensing were expressed at a lower level *in vivo* across all samples compared to *in vitro* conditions such as growth in laboratory media. Genes that were more highly induced in human samples included those involved in SOS response, long-chain fatty acid catabolism, efflux pumps, and expression of the AlgT sigma factor (also called σ^{22} or AlgU), which will be discussed in greater detail throughout this dissertation. Some of the benefits of this study are that

samples were from different patients, infected with different *P. aeruginosa* strains, and co-infected with different types of bacteria. These are important considerations when determining the therapeutic value of using a drug to treat a wide range of infections within a variable population.

P. aeruginosa has always been considered a ubiquitous organism, but the location of a *P. aeruginosa* natural reservoir and where infection isolates originate is still up for debate. Even though *P. aeruginosa* is thought of as a soil bacterium, unless the location is contaminated, it is difficult to isolate from soil or water (15-18). In fact, it is 7 times more likely to find *P. aeruginosa* in contaminated human-associated soil compared to uncontaminated soil (15). Further, uncontaminated water samples contain almost no *P. aeruginosa* (15, 19, 20). While there are limitations to these studies, the natural source of *P. aeruginosa* appears to be closely linked to humans. Thus, *P. aeruginosa* is not really as ubiquitous as once perceived and the natural environment may not be water or soil.

P. aeruginosa **in chronic infections.**

The resilient nature of *P. aeruginosa* supports rapid adaption and long-term survival of this bacterium in stressful niches. This is especially true when it comes to the establishment of chronic lung infections in people with CF (21, 22). CF is an autosomal recessive genetic disease caused by mutations in the cystic fibrosis transmembrane conductance regulator (*cftr*), a chloride anion channel found on epithelial cell membranes throughout the body (23, 24). Mutations in *cftr* alter ion transport significantly impairing cellular functions and causing multiorgan disease (23, 24). There are currently 30,775 people in the United States (US) who have CF, with 54.6% of this population comprising adults over 18 years of age (25). The most significant manifestation

of CF disease occurs in the lungs where there is increased inflammation, thick mucus accumulation, and reduced clearance of inhaled bacteria (26). CF lung infections can last decades since this altered lung environment leads to bacterial persistence and more difficult to treat infections (27-30). As a result, lung damage is the leading cause of morbidity and mortality in this population. To date, 44.4% of people with CF in the US cultured positive for *P. aeruginosa*.

While once considered the most predominant CF pathogen, *P. aeruginosa* prominence has decreased over the years likely due to robust detection and targeted treatment of infections. Now *Staphylococcus aureus* has surpassed *P. aeruginosa* as the most dominant pathogen detected (Fig. 1.2) (25). Upwards of 50% of people with CF actually test positive for both *S. aureus* and *P. aeruginosa*, indicating that these individuals are co-infected by both bacterium (31). People who are co-infected have worse lung function compared to those individually infected. Still, it is becoming more appreciated that there is an even greater polymicrobial community within the lungs of people with CF thanks to advances in culture-independent technologies. This CF lung community includes other well studied pathogens, anaerobic bacteria, fungi, and viruses (32-34). While most of our greatest discoveries have been made by studying bacteria in isolation, these findings point to the importance of studying bacteria in the complex environments in which they live. For example, when studying bacteria in the context of a CF lung infection, it was found that oral anaerobic bacteria surviving within the oxygen-limiting CF lung produce fermentative byproducts that provide additional carbon sources for co-infecting bacteria, such as *P. aeruginosa* (35).

P. aeruginosa persistence, survival, and adaption to this unique lung ecosystem is reflected by the expression of rare phenotypes (36). These phenotypes are collectively termed the

“CF phenotype” or the "chronic infection phenotype" and distinguishes chronic CF isolates from most other *P. aeruginosa* strains from other types of infections and environmental sources (Fig. 1.3) (36). These isolates are often mucoid, LPS-rough, nonmotile, and less virulent (37-42). We now know that these phenotypes are regulated at the genetic level by the AlgT sigma factor (38, 39, 43-48). I prefer to use the term “chronic infection phenotype” since mucoid strains have also been seen in chronic obstructive pulmonary disease (COPD) and urinary tract infection (UTI), although this is much more rare (49, 50). Still, it is not exactly known what selects for the permanent manifestation of these phenotypes. Some evidence suggests that conversion could be linked to conditions in the lung such as anaerobicity, dehydration, high osmolarity, and oxidative stress (51-54).

Due to the complex and multifaceted nature of CF pathophysiology, creating a reliable animal model to study infections has been difficult. While murine models of infection have been instrumental, mouse models of CF do not recapitulate the pathology of lung disease observed in humans and establishing long-term chronic bacterial infections in mice has been difficult (55, 56). At the moment, it is not possible to infect mice with nonmucoid *P. aeruginosa* and monitor the emergence of mucoid strains during the course of a lung infection. Therefore, we cannot rigorously test the selection for or the importance of the chronic infection phenotype in a host until a more appropriate model is established. More relevant models that may more closely mimic human disease that are being developed include the CF rat, the CF ferret, the CF rabbit, and the CF pig (55, 56). In one instance, a chronic CF rat infected with *P. aeruginosa* produced mucoid strains that possessed some of the characteristic phenotypes of chronic infection strains (57). The CF pig, although costly, has a longer lifespan and develops lung disease similarly to

humans and therefore would be a more ideal animal model for studying chronic bacterial infections. Presently, these studies have not yet been performed.

Alginate regulation, synthesis, and production.

As mentioned, the emergence of a mucoid colony morphology is correlated with the transition from an acute to a chronic lung infection. Researchers have spent decades unraveling the network that regulates alginate biosynthesis and production. It has long been appreciated that mucoid *P. aeruginosa* is almost exclusively isolated from chronic lung infections, primarily those with CF (58-62). Several early studies linked the composition of this mucoid slime exopolysaccharide to seaweed alginic acid (59, 63, 64). *P. aeruginosa* alginate is composed of repeating 1-4 linked D-mannuronic and L-guluronic acids and is O-acetylated, unlike seaweed alginate (37).

Alginate has been proposed to play may roles such as inhibition of phagocytosis, quenching of reactive oxygen species, resistance to antibiotics, and contributing to overall biofilm architecture (65). Recently, mucoid *P. aeruginosa* was shown to contribute to regional inflammation within the CF lung (66). Additionally, exogenous alginate was shown to induce downregulation of virulence factors produced by nonmucoid *P. aeruginosa* (67). Since nonmucoid and mucoid *P. aeruginosa* exist together within the CF lung along with other bacteria, alginate may be a shared resource used to influence gene expression of surrounding organisms.

Early genetic studies using nonmucoid revertants of mucoid *P. aeruginosa* strains and complementation analysis identified two main regions of the chromosome important for the production of alginate and the mucoid phenotype (44, 68-74). These loci ultimately mapped to the

algT sigma factor operon (region I) and the alginate biosynthesis operon (region II) (75). The alginate operon contains 12 genes in the following order; *algD, alg8, alg44, algK, algE, algG, algX, algL, algI, algJ, algF,* and *algA* (72). The biosynthesis enzymes, AlgA, AlgC, and AlgD, synthesize GDP-mannuronate, the primary sugar that constitutes alginate (76, 77). AlgA is a dual function enzyme and first uses phosphomannose isomerase activity to convert fructose-6-phosphate into mannose-6-phosphate (78, 79). AlgC, a phosphomannomutase located outside of the alginate biosynthesis operon, acts between the two enzymatic steps of AlgA to convert mannose-6-phosphate into mannose-1-phosphate (80, 81). Next, the GDP-mannose pyrophosphorylase activity of AlgA converts mannose-1-phosphate into GDP-mannose. The final enzymatic step involves AlgD, which converts GDP-mannose into GDP-mannuronate acid (76). Prior to transport, Alg8 and Alg44 polymerize GDP-mannuronate into a linear sugar chain while the epimerase AlgG converts some of the GDP-mannuronate sugars into GDP-guluronate. Next, the growing sugar chain is O-acetylated by AlgI, AlgJ, and AlgF to eventually form mature alginate (82-90). Alginate is then sliced by the alginate lyase AlgL and exported into the extracellular space by AlgX, AlgK, and AlgE. (91-95).

The *algT* operon was identified because mutations causing mucoid conversion and nonmucoid reversion both often mapped to this region (68, 73). Likewise, providing this region of the chromosome *in trans* could complement some nonmucoid strains to mucoid (44). The *algT* operon is now known to contain five genes in the following order: *algT*, *mucA, mucB, mucC*, and *mucD*. This operon is functionally similar to the *rpoE, rseA, rseB,* and *rseC* stress-response operon in *Escherichia coli* (96, 97). Further, the *algT* operon is driven by five promoters, two of which are AlgT-dependent resulting in positive autoregulation (73, 98). We have new evidence, presented in Chapter 5, that expression of genes in the alginate biosynthesis operon contributes to this AlgT

positive-eedback loop. AlgT is an extracytoplasmic function sigma factor that is under post-translational negative control by the anti-sigma factor MucA that itself is stabilized by the structural protein MucB (99-102). Recently, high resolution crystal structures of the N-terminus cytosolic portion of MucA bound to AlgT and the C-terminus periplasmic portion of MucA bound to MucB was solved (103).

Outer membrane and periplasmic stresses induce an intermembrane proteolysis (RIP) cascade that subjects MucA and MucB to degradation by periplasmic proteases releasing AlgT to direct transcription of AlgT-dependent promoters (96, 104). To do this, the interaction between MucB and MucA is destabilized and MucB no longer protects the C-terminus of MucA. As a result, the AlgW protease cleaves MucA making the truncated MucA available for cleavage by AlgO and MucP proteases (105, 106). This releases the N-terminus AlgT-bound fragment of MucA into the cytosol where it is finally completely degraded by the ClpPX proteasome. AlgT is then made available to promote transcription of the alginate biosynthesis operon as well as about 300 additional genes involved in responses to outer membrane stress and cell wall homeostasis (104, 107, 108). Based on experiments performed in Chapter 4 we also know, however, that regulating the amount of AlgT, through this RIP cascade, is important for maintaining cell viability.

Over the decades it has become appreciated that alginate biosynthesis and production is highly regulated and requires more than just AlgT. The first analysis of the alginate operon promoter, usually referred to as the *algD* promoter since *algD* is the first gene in the operon, identified the gene AlgR (also named AlgR1) as the first transcription factor directly linked to promoting expression of the operon (76, 109). The next transcription factor identified to be involved in regulating the alginate operon was the two-component response regulator AlgB (110,

111). While *algB* mutants still make low amounts of alginate, AlgB is still necessary for full induction of the operon. The final major transcriptional regulator of the alginate biosynthesis operon identified was AmrZ (originally named AlgZ) (112). AmrZ is also required for transcription of the alginate operon. Both AlgR and AmrZ are directly regulated by AlgT, but AlgT is not required for the expression of AlgB (113). While alginate regulation by AlgR, AlgB, and AmrZ has been extensively studied, each regulator has a vast regulon of their own (114-116). The histone-like protein AlgP has also been thought to regulate the alginate biosynthesis operon, although the exact nature of this regulation was unclear. However, based on the data presented in Chapter 2, we can now confidently say that AlgP does not regulate alginate biosynthesis or production. A simplified model for the regulation of the alginate biosynthesis operon and the production of alginate discussed here is presented in Figure 1.4.

P. aeruginosa isolates from CF lung infections often contain mutations in *mucA*, derestricting AlgT, and therefore no longer regulate alginate production through a RIP cascade (42, 117-120). The *mucA22* mutation, which is a deletion of a G in a string of 5 G's, is the most common clinical mutation observed and results in a truncated form of MucA that does not contain a C-terminus (51, 117). As a result, truncated MucA22 does not bind MucB, is continuously subjected to RIP, AlgT is always free, and the alginate biosynthesis operon is always expressed (76, 113). In order to shut down alginate production, mucoid strains can acquire secondary site mutations that result in nonmucoid reversion, often occurring in *algT* (73, 106, 121). Ultimately, nonmucoid revertants with mutations in *algT* can no longer become mucoid again. The experiments performed in Appendix 3 characterized novel mutations in *algT* that result in nonmucoid reversion and predicts how these mutations affect AlgT function.

Regulation and biosynthesis of lipopolysaccharide O antigen.

P. aeruginosa is a gram-negative bacterium and thus possesses a complex cell wall containing a heterogeneous outer membrane. The outer leaflet of the outer membrane primarily contains lipopolysaccharide (LPS), a complex glycolipid that shields the bacteria from the outside environment. Due to its location, LPS is likely the first part of the bacterium to come into contact with a surface. The LPS molecule can be divided into three domains; lipid A, core, and O antigen (Fig. 1.5). The O antigen portion of the molecule can be further divided into two categories; common O antigen and serotype specific O antigen (122). Historically, these are referred to as A-band and B-band, respectively (39). The lipid A, core, and common O antigen structures are mostly conserved across *P. aeruginosa* species although some modifications are observed in response to environmental stimuli, host immune molecules, and antibiotic treatment (123). The specific O antigen, on the other hand, varies in composition of sugars across strains. The sugars incorporated into the specific O antigen categorize the *P. aeruginosa* strains into 20 different serotype groups (124, 125).

Classically, gram-negative bacteria that attach O antigen sugars onto the lipid A-core of the LPS molecule are termed “smooth” and those that lack O antigen are termed “rough” (126). This is due to the fact that several enteric bacteria have rough colony edges when lacking O antigen compared to those that produced O antigen. This is not the case for *P. aeruginosa*, however, since isogenic O antigen producing and O antigen deficient strains have the same colony morphology when visualized by the naked eye. Still, the terms LPS rough and LPS smooth are used to describe O antigen deficient and O antigen proficient strains of *P. aeruginosa*, respectively.

P. aeruginosa specific O antigen is a heteropolymer composed of 2-5 repeating polysaccharide units and is synthesized and assembled in a pathway independent of common O antigen and core LPS (127). The composition and assembly of each unit is determined by the O antigen biosynthesis operon, which itself is serotype specific (128). This is because each operon varies in the total number of functional open reading frames, deletions, and/or large insertions (Fig. 1.6). Still, each operon is located in the same region of the chromosome (near *himD*) and begins and ends with the same genes; *wzz1* and *wbpM*. The first specific O antigen operon characterized was that of serotype O5 strain PAO1 (129, 130). It was quickly appreciated that the overall GC nucleotide content of the operon was ~10% lower than that of the rest of the PAO1 chromosome. This backs some of the evidence and speculation that the specific O antigen operon was originally acquired through horizontal gene transfer since this region of the chromosome is different from the rest.

Once the sugar repeat unit is synthesized by the serotype specific O antigen biosynthesis operon, the O antigen molecule is assembled by a Wzx/Wzy-dependent pathway (127, 131). First, a repeat sugar unit attached to a undecaprenyl pyrophosphate lipid carrier is flipped across the inner membrane into the periplasm by the Wzx flippase. Next, single repeat units are polymerized into a growing chain by Wzy. The length of the chain is determined by Wzz through an unknown mechanism. Finally, WaaL ligates the O antigen chain to the lipid A-core molecule. This whole molecule is transported through the periplasmic space and inserted into the oute rmembrane by the LPS transport pathway. A simplified model for the assembly and export of serotype specific O antigen is presented in Figure 1.7.

Classifying strains based on serotype is useful only if the strain is producing O antigen, which is the case for most environmental and acute infection isolates. However, *P. aeruginosa*

isolates from chronic infections are often LPS rough (36, 38, 119, 132-134). Therefore, sequencing of the serotype specific O antigen operon is necessary to determine the serotype of these strains. Further, mucoid isolates from people with CF are LPS rough (135, 136). It was originally hypothesized that alginate and O antigen are inversely expressed due to a competition for a shared sugar pool by O antigen and alginate biosynthesis pathways (137, 138). However, experiments performed in Chapter 3 of this dissertation show that this may not be the case since forcing expression of very long O antigen in mucoid strain PDO300 does not alter alginate production suggesting that sugar precursors are not limited between the two biosynthesis pathways.

O antigen chain length control; Wzz1 and Wzz2.

The serotype specific O antigen expressed by LPS smooth strains is bimodal and categorized based on the number of repeat units attached to the lipid A-core molecule. Ultimately, the lengths of each modality vary between each serotype, but they are always designated as long or very long. For serotype O5 strains, the long O antigen molecules possess 12-30 sugar repeats and the very long O antigen molecules possess 40-50 sugar repeats (122, 139, 140). Each length is determined by one of two Wzz chain-length control protein. Wzz1 regulates the assembly of long O antigen chain lengths while very long O antigen is regulated by the chain-length control protein Wzz2 (122, 139-141). The *wzz1* gene is located at the 5'-end of the serotype specific O antigen biosynthesis operon and the sequence of which is also serotype specific (129, 142). Conversely, *wzz2* is located elsewhere in the chromosome and is sequence conserved among *P. aeruginosa* strains (139, 141). Since each serotype O antigen modality is different, the experiments performed in Appendix 2 visualize the LPS and O antigen of all 20

serotypes and characterizes the effect of *wzz2* deletion on each strain. Further, preliminary experiments deciphering the biological importance of expressing very long O antigen in each serotype are described.

How Wzz1 and Wzz2 regulate chain length is still a topic of debate. There are up to four competing theories describing how Wzz proteins function each taking into consideration that O antigen chain length is determined before ligation to lipid A-core and that Wzz protein structures are fairly conserved (140). These are the chaperone model, the organizing scaffold model, the ruler model, and the chain feedback model (127). Recently, Islam et al. summarized the available experimental evidence for each model and proposed that the most likely mechanism of action is a hybrid combining the ruler and the chain feedback models (127). In this model, Wzy polymerizes the O antigen repeat units until they are long enough to interact with Wzz. This interaction stabilizes the growing chain allowing for continued polymerization. As the chain gets larger, it becomes rigid and unstable. At a certain length, the growing O antigen chain reaches the tip of Wzz and a mechanical force disengages the O antigen chain from Wzy making it available for ligation to lipid A-core. While a substantial number of experiments support portions of this model, it still does not account for why different serotypes can have extremely different chain length modalities.

Also, not much is known about how *wzz1* and *wzz2* are regulated at the transcriptional level. For example, we know that high temperatures, low pH, or low concentrations of phosphate or high concentrations of NaCl, $MgCl_2$, glycerol, or sucrose result in decreased amounts of very long O antigen, but whether these conditions affect expression of *wzz* genes has not been tested (143). Reporters built in Appendix 1 seek to provide a system to study *wzz1* and *wzz2* promoter expression across a wide range of environments and conditions. Ongoing experiments in our

laboratory aim to unravel pathways that regulate *wzz* expression in *P. aeruginosa*. Until now, no known transcriptional regulators of O antigen chain-length had been identified in nonmucoid *P. aeruginosa*. In Chapter 3, experiments identify and confirm that AmrZ, a transcription factor described earlier for its necessity in promoting alginate biosynthesis, is a negative regulator of *wzz2* promoter activity and very long O antigen expression. AmrZ is therefore the first transcriptional regulator of O antigen chain-length identified in *P. aeruginosa*.

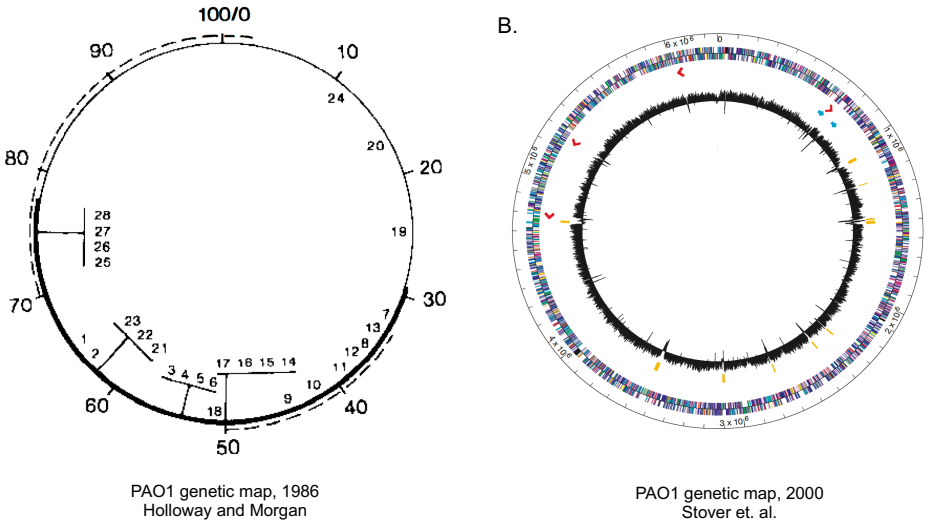

Figure 1.1. Genetic maps of *P. aeruginosa* strains PAO1. A) Genetic map of PAO1 by Holloway and Morgan. The auxotrophic rich region of the chromosome is shown with a thickened line and the regions of catabolic marker clustering is shown with dashed lines. Numbers refer to isofunctional markers (see paper for details). B) Genetic map of PAO1 by Stover et al. Key: The outermost circle indicates the chromosomal location in base pairs (each tick is 100 kb). The distribution of genes is depicted by colored boxes according to functional category and direction of transcription (outer band is the plus strand; inner band is the minus strand). Red arrows, the locations and direction of transcription of ribosomal RNA genes; green arrow, the inverted region that resulted from a homologous recombination event between *rrnA* and *rrnB*; blue arrows, location of two regions containing probable bacteriophages. The black plot in the center is percentage G+C content plotted as the average for non-overlapping 1-kb windows spanning one strand for the entire genome. Yellow bars, regions with G+C content of two standard deviations below the mean. *Modified from A) Holloway BW, Morgan AF. 1986. Genome Organization in Pseudomonas. Ann Rev Microbiol 40:79-105 and B) Stover C et al. 2000. Complete genome sequence of *Pseudomonas aeruginosa* PAO1, an opportunistic pathogen. Nature 406:959-964.

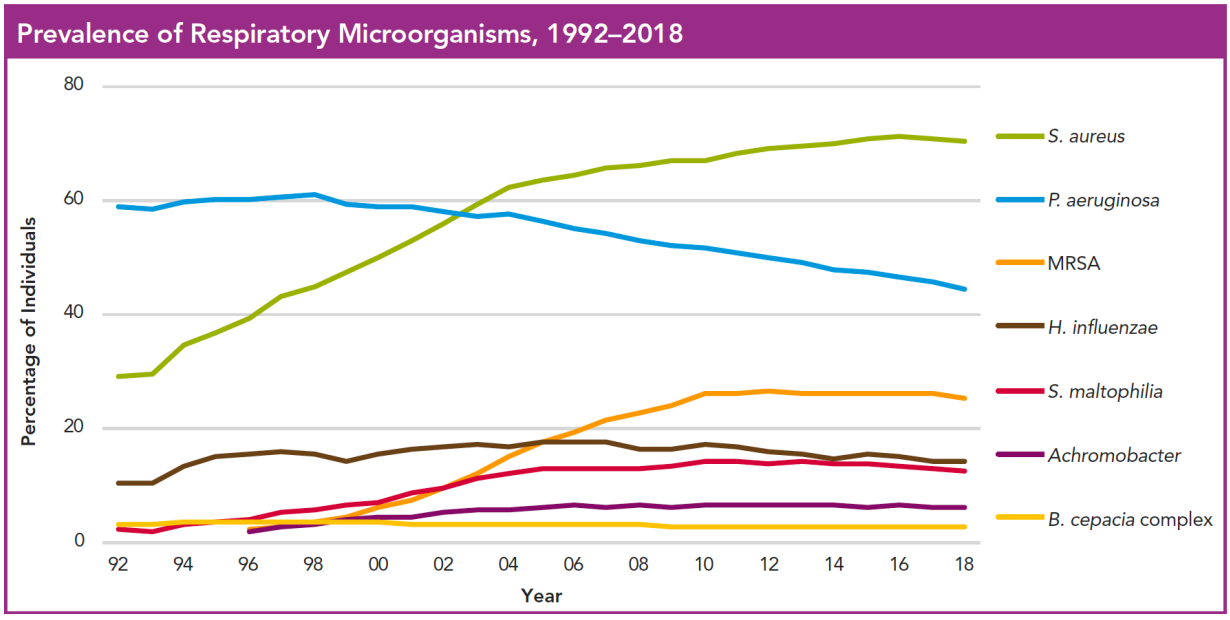

Figure 1.2. Prevalence of respiratory microorganisms in people with CF. *Pseudomonas aeruginosa* and *Staphylococcus aureus* are the predominant pathogens isolated from people with cystic fibrosis (CF). Figure and data from the 2018 CF Foundation Patient Registry Report.

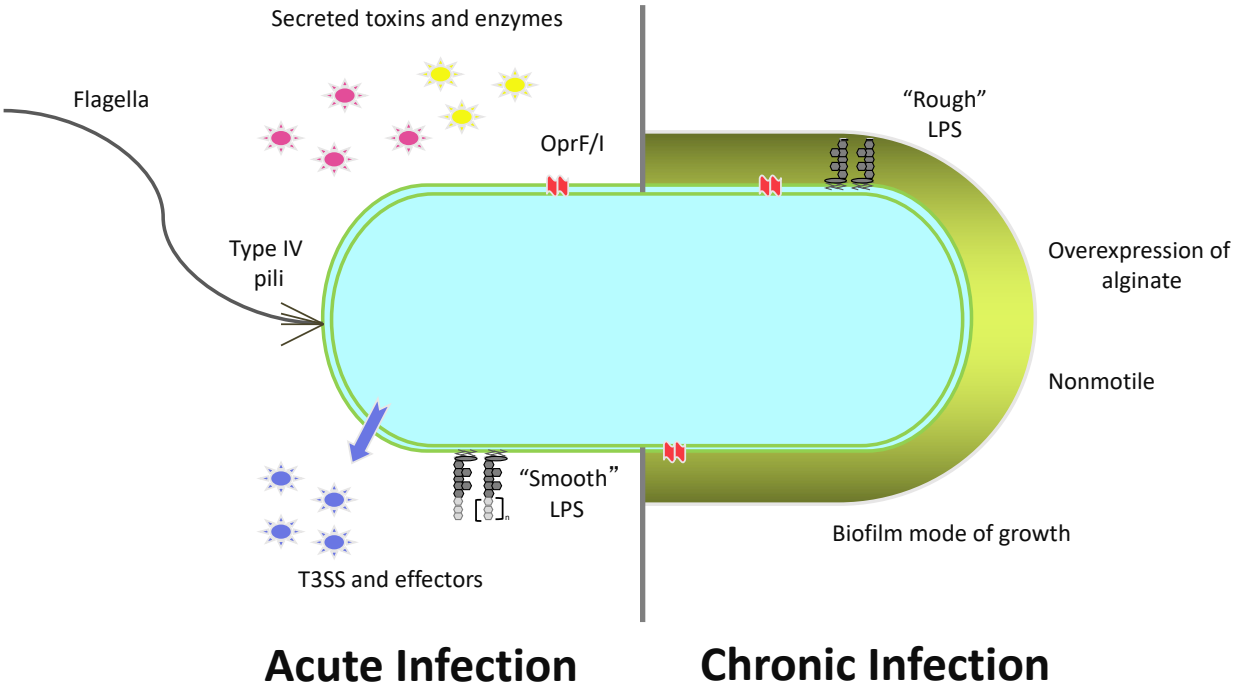

Figure 1.3. *P. aeruginosa* phenotypic changes that occur during the transition from an acute to chronic infection. Isolates from an acute or initial lung infection (left) are motile, nonmucoid, and express many virulence factors including toxins, O antigen ("smooth LPS"), and a type three secretion system (T3SS). However, after long-term adaption to the CF lung, the chronic infection phenotype (right) is established leading to the overproduction the exopolysaccharide alginate, loss of flagella and motility, more robust biofilm formation, and incomplete LPS ("rough" LPS). Adapted from a model generated by Dr. Joanna B. Goldberg.

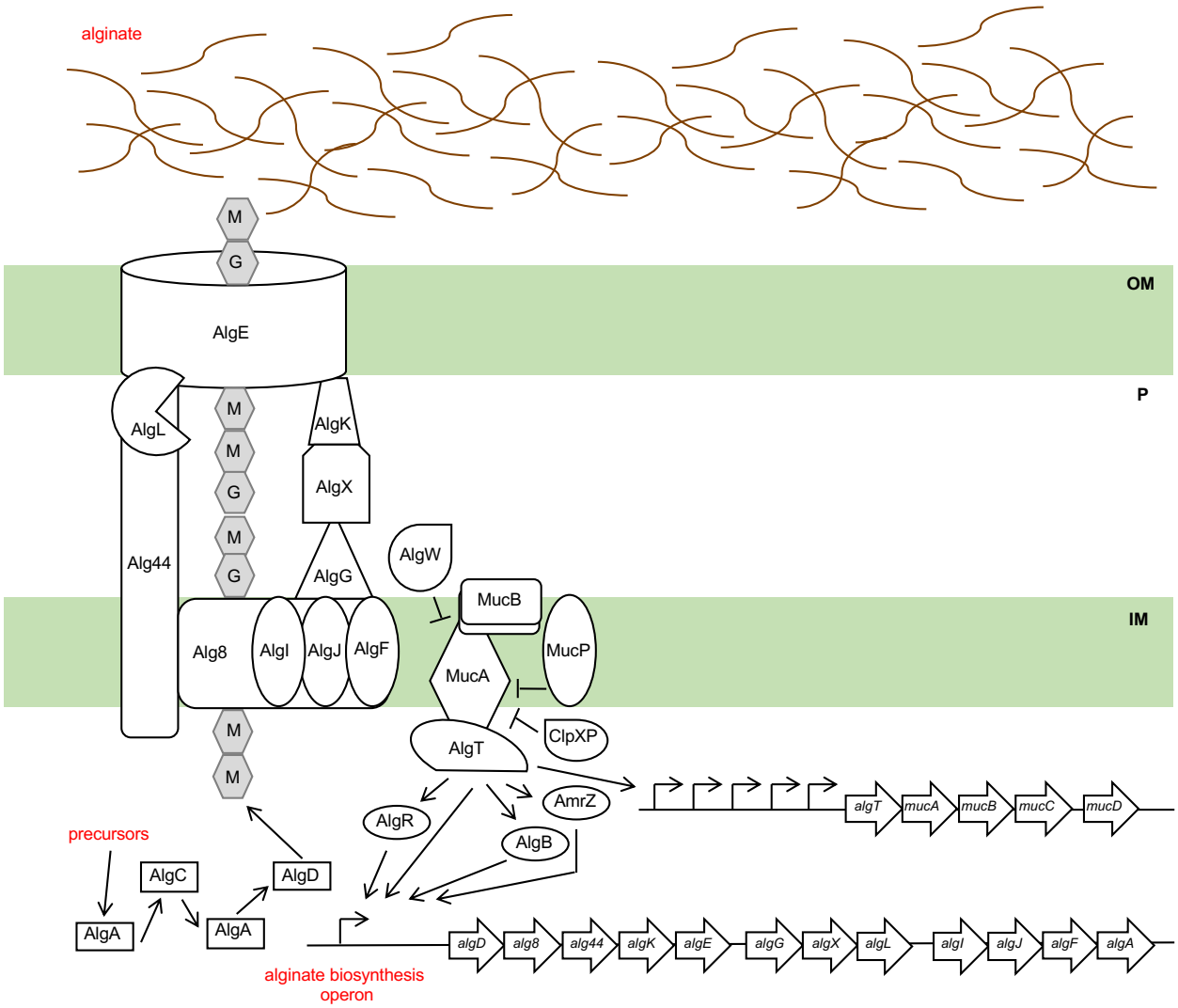

Figure 1.4. Model for alginate biosynthesis. Outer membrane and periplasmic stresses induce an intermembrane proteolysis (RIP) cascade that subjects MucA and MucB to degradation by periplasmic proteases AlgW and MucP. This releases the N-terminus AlgT-bound fragment of MucA into the cytosol where it is finally completely degraded by the ClpPX proteasome. AlgT is then made available to promote transcription of the alginate biosynthesis operon and the *algT* operon. The *algT* operon is now known to contain five genes in the following order: *algT*, *mucA, mucB, mucC*, and *mucD*. The *algT* operon is positive autoregulation by AlgT. The transcription facrors AlgR, AmrZ, and AlgB, along with AlgT, are all required to promote transcription of the

alginate biosynthesis operon. The biosynthesis enzymes, AlgA, AlgC (located outside of the operon), and AlgD synthesize GDP-mannuronate (M), the primary sugar that constitutes alginate. Prior transport, Alg8 and Alg44 polymerize GDP-mannuronate into a linear sugar chain while the epimerase AlgG converts some of the GDP-mannuronate sugars into GDP-guluronate. Next, the growing sugar chain is O-acetylated by AlgI, AlgJ, and AlgF to eventually form mature alginate. Alginate is then sliced by the alginate lyase AlgL and exported into the extracellular space by AlgX, AlgK, and AlgE. Key- OM: outer membrane, P: periplasmic space, IM: inner membrane.

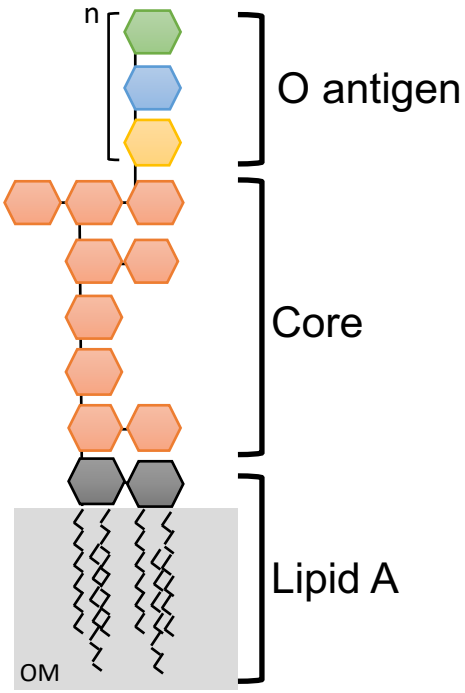

Figure 1.5. Structure of lipopolysaccharide. The lipopolysaccharide (LPS) molecule is divided into three domains. The most proximal portion is the lipid A core that is embedded in the outer leaflet of the outer membrane (OM). Attached to lipid A is the core polysaccharide. Both lipid A and core are mostly conserved between *P. aeruginosa* strains. The distal portion of the LPS molecule is capped with a repeating (n) sugar unit composed outwards from the cell. Common O antigen is the same between *P. aeruginosa* serotypes while serotype specific O antigen distinguishes *P. aeruginosa* into 20 different serotype groups. This is based on the composition of sugars in the repeat unit. Strains that produce O antigen are termed "LPS smooth" while strains that do not cap LPS with O antigen are termed "LPS rough".

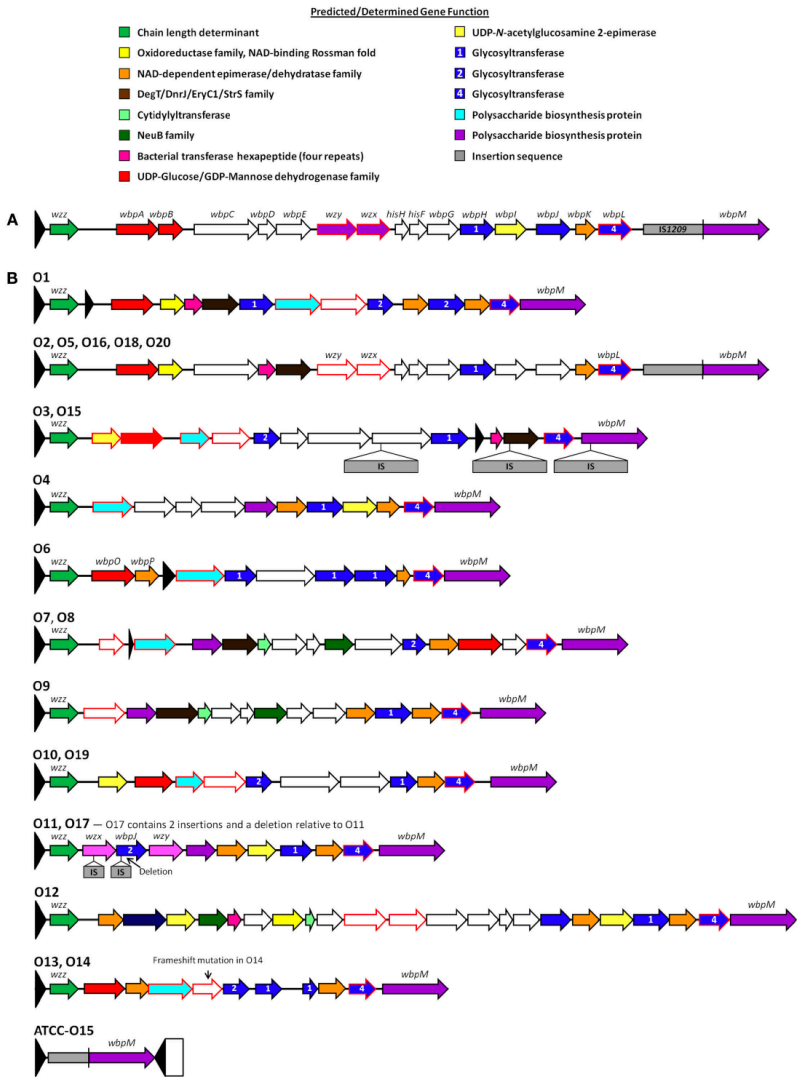

Figure 1.6. Organization of genes within the O antigen biosynthesis clusters in each *P. aeruginosa* serotype. A) O antigen gene arrangement in serotype O5 strain PAO1. B) The 20 different O antigen serotype biosynthesis operons are clustered into 11 groups based off of sequence conservation. A red outline depicts an ORF with potential transmembrane-spanning domains. Previously identified genes are labeled above the respected cluster if present within the serotype. Insertion sequences (IS) present within genes are depicted by a secondary gray box. *Modified from Lam JS, Taylor VL, Islam ST, Hao Y, Kocincova D. 2011. Genetic and Functional Diversity of *Pseudomonas aeruginosa* Lipopolysaccharide. Front Microbiol 2:118.

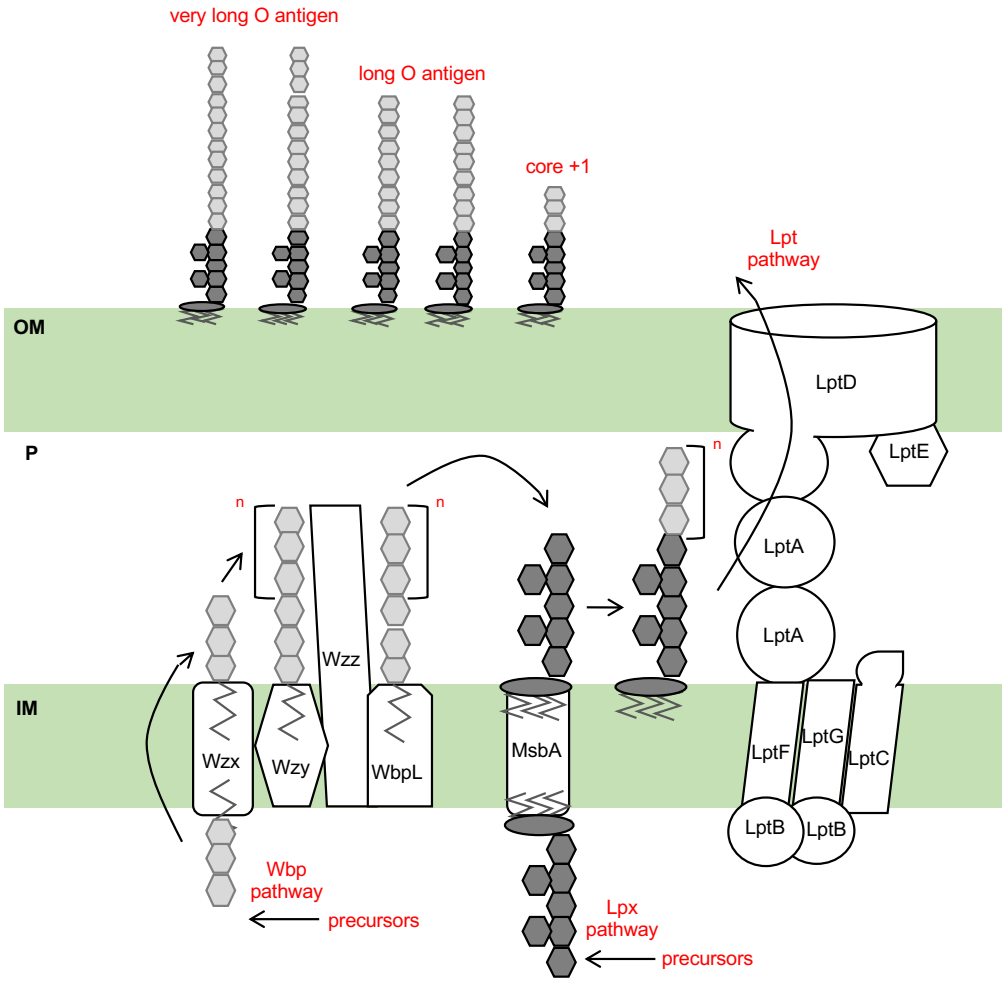

Figure 1.7. Model for O antigen biosynthesis. The O antigen repeat unit is assembled onto a a undecaprenyl pyrophosphate lipid carrier based on the biosynthetic genes of the serotype specific O antigen operon (Wbp pathway). Next, the repeat sugar unit attached to a undecaprenyl pyrophosphate lipid carrier is flipped across the inner membrane (IM) into the periplasm by the Wzx flippase. Single repeat units are then polymerized into a growing chain (n) by Wzy. The length of the chain is determined by Wzz1/Wzz2. Finally, WaaL ligates the O antigen chain to the lipid A-core molecule, which is assembled by the Lpx biosynthesis operon and flipped across the inner membrane by MsbA. The lipid A-core-O antigen molecule is then transported through the periplasmic space (P) and inserted into the outer membrane (OM) by the Lpt transport pathway.

Table 1.1. Functional class of predicted open reading frames in PAO1.

Function class	ORFS	% of ORFS
Adaptation, protection (for example cold shock proteins)	60	1.1
Amino acid biosynthesis and metabolism	150	2.7
Antibiotic resistance and susceptibility	19	0.3
Biosynthesis of cofactors, prosthetic groups and carriers	119	2.1
Carbon compound catabolism	130	2.3
Cell division	26	0.5
Cell wall, LPS	83	1.5
Central intermediary metabolism	64	1.1
Chaperones & heat shock proteins	52	0.9
Chemotaxis	43	0.8
DNA replication, recombination, modifcation and repair	81	1.5
Energy metabolism	166	3.0
Fatty acid and phospholipid metabolism	56	1.0
Membrane proteins	7	0.1
Motility & attachment	65	1.2
Nucleotide biosynthesis and metabolism	60	1.1
Protein secretion/export apparatus	83	1.5
Putative enzymes	409	7.3
Related to phage, transposon or plasmid	38	0.7
Secreted factors (toxins, enzymes, alginate)	58	1.0
Transcription, RNA processing and degradation	45	0.8
Transcriptional regulators	403	7.2
Translation, post-translational modification, degradation	149	2.7
Transport of small molecules	555	10.0
Two-component regulatory systems	118	2.1
Hypothetical	1,774	31.8
Unknown (conserved hypothetical)	757	13.6
Total	**5,570**	**100%**

**adapted from Stover et al. 2000. Nature. 406:959-64.*

Table 1.2. Summary of PAO1 genomes from different sources.

Strain name	GenBank accession no.	Source	Genome size (bps)	% GC content
H103 PAO-1 AK957	QZFW00000000	R. Hancock, University of British Columbia	6,218,105	66.57
PAO-1	QZFX00000000	J. Burns, University of Washington	6,200,122	66.56
PAO-1 (B. Iglewski)	QZFY00000000	E. P. Greenberg, University of Washington	6,219,177	66.57
PAO-1 (B. Holloway)	QZFZ00000000	D. Ohman, Virginia Commonwealth University	6,229,074	66.53
MPAO-1 (C. Manoil)	QZGA00000000	C. Manoil, University of Washington	6,221,774	66.57
PAO-1 V	QZGB00000000	J. Goldberg, University of Virginia	6,219,532	66.57
PAO-1 H	QZGC00000000	H. Nikaido, University of California, Berkeley	6,218,750	66.57
PAO-1 A	QZGD00000000	A. Prince, Columbia University	6,217,973	66.50
MPAO-1 (C. Manoil)	QZGE00000000	C. Manoil, University of Washington	6,218,510	66.57
PAO-1 ATCC	NZ_CP017149.1	ATCC	6,276,434	66.50

**adapted from Chandler et al. 2019. J Bacteriol. 201(5).*

Chapter 2

The AlgP histone-like protein regulon is distinct in nonmucoid and mucoid *Pseudomonas aeruginosa* and does not include alginate biosynthesis genes

Adapted from the submitted publication

"The AlgP histone-like protein regulon is distinct in nonmucoid and mucoid *Pseudomonas aeruginosa* and does not include alginate biosynthesis genes"

Ashley R. Cross, Erika E. Csatary, Vishnu Raghuram, Frances L. Diggle, Marvin Whiteley, William M. Wuest, and Joanna B. Goldberg

Accepted with minor revisions

ABSTRACT

The opportunistic bacterial pathogen *Pseudomonas aeruginosa* causes acute and chronic infections that are notoriously difficult to treat. In people with cystic fibrosis, *P. aeruginosa* can cause lifelong lung infections and isolation of mucoid *P. aeruginosa*, resulting from the overproduction of alginate, is associated with chronic infection. The histone-like protein AlgP has been implicated in the control of alginate gene expression, but this regulation is unclear. To explore AlgP in further detail, we deleted *algP* in mucoid strains and demonstrate that deletion of *algP* did not result in a nonmucoid phenotype or reduced alginate production. We show that the *algP* promoter is expressed by both the nonmucoid strain PAO1 and the isogenic mucoid strain PDO300, suggesting that there may be genes differentially regulated between these strains. In support of this, we found that deletion of *algP* in PAO1 increased expression of the nitric-oxide operon *norCBD* and the nitrous-oxide reductase genes *nosRZ*, while deletion of *algP* in PDO300 increased expression of the potassium transport operon *kdpABCD*. Surprisingly, we found no significant overlap of the PAO1 and PDO300 AlgP regulons and furthermore, that *algP* did not regulate genes in the alginate biosynthesis operon. This study helps clarify the existing literature surrounding AlgP and elucidates a narrow regulatory network controlled by AlgP.

ABBREVIATED SUMMARY

Transition of *Pseudomonas aeruginosa* from a nonmucoid to a mucoid phenotype, characterized by the overproduction of alginate, correlates with the establishment of a chronic lung infection in people with cystic fibrosis. The histone-like protein AlgP has been proposed to regulate alginate production. Here, we define the AlgP transcriptome in both nonmucoid and mucoid *P. aeruginosa* and find that the AlgP regulon is distinct in each background, but that alginate genes were not a significant component.

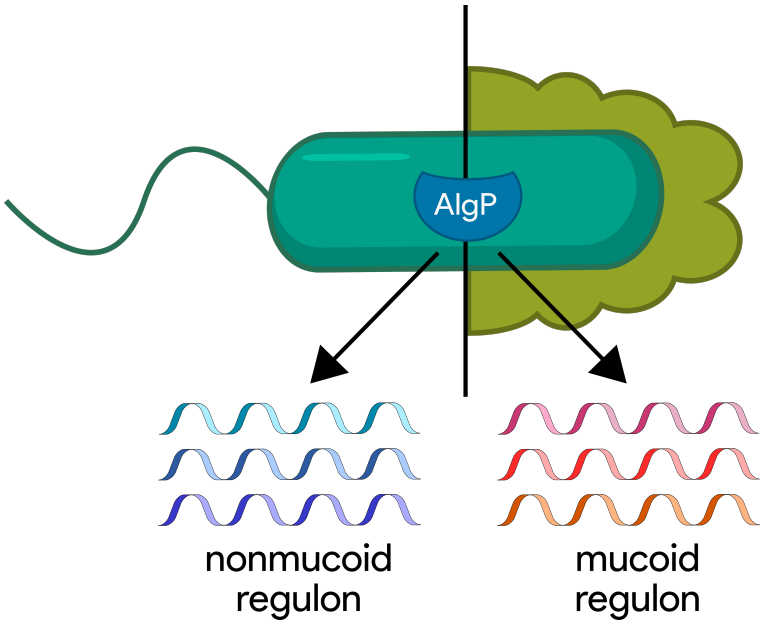

INTRODUCTION

Pseudomonas aeruginosa is an opportunistic pathogen with the ability to persist in many complex environments due to a large genome encoding an extensive repertoire of virulence factors, toxins, and exopolysaccharides (2). In order to coordinate the expression of many genes *P. aeruginosa* strain PAO1, for example, is predicted to encode 118 two-component response regulators, 403 transcriptional regulators (2), over 20 known or predicted sigma factors (144), and 4 quorum sensing networks (145, 146). *P. aeruginosa* causes a variety of acute and chronic illnesses and is one of the most common microbes colonizing the lungs of people with cystic fibrosis (CF) (21, 22, 27). People living with CF have impaired lung function and a reduced ability to clear inhaled bacteria that can result in the establishment of chronic and sometimes lifelong infections (23, 24, 26, 147).

During long-term respiratory infection in CF, *P. aeruginosa* can accumulate genetic mutations that rewire regulatory circuits to be better suited to this environment. Some mutations result in dramatic phenotypic changes such as the transition from a nonmucoid to a mucoid phenotype. Emergence of mucoid colonies correlates with the establishment of a chronic infection, increased inflammation, and worsening lung disease (61, 65, 66). Over 80% of mutations leading to mucoid conversion, characterized by the overproduction of the exopolysaccharide alginate, occur in the *mucA* gene encoding an anti-sigma factor (42, 51, 120, 148, 149). The most commonly observed *mucA* mutation is called "*mucA22*" and results from the deletion of a G in a string of 5 G nucleotides (44, 45, 101). MucA is a critical negative regulator for maintaining control of alginate production. When MucA is inactivated, it no longer binds the sigma factor AlgT, which is then free to continuously direct transcription of the alginate biosynthesis operon as well as about 300 other genes (76, 108). The alginate operon is composed

of 12 genes that are necessary for synthesizing and transporting alginate outside of the cell and is typically expressed in response to external stresses (104, 107).

Transcription of the alginate operon is highly regulated. Histone-like proteins are unique transcriptional regulators that can control virulence expression in *P. aeruginosa* and some have been shown to regulate alginate production (150-152). One such histone-like protein is AlgP (also called AlgR3 and Hp-1). AlgP was originally identified on a large region of DNA that, when provided in *trans*, could weakly complement a nonmucoid clinical isolate containing an unknown alginate regulatory mutation back to a mucoid phenotype (153). Unlike other known regulators of alginate biosynthesis that are highly expressed in only mucoid strains, *algP* mRNA is produced by both nonmucoid and mucoid strains from a sigma 70-like promoter (154, 155). Sequence analysis of *algP* revealed that the carboxyl-terminal domain contains multiple KPAA amino acid repeat units and that AlgP is highly basic resulting in a high affinity for DNA (153, 154, 156). Konyecsni and Deretic purified a short repeat peptide from the lysine-rich region of *algP* and demonstrated that this peptide bound multiple upstream regions of the alginate promoter using a gel mobility shift assay, however this peptide also bound to nonspecific DNA (156). Therefore, the exact role for AlgP in the regulation of the mucoid phenotype is still unclear.

To determine the genes, including alginate genes, regulated by *algP*, we dissected the AlgP regulon in the well-studied nonmucoid strain PAO1 and isogenic mucoid strain PAO1 *mucA22*, which is referred to as PDO300 (51). Our results show that there are few *algP* regulated genes, that there is no significant overlap in the PAO1 and PDO300 AlgP regulons, and, most surprisingly, that the alginate biosynthetic genes are not impacted by deletion of *algP*. Altogether these results suggest that AlgP is not a major regulatory factor controlling alginate production.

RESULTS

Deletion of *algP* from mucoid strains does not alter alginate levels. Based on published data, we hypothesized that deletion of *algP* in the mucoid PAO1 strain, PDO300, would result in a nonmucoid phenotype due to decreased alginate production (153, 156). To test this, we generated a PDO300 Δ*algP* mutant containing a deletion of *algP*. Surprisingly, when visualized on an L agar plate, PDO300 Δ*algP* was still mucoid and was indistinguishable from PDO300 (Fig. 2.1A). We considered that small differences in alginate production might not be visible, so we quantified how much alginate was produced by each strain and observed no significant difference in the amount of alginate produced by PDO300 and PDO300 Δ*algP* in MOPS succinate minimal media (Fig. 2.1A) as well as rich L broth (Fig. S2.1).

Since the original role for AlgP was described in a mucoid clinical isolate (156), we reasoned that the regulation of alginate by AlgP might be dependent on strain background. To attempt to reconcile our findings with those in the literature, we examined whether deletion of *algP* in a mucoid clinical isolate would render this strain nonmucoid. Therefore we deleted *algP* in 2192, a mucoid strain isolated from a person with cystic fibrosis (157). 2192 Δ*algP* was still mucoid and produced similar levels of alginate to the parent strain 2192 (Fig. 2.1B, Fig. S2.1).

***algP* expression is reduced in PDO300 compared to PAO1.** Through mapping of the *algP* transcriptional start site, Konyecsni and Deretic observed that *algP* mRNA was produced by nonmucoid and mucoid clinical isolates, likely due to the presence of a sigma 70 promoter (154). To expand on this observation, we measured *algP* promoter activity in PAO1 and PDO300. We constructed a transcriptional-*lacZ* reporter by fusing the predicted *algP* promoter sequence to a promoterless-*lacZ* (P_{algP}-*lacZ*) and inserted this construct, in single copy, into the chromosome of PAO1 and PDO300. Using ß-galactosidase assays, we compared expression of the *algP* promoter in each strain. We found that, while the *algP* promoter was indeed expressed

in both PAO1 and PDO300, there is a 40% decrease in PDO300 *algP* promoter activity compared to PAO1 (Fig. 2.2).

AlgP is a positive and negative regulator of genes in PAO1 and PDO300. We next wanted to know what genes were AlgP-regulated. Because the *algP* promoter is expressed by both PAO1 and PDO300, we hypothesized that AlgP may regulate different genes in a nonmucoid background compared to a mucoid background. To determine the AlgP regulon of PAO1 and PDO300, we used RNA sequencing to assess gene expression differences in each strain when *algP* is deleted. We confirmed that there are no growth differences in either PAO1 or PDO300 when *algP* is deleted (Fig. S2.2) and then isolated mRNA from wild type and Δ*algP* PAO1 and PDO300 at exponential phase.

There were 26 differentially regulated genes between PAO1 and PAO1 Δ*algP* (Table 2.1). A similar number of genes were obtained for PDO300 and PDO300 Δ*algP* with 19 genes differentially regulated (Table 2.2). Of particular interest, none of the alginate biosynthetic genes were found to be differentially regulated due to the deletion of *algP*. However, these genes were significantly up-regulated in PDO300 compared to PAO1, as expected. In both PAO1 and PDO300 strain backgrounds, AlgP acts as both a positive and negative regulator of gene expression. Of note, the genes for the operons *norCBD* and *nosRZ* controlling nitric-oxide and nitrous-oxide reductase enzymes, respectively, were significantly increased in expression in PAO1 when *algP* was deleted. On the other hand, the *kdpABCD* operon, implicated in potassium transport, was significantly increased in expression when *algP* was deleted from PDO300.

It was surprising to us that there was no significant overlap in the PAO1 and PDO300 AlgP regulons. One hypothesis for this might be that MucA/AlgT regulates all of the genes and result in differential expression of the genes between PAO1 and PDO300 independent of AlgP.

However, of the 45 genes in the PAO1 and PDO300 AlgP regulons, there were only 4 AlgT-regulated genes and these were different between the PAO1 and PDO300 datasets. The AlgT-regulated genes were PA1301 (*kdpA*) and PA5526 (hypothetical protein) in PAO1 and PA1196 (*ddaR*) and PA5535 (hypothetical protein) in PDO300.

Deletion of *algP* increases survival of PAO1 during anaerobic growth. We confirmed mRNA expression differences of the nitric oxide reductase subunit C *norC* in PAO1, PDO300, and each respective *algP* mutant, using qPCR performed on the original RNA isolated for RNA sequencing. We found a 2.9-fold change in *norC* steady-state levels in PAO1 Δ*algP* compared to PAO1, similar to that found by RNA sequencing. As anticipated from the RNA sequencing results, we did not see a significant difference in *norC* steady-state levels between PDO300 and PDO300 Δ*algP*, with only a -0.3-fold difference between strains. Previous studies have shown that expression of nitric oxide reductase and nitrous oxide reductase are necessary for denitrification and growth of *P. aeruginosa* during anaerobic respiration and a PAO1 *norCB* mutant has a decreased growth rate under anaerobic conditions compared to wild type PAO1 (158). Based on this result, we hypothesized that PAO1 Δ*algP,* which has increased *norCB and nosRZ* expression*,* would grow better anaerobically compared to PAO1. To test this, we grew PAO1 and PAO1 Δ*algP* anaerobically with nitrate as a terminal electron acceptor and calculated colony forming units (CFUs) after 24 and 48 hours of growth. In support of our hypothesis, deletion of *algP* significantly increased survival of PAO1 after 48 hours of anaerobic growth (Fig. 2.3). Complementation of *algP* in single copy under control of the native *algP* promoter (PAO1 Δ*algP* Tn7::P_{algP}-*algP*) returned growth to wild type levels. We also monitored growth of PDO300 and PDO300 Δ*algP.* Since there is no difference in *norCB* and *nosRZ* levels between these two strains, we hypothesized that deletion of *algP* would result in no difference in growth

under anaerobic conditions. Consistent with the RNA sequencing results, there was no difference in growth of PDO300, PDO300 Δ*algP*, and PDO300 Δ*algP* Tn7::P_{algP}-*algP* (Fig. 2.3). We used a PAO1 *norC* transposon mutant (PAO1 *norC*::IS*lacZ*hah) as a control for a strain with slow growth under anaerobic conditions.

***algP* promoter activity is increased in stationary phase independent of RpoS.** Recent work by Babin, *et al.* observed that expression of the *algP* promoter correlated with *rpoS* promoter expression (159). RpoS is a sigma factor that regulates or contributes to the regulation of over 700 genes including many stationary phase genes (160, 161). Based on this data we hypothesized that *algP* may be more highly expressed in stationary phase. Using the P_{algP}-*lacZ* reporter described above, we measured *algP* promoter activity in exponential and stationary phase grown cultures. We used an *rpoD* promoter-*lacZ* transcriptional fusion (P_{rpoD}-*lacZ*) as a control for a gene that is not differentially regulated in different growth phases (162). In support of our hypothesis, *algP* promoter activity in PAO1 and PDO300 is increased 3- to 5-fold in stationary phase compared to *algP* promoter activity in exponential phase (Fig. 2.4), while *rpoD* promoter expression was unchanged between exponential and stationary phase in both PAO1 and PDO300 (Fig. 2.4).

To test if the increase in *algP* promoter activity in stationary phase is dependent on RpoS production, we constructed a PDO300 *rpoS* mutant by replacing the wild type *mucA* gene in PAO1 *rpoS*::hah with the *mucA22* allele. We then inserted P_{algP}-*lacZ* into both PAO1 *rpoS*::hah and PDO300 *rpoS*::hah (163, 164). We hypothesized that *rpoS* would be necessary for the increase in *algP* promoter activity when bacteria transition to stationary phase. However, when *algP* promoter activity was quantified in both PAO1 *rpoS*::hah and PDO300 *rpoS*::hah, there was still a significant increase in promoter activity between exponential and stationary phase. This

rejects our hypothesis and indicates that RpoS is not required for the increase in *algP* promoter expression upon entry into stationary phase (Fig. 2.4).

DISCUSSION

Alginate regulation in *P. aeruginosa* is complex and has been well studied (45, 102, 107, 111, 113, 120, 165). The histone-like protein AlgP was one of the first regulators discovered and has not been thoroughly reinvestigated until now. Originally, *algP* was recognized by its ability to partially complement a nonmucoid clinical *P. aeruginosa* isolate back to a mucoid phenotype by providing *algP* in trans; other studies showed that this complementation required expression of an additional gene, *algQ* (153, 154). This suggests that disruption of *algP* may not have been the reason for the nonmucoid phenotype. And while AlgP had been described for its ability to bind to the alginate promoter, the AlgP peptide used for these studies also bound nonspecific DNA indicating the lack of specificity of this interaction (156).

Considerable evidence and speculation also suggested that the number of KPAA repeats present in the C-terminus of *algP* play a vital role in regulating alginate production (154-156). Nonmucoid revertants of clinical isolates have been found to contain large rearrangements spanning the *algP* region. However, rearrangements were also observed in mucoid isolates (156) . More recently, three studies on genomic variation, evolution, and polymorphisms of clinical isolates found *algP* to be a hot spot for mutations (166-168). However, there was no significant relationship between the mutations found and the mucoid or nonmucoid phenotype of each strain.

Despite these studies, there remained a significant gap in knowledge about AlgP so we chose to reexamine the relationship between AlgP and alginate. The results presented here help to explain a regulatory role for AlgP in *P. aeruginosa*. We provide evidence that alginate production is not greatly impacted by AlgP, countering the long-standing premise in the field. This was found to be the case for two different mucoid strains and independent of culture

conditions. We found in MOPS succinate minimal media, the 2192 strains produced 40 times as much alginate as PDO300 (Fig. 2.1), while in lysogeny broth (LB) PDO300 produces similar levels of alginate to 2192. The differences are likely due to the many genotypic differences between the two wildtype strains. However, in all cases, the Δ*algP* mutants produced similar amounts of alginate as the wildtype parental strains.

A broad regulatory role has been reported for histone-like proteins MvaT and MvaU in *P. aeruginosa*. These two proteins regulate a specific subset of genes and phenotypes in nonmucoid *P. aeruginosa* that include biofilm formation, pyocyanin production, quorum sensing, and swarming motility (150, 151). We reasoned that this might also be true for AlgP and further that there may be different subsets of genes regulated between nonmucoid and mucoid backgrounds. We performed RNA sequencing of isogenic nonmucoid and mucoid strains to decipher the AlgP regulon. As a result, we identified 45 AlgP-regulated genes, 26 in PAO1 and 19 in PDO300. AlgP repressed expression of most of the genes identified, either directly or indirectly, and positively regulated only 7. As an internal control, the differences we found in gene expression between PAO1 and PDO300 were similar to those previously reported and included genes for alginate biosynthesis (169). We found no significant difference in *algP* mRNA levels between PAO1 and PDO300 based on the RNA sequencing results, even though there is a slight decrease in *algP* promoter activity in PDO300 compared to PAO1 (Fig. 2.2).

Additionally, we found that the *norCBD* and *nosRZ* are up regulated in PAO1 Δ*algP* compared to PAO1, but not significantly altered in PDO300 and PDO300 Δ*algP*. We confirmed this on the same samples using qPCR and further validated this observation phenotypically and showed that PAO1 Δ*algP* survives better under anaerobic growth conditions compared to PAO1 while deletion of *algP* from PDO300 resulted in no increase in survival. Down regulation of

algP in PAO1 may promote survival during an initial infection where *P. aeruginosa* must quickly adapt to growth in the thick oxygen-deplete mucus found in the lungs of people with CF (170, 171).

Recent published data implicates AlgP in the regulation of the small molecules pyoverdine and pyocyanin (172), but we did not find genes for the biosynthesis or transport of these molecules in our RNA sequencing results. Additionally, AlgP was implicated in the regulation of biofilm formation and that this may be RpoS-dependent (159). We found that the *algP* promoter is up regulated in stationary phase, but that this is independent of RpoS. This agrees with published RpoS ChIP-sequencing (173) that does not show binding of RpoS to the *algP* promoter and published microarray data (160) that does not show regulation of *algP* mRNA by RpoS. Regardless, since *algP* expression is increased in stationary phase, there may be more genes regulated by AlgP at this later growth phase in both strains. However, in line with our original observations, deletion of *algP* does not alter alginate production or gene expression during stationary or exponential growth, respectively (Fig. 2.1, Table 2.1, Table 2.2). Babin *et al*. also found that AlgP as well as the *algP* promoter are more highly expressed in cells contained within the interior of four-day-old biofilms (159). However, our RNA sequencing results found no genes known to be involved in biofilm formation regulated by AlgP.

It was surprising to us that there were only 4 of the AlgP-regulated genes were also differentially regulated between PAO1 and PDO300. Therefore, most of the genes identified are not MucA/AlgT regulated. While we have not reconciled why this is the case, the mechanisms responsible could be (1) that different co-factors that are only expressed in either a nonmucoid or mucoid background may be required for AlgP function, (2) that AlgP may be modified in one strain background compared to the other resulting in different DNA-binding preferences, and/or

(3) that a large production of alginate alters AlgP function and preference for targets. While it appears that the most accepted way for *P. aeruginosa* to rewire gene expression during chronic infection is through *mucA* mutation and overexpression of AlgT (108), this may not be the only way. Another way could be to alter the gene targets of a regulator that is already expressed, such as we see with AlgP. Still, since we only saw a small subset of genes significantly regulated by AlgP and most of the regulation we see is small, AlgP might be more involved in fine tuning gene expression rather than regulating genes on or off. A thorough understanding of the multifaceted regulatory systems in *P. aeruginosa* will provide knowledge on how this complex opportunistic pathogen adapts to many environments, cause infections, and persist.

MATERIALS AND METHODS

Bacterial strains and culture conditions. Bacteria were maintained with lysogeny broth (LB, Teknova) plates or broth. When appropriate, media was supplemented with 10 µg ml-1 tetracycline, 15 µg ml-1 gentamycin, 100 µg ml-1 carbenicillin, or 30 µg ml-1 kanamycin for *Escherichia coli* and 100 µg ml-1 tetracycline, 300 µg ml-1 carbenicillin or 60 µg ml-1 gentamycin for *P. aeruginosa*. All growth experiments were performed in MOPS supplemented with 20 mM succinate (174). For allelic exchange, Vogel-Bonner minimal medium (VBMM) supplemented with gentamicin and no salt L agar (LA, 10 g l-1 tryptone and 5 g l-1 yeast extract) plates containing 15% sucrose were used for sucrose counterselection. All plates were supplemented with 1.5% agar (Apex). Strains were grown at 37°C except for conjugations and sucrose counterselections, which were performed at 30°C. Growth curves were performed by diluting an overnight culture of each strain to an OD_{600} of 0.01 in fresh media in a 6-well plate and growth, as determined by OD_{600}, was continuously monitored in a BioTek Synergy H1 plate reader. For anaerobic growth, overnight cultures of aerobically grown bacteria were back-diluted to an OD_{600} of 0.1 in LB supplemented with 1% potassium nitrate and grown in a GasPak EZ Anaerobe Container System with indicator (BD BDL) at 37°C. CFUs were plated at time 0, 24, and 48 hours on LA and incubated aerobically at 37°C. Survival was calculated as (final CFU/ml- initial CFU/ml). A complete list of strains, plasmids, and primers are available in supplemental table 1 (Table S1).

Plasmid and mutant construction. A detailed description of plasmid construction and generation of PAO1 Δ*algP,* PDO30*0* Δ*algP,* and PDO300 *rpoS::Tn* mutants can be found in Text S1 in the supplemental material.

Alginate isolation and quantification. Alginate was purified and quantified as described previously (175) with modifications (48).

ß-galactosidase assay. Assays for *algP* were performed as described previously (176) with modifications (48).

RNA sequencing. A detailed description of the RNA sequencing methods can be found in Text S1 in the supplemental material.

RT-qPCR. Total RNA was isolated from 1 ml of exponentially growing culture and quantitative PCR was performed as previously described (48). Primers oAC03/oAC04 were used to amplify *rpoD* and primers VRp015/VRp016 were used to amplify *norC*.

Additional statistical analysis. GraphPad Prism Software (version 6) was used to analyze the data. All data represent biological replicate data with technical replicates. Graphs show mean values and error bars represent standard deviation (SD). *: $P<0.05$; **, $P<0.01$: ***, $P<0.001$: ****: $P<0.0001$. ns, not significant.

SUPPLEMENTAL TEXT S2.1.

Plasmid Construction. To generate pEXG2-Δ*algP* 1000 bps of the upstream region of *algP* was PCR amplified from PAO1 genomic DNA using oAC225/oAC226 and 1000 bps of downstream *algP* sequence was amplified using oAC227/oAC228. These two fragments were then inserted into HindIII digest pEXG2 using isothermal assembly (Gibson Assembly Master Mix, New England BioLabs) following the manufacturers protocol. The reaction was then transformed by heat-shock into chemically competent DH5α and selected for on gentamicin. Plasmids were extracted (Qiagen Miniprep Kit) from isolated colonies and PCR verified using oAC91/oAC92. Plasmid pEXG2-Δ*algP* was then transformed into chemically competent SM10 in the same way described for DH5α.

To make pP_{lac}-*cre* the P_{lac}-*cre* sequence was amplified from pCM157 using oJM521/oJM522. This fragment was then ligated into BamHI/SacI double-digest pFLP2 using isothermal assembly (Gibson Assembly Master Mix, New England BioLabs) following the manufacturers protocol. The reaction was then transformed by heat-shock into chemically competent DH5α and selected for on carbenicillin. Plasmids were extracted (Qiagen Miniprep Kit) from isolated colonies and verified by restriction digest.

To construct the *algP* reporter, 125 bps of the upstream *algP* region containing the predicted *algP* promoter was amplified using oAC235/oAC236 and inserted into HindIII digest miniCTX1-optRBS-*lacZ* using isothermal assembly (Gibson Assembly Master Mix, New England BioLabs) following the manufacturers protocol, to generate miniCTX1-P_{algP}-optRBS-*lacZ*. The reaction was transformed into chemically competent DH5α and selected for on

tetracycline. Plasmids from single colonies were isolated and screened for the *algP* promoter insertion using oAC32/oAC33. Once confirmed, miniCTX1-P_{algP}-optRBS-*lacZ* was then electroporated into electrocompetent PAO1 and PDO300 as previously described (177) to generate PAO1 attCTX1::P_{algP}-optRBS-*lacZ* and PDO300 attCTX1::P_{algP}-optRBS-*lacZ*.

Construction of PAO1 Δ*algP*, PDO300 Δ*algP*, and PDO300 *rpoS::Tn*. SM10 containing pEXG2-Δ*algP* was conjugated with PAO1 and PDO300 and SM10 containing pEXG2-*mucA22* was conjugated with PAO1 *rpoS*::Tn following the puddle-mating protocol, in a 3:1 ratio as previously described (178). After sucrose counterselection, single colonies were patched onto LA and LA containing gentamicin. Gentamicin sensitive colonies were screened for loss of *algP* by single-colony PCR using primers oAC225/oAC228. Insertion of the *mucA22* allele was confirmed by PCR amplification of the *mucA* gene by oAC89/oAC90 and Sanger sequencing by Genewiz.

Removal of antibiotic marker from PAO1 *rpoS* transposon mutant. The antibiotic marker was removed from PAO1 *rpoS* transposon mutant PW7152 using plasmid pP_{lac}-*cre*. This leaves a scar containing an influenza-hemagglutinin epitope and a hexahistidine tag (hah) and generates strain PAO1 *rpoS*::hah (179). To do this, pP_{lac}-*cre* was transformed into electrocompetent PW7152, prepared as previously described (177), and selected for on LA plates containing carbenicillin and 1 mM IPTG. Colonies were then patched on LA, LA+tetracycline, and LA+carbenicillin. Tetracycline sensitive and carbenicillin resistant colonies were streaked onto no salt LB containing 15% sucrose. Sucrose resistant colonies were then patched again onto LA, tetracycline, and carbenicillin. Tetracycline and carbenicillin sensitive colonies were used for

these studies. miniCTX1-P_{algP}-optRBS-*lacZ* was then electroporated into this strain as described above to generate PAO1 *rpoS*::hah attCTX::P_{algP}-optRBS-*lacZ* and PDO300 *rpoS*::hah attCTX::P_{algP}-optRBS-*lacZ*.

RNA sequencing sample collection and RNA isolation. Overnight cultures of PAO1, PAO1 Δ*algP*, PDO300, and PDO300 Δ*algP* were grown in 3ml MOPS-succinate, cultures were back diluted to an OD_{600} of 0.01 in 20 ml MOPS-succinate and allowed to grow to exponential phase, shaking at 200 rpm. 2 ml aliquots from each culture were added directly to 10ml of RNAlater (Thermo Fisher Scientific). This suspension was stored at 4°C for 24 hours and then transferred to -80°C until samples were processed. Each sample was collected in biological triplicate and matched to 0.56 +/- 0.02 OD_{600}. RNA extraction and preparation of sequencing libraries were performed as described recently (14) with some modifications. Briefly, cultures stored in RNAlater were pelleted at 12,000 x g for 30 min at 4°C, resuspended in 300 µl RNase Free TE buffer containing 6 µl of lysozyme (50 mg ml-1), transferred to Benchmark Bead Bug tubes, and lysed by bead beating for 30 s. Samples were incubated at 37°C for 30 mins prior to adding 1 ml of RNA-bee (Tel-Test Inc.). The contents were homogenized by bead beating 3X for 30 s, resting on ice for 60 s between sets, transferred to a clean microcentrifuge tube, and 200 µl of chloroform added. Next, samples were shaken vigorously for 45s and stored on ice for 1 hr. The phases were separated by centrifugation at 13000 x g for 30 min at 4°C and the aqueous phase transferred to a new tube. 500 µl of isopropanol and 2 µl of linear acrylamide (5mg ml-1, Invitrogen) were added to each sample and these were stored at -80°C overnight. Overnight samples were thawed and centrifuged at 13,000 × g for 15 min at 4°C. The pellets were washed twice with 1 ml 75% ethanol, air dried for 5 min, and dissolved in 100 µL of RNase-free water.

The RNA concentration for each sample was determined using a NanoDrop 100 spectrophotometer (Thermofisher). Next, 10 µg of RNA was DNase (Promega) treated and the RNA-bee extraction protocol used to clean-up and recover the RNA was repeated.

Preparation of RNA sequencing libraries. Ribosomal RNA was depleted and mRNA enriched from 2 µg of DNase-treated RNA using the MICROB*Express* (Ambion) kit and then precipitated by adding 1/10th the volume of 3M sodium acetate, 2 µl linear acrylamide (5 mg ml-1), and 3 volumes cold ethanol, vortexing, and storing overnight at -80°C. The enriched mRNA was recovered as described before and then 250 ng was fragmented using the Magnesium RNA Fragmentation Module (NEBNext) kit. The fragmented mRNA was precipitated and recovered as described above and then resuspended in 13 µl of RNase free water. Finally, libraries were prepared using the Multiplex Small RNA Library Prep Set for Illumina (NEBNext) kit and PCR purified (Qiagen). For quality control and size selection, the purified libraries were separated by size in a 5% TBE gel (BioRad), stained using SYBR Gold nucleic acid gel stain (Invitrogen), and visualized using a UV transilluminator. The bands between 147/160 bps to 307 bps were cut from the gel, eluted, and transferred to a gel filtration column (Costar). After centrifugation the eluate was precipitated and recovered as described above. Purified libraries were sequenced using NextSeq at Georgia Tech by the molecular evolution core.

Bioinformatics analysis. RNAseq reads were trimmed using cutadapt v2.3 with a minimum length cutoff of 18 bp (180). The reads were then mapped to PAO1 refseq genome NC_002516.2 using bowtie2 v2.3.5 with end-to-end alignment (181). The number of reads mapped to each genomic feature was calculated using HTSeq v11.1 and features with less than 10 mapped reads

were discarded (182). The normalized read counts can be found in Supplementary tables S2.2-2.4 (Table S2.2, Table S2.3, Table S2.4). The final dataset consists of 5590 genes. Differential expression analysis was performed using the R package DESeq2 (183).

ACKNOWLEDGEMENTS

We thank Dr. Jeffrey Meisner for the construction of pP_{lac}-*cre*. ARC was supported by a predoctoral fellowship from the Cystic Fibrosis Foundation (CFF)-funded CF@LANTA RDP Center (MCCART15R0) and a NRSA predoctoral fellowship from the National Institutes of Health (NIH) under award number F31AI136310. Additional funding was provided under award numbers R21AI122192 (JBG), GOLDBE16G0 (JBG), R01GM116547 (MW), R56HL142857 (MW), WHITEL19P0 (MW), WHITEL16G0 (MW), and GM119426 (WMW). The content of the manuscript does not represent the official views of the NIH who had no role in study design, data collection, or interpretation of the data.

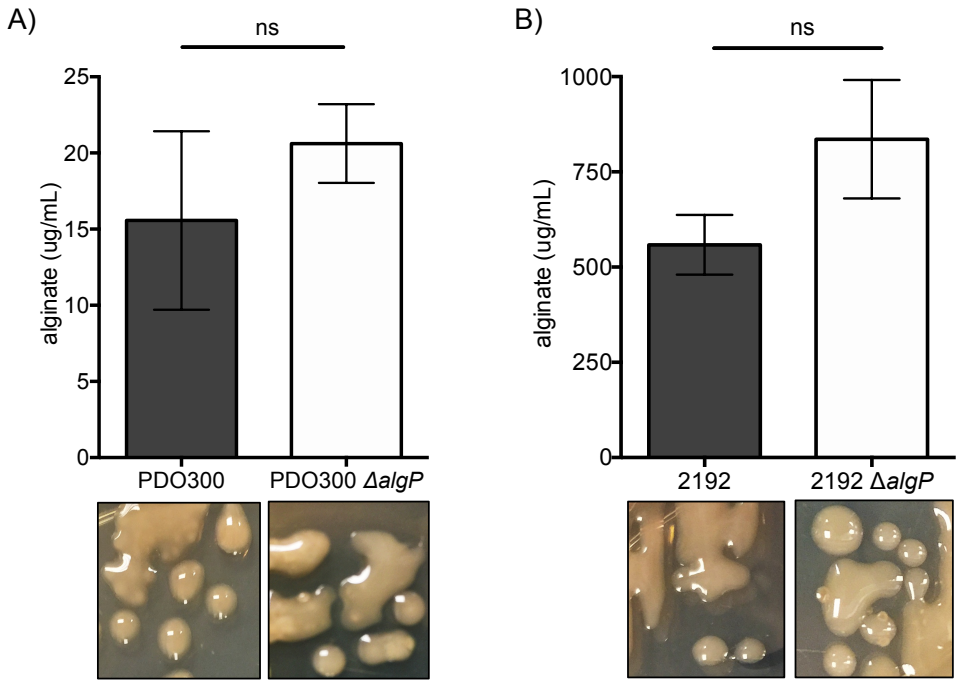

Figure 2.1. Deletion of *algP* from mucoid strains does not decrease alginate levels. Alginate was purified from 24-hour cultures grow in MOPS succinate minimal media and quantified using a carbazole assay. Deletion of *algP* from mucoid laboratory strain PDO300 (A) or mucoid CF isolate 2192 (B) does not result in decreased alginate production. Significance was determined using an unpaired t-test. Error bars represent SD of three biological replicates. A picture of the mucoid phenotype of each strain grown on lysogeny agar (LA) is shown below each bar. ns: not significant.

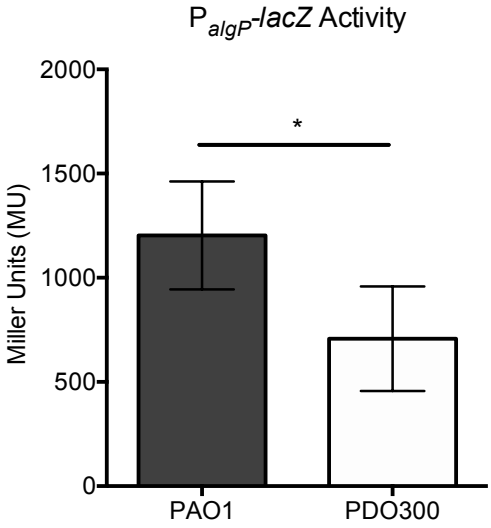

Figure 2.2. *algP* promoter expression is reduced in PDO300 compared to PAO1. The *algP* promoter was transcriptionally fused to a promoterless-*lacZ* to construct a P_{algP}-*lacZ* reporter. The reporter was inserted, in single copy, at an ectopic site in the chromosome of PAO1 and PDO300. ß-galactosidase activity was determined during exponential phase growth in MOPS succinate minimal media. Significance was determined using an unpaired t-test. Error bars represent SD of three biological replicates. *: $p<0.05$.

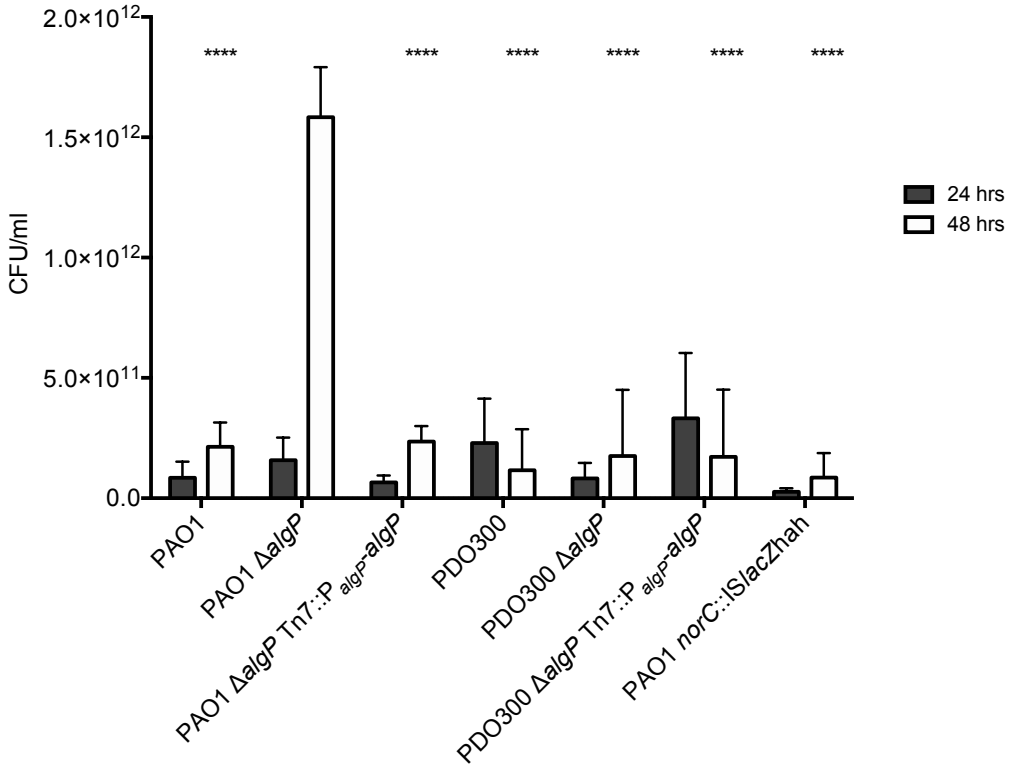

Figure 2.3. Deletion of *algP* increases survival of PAO1 during anaerobic growth. Strains were grown anaerobically in LB supplemented with potassium nitrate and CFUs were plated at time 0, 24, and 48 hours. Growth was calculated as (final CFU/ml- initial CFU/ml). Significance was determined using a two-way ANOVA with Sidak's multiple comparisons analysis. Error bars represent SD of three biological replicates. ****: $p<0.0001$.

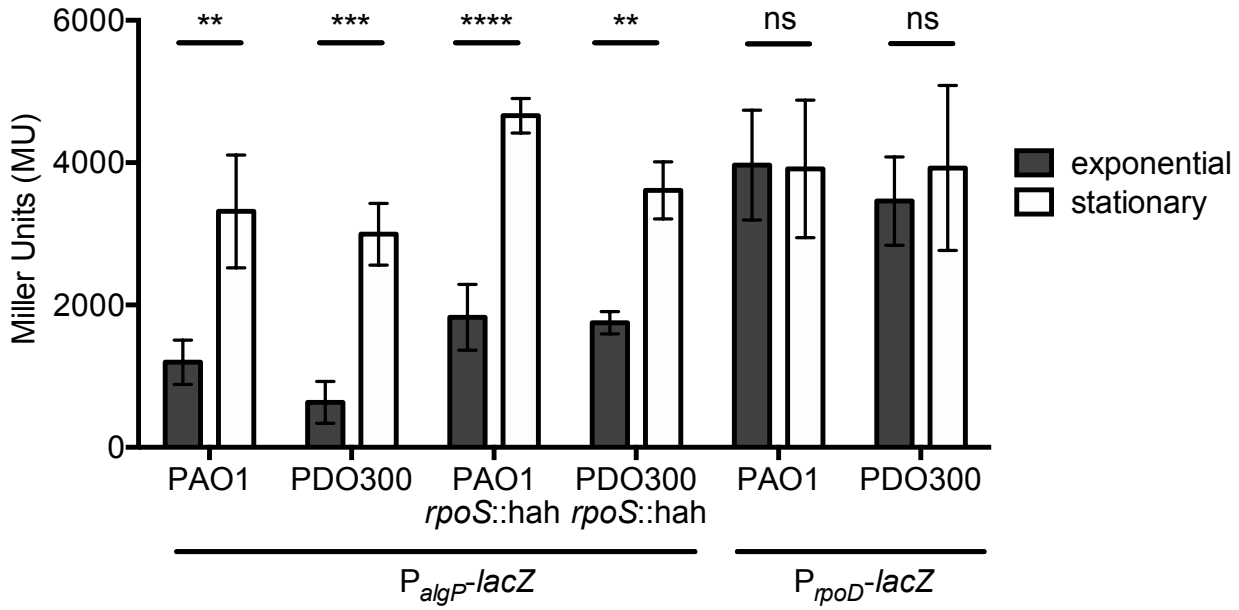

Figure 2.4. *algP* promoter activity is increased in stationary phase independent of RpoS. The P_{algP}-*lacZ* reporter or the P_{rpoD}-*lacZ* reporter was inserted, in single copy, at an ectopic site in the chromosome of each strain. ß-galactosidase activity was determined during exponential and stationary phase growth in MOPS succinate minimal media. Significance was determined using a two-way ANOVA with Sidak's multiple comparisons analysis. Error bars represent SD of three biological replicates. **: $p<0.01$, ***: $P<0.001$, ****: $P<0.0001$, ns: not significant.

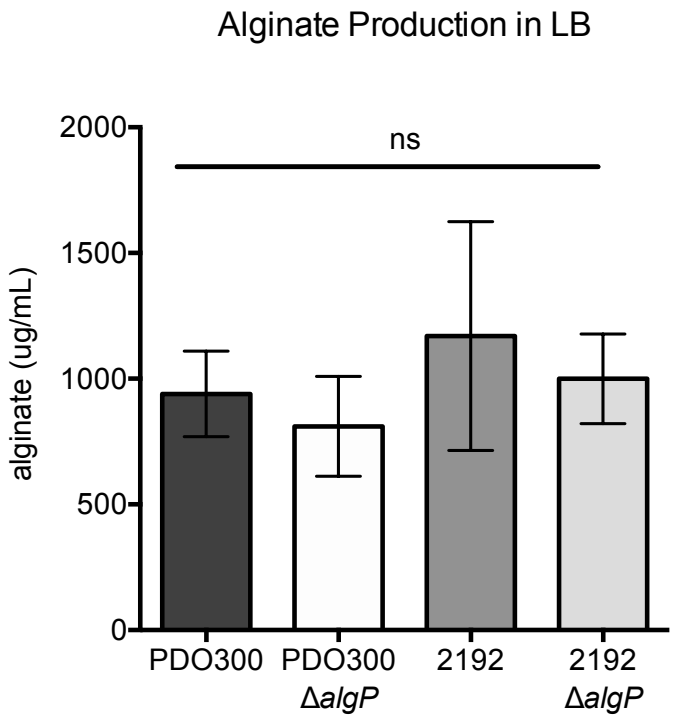

Figure S2.1. Deletion of *algP* does not significantly alter alginate production in LB. Alginate was purified from 24-hour cultures grown in LB and quantified using a carbazole assay. Significance was determined using a one-way ANOVA. Error bars represent SD of three biological replicates. ns: not significant.

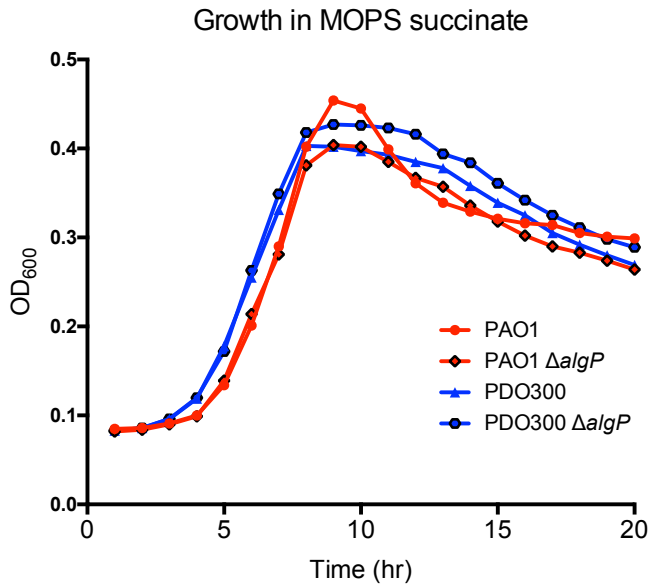

Figure S2.2. Growth of PAO1 and PDO300 is unaltered when *algP* is deleted. Strains were grown in MOPS succinate minimal media for 20 hours in 6-well plates and OD_{600} measurements were taken every 20 minutes in a BioTek Synergy H1 plate reader.

Table 2.1. PAO1 v. PAO1 Δ*algP* significant expression differences.

Gene ID	Gene Name	Gene Product	Log_2 Fold Change	p-value
PA0094	*eagT6*	Type VI secretion system associated protein/chaperone	1.31	4.84E-04
PA0523	*norC*	nitric-oxide reductase subunit C	2.06	1.30E-03
PA0524	*norB*	nitric-oxide reductase subunit B	1.46	1.44E-03
PA0525	*norD*	probable dinitrification protein	1.81	2.02E-03
PA0637		conserved hypothetical protein	-1.64	3.78E-03
PA1301		probably transmembrane sensor	-3.54	2.38E-05
PA1389		probably glycosyl transferase	1.15	1.93E-03
PA1537		probable short-chain dehydrogenase	1.14	3.49E-03
PA2282		hypothetical protein	1.99	5.50E-04
PA2930		probable transcriptional regulator	1.81	6.02E-04
PA3116		probable aspartate-semialdehyde dehydrogenase	1.04	3.42E-03
PA3278		hypothetical protein	1.09	2.76E-03
PA3309		conserved hypothetical protein	1.75	1.38E-04
PA3359		hypothetical protein	2.39	2.36E-04
PA3391	*nosR*	nitrous-oxide reductase regulatory protein	2.18	1.66E-05
PA3392	*nosZ*	nitrous-oxide reductase precursor	1.58	2.52E-03
PA3443		probable permease of ABC transporter	1.33	1.99E-03
PA3754		hypothetical protein	1.13	6.44E-04
PA4242	*rpmJ*	50S ribosomal protein L36	1.20	1.04E-03
PA4373		hypothetical protein	-1.02	2.16E-03
PA4610		hypothetical protein	2.74	8.98E-06
PA4705	*phuW*	haem uptake ABC transporter component	-1.28	1.18E-03
PA4849		hypothetical protein	1.64	6.86E-04
PA5029		probable transcriptional regulator	1.22	1.24E-03
PA5253	*algP*	histone-like protein	-7.63	1.04E-12
PA5446		hypothetical protein	1.23	1.63E-03
PA5526		hypothetical protein	1.15	1.42E-03

Table 2.2. PDO300 v. PDO300 Δ*algP* significant expression differences.

Gene ID	Gene Name	Gene Product	Log_2 Fold Change	p-value
PA0076	*tagF1*	Type VI secretion system associated protein	-1.24	1.51E-03
PA0509	*nirN*	electron-bifurcating dehydrogenase	1.01	2.35E-03
PA0622		probably bacteriophage protein	1.13	2.89E-03
PA0985	*pyoS5*	pyocin S5	1.69	5.62E-04
PA1196	*ddaR*	transcriptional regulator	-1.27	4.50E-04
PA1633	*kdpA*	potassium-transporting ATPase, A chain	1.68	2.31E-04
PA1634	*kdpB*	potassium-transporting ATPase, B chain	2.30	2.70E-07
PA1635	*kdpC*	potassium-transporting ATPase, C chain	2.11	9.76E-06
PA1636	*kdpD*	two-component sensor	1.14	2.42E-03
PA2310		hypothetical protein	1.02	2.43E-03
PA3441		probable molybdopterin-binding protein	1.12	8.79E-04
PA3515		hypothetical protein	1.93	1.97E-05
PA3516		probably lyase	1.69	1.85E-03
PA3931		conserved hypothetical protein	1.75	3.21E-05
PA4670	*prs*	ribose-phosphate pyrophosphokinase	1.44	6.16E-04
PA4970		conserved hypothetical protein	-1.16	1.94E-03
PA5172	*arcB*	ornithine carbamoyltransferase, catabolic	1.66	1.15E-03
PA5252		probable ATP-binding component of ABC transporter	1.06	7.22E-04
PA5253	*algP*	histone-like protein	-7.34	1.31E-15
PA5535		conserved hypothetical protein	3.45	2.20E-07

Table S2.1. Strains, plasmids, and primers used in this study.

Name	Description	Reference
E. coli		
DH5a	cloning background, plasmid maintenance	Invitrogen
SM10	bi-parental mating, conjugation proficient	9
P. aeruginosa		
PAO1	nonmucoid laboratory strain	10
PAO1 *norC*::IS*lacZ*hah	PAO1 transposon mutant PW1959	11, 12
PAO1 attCTX::optRBS-*lacZ*	promoterless-*lacZ* control	13
PAO1 attCTX::PrpoD-optRBS-*lacZ*	*rpoD* promoter reporter inserted in single-copy	13
PAO1 attCTX::PalgP-optRBS-*lacZ*	*algP* promoter reporter inserted in single-copy	This study
PAO1 Δ*algP*	*algP* clean deletion	This study
PAO1 Δ*algP* Tn7::P*algP-algP*	*algP* mutant complemented with *algP* and native promoter in single copy	This study
PAO1 *rpoS*::IS*lacZ*hah	PAO1 transposon mutant PW7152	11, 12
PAO1 *rpoS*::hah	*rpoS* transposon mutant PW7152 with antibiotic marker removed	This study
PAO1 *rpoS*::hah attCTX::PalgP-optRBS-*lacZ*	algP promoter reporter inserted in single-copy	This study
PDO300	mucoid PAO1 containing *mucA22* allele	14
PDO300 attCTX::PrpoD-optRBS-*lacZ*	*rpoD* promoter reporter inserted in single-copy	13
PDO300 attCTX::PalgP-optRBS-*lacZ*	*algP* promoter reporter inserted in single-copy	This study
PDO300 Δ*algP*	*algP* clean deletion	This study
PDO300 Δ*algP* Tn7::P*algP-algP*	*algP* mutant complemented with *algP* and native promoter in single copy	This study
PDO300 *rpoS*::hah attCTX::PalgP-optRBS-*lacZ*	PAO1 *rpoS*::hah containing *mucA22* and *algP* promoter reporter inserted in single-copy	This study
Plasmids		
pEXG2	allelic exchange vector	15
pEXG2-Δ*algP*	*algP* clean deletion vector	This study
pEXG2-*mucA22*	*mucA22* allelelic replacement vector	13
miniCTX1-optRBS-*lacZ*	promoterless-*lacZ* reporter with optimized RBS	13
miniCTX1-PrpoD-optRBS-*lacZ*	miniCTX1-optRBS-*lacZ* containing *rpoD* promoter	13
miniCTX1-PalgP-optRBS-*lacZ*	miniCTX1-optRBS-*lacZ* containing *algP* promoter	This study
miniTn7	single copy insertion plasmid for Tn7 site	19
miniTn7-P*algP-algP*	miniTn7 containing *algP* promoter and coding sequence	This study
pFLP2	Flp-FRT recombinase system, back-bone for construction of pPlac-*cre*	16
pCM157	Back-bone for Plac-*cre* amplification	17
pPlac-*cre*	Cre recombinase vector for antibiotic excision of transposon mutant, IPTG inducible	This study
Primers		
oAC03	GGGCGAAGAAGGAAATGGTC	18
oAC04	CAGGTGGCGTAGGTGGAGAA	18
oAC32	GACCCACTCTCAGGAGTGAAC	13
oAC33	CTCTTCGCTATTACGCCAGCTG	13
oAC89	ATGAGTCGTGAAGCCCTGCA	13
oAC90	TCAGCGGTTTTCCAGGCTGG	13
oAC91	CCACACATTATACGAGCCGGAAGC	13
oAC92	GGTACCGAATTCGAGCTCGAGC	13
oAC225	TTCCACACATTATACGAGCCGGAAGCATAAATGTAAAGCAcgcgctgaacttcaacgacc	This study
oAC226	CTTTGCTGGTGCTTGGCTCGGCGGCTTTGCAGACAGCGCCgacgtgcctccaggcggacg	This study
oAC227	ggcgctgtctgcaaagccgc	This study
oAC228	CGAGCTCGAGCCCGGGGATCCTCTAGAGTCGACCTGCAGAaggttcaggcgcatcctcca	This study
oAC235	CTGGAGCTCCACCGCGGTGGCGGCCGCTCTAGAACTAGTGcatacccaggcgggcgccta	This study
oAC236	AATCATGGTCATAGCTGTTCCTCCTTACTGCAGCCCGGGGgacgtggttgcgcccatac	This study
oAC231	CTCACTAGTGGATCCCCCGGGCTGCAGGAATTCCTCGAGAcgcgccgatgccgttacctt	This study
oAC232	TCTGGTTGGCCTGCAAGGCCTTCGCGAGGTACCGGGCCCAcgcccttgcggagcgtgagg	This study
VRp015	ATTTCGGCGGGAGTGTGTTCTTC	This study
VRp016	GCACGTTCAGCGGCTGGATATT	This study
oJM521	aaaaaggatcgatcctctagagGAGCGCAACGCAATTAATGTG	This study
oJM522	accatgattacgaattcgagctCAGGGTTTTCCCAGTCACGAC	This study

*lowercase nucleotides anneal to plasmid sequence during isothermal assembly

Chapter 3

Remodeling of O antigen in mucoid *Pseudomonas aeruginosa* via transcriptional repression of *wzz2*

Adapted from the publication

"Remodeling of O antigen in mucoid *Pseudomonas aeruginosa* via transcriptional repression of *wzz2"*

Ashley R. Cross and Joanna B. Goldberg

mBio 2019, 10 (1) e02914-18
DOI: 10.1128/mBio.02914-18

ABSTRACT

Pseudomonas aeruginosa is an opportunistic pathogen that causes chronic lung infections in people with cystic fibrosis (CF). Chronic *P. aeruginosa* isolates generally do not express O antigen and often have a mucoid phenotype, the latter of which is characterized by the overproduction of the exopolysaccharide alginate. Therefore, O antigen expression and the mucoid phenotype may be coordinately regulated upon chronic adaption to the CF lung. Here we demonstrate that PDO300, a mucoid strain derived from the nonmucoid laboratory isolate PAO1, does not produce very long O antigen due to decreased expression of Wzz2, the very long O antigen chain-length control protein, and that mucoid clinical isolates express reduced levels of Wzz2 compared to nonmucoid isolates. Further we show that forcing the expression of very long O antigen by PDO300, by providing *wzz2 in trans*, does not alter alginate production suggesting that sugar precursors are not limited between the two biosynthesis pathways. Moreover, we confirm that AmrZ, a transcription factor highly expressed in mucoid strains, is a negative regulator of *wzz2* promoter activity and very long O antigen expression. These experiments identify the first transcriptional regulator of O antigen chain-length in *P. aeruginosa* and support a model where transition to a chronic mucoid phenotype is correlated with down regulation of very long O antigen through decreased Wzz2 production.

IMPORTANCE

Detection of mucoid *Pseudomonas aeruginosa*, characterized by the overproduction of alginate, is correlated with the establishment of a chronic pulmonary infection and disease progression in people with cystic fibrosis (CF). In addition to the overproduction of alginate, loss of O antigen lipopolysaccharide production is also selected for in chronic infection isolates. In this study, we have identified the regulatory network that inversely regulates O antigen and alginate production. Understanding the regulation of these chronic phenotypes will elucidate mechanisms that are important for the establishment of a long-term *P. aeruginosa* lung infection and ultimately provide an opportunity for intervention. Preventing *P. aeruginosa* from chronically adapting to the CF lung environment could provide a better outcome for people who are infected.

INTRODUCTION

Pseudomonas aeruginosa is capable of causing chronic lung infections in people with cystic fibrosis (CF) (21, 22). Upwards of 50% of people with CF are infected with *P. aeruginosa* and life-long infections are the leading cause of morbidity and mortality (27-30). CF is caused by mutations in the cystic fibrosis transmembrane conductance regulator (*cftr*) that results in altered ion transport and improper lung function (23, 24). This altered lung environment increases mucus accumulation in the lungs, reducing mucociliary clearance that ultimately leads to bacterial persistence (26). Attempts at treating these life-threatening infections have fallen short due to *P. aeruginosa's* ability to adapt to the CF lung and survive in the altered lung environment (184). This survival is reflected by the expression of rare phenotypes that distinguish chronic CF isolates from *P. aeruginosa* obtained from other sources or types of infections. The accumulation of these features is often referred to as the "chronic infection phenotype" (36).

One distinct chronic phenotype that has been observed is related to the expression of lipopolysaccharide (LPS). Environmental and acute infection isolates express an LPS-smooth phenotype, while *P. aeruginosa* isolates from chronic pulmonary infections are often LPS-rough, meaning they do not express O antigen (36, 38, 119, 132-134). In LPS-smooth strains, the serotype specific O antigen expressed is characterized based on size; long O antigen is regulated by the chain-length control protein Wzz1, while very long O antigen is regulated by the chain-length control protein Wzz2 (122, 139-141)

In addition to the loss of O antigen expression *P. aeruginosa* strains isolated from chronic infections are often mucoid (42, 148). Furthermore, these mucoid clinical strains are LPS-rough (135, 136). Detection of the mucoid phenotype, characterized by the overproduction of the

exopolysaccharide alginate, is correlated with pulmonary disease progression (58, 61, 65, 185). The most common mutations that lead to mucoid conversion in CF isolates are found in *mucA* (42, 106, 120, 121). MucA is an anti-sigma factor responsible for sequestering AlgT, the sigma factor that initiates transcription of the alginate biosynthesis operon and approximately 300 other genes of the AlgT regulon (104). When MucA is inactivated, AlgT constitutively transcribes the alginate biosynthesis operon resulting in overproduction of alginate and the mucoid phenotype.

Given the apparent correlation between alginate overexpression and loss of O antigen in chronic infection isolates, it has been speculated that alginate and O antigen are coordinately controlled. In support of this premise, Kelly et al. compared the LPS profiles of the nonmucoid laboratory strain PAO1 and a series of phage-induced mucoid variants (137). They noted that the mucoid strains had lost expression of the high molecular weight portion of the LPS molecule and that nonmucoid reversion could restore production. Ma et al. expanded upon the results of Kelly et al. by comparing O antigen production of PAO1 to PDO300, a well-studied isogenic mucoid variant of PAO1 (51). PDO300 contains the most common clinically observed *mucA* mutation *mucA22* (42). The authors observed that high molecular weight O antigen was reduced in PDO300 compared to PAO1. Both groups suggested that the overproduction of multiple mannose-rich exopolysaccharides results in a competition for a shared sugar pool by O antigen and alginate biosynthesis pathways. However, these results do not account for why the low molecular weight fractions of O antigen are unaffected since both low and high molecular weight O antigen contains the same sugars.

Previous research has primarily focused on the mucoid phenotype and the regulation of alginate biosynthesis. Contrary, it is not known how O antigen is regulated during chronic infections even though loss of O antigen expression is a common chronic phenotype. Given the

failure of the shared precursor model to adequately explain why nonmucoid reversion of clinical isolates does not restore O antigen production or why only one chain-length of O antigen is affected by mucoid conversion, we fill this gap in knowledge by, instead, identifying an overlapping transcriptional regulator that inversely controls alginate and O antigen expression at a genetic level. Understanding the coordinated regulation between the mucoid phenotype and O antigen production will elucidate mechanisms that are selected for during the establishment of a long-term infection and inform us about host-pathogen interactions during chronic infections. We suggest that interfering with the expression of these chronic infection phenotypes and the subsequent adaption of *P. aeruginosa* to the CF lung environment could provide a better outcome for people living with CF.

RESULTS

Mucoid strains produce less Wzz2 compared to nonmucoid strains resulting in less very long O antigen. Previous studies by Kelly et al. and Ma et al. showed that mucoid strains often do not express high molecular weight O antigen (137, 138). To begin to understand the mechanism responsible for the change in O chain length expression in mucoid strains, we first sought to confirm the observation made by Ma et al. We isolated LPS and compared the O antigen profiles between from nonmucoid (NM) PAO1 and mucoid (M) derivative PDO300 (51). When PAO1 LPS was separated based on size and probed using serotype O5 specific antigen antibodies, long and very long O antigen modalities are clearly visible (Fig 3.1A). When LPS isolated from PDO300 was separated in the same manner, little high molecular weight O antigen was observed (Fig 3.1A) as previously reported (138). We specifically noted that the O antigen modality of PDO300 looks similar to that of a PAO1 *wzz2::*Tn transposon mutant (140). This transposon is inserted in the first half of *wzz2*, likely disrupting Wzz2 protein function. Wzz2 is known to regulate the very long O antigen lengths, and, in the absence of *wzz2*, PAO1 does not make very long O antigen (Fig 3.1A).

We therefore hypothesized that loss of this high molecular weight O antigen is the specific loss of very long O antigen chain-lengths in PDO300 and further that this is likely due to decreased production of Wzz2. Using polyclonal antibody to Wzz2 in western blot analysis of protein extracts from PAO1, PDO300, and PAO1 *wzz2*::Tn, Wzz2 production of each strain was examined; reactivity is seen with an ~49 kDa protein, as expected. Reactivity was also consistently seen with a protein ~65 kDa in all of the samples tested, including the *wzz2* mutant. Because of this, we are confident this cross-reacting band does not belong to Wzz2 and it has been cropped from the images. In support of our hypothesis, Wzz2 production was reduced in

PDO300 compared to PAO1 (Fig 3.1A). Comparison of protein levels by densitometry analysis determined that PDO300 makes about 65% less Wzz2 than PAO1. PAO1 *wzz2*::Tn, as expected, does not make Wzz2 (Fig 3.1A). Altogether, these data indicate that the loss of high molecular weight O antigen expression in PDO300 is due to decreased expression of Wzz2 and thereby loss of very long O antigen modalities.

As Wzz2 is conserved among *P. aeruginosa* strains (140) we also compared Wzz2 and O antigen production in serotype O10 laboratory strain PA14 and a mucoid derivative that we generated (PA14 *mucA22*). PA14 *mucA22* has reduced levels of Wzz2 and fewer high molecular weight O antigen chain-lengths compared to PA14 (Fig S3.1) confirming that the inverse relationship between alginate production and O antigen chain-length is not strain or serotype specific.

Since loss of O antigen expression is a recognized phenotype of CF isolates, we next determined whether decreased expression of Wzz2 by PDO300 held true in mucoid *P. aeruginosa* CF isolates. We used the Wzz2 polyclonal antibody to screen a series of random nonmucoid and mucoid CF isolates obtained from the Cystic Fibrosis Biospecimen Registry (CFBR). CFBRPA10, 34, 44, and 20 are all nonmucoid strains and, overall, expressed higher levels of Wzz2 compared to the mucoid isolates CFBRPA08, 11, 33, and 32 (Fig 3.1C). Wzz2 was barely detectable in all of the mucoid isolates and these appeared similar to the PAO1 *wzz2*::Tn control. CF isolates are generally LPS-rough and nontypable (186), thus O antigen production was not monitored in these strains.

Overexpression of *wzz2* in PDO300 increases very long O antigen production. We next wanted to determine if we could restore expression of Wzz2 and very long O antigen to PDO300 by providing *wzz2 in trans* and whether this would alter alginate production. If there is

a shared pool of precursor sugars, we should not be able to express very long O antigen in PDO300 without compromising alginate production. To test this, we cloned *wzz2* behind an arabinose-inducible promoter contained on the plasmid pHERD20T (187) to generate pHERD20T-*wzz2*. This plasmid has a *P. aeruginosa* origin of replication and can be maintained in multi-copy to facilitate overexpression of genes. pHERD20T-*wzz2* were transferred into PAO1 and PDO300 and production of Wzz2 and very long O antigen were monitored when *wzz2* was induced using 0.4% L-arabinose and compared to a vector only (pHERD20T) control. When *wzz2* was overexpressed in PAO1, which already expresses very long O antigen, there was a modest increase in the amount of very long O antigen produced (Fig 3.2). When *wzz2* was overexpressed in PDO300 we successfully restored Wzz2 and very long O antigen production to PAO1 levels (Fig 3.2). There was no effect on Wzz2 or very long O antigen production when PAO1 pHERD20T and PDO300 pHERD20T vector only controls were grown in 0.4% L-arabinose.

To determine if alginate production had been impacted in PDO300 when *wzz2* and very long O antigen were overexpressed, we monitored the mucoid phenotype. When grown on a plate containing 0.4% L-arabinose to induce *wzz2* expression, PDO300 pHERD20T-*wzz2* maintained a mucoid phenotype (data not shown). We quantified the amount of alginate that was made by PDO300, a PDO300 vector only control (PDO300 pHERD20T), and PDO300 pHERD20T-*wzz2* when each strain was grown to stationary phase in the absence or presence of the inducer. PDO300 pHERD20T-*wzz2* grown without inducer produced 570.52 µg/ml of alginate (Table 3.1). When grown in inducer, PDO300 pHERD20T-*wzz2* had a 12% decrease in alginate production. As a control, we also compared alginate expression of the vector only PDO300 control and noted a 21% decrease in alginate production when this strain was grown

with inducer compared to without (Table 3.1). Altogether this suggests that there is no major difference in alginate produced when very long O antigen is made by a mucoid strain suggesting that a limited pool of sugar precursors, under these conditions, does not account for loss of very long O antigen production in PDO300. This supports our hypothesis that decreased very long O antigen in PDO300 results from decreased expression of Wzz2 rather than a competition of sugar precursors.

The *wzz2* steady-state mRNA levels and promoter activity are repressed in PDO300. To determine how Wzz2 is regulated in PDO300, we investigated both *wzz2* steady-state mRNA levels and transcription initiation. We utilized quantitative reverse transcriptase PCR with *wzz2* gene-specific primers, which anneal on sites upstream and downstream of the transposon insertion, to measure relative *wzz2* transcript levels in PAO1, PDO300, and control strain PAO1 *wzz2*::Tn, which does not express *wzz2* (Fig. 3.3A). Transcript levels were normalized to the housekeeping gene *rpoD* (162). When compared, PDO300 expressed about one-third the relative number of *wzz2* transcripts compared to PAO1 (Fig. 3.3A). Since *wzz2* mRNA expression is reduced in PDO300, we suspected that *wzz2* is transcriptionally repressed in this strain. To test this, we fused the 5' promoter region of *wzz2* to a promoterless-*lacZ* and inserted this construct, in single-copy, into the CTX phage attachment site in PAO1 and PDO300. Subsequently, ß-galactosidase enzymatic activity was used as readout of *wzz2* promoter activity in each strain. As speculated, analysis of *wzz2* promoter activity revealed that PDO300 had a significant 17-fold decrease in *wzz2* promoter activation compared to PAO1 (Fig. 3.3B) indicating that *wzz2* is transcriptionally repressed in PDO300.

Nonmucoid isolates of mucoid strains express more Wzz2 and very long O antigen. To further interrogate the relationship between Wzz2 and alginate production, we monitored

Wzz2 expression in nonmucoid revertants of two mucoid CF isolates (188). The mucoid phenotype is unstable and these strains frequently revert to nonmucoid in the laboratory (43). We hypothesized that loss of alginate production by a mucoid strain would restore Wzz2 expression. Importantly, isolation of nonmucoid revertants also allows us to study the effect of alginate and Wzz2 regulation in isogenic clinical isolates. We used western blot analysis to compare Wzz2 production in mucoid clinical isolates CFBRPA32 and CFBRPA43 as well as two isogenic nonmucoid revertants of each. Each pair of nonmucoid revertants was obtained from the same mucoid parental culture. Both pairs of nonmucoid revertants, nmr1 and nmr2, had substantial increases in Wzz2 expression compared to each isogenic mucoid parental strain (Fig. 3.4A).

Frequently, nonmucoid reversion results from inactivating mutations in the sigma factor *algT* (44, 73, 106, 121). We sequenced *algT* in each nonmucoid revertant and discovered that three of the four strains contained mutations in the *algT* coding sequence. CFBRPA32nmr1 and nmr2 both had an in-frame duplication of basepairs 127-135 (GACGCCCAG). This results in insertion of amino acids DAQ. Since both revertants had the same mutation, this is likely a result of a single clone overtaking the entire population early in passaging of this culture. CFBRPA43nmr1 had no mutations identified in the *algT* coding sequence and therefore a mutation upstream in the regulatory region or elsewhere in the chromosome resulted in nonmucoid reversion. Finally, CFBRPA43nmr2 had a C to A transversion at nucleotide 245 of *algT* resulting in a threonine to asparagine change at amino acid 82. Both amino acids are polar and uncharged. These data provide a connection between *algT* and the regulation of Wzz2.

Since clinical isolates are often LPS-rough (135, 136), whether nonmucoid reversion is sufficient to restore very long O antigen expression remained unclear. Therefore, we utilized PDO300, which can express O antigen, to determine if nonmucoid reversion would restore very

long O antigen production. We isolated a nonmucoid revertant of PDO300, PDO300nmr1, by daily serial passaging in a static broth culture. Interestingly, sequencing of *algT* in this nonmucoid revertant revealed the same duplication of basepairs 127-135 in *algT* as described for the CFBRPA32 nonmucoid revertants. We isolated and separated LPS by SDS-PAGE and analyzed O antigen expression using serotype specific antibodies. As predicted, nonmucoid reversion of PDO300 restored very long O antigen production and resulted in increased Wzz2 production compared to PDO300 (Fig. 3.4B).

Overexpression of *algT* results in less very long O antigen and decreased *wzz2* promoter activity. To expand upon our observations that mutations in *algT* result in increased Wzz2, we next sought to determine if overexpression of *algT in trans* would decrease Wzz2 and very long O antigen. To do this we overexpressed *algT* on multi-copy plasmid pHERD20T in PAO1, which usually does not express high amounts of *algT*. We then compared the effects of uninduced and induced pHERD20T-*algT* in PAO1 on Wzz2 and O antigen production. PAO1 grown without inducer and therefore low *algT* expression produced both Wzz2 and very long O antigen. In contrast, when *algT* was induced with 0.4% arabinose, PAO1 produced no Wzz2 or very long O antigen and looked strikingly similar to PDO300 (Fig 3.5A).

We next investigated whether overexpression of *algT* would repress *wzz2* promoter activity. To test this, we cloned *algT* behind an IPTG inducible promoter in a miniTn*7*T plasmid and inserted this construct in single copy into PAO1 and PDO300nmr1 at the Tn*7* transposon insertion sites. When *algT* is overexpressed nonmucoid strains become mucoid (73, 102). We measured the amount of alginate produced by PAO1 and PDO300nmr1 when *algT* was induced compared to uninduced. PAO1 became mucoid when grown on inducer and produced a large 161.85-fold increase in alginate compared to when *algT* was uninduced (Table S3.1).

Contrariwise, when we quantified alginate production from PDO300nmr1 when *algT* was overexpressed the mucoid phenotype was slightly restored. However, there was no significant increase in the amount of alginate that was made compared to uninduced conditions (Table S3.1). Since AlgT is known to regulate its own transcription in a positive-feedback loop (45, 73), we suspect that disrupting this auto-regulation and only supplying *algT* in single copy fails to promote alginate overexpression. It could also be possible that this particular mutation in *algT* results in a dominant negative phenotype inactivating AlgT.

To measure *wzz2* promoter activity when *algT* was overexpressed, we inserted the *wzz2* promoter-*lacZ* fusion at the CTX site of PAO1 and PDO300nmr1. Both strains contain an IPTG-inducible copy of *algT* at the Tn*7* site. First, we measured *wzz2* promoter activity in PAO1 when *algT* was overexpressed. When *algT* was induced, PAO1 had a significant 18-fold decrease in *wzz2* promoter activity compared to when *algT* was uninduced (Fig. 3.5B). We also measured *wzz2* promoter activity in PDO300nmr1 grown without inducer. When *algT* was uninduced, PDO300nmr1 had high levels of *wzz2* promoter activity (Fig. 3.5B). When PDO300nmr1 was grown on inducer to express *algT*, *wzz2* promoter activity was reduced 6-fold. Taken together, these data pinpoint AlgT as the critical regulator of alginate production and very long O antigen.

Overexpression of *amrZ* represses *wzz2* promoter activity. When active, AlgT transcribes the genes encoding three global transcriptional regulators: AlgB, AlgR, and AmrZ (111, 165, 189, 190). We reasoned that one of these regulators would be a likely candidate for regulating *wzz2* transcription. Published microarray data for AlgB and AlgR did not provide evidence that *wzz2* was part of either regulon under the conditions tested (116, 191, 192). On the other hand, published RNA-sequencing and ChIP-sequencing data by Jones et al. provided evidence that, when *amrZ* is overexpressed in PAO1, AmrZ will bind upstream of *wzz2* and

reduce *wzz2* mRNA production (114). The predicted binding site of AmrZ is CGATAGCATAATG at –88 to –75 nucleotides upstream of the *wzz2* start codon (114). In order to directly test whether AmrZ regulates *wzz2* transcription initiation we reproduced an experiment similar to the one performed by Jones et al. by overexpressing *amrZ* in PAO1 and then measured *wzz2* promoter activity. To do this, we inserted the *amrZ* coding sequence downstream of an IPTG-inducible promoter and inserted this construct at the Tn*7* attachment site of PAO1. This strain (PAO1 P_{tac}-*amrZ*) also contains the *wzz2* promoter-*lacZ* fusion at the CTX site so that we can measure *wzz2* promoter activity when *amrZ* is being overexpressed. When *amrZ* expression is induced in the PAO1 background, this strain background had 4-fold less *wzz2* promoter activity compared to uninduced conditions (Fig. 3.6). This was comparable to wzz2 promoter levels in the PDO300 background (PDO300 P_{tac}-*amrZ*), which are not altered when *amrZ* was induced or uninduced.

Likewise, to determine if disruption of *amrZ*, in the context of a mucoid strain*,* would alleviate repression of *wzz2,* we inserted the *mucA22* allele from PDO300 into a PAO1 *amrZ* transposon mutant to generate PAO1 *mucA22 amrZ*::Tn. Inserting *mucA22* into PAO1 replicates the original construction of PDO300. We then assayed *wzz2* promoter activity in PAO1 *mucA22 amrZ*:Tn by inserting the *wzz2* promoter-*lacZ* fusion at the CTX site of this strain. Supporting our premise, when *amrZ* was inactivated and grown under uninduced conditions, PAO1 *mucA22 amrZ*::Tn had about a 14-fold increase in *wzz2* promoter activity compared to PDO300 (Fig. 3.6). We then complemented the *amrZ* defect by providing *amrZ in trans*. When *amrZ* was overexpressed in PAO1 *mucA22 amrZ*::Tn, *wzz2* promoter activity was reduced 3-fold, close to native PDO300 levels (Fig. 3.6). These data validate AmrZ as a negative regulator of *wzz2* promoter activity and therefore very long O antigen in mucoid *P. aeruginosa.* We also tested whether overexpression of

amrZ in PAO1 *mucA22 amrZ*::Tn would complement this strain back to mucoid. When *amrZ* was induced this strain became mucoid and alginate production was increased almost 50-fold (Table 3.2). Although there was a large increase in alginate produced when *amrZ* was induced, this was still 4 times less than the amount of alginate made by PDO300. As expected, overexpression of *amrZ* in PAO1 or PDO300 did not alter alginate production of these strains; PAO1 remained nonmucoid and PDO300 remained mucoid.

Disruption of *amrZ* restores Wzz2 production in mucoid strains. We also wanted to confirm that disruption of *amrZ* in the context of *mucA22* would restore very long O antigen production. When protein and O antigen from PAO1 *mucA22 amrZ*::Tn was visualized using western blot analysis, both Wzz2 and very long O antigen were restored to wild type PAO1 levels (Fig. 3.7A). This supports our hypothesis that AmrZ also regulates very long O antigen production. To confirm that this regulation is dependent on *mucA22*, we measured O antigen in PAO1 *amrZ*::Tn. There is no difference in Wzz2 or very long O antigen when *amrZ* is disrupted in PAO1, which is expected since PAO1 does not characteristically produce high levels of *amrZ* (Fig. S3.3). This indicates that AmrZ does not regulate very long O antigen in the absence of *mucA* disruption. Finally, to support the finding that *amrZ* negatively regulates Wzz2 in our laboratory strains, we also wanted to determine if deletion of *amrZ* in a mucoid clinical isolate would restore Wzz2 production. Therefore, we tested Wzz2 levels in mucoid LPS-rough CF isolate FRD1 and an isogenic FRD1 *amrZ* mutant (43, 135, 165, 193). Comparable to other mucoid CF isolates, FRD1 does not produce detectable levels of Wzz2 (Fig. 3.7B). Deletion of *amrZ* in FRD1, however, greatly increases Wzz2 production levels. Expression of Wzz2 in the FRD1 *amrZ* mutant provides evidence that AmrZ inhibits Wzz2 expression in mucoid clinical isolates.

DISCUSSION

P. aeruginosa isolates from chronic pulmonary infections exhibit unique characteristics, collectively termed the "chronic infection phenotype", compared to isolates from other types of infections (36). These strains are typically mucoid, non-motile, and have an LPS-rough phenotype, defined as lacking the O antigen portion of LPS (36, 38, 132-134). Mucoid conversion is well studied (46, 47), as is the mechanism responsible for the nonmotile phenotype of chronic infections isolates (190, 194). On the other hand, little progress has been made in understanding how O antigen and the LPS-rough phenotype are regulated in the context of a chronic infection.

To fill this gap in knowledge, we first focused our studies on LPS-smooth mucoid laboratory strains in order to determine why O antigen production is altered in these strains and to identify possible regulators of O antigen chain-length. In concentrating our studies on known transcription factors that are up regulated in mucoid strains, we found that AmrZ, which is an activator alginate biosynthesis and a repressor of motility (114, 190, 194-196), negatively regulates *wzz2* promoter activity and therefore very long O antigen production (Fig. 3.6). From the data presented here, we can now build a model for the regulation of very long O antigen in mucoid *P. aeruginosa* (Fig. 3.8). Nonmucoid strains expressing wildtype *mucA* have little AlgT activity. Under these conditions the *algT* regulon, including the alginate biosynthesis operon, *algB*, *algR*, and *amrZ*, are not transcribed. Because AmrZ is not produced, *wzz2* transcription is high and Wzz2 is free to mediate the assembly of very long O antigen. When *algT* expression is induced or *mucA* acquires mutations, AlgT is unrestricted and *amrZ* expression is induced. Overproduction of AmrZ represses *wzz2* expression and results in loss of very long O antigen chain-lengths (Fig 3.8).

While we are closer to understanding regulation of O antigen in mucoid *P. aeruginosa*, there may be other factors responsible for regulating chain-length in other contexts. For example, McGroarty and Rivera reported that high temperatures, low pH, or low concentrations of phosphate or high concentrations of NaCl, $MgCl_2$, glycerol, or sucrose resulted in decreased amounts of very long O antigen (143), but whether these conditions affect expression of *wzz2* has not been tested. Consequently, no known transcriptional regulators of O antigen chain-length have been identified in nonmucoid *P. aeruginosa*. Conversely, temperature was shown to regulate transcription of the O antigen gene cluster in *Yersinia enterocolitica* (197). Additionally, the PmrA/B and Rcs systems were reported to directly regulate transcription of *wzz* genes in *Salmonella enterica* serovar Typhimurium (197, 198). Ongoing experiments in our laboratory aim to unravel additional circuits that regulate *wzz* expression in *P. aeruginosa*.

It is postulated that nonmucoid, mucoid, and nonmucoid revertant *P. aeruginosa* strains co-exist during infection (199). In a recent study, 54% of nonmucoid CF isolates from 40 patients contained *mucA* mutations (149). Half of these also contained *algT* mutations leading the authors to classify these strains as nonmucoid revertants. Surprisingly, the CFBRPA32 nonmucoid revertants and the PDO300 nonmucoid revertant we isolated each had an in-frame duplication of basepairs 127-135. Cacador et al. also described a 9 basepair insertion in this region. Sequence alignment of AlgT to *Escherichia coli* RpoE by Sautter et al., who also described mutations in this area, predict that this region is involved in promoter melting (121). Mutations here may represent a hot spot for *algT* mutations that result in nonmucoid reversion.

Altogether, it appears that coordinating the overproduction of alginate with decreased Wzz2 and thereby very long O antigen is an important first step involved in establishing the chronic phenotype and may represent an intermediate phenotype between the transition from a

nonmucoid LPS-smooth isolates to a mucoid LPS-rough isolate. Importantly, we have shown that different serotypes regulate very long O antigen through down regulation of Wzz2 (Fig. S3.1) and that independent clinical isolates also down regulate Wzz2 (Fig. 3.1B, Fig. 3.4A, and Fig. 3.7B). Translating this across laboratory strains and CF isolates strengthens the relevance of our findings. Unlike *wzz1*, which is serotype specific and located at the beginning of the O antigen biosynthesis operon, *wzz2* is highly conserved among *P. aeruginosa* strains so having a regulatory circuit maintained within strains is not unexpected.

In support of this, nonmucoid strains of *P. aeruginosa* begin to express alginate during initial colonization of the lung (200), implying that *wzz2* and very long O antigen are also likely being repressed at this time. Loss of O antigen regulation was also observed for LPS-rough mucoid CF isolate 2192 (136). When the mutation responsible for the LPS-rough phenotype was identified and complemented back *in trans*, 2192 produced low molecular weight O antigen, but not high molecular weight O antigen. This provides evidence that even mucoid LPS-smooth strains from CF still do not make very long O antigen. Still, these strains are usually LPS-rough so why repress Wzz2? The benefit of regulating only Wzz2 and very long O antigen upon mucoid conversion, when the LPS-rough phenotype is ultimately selected, remains unexplained.

A long-term chronic *P. aeruginosa* infection model has not been established, but will be crucial to determine the benefits of the co-regulation of alginate and very long O antigen as well as the intermediate steps involved in the establishment of an LPS-rough phenotype. Understanding the coordinated regulation between the mucoid phenotype and O antigen expression will elucidate mechanisms that are selected for during the establishment of a long-term infection. Interfering with the expression of chronic infection phenotypes and subsequent adaption of *P. aeruginosa* to the CF lung could provide a better outcome for people with CF.

MATERIALS AND METHODS

Bacterial strains and culture conditions. *Escherichia coli* DH5α and SM10 were maintained on lysogeny broth (LB, Teknova) plates or in broth with or without 10 μg/ml tetracycline, 15 μg/ml gentamycin, 100 μg/ml carbenicillin, or 30 μg/ml kanamycin, as appropriate. *P. aeruginosa* strains were grown in LB medium or Vogel-Bonner minimal medium (VBMM) (201) supplemented with 100 μg/ml tetracycline, 60 μg/ml gentamycin, or 300 μg/ml carbenicillin, where necessary. For allelic exchange, 15% sucrose was used in no salt LB plates (10 g/l tryptone and 5 g/l yeast extract). All plates were supplemented with 1.5% agar (Apex). Strains were grown at 37°C and all conjugations were performed at 30°C as previously reported (178). Plasmids were transformed into electrocompetent PAO1 and PDO300, as previously described (177, 202). A complete list of strains and plasmids is available in Table S3.2 and a complete list of primers is available in Table S3.3. A detailed description of the construction of plasmids can be found in Text S2.1 in supplemental material.

Mucoid to nonmucoid reversion. CFBRPA32 and CFBRPA43 nonmucoid revertants were isolated as previously described (188). Passaging PDO300 in LB, without shaking, daily for 5 days isolated PDO300 nonmucoid revertant PDO300nmr1. Single colony PCR using primers oAC221/oAC222 was used to amplify *algT*, which was then column purified (Qiagen Miniprep Kit) and sent to Genewiz for sequencing to identify *algT* mutations.

Construction of PAO1 *mucA22 amrZ::*Tn and PA14 *mucA22*. pEXG2-*mucA22* was transformed into chemically competent SM10 and then mated with PA14 or the PAO1 *amrZ*::Tn transposon mutant (163, 164) in a 3:1 ratio, following the puddle-mating protocol described by

Hmelo et. al (178). After patching, single colony PCR using primers oAC089/oAC090 was used to amplify *mucA* from gentamicin sensitive colonies. PCR purified products were then sent to Genewiz for sequencing and verification that the *mucA22* allele had inserted into the strain.

Sample preparation and western blot analysis. Exponential phase bacterial cultures were normalized to an OD_{600} of 0.5 in 1 ml and centrifuged at 12,000 x g for 2 minutes. The cell pellet was resuspended in 50 µl of lysis solution (20 mM Tris, 1 mM EDTA, 10 mM $MgCl_2$, 10 µg/mL DNase, 10 µg/mL RNase, and 1X GoldBio ProBlock Protease Inhibitor) and incubated at 37°C for 15 minutes. 50 µl of 2X Laemmli Buffer (BioRad) was added, and the reaction was boiled for 5 minutes, LPS was prepared as previously reported (203), but without organic extraction by stopping after the proteinase K treatment. Proteins and LPS were separated by SDS-PAGE and transferred to a polyvinylidene difluoride membrane (PVDF, Bio-Rad). The membranes were blocked in PBS-T containing 5% instant nonfat dry milk (Publix) and probed using specific polyclonal antibodies. Detailed sample preparation and western blot analysis can be found in Text S1 in supplemental material.

qRT-PCR. Quantitative reverse transcriptase PCR (qRT-PCR) was performed as previously described (119) with modifications described in Text S2.1 in supplemental material.

β-galactosidase assay. Reporter assays were performed as described previously by Miller (176) with modifications (204).

Alginate isolation and quantification. Alginate was purified and quantified as described

previously (175) with modifications described in Text S2.1 in supplemental material.

Statistical analysis. Data were analyzed using GraphPad Prism Software (version 6). Experiments were compared using one-way analysis of variance (ANOVA) with Tukey's multiple comparisons analysis or two-way ANOVA with Sidak's multiple comparisons analysis. All data represent biological triplicate data with technical replicates. Graphs show mean values and error bars represent standard deviation (SD). *, $P<0.05$; **, $P<0.01$; ***, $P<0.001$; ****, $P<0.0001$.

SUPPLEMENTAL TEXT S3.1

Plasmid Construction. To generate pHERD20T-*wzz2*, the *wzz2* coding region was amplified using oAC017/oAC018 and the PCR product, along with pHERD20T, were digested using NcoI and HindIII (New England BioLabs). The *wzz2* fragment and digested pHERD20T were gel purified, ligated (New England BioLabs) in a 2:1 ratio, and the reaction was then transformed via heat-shock into chemically competent DH5α (Invitrogen) and selected for resistance on carbenicillin. Plasmids were PCR verified using oAC039/oAC040 and sequence confirmed.

Construction of miniCTX1-P_{wzz2}-optRBS-*lacZ* was accomplished by amplifying *lacZ* from miniCTX-*lacZ* using oJM524, which containing an consensus ribosome-binding site (taaggagg) (204), and oJM456. This PCR product, along with miniCTX1, was cut with PstI-HindIII (New England BioLabs) and ligated together to generate miniCTX1-optRBS-*lacZ*. Next, 500 bps of the upstream *wzz2* promoter region was amplified using oAC053/oAC054 and inserted into HindIII digest miniCTX1-optRBS-*lacZ* using isothermal assembly (Gibson Assembly Master Mix, New England BioLabs) following the manufacturers protocol. The

reactions were transformed into chemically competent DH5α and selected for on the appropriate antibiotic. Plasmids were extracted from isolated colonies, PCR verified using oAC032/oAC033, and sequence verified. miniCTX1-P_{wzz2}-optRBS-*lacZ* was electroporated into electrocompetent PAO1, PDO300, PDO300nmr1, and PAO1 *mucA22 amrZ*::Tn as previously described (177, 202) to generate PAO1 attCTX::P_{wzz2}-optRBS-*lacZ*, PDO300 attCTX::P_{wzz2}-optRBS-*lacZ*, PDO300nmr1 attCTX::P_{wzz2}-optRBS-*lacZ*, and PAO1 *mucA22 amrZ*::Tn attCTX::P_{wzz2}-optRBS-*lacZ.* Insertions at the CTX site were verified using oAC056/oAC057.

In order to generate the inducible constructs miniTn*7*T-lacIq-Ptac-*amrZ* and miniTn*7*T-lacIq-Ptac-*algT* we amplified the coding sequence of *amrZ*, using oAC137/oAC138, or *algT,* using oA221C/oAC222*,* from PAO1 using PCR. The amplified sequence was then inserted into HindIII digest miniTn*7*T-Gm-lacIq-P_{tac} using isothermal assembly (Gibson Assembly Master Mix, New England BioLabs) following the manufacturers protocol. All reactions were transformed into chemically competent DH5α and selected for on the appropriate antibiotic. Plasmids were extracted from isolated colonies, PCR verified using oAC148/oAC149, and sequence verified. miniTn*7*T-lacIq-Ptac-*amrZ* was electroporated into electrocompetent PAO1 attCTX::P_{wzz2}-optRBS-*lacZ,* PDO300 attCTX::P_{wzz2}-optRBS-*lacZ*, and PAO1 *mucA22 amrZ*::Tn attCTX::P_{wzz2}-optRBS-*lacZ* as previously described (177, 202) to generate PAO1 attCTX::P_{wzz2}-optRBS-*lacZ* attTn*7*::lacIq-Ptac-*amrZ,* PDO300 attCTX::P_{wzz2}-optRBS-*lacZ* attTn*7*::lacIq-Ptac-*amrZ*, and PAO1 *mucA22 amrZ*::Tn attCTX::P_{wzz2}-optRBS-*lacZ* attTn*7*::lacIq-Ptac-*amrZ.* miniTn*7*T-lacIq-Ptac-*algT* was electroporated into electrocompetent PAO1 attCTX::P_{wzz2}-optRBS-*lacZ* and PDO300nmr1 attCTX::P_{wzz2}-optRBS-*lacZ* to generate PAO1 attCTX::P_{wzz2}-optRBS-*lacZ* attTn7::lacIq-Ptac-*algT,* and PDO300nmr1 attCTX::P_{wzz2}-optRBS-*lacZ*

attTn7::lacIq-Ptac-*algT*. 500 ng of pTNS3 helper plasmid was also included when transforming miniTn*7*T vectors. Insertions at the Tn*7* site were verified using oAC129/oAC130.

To generate pEXG2-*mucA22* the *mucA22* allele was PCR amplified from PDO300 using oAC089/oAC090 and inserted into HindIII digest pEXG2 using isothermal assembly (Gibson Assembly Master Mix, New England BioLabs) following the manufacturers protocol. The reactions were transformed into chemically competent DH5α and selected for on the appropriate antibiotic. Plasmids were extracted from isolated colonies, PCR verified using primers oAC091/oAC092, and sequence verified.

To overexpress *wzz2* in order to generate polyclonal antibody the *wzz2* coding region from nucleotides 150-1173 (to exclude transmembrane sequences in the first and last 150 bps of the gene) was PCR amplified from *P. aeruginosa* strain PA103 using primers oJM483/oJM484 and cloned into pET28a digested with NdeI-XhoI (New England BioLabs) by isothermal assembly to construct pET28a-his6-*wzz2deltaTMS*. The Wzz2 N-terminus contains a 6X His-tag.

Generation of Wzz2 polyclonal antibodies. *E. coli* BL21(DE3) containing pET28a-his6-*wzz2deltaTMS* was induced with 0.2 mM IPTG at 16°C overnight in a 2.8 L Fernbach flask containing 1 L LB containing kanamycin. Cells were then lysed using a French press and protein was purified first by a nickel column and then by size exclusion (HiLoad16/60 Superdex200 FPLC). Purified Wzz2 was sent to and used by Covance (Princeton, NJ) to generate polyclonal antibodies in White New Zealand Rabbits.

Western blot analysis. Protein and LPS samples were thawed at room temperature, boiled for 5 minutes, and then cooled to room temperature. Proteins were separated by 10% SDS-PAGE and

LPS was separated by 12% SDS-PAGE (Bio-Rad). Both were transferred to a polyvinylidene difluoride membrane (PVDF, Bio-Rad). The membranes were blocked in PBS-T containing 5% instant nonfat dry milk (Publix) and probed using specific polyclonal antibodies for O5 serotype antigen (1:2,500, Denka Seiken Co. Ltd. Group B), O10 serotype antigen (1:5,000 Denka Seiken Co. Ltd. Group H) Wzz2 (1:10,000), or a monoclonal antibody for EF-Tu (1:10,000, LS Bio) followed by a 1:10,000 dilution of horseradish peroxidase-conjugated anti-rabbit IgG (O5 antigen, O10 antigen, and Wzz2) or anti-mouse IgG (EF-Tu) immunoglobulin antibody (Sigma-Aldrich). Detection was performed using Pierce ECL Western Blotting Substrate (following manufacturer's instructions) and chemiluminescence detection. Images were obtained using a ChemiDoc Imaging System (Bio-Rad) and densitometry analyzed was performed using Image Lab volume 5.2.1 software (Bio-Rad) relative quantity tool.

qRT-PCR. 500 µl of exponential phase culture was added to 1 ml of RNA Protect (Qiagen), incubated at room temperature for 5 minutes, and then centrifuged at 5,000 x g for 10 minutes. Pellets were air-dried and stored at -80°C. Total RNA was extracted using the MasterPure RNA Purification Kit (Epicentre) following the manufacturers protocol and 10 µg of total RNA was converted into cDNA using the SuperScript III First-Strand Synthesis System Kit (Invitrogen) following the manufacturer's instructions. Random hexamers were used to convert 1 µg of RNA to cDNA. Finally, cDNA was used to perform qPCR using *wzz2* specific primers oAC001/oAC002 and Fast Start Universal SybrGreen Master Mix (Roche) for detection. The amount of *wzz2* expressed was quantified based on cycle threshold (C_T) and primer efficiencies were determined using a standard curve of purified genomic DNA. All samples were then normalized to the housekeeping gene *rpoD* that was detected using oAC003/oAC004.

Alginate isolation and quantification. Single colonies were used to inoculate 3 ml LB and allowed to grow, rolling at 37°C, until turbid. This culture was back-diluted to an OD_{600} of 0.01 into 20 ml LB and allowed to grow overnight at 37°C, shaking. 10 ml of overnight culture was combined with 10 ml of 0.85% sodium chloride (Sigma) in a 50 ml conical tube, vortexed, and centrifuged at 12,000 x g for 30 minutes to remove cell material. The supernatant was transferred to a clean 50 ml conical tube and combined with 20 ml of 2% cetyl pyridinium (ACROS Organics), inverted 10 times to precipitate the alginate, and then centrifuged for at 12,000 x g for 10 minutes. The supernatant was carefully poured off of the pellet and discarded. The alginate pellet was resuspended in 10 ml of 1 M sodium chloride, vortexed thoroughly, a pipet was used to break up the pellet, and then incubated at room temperature for 30 minutes to ensure pellet had gone into solution. 10 ml of isopropanol (Fisher Scientific) was added to the solution, inverted 10 times to reprecipitate the alginate, vortexed thoroughly, and then the solution was centrifuged again at 12,000 x g for 10 minutes. The supernatant was carefully poured off of the clear alginate pellet and a pipet was used to remove any residual isopropanol. Finally, the alginate pellet was resuspended in 10 ml 0.85% sodium chloride and a pipet was used to break up the pellet. Final suspension was incubated at 4°C overnight.

Alginate was quantified by heating at 55°C in a borate-carbazole solution. All values were compared to a standard curve generated by diluting laboratory grade alginic acid (Sigma) in 0.85% sodium chloride to concentrations of 100-900 µg/ml. Briefly, 6 µl of purified alginate or standard was added to 200 µl of 0.1 M H_3BO_3 reagent (created by adding 5 ml of 2 M BO_3^{-3} added to 95 ml of ACS- grade H_2SO_4). The 2 M BO_3^{-3} stock was created by adding 24.74g H_3BO_3 to 45 ml 4 M KOH, with heat, and then diluted to 200 ml in water. Next, 6 µl of 0.1%

carbazole reagent (Sigma) was added and this solution was incubated at 55°C for 30 minutes in a water bath to allow for sufficient purple color to develop. After incubation, the solution was mixed and transferred to a 96-well plate. Absorbance was measured at 530 nm in a BioTek Synergy H1M plate reader and values were compared to the standard curve generated.

ACKNOWLEDGEMENTS

We would like to thank Dr. Jeffrey Meisner for purification of Wzz2 and construction of miniCTX-optRBS-*lacZ* and Dr. Dominique Limoli for the isolation of CFBRPA32 and CFBRPA43 nonmucoid revertants. Clinical isolates were obtained from the Cystic Fibrosis Biospecimen Registry (CFBR), which is maintained by Emory University and the Children's Healthcare of Atlanta Center for Cystic Fibrosis and Airways Disease Research (CF-AIR).

This work was partially supported by a predoctoral fellowship to A.R.C. from the Cystic Fibrosis Foundation (CFF) funded CF@LANTA RDP Center (MCCART15R0), CF-AIR, components of the Emory+Children's CF Center of Excellence at Emory University, and Children's Healthcare of Atlanta. The National Institute of Allergy And Infectious Diseases (NIAID) of the National Institutes of Health (NIH) under award number F31AI136310 also supported A.R.C. Additional funding was awarded by the NIH and the CFF to J.B.G. under award numbers R21AI122192 and GOLDBE16G0, respectively. The content of this manuscript is solely the responsibility of the authors and does not necessarily represent the official views of the NIH. The funders had no role in study design, data collection and interpretation, or the decision to submit the work for publication.

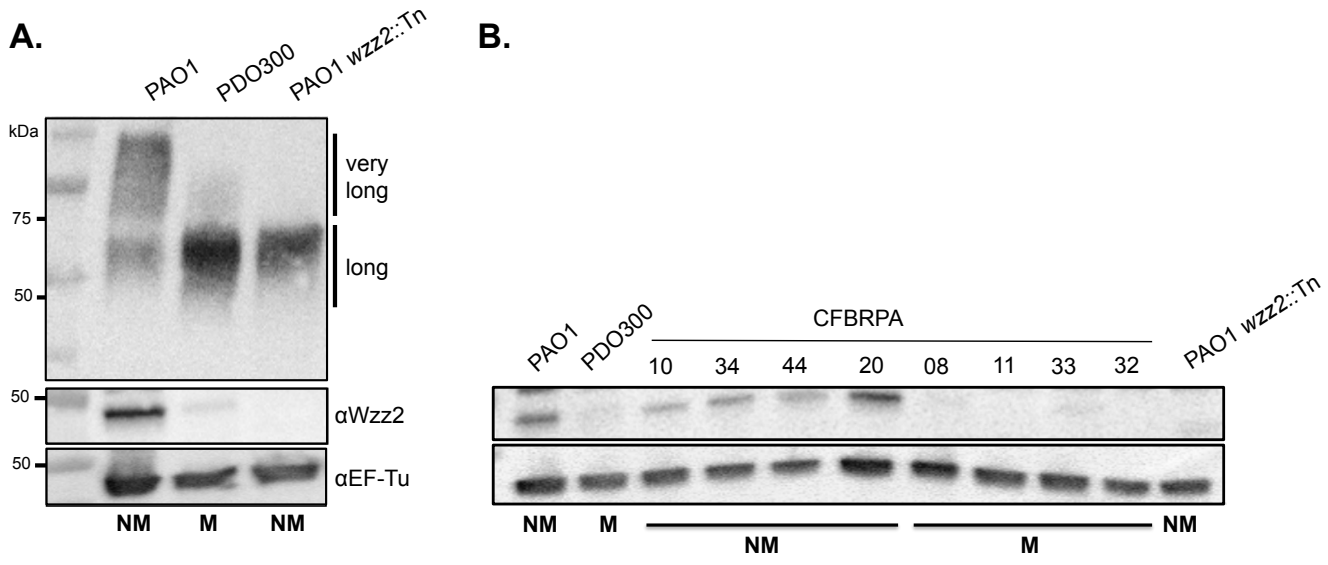

Figure 3.1. Mucoid strains produce less Wzz2 compared to nonmucoid strains resulting in less very long O antigen. A) Analysis of protein and LPS extracts from nonmucoid and mucoid strains by western blot. Wzz2 or EF-Tu (loading control) was visualized using αWzz2 or αEF-Tu antibodies. Serotype O5 specific antibodies were used to visualize O antigen production. PAO1 *wzz2*::Tn is a transposon mutant from the PAO1 library (163, 164) and is used as a control for no Wzz2 or very long O antigen production. B) CF isolates CFBRPA10, 34, 44, and 20 are nonmucoid while CF isolates CFBRPA08, 11, 33, and 32 are mucoid. These isolates were obtained from the Emory-Children's Healthcare Cystic Fibrosis Biospecimen Registry (CFBR). All western blots are representative of three or more independent experiments. Key: NM, nonmucoid; M, mucoid; Tn, transposon.

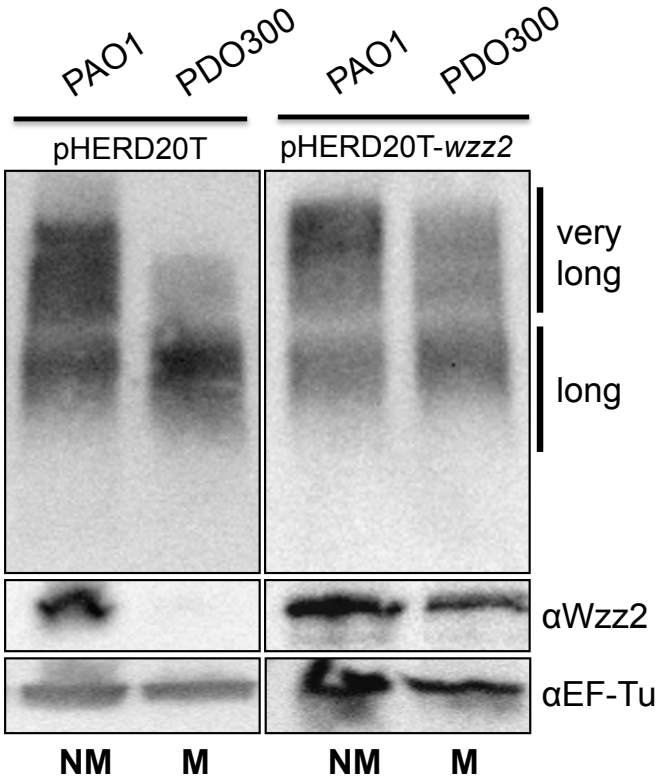

Figure 3.2. Overexpression of *wzz2* in PDO300 increases very long O antigen production. O antigen and Wzz2 production of strain overexpressing *wzz2* on pHERD20T (right) compared to vector only control (left). All strains were grown in 0.4% L-arabinose inducer. Western blot was performed as described in Figure 3.1. Key: NM, nonmucoid; M, mucoid.

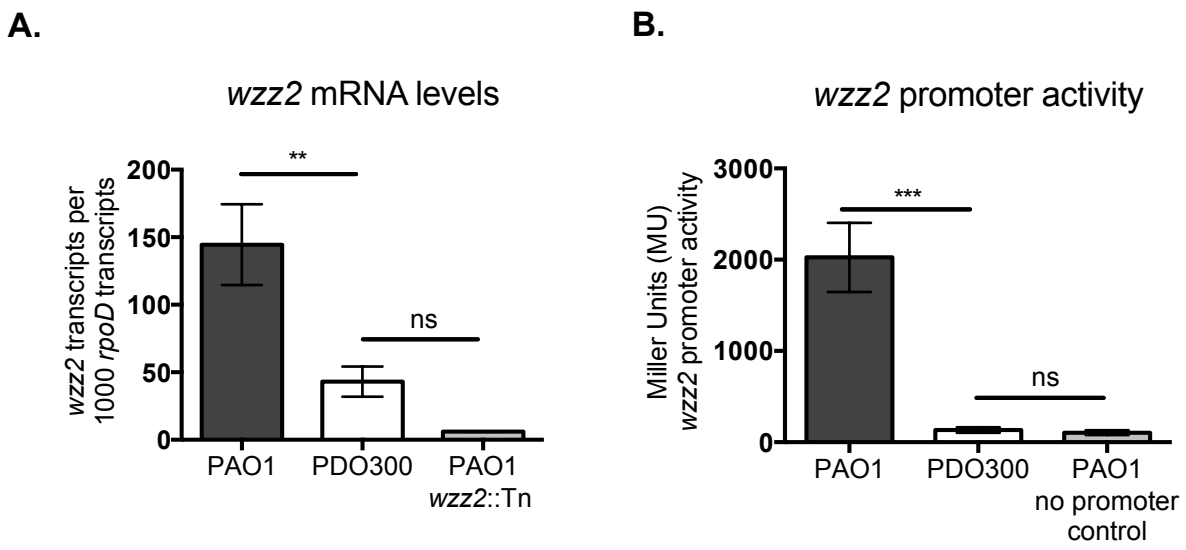

Figure 3.3. The *wzz2* steady-state mRNA levels and promoter activity are repressed in PDO300. A) qRT-PCR to examine mRNA expression in PAO1 compared to PDO300. qPCR was performed using primers specific to *wzz2* and normalized to the housekeeping gene *rpoD*, which is known to be stably expressed (162). The PAO1 *wzz2* transposon mutant (PAO1 *wzz2*::Tn) was used as a negative control. B) The *wzz2* was fused to a promoterless-*lacZ* containing an optimized ribosome-binding site (RBS) to make a transcriptional fusion. This fusion was used to measure *wzz2* promoter activity in each strain using β-galactosidase assays. Significance for each experiment was determined using one-way ANOVA with Tukey's multiple comparisons analysis. Error bars represent SD of three biological replicates with technical triplicates. **P<0.01; ***P<0.001; ns, not significant.

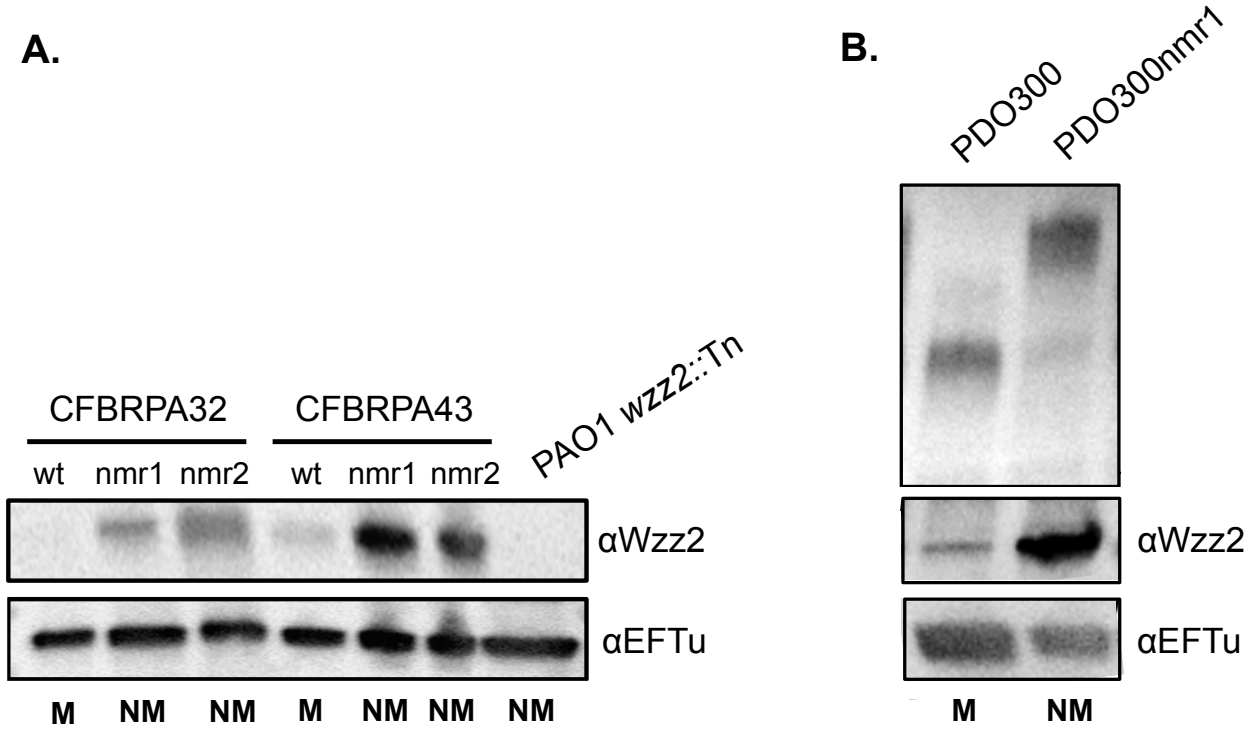

Figure 3.4. Nonmucoid isolates of mucoid strains express more Wzz2 and very long O antigen. A) Nonmucoid revertants of mucoid CF isolates were isolated by daily passage in the laboratory. B) PDO300nmr1 is a nonmucoid revertant of PDO300. Western blot was performed as described in Figure 3.1. Key: NM, nonmucoid; M, mucoid.

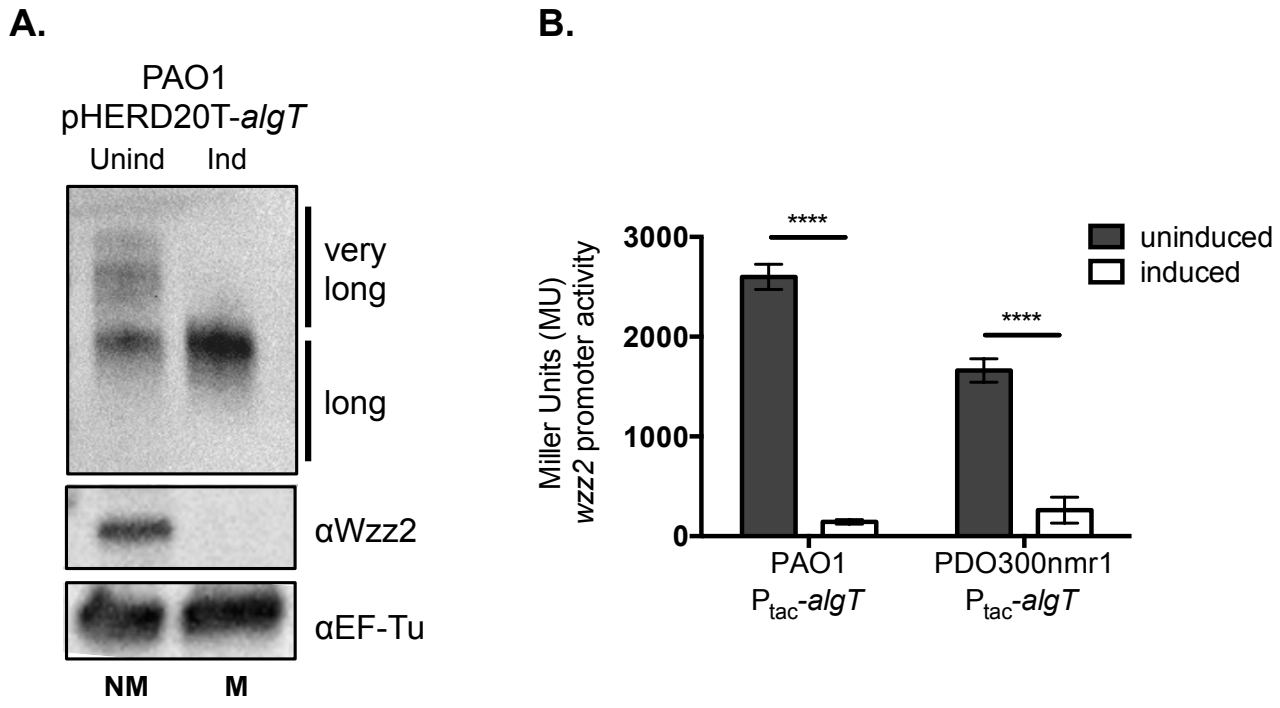

Figure 3.5. Overexpression of *algT* results in less very long O antigen and decreased *wzz2* promoter activity. A) Wzz2 and O antigen where monitored when *algT* was overexpressed using pHERD20T. Uninduced (Unind) expression indicates growth without inducer and induced (Ind) indicates growth in 0.4% L-arabinose. Western blot was performed as described in Figure 3.1. Key: NM, nonmucoid; M, mucoid. B) *wzz2* promoter activity was monitored when *algT* was uninduced or induced using 1 mM IPTG. β-galactosidase assays were performed as described in Figure 3.3B. Error bars represent SD of three biological replicates with technical triplicates. Significance was determined using two-way ANOVA with Sidak's multiple comparisons analysis. ****P<0.0001.

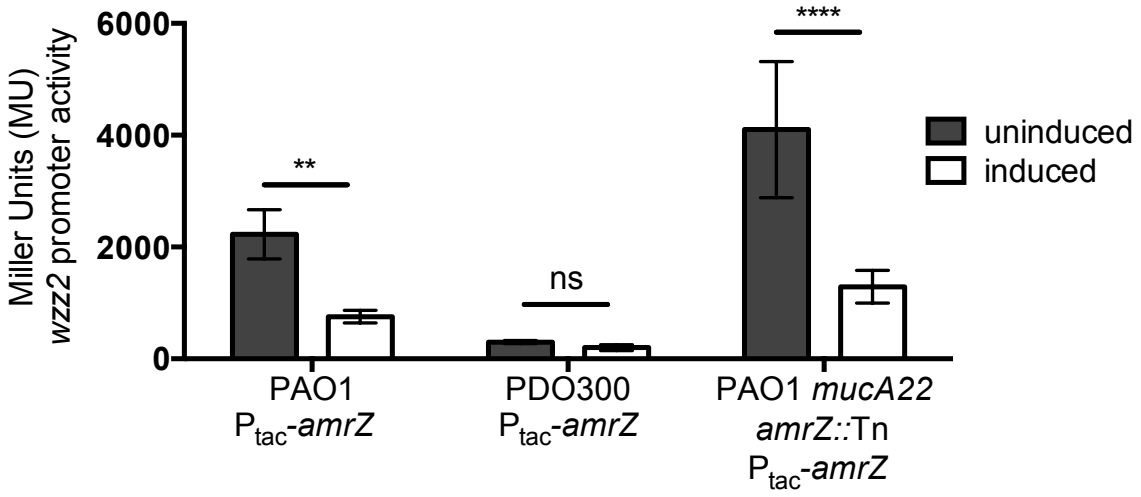

Figure 3.6. Overexpression of *amrZ* represses *wzz2* promoter activity. *wzz2* promoter activity was monitored when *amrZ* expression was uninduced or induced using 1 mM IPTG. β-galactosidase assays were performed as described in Figure 3.3B. The *mucA22* allele was inserted into PAO1 *amrZ*::Tn, a transposon mutant from the PAO1 library (163, 164), to generate PAO1 *mucA22 amrZ*::Tn. Error bars represent SD of three biological replicates with technical triplicates. Significance was determined using two-way ANOVA with Sidak's multiple comparisons analysis. **P<0.01, ****P<0.0001, ns; not significant.

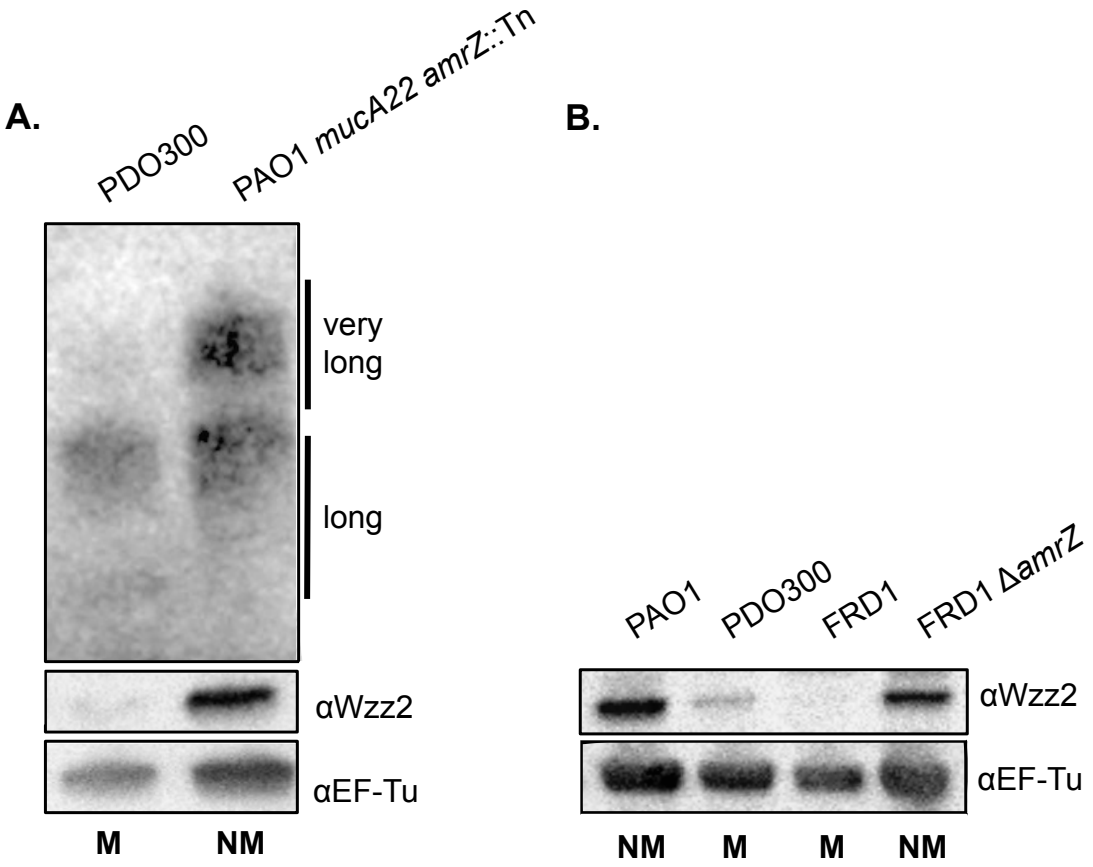

Figure 3.7. Disruption of *amrZ* restores Wzz2 production in mucoid strains. A) Wzz2 and very long O antigen were monitored when *amrZ* was disrupted. B) Mucoid LPS-rough clinical isolate FRD1 was originally isolated from a person with CF (43) and nonmucoid FRD1 Δ*amrZ* contains a clean deletion of *amrZ* (193). Western blot was performed as described in Figure 3.1. Key: NM, nonmucoid; M, mucoid.

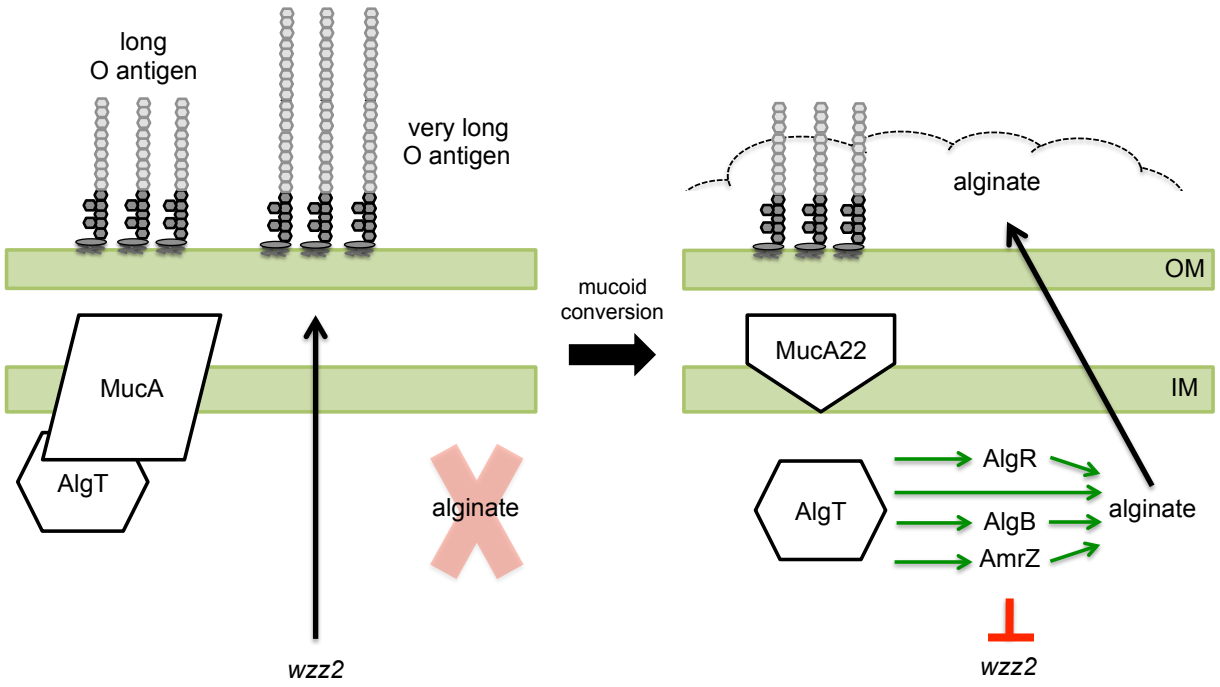

Figure 3.8. Model for the inverse regulation of alginate and very long O antigen in mucoid *P. aeruginosa*. Left: In LPS-smooth nonmucoid *P. aeruginosa*, wildtype MucA sequesters the sigma-factor AlgT rendering it inactive. When AlgT is inactive, the AlgT regulon, including AmrZ and the alginate operon, are not transcribed. Therefore, *wzz2* and very long O antigen are expressed. Right**:** When MucA acquires mutations, such as *mucA22*, AlgT is free to transcribe genes of its regulon. AmrZ now represses *wzz2* resulting in loss of very long O antigen production. Key: IM; inner membrane, OM; outer membrane.

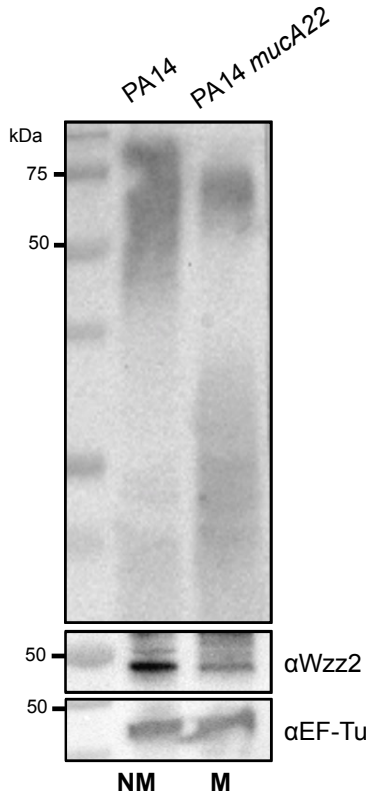

Figure S3.1. Mucoid PA14 has reduced levels of Wzz2 and fewer very long O antigen chain-lengths compared to nonmucoid PA14. Analysis of Wzz2 and serotype O10 antigen production. Samples were prepared and western blot was performed as described in Figure 3.1. Key: NM, nonmucoid; M, mucoid.

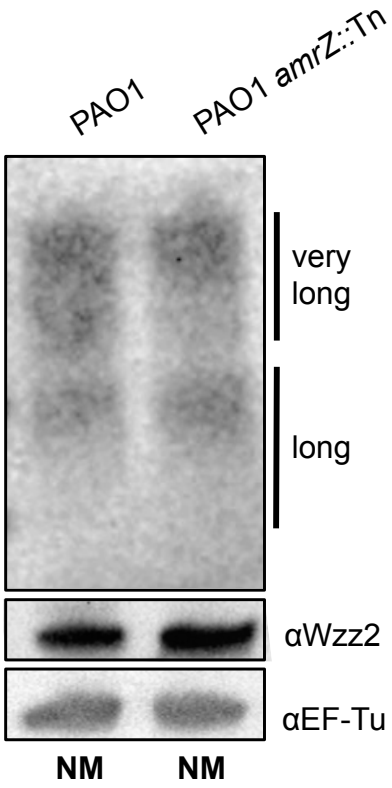

Figure S3.2. Disruption of *amrZ* in PAO1 does not alter Wzz2 or O antigen production. Wzz2 and serotype O5 antigen were monitored in each strain. PAO1 *amrZ*::Tn is a transposon mutant from the PAO1 library (163, 164). Samples were prepared and western blot was performed as described in Figure 3.1. Key: NM, nonmucoid; M, mucoid.

Table 3.1. Alginate produced by strains overexpressing *wzz2*.

Strain	Inducer (0.4% L-arabinose)	Alginate (µg/ml)	SD[a]	Fold Change
PDO300	-	615.89	75.94	
	+	610.50	126.59	0.99
PDO300 pHERD20T	-	706.99	142.33	
	+	555.00	210.39	0.79
PDO300 pHERD20T-*wzz2*	-	570.52	213.50	
	+	503.03	181.18	0.88

[a]Standard Deviation

Table 3.2. Alginate produced by strains overexpressing *amrZ*.

Strain	Inducer (1mM IPTG)	Alginate (µg/ml)	SD[a]	Fold Change
PAO1 P_{tac}-*amrZ*	-	BD[b]		
	+	BD[b]		
PDO300 P_{tac}-*amrZ*	-	184.75	23.10	
	+	187.28	37.76	1.01
PAO1 *mucA22 amrZ*::Tn P_{tac}-*amrZ*	-	1.07	4.40	
	+	52.17	1.47	48.76

[a]Standard Deviation
[b]Below Detection

Table S3.1. Alginate produced by strains overexpressing *algT*

Strain	Inducer (1mM IPTG)	Alginate (µg/ml)	SD[a]	Fold Change
PDO300nmr1 P_{tac}-*algT*	-	29.48	19.02	
	+	26.52	21.40	0.90
PAO1 P_{tac}-*algT*	-	6.80	5.12	
	+	1101.15	76.90	161.85

[a]Standard Deviation

Table S3.2. Strains and plasmids used in this study.

Bacterial Strain or Plasmid	Description	Location	Reference
E. coli			
DH5α	plasmid maintenance		Invitrogen
BL21(DE3)	protein expression and purification		Invitrogen
SM10	bi-parental mating		Simon R et al. 1983
P. aeruginosa			
PAO1	nonmucoid laboratory strain, serotype O5		Hancock REW and Carey AM. 1979
PAO1 *wzz2*::Tn	PAO1 transposon mutant PW2707	PAC03	Held K et al. 2012; Jacobs MA et al. 2003
PAO1 *amrZ*::Tn	PAO1 transposon mutant PW6710	PAC04	Held K et al. 2012; Jacobs MA et al. 2003
PDO300	mucoid PAO1 containing *mucA22* allelle	PAC01	Mathee K et al. 1999
PDO300nmr1	nonmucoid revertant of PDO300, *algT* 127-135 duplication	PAC273	This study
PAO1 *mucA22 amrZ*::Tn	PAO1 transposon mutant PW6710 with *mucA22* allele	PAC33	This study
PA14	nonmucoid laboratory strain, serotype O10	PAC40	Rahme LG et al. 1995
PA14 *mucA22*	mucoid PA14 containing *mucA22* allelle	PAC431	This study
Clinical P. aeruginosa isolates			
CFBRPA10	cystic fibrosis nonmucoid clinical isolate	CFBR	This study
CFBRPA34	cystic fibrosis nonmucoid clinical isolate	CFBR	This study
CFBRPA44	cystic fibrosis nonmucoid clinical isolate	CFBR	This study
CFBRPA20	cystic fibrosis nonmucoid clinical isolate	CFBR	This study
CFBRPA08	cystic fibrosis nonmucoid clinical isolate	CFBR	This study
CFBRPA11	cystic fibrosis mucoid clinical isolate	CFBR	This study
CFBRPA33	cystic fibrosis mucoid clinical isolate	CFBR	This study
CFBRPA32	cystic fibrosis mucoid clinical isolate	PAC420	This study
CFBRPA32nmr1	nonmucoid revertant of CFBRPA32, *algT* 127-135 duplication	PAC421	This study
CFBRPA32nmr2	nonmucoid revertant of CFBRPA32, *algT* 127-135 duplication	PAC422	This study
CFBRPA43	cystic fibrosis mucoid clinical isolate	PAC423	Limoli DH et al. 2017
CFBRPA43nmr1	nonmucoid revertant of CFBRPA43, mutations not in *algT*	PAC424	This study
CFBRPA43nmr2	nonmucoid revertant of CFBRPA43, *algT* C245A transversion	PAC425	This study
FRD1	mucoid clinical CF isolate	PAC08	Ohman DE & Chakrabarty AM, 1981
FRD1 Δ*amrZ*	FRD1 with *amrZ* deleted	PAC11	Ramsey DM et al. 2005.
Plasmids (alternative name)			
miniCTX1 (pARC34)	attCTX integration proficient	ECAC02	Hoang TT et al. 200
miniCTX1-lacZ (pARC07)	miniCTX1 containing promoterless-*lacZ* reporter	ECAC11	Becher A & Schweizer H. 2000
miniCTX1-optRBS-lacZ (pARC11)	miniCTX1 promoterless-*lacZ* reporter with optimized RBS	ECAC16	This study
miniCTX1-Pwzz2-optRBS-lacZ (pARC15)	contains -25 to -500 bp of *wzz2* promoter	ECAC13	This study
pEXG2 (pARC28)	allelelic exchange vector	ECAC42	Rietsch A et al. 2005
pEXG2-mucA22 (pARC29)	contains *mucA22* allele amplified from PDO300	ECAC52	This study
miniTn7T-Gm-laclq-Ptac (pARC22)	attTn*7* integration proficient, IPTG inducible	ECAC73	Meisner J & Goldberg JB. 2016
miniTn7T-Gm-laclq-Ptac-algT (pARC57)	contains coding region of *algT* for overexpression	ECAC141	This study
miniTn7T-Gm-laclq-Ptac-amrZ (pARC39)	contains coding region of *amrZ* for overexpression	ECAC88	This study
pET28a	protein expression vector	ECAC30	Addgene
pET28a-his6-wzz2deltaTMS (pJM137)	expression vector containing His-tagged *wzz2* (without TMS)	ECJM109	This study
pHERD20T (pARC06)	multicopy overexpression plasmid, arabinose inducible	ECAC09	Qiu D & Damron FH et al. 2008
pHERD20T-wzz2 (pARC05)	contains *wzz2* coding sequence for multicopy expression	ECAC10	This study
pHERD20T-algT (pARC19)	contains *algT* coding sequence for multicopy expression	ECAC25	Qiu D & Damron FH et al. 2008
pTNS3	transposase helper	ECAC03	Choi KH et al. 2008

Table S3.3. Primers used in this study.

Primer	Sequence	Description
oJM483	ctggtgccgcgcggcagccatatgACCTACCAGGTGGATGTCCTG	This study
oJM484	agtggtggtggtggtggtgctcaCTTGCGTGGCTTGATCGGTC	This study
oJM456	gcgaagcttTTATTTTTGACACCAGACCAACTG	This study
oJM524	cgcctgcag**taaggagg**AACAGCTATGACCATGATTACG	This study
oAC129	GCACATCGGCGACGTGCTCTC	Choi KH and Schweizer HP. 2006
oAC130	CACAGCATAACTGGACTGATTTC	Choi KH and Schweizer HP. 2006
oAC032	GACCCACTCTCAGGAGTGAAC	This study
oAC033	CTCTTCGCTATTACGCCAGCTG	This study
oAC053	AATCATGGTCATAGCTGTTCCTCCTTACTGCAGCCCGGGGtagcccacagatgcacgcaa	This study
oAC054	CTGGAGCTCCACCGCGGTGGCGGCCGCTCTAGAACTAGTGcgcgcagatcaagcaactta	This study
oAC056	GACGGCGGAGTTCAGCTGATAT	This study
oAC057	GTCTGCTGAATCAGGCGCTG	This study
oAC221	CACAGGAAACAGACTAGTGCTCTGCAGGAATTCCTCGAGAatgctaacccaggaacagga	This study
oAC222	TCTGGTTGGCCTGCAAGGCCTTCGCGAGGTACCGGGCCCAtcaggcttctcgcaacaaag	This study
oAC137	CACAGGAAACAGACTAGTGCTCTGCAGGAATTCCTCGAGAatgcgcccactgaaacaggc	This study
oAC138	TCTGGTTGGCCTGCAAGGCCTTCGCGAGGTACCGGGCCCAtcaggcctgggccagctccg	This study
oAC148	CGCACTCCCGTTCTGGATA	This study
oAC149	TGCTTCGGGGTCATTATAGCGA	This study
oAC089	TTCCACACATTATACGAGCCGGAAGCATAAATGTAAAGCAatgagtcgtgaagccctgca	This study
oAC090	CGAGCTCGAGCCCGGGGATCCTCTAGAGTCGACCTGCAGAtcagcggttttcaggctgg	This study
oAC091	CCACACATTATACGAGCCGGAAGC	This study
oAC092	GGTACCGAATTCGAGCTCGAGC	This study
oAC039	ATCGCAACTCTCTACTGTTTCT	Qiu D and Damron FH et al. 2008
oAC040	TGCAAGGCGATTAAGTTGGGT	Qiu D and Damron FH et al. 2008
oAC018	GCGCCATGGCCGCCTATCGAAAAGGACGTTGG	This study
oAC017	GCGAAGCTTTCAGGTCCCTGAAAGGCTCCGGTC	This study
oAC001	CAGGATATCGAAGGCAAGCG	This study
oAC002	GGATAGCCTCGTTGAGCTGC	This study
oAC003	GGGCGAAGAAGGAAATGGTC	Savli H, et al. 2003
oAC004	CAGGTGGCGTAGGTGGAGAA	Savli H, et al. 2003

lowercase nucleotides anneal to plasmid sequence during isothermal assembly
restriction sites are underlined
optimized ribosome binding site is in bold

Chapter 4

Overexpression of the AlgT sigma factor is lethal to mucoid *Pseudomonas aeruginosa*

Ashley R. Cross, Vishnu Raghuram, and Joanna B. Goldberg

unpublished data

ABSTRACT

Pseudomonas aeruginosa isolates from chronic lung infections often constitutively produce alginate, termed the mucoid phenotype. Isolation of mucoid strains correlates with a poor patient prognosis. The most common mutation that leads to the mucoid phenotype is called *mucA22* and results in a truncated form of the anti-sigma factor MucA. MucA22 does not contain a C-terminus and, as a result, is continuously subjected to proteolysis. When a functional MucA is absent, the cognate sigma factor AlgT is no longer sequestered and continuously transcribes the alginate biosynthesis operon leading to alginate overproduction. In this work, we report that in the absence of wild type MucA, overexpression of exogenous AlgT *in trans* is toxic. This is intriguing since mucoid strains endogenously possess very high levels of AlgT. Furthermore, we show that suppressors of toxic AlgT production have mutations in *mucP*, a protease involved in MucA degradation. Our findings support a model where mutations in *mucP* stabilize the truncated form of MucA22 rendering it partially functional. Functional MucA22 is therefore able to reduce AlgT toxicity by properly sequestering AlgT to the inner membrane.

INTRODUCTION

Alginate production by the opportunistic pathogen *Pseudomonas aeruginosa* results in a mucoid phenotype and correlates with the establishment of a chronic infection (42, 58, 61, 65, 148, 185). Production of alginate is highly regulated and is usually a response to external and internal membrane stressors (104, 107, 205). In nonmucoid strains, the anti-sigma factor MucA is inserted into the inner membrane where the cytosolic N-terminus interacts with the AlgT sigma factor (also called σ^{22} or AlgU). AlgT is the master regulator of alginate biosynthesis as well as about 300 other genes and phenotypes including pigment production, motility, and very long O antigen production (47, 48, 114, 169, 191, 194). When AlgT is sequestered by MucA, the alginate biosynthesis operon is not transcribed and these strains produce little to no alginate.

When AlgT is activated, however, alginate biosynthesis is triggered by a regulated intermembrane proteolysis (RIP) cascade that is activated by periplasmic proteases (96). First, activated AlgW cleaves the C-terminus of MucA releasing MucB. The truncated periplasmic portion of MucA is then made available for cleavage by AlgO and MucP (105, 106). This releases the N-terminus AlgT-bound fragment of MucA into the cytosol where it is finally completely degraded by the ClpPX proteasome. Once free of MucA, AlgT transcribes the global transcription factors AlgR, AlgB, and AmrZ (45, 101). All three regulators are needed, in combination with AlgT, to initiate transcription of the alginate biosynthesis operon.

AlgT itself is the first gene in an operon followed by *mucA, mucB, mucC*, and *mucD*. This operon is highly similar to the *rpoE, rseA, rseB,* and *rseC* operon in *Escherichia coli* (96, 97). Likewise, the proteins encoded by this operon are functionally similar to those in *P. aeruginosa*. AlgT and RpoE are 66% similar and functionally interchangeable, with RpoE capable of complementing *algT* null mutants of *P. aeruginosa* (206). AlgT is driven by five promoters with

two of these promoters themselves being AlgT-dependent (73, 98). Therefore, *algT* is positively autoregulated.

While nonmucoid strains are capable of producing and regulating alginate in certain environments, *P. aeruginosa* isolates from CF lung infections often constitutively produce alginate, termed the mucoid phenotype (36, 37, 42, 148, 149). The most common mutations that result in the mucoid phenotype are found in *mucA* (42, 120). The *mucA22* mutation, which is a deletion of a G in a string of 5 G's, is the most common clinical mutation observed and results in a truncated form of MucA that does not contain a C-terminus (51). As a result, MucA22 is continuously subjected to RIP, AlgT is always free, and the alginate biosynthesis operon is always expressed (76, 113). Since AlgT promotes transcription of its own promoter, mucoid strains have extremely high AlgT activity and no longer respond to membrane stresses in the same way as nonmucoid strains.

Despite the many discoveries surrounding the regulation of AlgT in nonmucoid strains, it is still unclear if mucoid strains are capable of regulating AlgT production in the absence of wild type MucA. Therefore, we sought to primarily study AlgT in the context of mucoid strain PDO300. In this work, we report that in the absence of wild type MucA the over production of exogenous AlgT is actually lethal. This is surprising since mucoid strains are thought to overproduce AlgT to very high levels. Further, we show that suppressors of toxic AlgT production have mutations in *mucP*, a protease involved in MucA degradation. Our findings support a model where mutations in *mucP* stabilize the MucA22-AlgT complex ultimately rendering MucA22 functional and capable of sequestering AlgT. Since it has been reported that deletion of *mucA* is lethal, we propose that this is likely due to deregulation of AlgT. Future experiments aim to determine through what mechanism overproduction of AlgT leads to cell death.

RESULTS AND DISCUSSION

Overproduction of *algT* is lethal in *mucA22* strains. To study the expression of AlgT in *P. aeruginosa*, we inserted an IPTG-inducible copy of *algT* (P_{tac}-*algT)* in single copy at an ectopic site in both PAO1 and PDO300. We then compared uninduced and induced expression of this second copy of *algT* on each strain. When grown on L agar containing no inducer, PAO1 is nonmucoid since *algT* expression is low (Fig. 4.1). PDO300 is mucoid because this strain inherently produces AlgT and therefore alginate (Fig. 4.1). When grown on increasing concentrations of IPTG to induce *algT* expression, PAO1 became mucoid, as expected. Surprisingly, at low concentration of IPTG the ectopic expression of *algT* inhibited growth of PDO300 with high levels of *algT* being entirely lethal. We were curious if alginate production played a role in the regulation of AlgT. We therefore deleted *algD*, the first gene in the alginate biosynthesis operon, in both PAO1 and PDO300 rendering both strains nonmucoid on all concentrations of inducer (Fig. 4.1A). PAO1 Δ*algD* still survived on high levels of inducer where *algT* expression was high while PDO300 Δ*algD* behaved similarly to PDO300 and did not grow on high concentrations of inducer (Fig. 4.1A). We also monitored growth of PAO1, PAO1 Δ*algD*, PDO300, and PDO300 Δ*algD* over time when grown in liquid broth culture. All strains grew to high density when no inducer was added and *algT* expression was uninduced (Fig. 4.1B, left). Conversely, when grown in the presence of inducer, PDO300 and PDO300 Δ*algD* grew slower and had a decreased growth rate compared to the PAO1 strains (Fig. 4.1B, right). Altogether, these data suggest that in mucoid strains, such as PDO300, tightly controlled expression of *algT* is essential for growth and that this is not dependent on *algD*.

Complementation with wild type *mucA* partially rescues *algT* lethality. Since the only difference between the PAO1 and PDO300 strains is the *mucA22* mutation, we

hypothesized that *algT* lethality is dependent on *mucA22*. To test this, wild ype *mucA* was overexpressed in trans, from an arabinose-inducible promoter, to determine if we could rescue PDO300 from the toxic effects of *algT* overexpression. On low levels of IPTG to express *algT* and on high levels of arabinose to express *mucA*, PDO300 became nonmucoid and, in support of our hypothesis, growth of PDO300 and PDO300 Δ*algD* was no longer inhibited by the ectopic expression of *algT* (Fig. 4.2). However, on higher levels of IPTG and therefore very high expression of *algT*, providing wildtype *mucA* in trans did not rescue growth of either strain (Fig. 4.2). This is likely because not enough MucA is being produced to sequester enough AlgT when maximally induced, even though it is enough to render the strain nonmucoid.

Identification of mutations that suppress *algT* lethality. Over the course of our experiments we observed PDO300 and PDO300 Δ*algD* colonies that were able to grow when *algT* was overexpressed. To determine if these were suppressors, we isolated four colonies from each strain, grew them overnight without inducer, and then plated on high levels of IPTG to produce toxic levels of AlgT. All eight colonies screened grew on IPTG and this growth was comparable to the uninduced controls (Fig. 4.3). Therefore, these strains are able to bypass the lethality caused by overexpression of *algT*. The most likely way to suppress *algT* toxicity would be to acquire mutations in one of the two copies of *algT*. To determine if this was the case, we sequenced both the native and Tn7 overexpression copies of *algT*. We found that two suppressors had mutations in the overexpression copy of *algT*. One had acquired a 9 bp duplication of nucleotides 136-144 (GAAGCCCAG) while the other had a C to T transition at nucleotide 400 that results in a stop codon.

To determine what mutations were acquired that allowed for survival when *algT* was overexpression in the other 6 mutants we chose to perform whole genome sequencing. We found

mutations in a number of hypothetical proteins, but of most interest to us were the SNPs found in the *mucA* protease *mucP* in 3 out of the 6 suppressors (Table 4.1). We also identified a number of alginate gene mutations that were unique to PDO300 Δ*algD* compared to PDO300 (Table 4.1). These were located upstream of *algD* in the promoter and in *alg8*, which is located just downstream of *algD*. While overexpression of *algT* is lethal to both PDO300 and PDO300 Δ*algD*, there is a difference that is dependent on strain background. We also identified PA1352 and PA4059 mutations in all of the suppressors (Table 4.1). Both are hypothetical proteins and it is not clear how mutations in these genes would suppress *algT* lethality. In *P. putida*, PA4059 is an ortholog of a type 12 methyltransferase while PA1352 is a major facilitator superfamily transporter.

Mutations identified in *mucP*. In our experiments, we found one *mucP* suppressor mutation in the PDO300 background, named PDO300 sup4, and two *mucP* suppressor mutations in the PDO300 Δ*algD* background, named PDO300 Δ*algD* sup1 and PDO300 Δ*algD* sup4 (Fig. 4.4). MucP is a protease that participates in the proteolytic cascade that degrades MucA (105, 106, 207). Delgado et al. analyzed the MucP sequence and found four possible transmembrane domains (amino acids 4-24, 97-122, 378-411, and 424-444) and one beta-loop domain (amino acids 55-72) (208). There also exists a metalloprotease zinc-binding motif (amino acids 21-25), two PDZ binding domains (amino acids 111-190 and 211-287), and a RIP motif (amino acids 401-403). PDO300 sup1 had an insertion of a "C" after nucleotide 355 leading to truncation of the protein after 122 amino acids. PDO300 Δ*algD* sup1 had a deletion of nucleotides 906-912, encoding "GGG GGC G", leading to truncation of the protein after 316 amino acids. Interesting, Delgado et al. found a similar 7 nucleotide MucP mutation due to a deletion of nucleotides 910-917 when looking for mutations that cause nonmucoid reversion (106). This region of the protein

contains a predicted unstructured periplasmic loop domain. Since we hypothesize that mutations here result in less available AlgT, it would make sense that these mutants would have decreased alginate production and be rendered nonmucoid. Lastly, PDO300 Δ*algD* sup4 had an in-frame deletion of nucleotides 1019-1033, encoding "TAA CGC TCG ACT CCA", leading to early truncation of the protein after 445 amino acids. This mutation is also located within the predicted unstructured periplasmic loop domain. Overall, each of these mutations we expect interferes with the ability of MucP to degrade MucA.

Complementation of *mucP* suppressor mutants restores sensitivity to *algT* overexpression. We hypothesize that mutations in *mucP* would stabilize the MucA-AlgT complex ultimately reducing AlgT activity. Multiple attempts at making clean deletions of *mucP* in PAO1 and PDO300 were unsuccessful and therefore we could not test the hypothesis that deletion of *mucP* from PDO300 or PDO300 Δ*algD* would allow for growth when *algT* is overexpressed. Therefore, we chose to overexpress *mucP* in suppressors that contain *mucP* mutations (PDO300 sup 4 and PDO300 Δ*algD* sup 1). We hypothesized that providing wild type MucP in trans would render the suppressors sensitive to the overproduction of AlgT. To test this, we cloned the *mucP* gene on a multicopy arabinose-inducible plasmid and inserted this into each of our strains. First, we confirmed that overexpression of *algT*, in the presence of this plasmid, was still lethal to PDO300 and PDO300 Δ*algD* and that both suppressors still grew to high densities when *algT* was overexpressed (Fig. 4.5). Overexpression of *mucP* by itself did not inhibit growth of any of the strains (Fig. 4.5). When *algT* and *mucP* are both overexpressed, however, growth of all strains was inhibited (Fig. 4.5). PDO300 and PDO300 Δ*algD* are likely dead due to overexpression of *algT.* The suppressors are now dead due to complementation of

the *mucP* suppressor mutations. Therefore, mutations in *mucP* are a mechanism to circumvent toxicity due to AlgT over expression.

MATERIALS AND METHODS

Bacterial strains and culture conditions. Bacteria were maintained on lysogeny agar (LA) containing 1.5% agar and grown in lysogeny broth (LB). When appropriate, media was supplemented with 10 µg/ml tetracycline, 15 µg/ml gentamycin, or 100 µg/ml carbenicillin for *Escherichia coli* and 100 µg/ml tetracycline, 60 µg/ml gentamycin, or 100 µg/ml carbenicillin for *Pseudomonas aeruginosa*. Vogel-Bonner minimal medium (VBMM) plates supplemented with gentamicin and no salt LB (10 g/l tryptone and 5 g/l yeast extract) containing 15% sucrose were used for allelic exchange (178). Strains were grown at 37°C. Conjugations and sucrose counterselections were performed at 30°C. A list of strains, plasmids, and primers used are available in Table 4.2. For serial dilutions, overnight cultures of each strain grown without inducer were normalized to an OD_{600} of 0.5 and 10-fold serially-diluted were plated.

Construction of PDO300 Δ*algD*. SM10 containing pEXG2-*mucA22* (48) was conjugated with PAO1 Δ*algD* following the puddle-mating protocol described by Hmelo et al. (178). After sucrose counterselection, single colonies were patched onto LA and LA containing gentamicin. Next, *mucA* was amplified, by single colony PCR, from gentamicin sensitive colonies using oAC089/oAC090 and sent to Genewiz for sequencing to identify colonies that contained the *mucA22* mutations.

Construction of pHERD20T-*mucP*. The *mucP* gene was amplified using oAC276/oAC277. This fragment was PCR purified (Qiagen) and ligated into HindIII digested gel-purified pHERD20T using isothermal assembly (Gibson Assembly Master Mix, New England BioLabs). Plasmids were miniprepped (Qiagen) from carbenicillin resistant colonies and screened for the

mucP insertion using oAC039/oAC040.

Generation of reporter strains, *algT* overexpression strains, *mucA* overexpression strains, and *mucP* overexpression strains. All plasmids were electroporated into *P. aeruginosa* strains as previously described (177). miniTn7-P_{tac}-*algT* (48) was selected for on gentamicin while pHERD20T-HA-*mucA* (97) and pHERD20T-*mucP* were selected for on carbenicillin.

Isolation of suppressors and whole genome sequencing and analysis. Overnight cultures of each suppressor strain grown without inducer were normalized to an OD_{600} of 0.5 and serially-diluted onto increasing concentrations of IPTG. Colonies that grew on high concentrations were considered suppressors of toxic *algT* expression. Genomic DNA was isolated using a DNeasy blood and tissue kit (Qiagen) and sent to the Microbial Genome Sequencing (MiGS) Center (migscenter.com). Genomes were quality trimmed using TrimGalore! v0.6.2 and reads having quality > 20 were assembled using SPAdes v3.13.1 (180, 209). Variant calling was performed using Snippy v4.4.0 (https://github.com/tseemann/snippy) using PAO1 as the reference genome (Assembly accession ASM676v1). Vishnu Raghuram assembled the whole genome sequences.

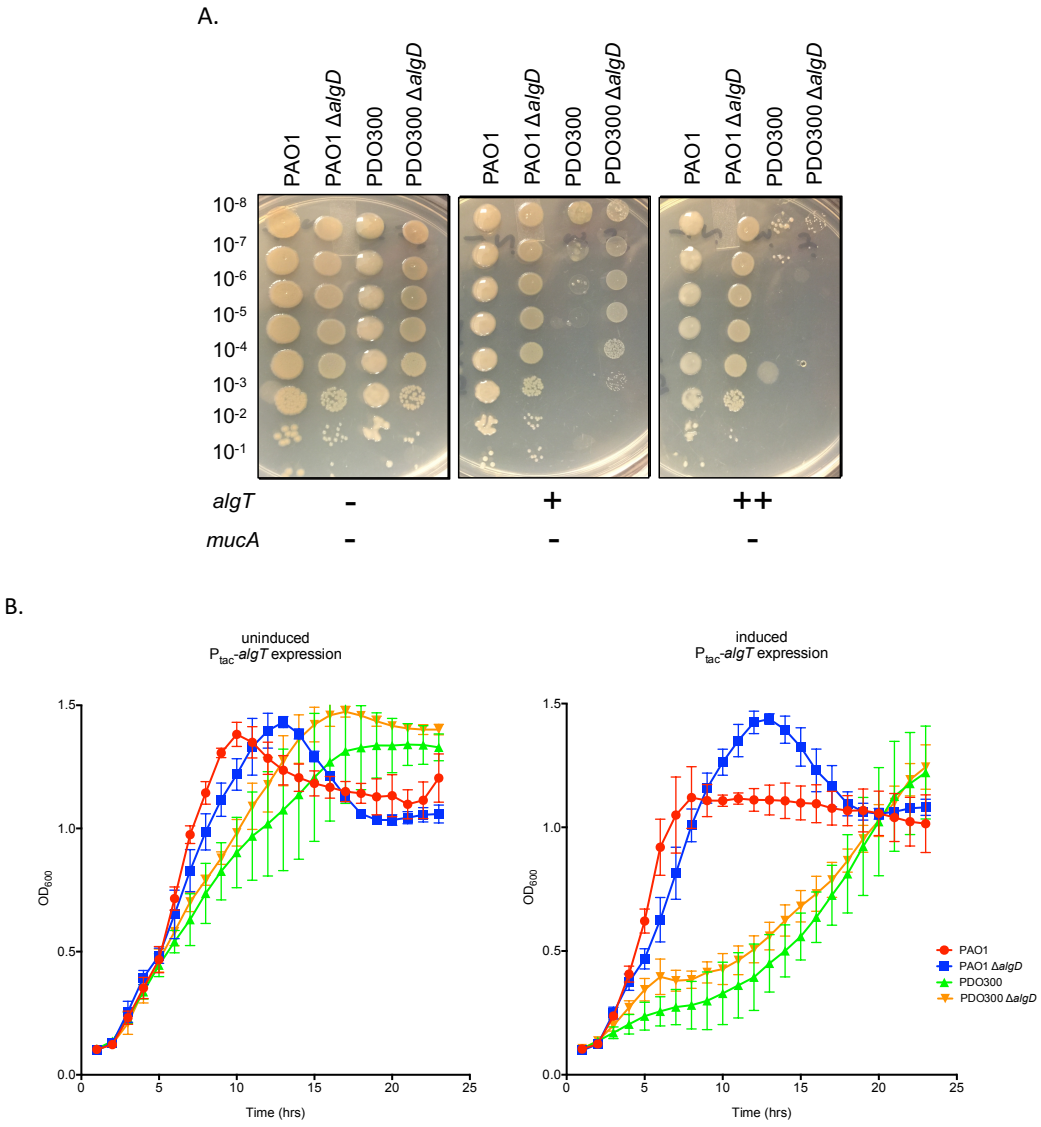

Figure 4.1. Overproduction of *algT* is lethal in *mucA22* strains. The *algT* coding sequence was cloned downstream of an IPTG inducible tac promoter and inserted, in single copy, at the Tn7 site of each strain (Tn7::P_{tac}-*algT*). A) Overnight cultures were grown without inducer, normalized to an optical density of 0.5, and then serially diluted onto LA containing no inducer (-), 0.1 mM IPTG (+), and 1 mM IPTG or (++). IPTG induces expression of *algT*. PAO1 becomes mucoid when *algT* is overexpressed. B) Growth curves of each strain grown in LB (uninduced, left) or LB containing 0.1 mM IPTG (induced, right). Over expression of *algT* in PDO300 strains is lethal.

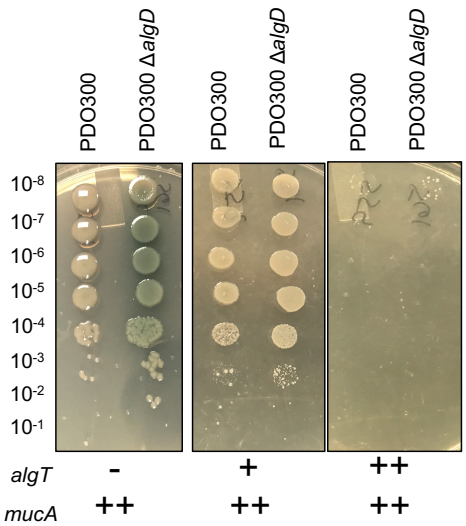

Figure 4.2. Complementation with wild type *mucA* partially rescues *algT* lethality. Each strain contains Tn7::P_{tac}-*algT* inserted in single copy as well as multicopy plasmid pHERD20T-*mucA*. Overnight cultures were grown without inducer, normalized to an optical density of 0.5, and then serially diluted onto LA supplemented with carbenicillin and containing either no inducer (-), 0.1 mM IPTG or 0.1% arabinose (+), or 1 mM IPTG or 1% arabinose (++). IPTG induces expression of *algT* while arabinose induces expression of *mucA*. Toxic *algT* expression is partially blocked when wildtype *mucA* is provided in trans.

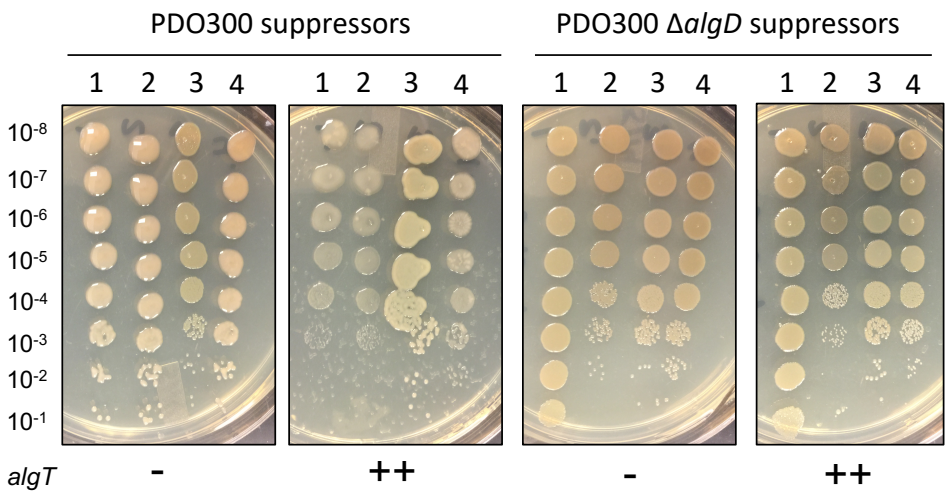

Figure 4.3. Identification of suppressors. PDO300 and PDO300 Δ*algD* colonies that were able to grow on high levels of IPTG where grown overnight and plated in the same way described in Figure 1. Suppressors of toxic *algT* expression survive similarly on high levels of IPTG (++) as they do on LA containing no inducer (-).

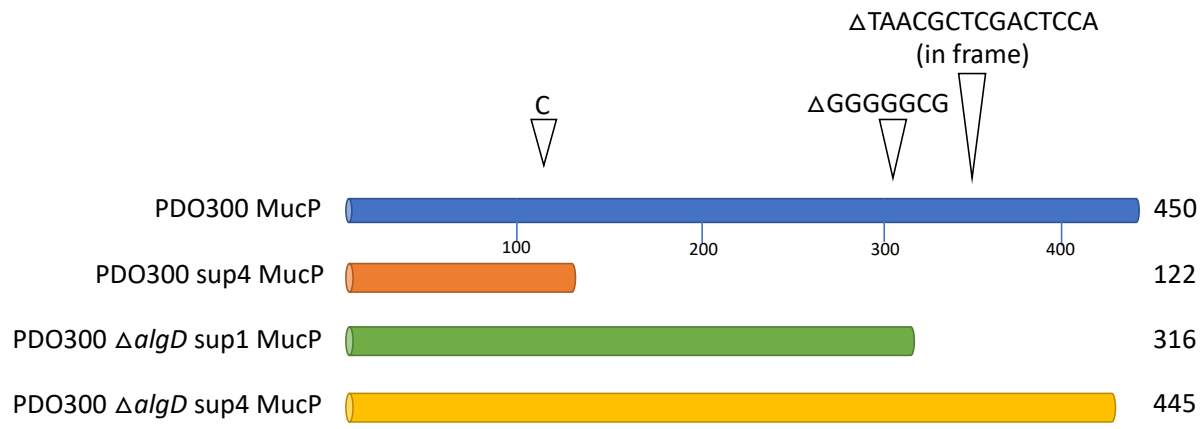

Figure 4.4. Mutations identified in *mucP*. Depiction of the primary protein structure of wild type MucP (blue) and suppressors are depicted with the nucleotide mutations shown above. The amino acid length of each protein is shown on the right. The PDO300 sup4 (orange) mutant has an insertion of a "C" after nucleotide 355 leading to truncation of the protein after 122 amino acids. PDO300 Δ*algD* sup1 (green) has a deletion of nucleotides 906-912, encoding "GGG GGC G", leading to truncation of the protein after 316 amino acids. PDO300 Δ*algD* sup4 (yellow) has an in-frame deletion of nucleotides 1019-1033, encoding "TAA CGC TCG ACT CCA", leading to truncation of the protein after 445 amino acids.

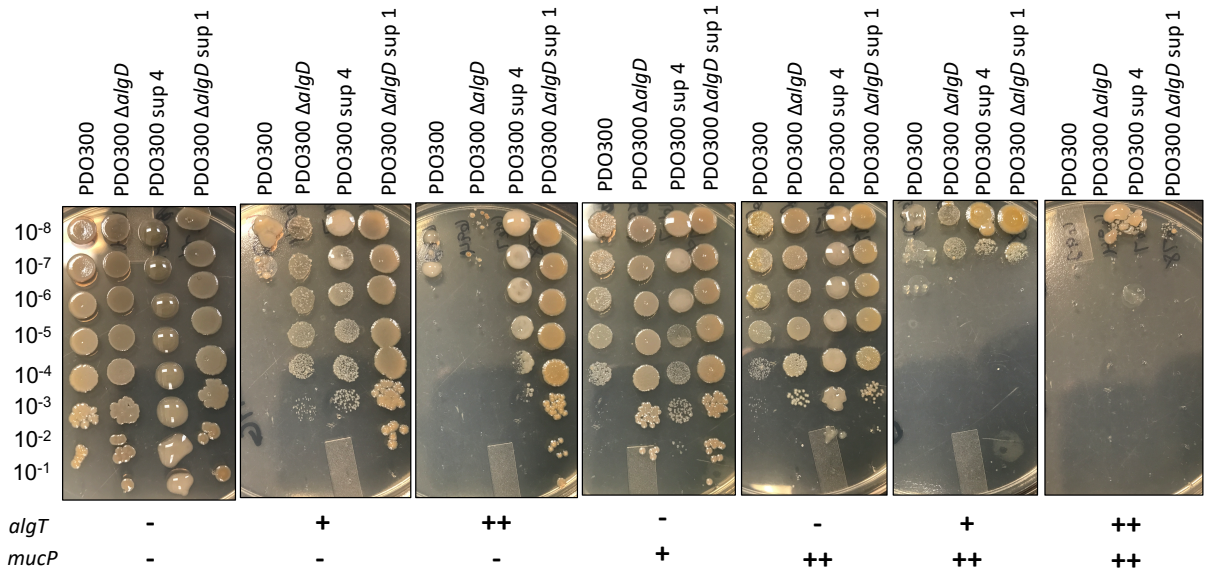

Figure 4.5. Complementation of *mucP* suppressor mutants restores *algT* sensitivity. Overnight cultures were grown without inducer, normalized to an optical density of 0.5, and then serially diluted onto LA containing no inducer (-), 0.1 mM IPTG or 0.1% arabinose (+), and 1 mM IPTG or 1% arabinose (++). IPTG induces expression of *algT* while arabinose induces expression of *mucP*. PDO300 sup 4 and PDO300 Δ*algD* sup 1 genotypes are listed in Table 4.1.

Table 4.1. Suppressor mutations.

Strain	Location	Mutation	Annotation
PDO300			
sup 1	PA1352 - PA1353	C*GCG	conserved hypothetical proteins
	PA4059	G*GC	hypothetical protein
sup 2	PA1352 - PA1353	C*GCG	conserved hypothetical proteins
	PA2000 - PA2001	G*GC	*dhcB* → *atoB*
	PA4059	G*GC	hypothetical protein
sup 4	PA1352 - PA1353	C*GCG	conserved hypothetical proteins
	PA2828 - PA2829	T*G	probable aminotransferase → hypothetical protein
	PA3649	A*AG	*mucP* protease
	PA4059	G*GC	hypothetical protein
PDO300 Δ*algD*			
sup 1	PA3539 - PA3540	A*G , G*A, C*A, G*A, G*T	*yaaA* → *algD*
	PA0424 - PA0425	C*T	*mexR* → *mexA*
	PA3541	A*G	*alg8* , alginate biosynthesis
	PA3649	A*AG	*mucP* protease
	PA4059	G*GC	hypothetical protein
sup 2	PA3539 - PA3540	A*G , G*A, C*A, G*A, G*T	*yaaA* → *algD*
	PA3541	A*G	*alg8* , alginate biosynthesis
	PA4059	G*GC	Hypothetical protein
sup 4	PA3539 - PA3540	A*G , G*A, C*A, G*A, G*T	*yaaA* → *algD*
	PA0424 - PA0425	C*T	*mexR* → *mexA*
	PA1352 - PA1353	C*GCG	conserved hypothetical proteins
	PA3541	A*G	*alg8* , alginate biosynthesis
	PA3649	A*AG	*mucP* protease
	PA4059	G*GC	hypothetical protein
	PA4938	G*A	*purA* , adenylosuccinate synthetase

Table 4.2. Strains, plasmids, and primers used in this study.

Name	Description	Location	Reference
E. coli			
DH5a	cloning background, plasmid maintenance		Invitrogen
SM10	bi-parental mating, conjugation proficient		Simon R et al. 1983
P. aeruginosa			
PAO1	nonmucoid laboratory strain		Hancock REW & Carey AM, 1979
PDO300	mucoid PAO1 containing *mucA22* allele	PAC01	Mathee K et al., 1999
PAO1 Δ*algD*	*algD* clean deletion	PAC342	Tseng BS et al. 2013
PDO300 Δ*algD*	*algD* clean deletion	PAC437	This study
PAO1 CTX::P5*algT*-optRBS-*lacZ* Tn7::Ptac-*algT*	*algT* promoter reporter inserted in single-copy and IPTG inducible *algT* inserted in single-copy	PAC541	This study
PAO1 Δ*algD* CTX::P5*algT*-optRBS-*lacZ* Tn7::Ptac-*algT*	*algT* promoter reporter inserted in single-copy and IPTG inducible *algT* inserted in single-copy	PAC501	This study
PDO300 CTX::P5*algT*-optRBS-*lacZ* Tn7::Ptac-*algT*	used to isolate suppressors	PAC539	This study
PDO300 Δ*algD* CTX::P5*algT*-optRBS-*lacZ* Tn7::Ptac-*algT*	used to isolate suppressors	PAC543	This study
PDO300 CTX::P5*algT*-optRBS-*lacZ* Tn7::Ptac-*algT* pHERD20T-HA-*mucA*	contains arabinose inducible *mucA* in multicopy	PAC559	This study
PDO300 Δ*algD* CTX::P5*algT*-optRBS-*lacZ* Tn7::Ptac-*algT* pHERD20T-HA-*mucA*	IPTG inducible *algT* inserted in single-copy and arabinose inducible *mucA* in multicopy	PAC561	This study
PDO300 CTX::P5*algT*-optRBS-*lacZ* Tn7::Ptac-*algT* pHERD20T-*mucP*	contains arabinose inducible *mucP* in multicopy	PAC692	This study
PDO300 Δ*algD* CT X::P5*algT*-optRBS-*lacZ* Tn7::Ptac-*algT* pHERD20T-*mucP*	contains arabinose inducible *mucP* in multicopy	PAC694	This study
PDO300 CTX::P5algT-optRBS-lacZ Tn7::Ptac-*algT* sup 4 pHERD20T-*mucP*	suppressor containing arabinose inducible *mucP* in multicopy	PAC667	This study
PDO300 Δ*algD CTX::P5algT-optRBS-lacZ* Tn7::Ptac-*algT* sup 1 pHERD20T-*mucP*	suppressor containing arabinose inducible *mucP* in multicopy	PAC678	This study
Suppressors			
PDO300 CTX::P5*algT*-optRBS-*lacZ* Tn7::Ptac-*algT* sup 1	suppressor of toxic *algT* expression	PAC575	This study
PDO300 CTX::P5*algT*-optRBS-*lacZ* Tn7::Ptac-*algT* sup 2	suppressor of toxic *algT* expression	PAC576	This study
PDO300 CTX::P5*algT*-optRBS-*lacZ* Tn7::Ptac-*algT* sup 3	suppressor of toxic *algT* expression	PAC578	This study
PDO300 CTX::P5*algT*-optRBS-*lacZ* Tn7::Ptac-*algT* sup 4	suppressor of toxic *algT* expression	PAC577	This study
PDO300 CTX::P5*algT*-optRBS-*lacZ* Δ*algD* Tn7::Ptac-*algT* sup 1	suppressor of toxic *algT* expression	PAC579	This study
PDO300 CTX::P5*algT*-optRBS-*lacZ* Δ*algD* Tn7::Ptac-*algT* sup 2	suppressor of toxic *algT* expression	PAC580	This study
PDO300 CTX::P5*algT*-optRBS-*lacZ* Δ*algD* Tn7::Ptac-*algT* sup 3	suppressor of toxic *algT* expression	PAC581	This study
PDO300 CTX::P5*algT*-optRBS-*lacZ* Δ*algD* Tn7::Ptac-*algT* sup 4	suppressor of toxic *algT* expression	PAC582	This study
Plasmids (alternative name)		*DH5α*	
miniTn7-Gm (pARC41)	Tn7 single copy insertion vector	ECAC87	Meisner J & Goldberg JB. 2016
miniTn7-Gm-Ptac-*algT* (pARC57)	IPTG inducible *algT* in single copy	ECAC141	Cross AR & Goldberg JB, 2019
pHERD20T (pARC06)	arabinose-inducible mutlicopy plasmid	ECAC09	Qiu D & Damron FH et al. 2008
pHERD20T-*algD*	arabinose inducible wildtype algD, multicopy	ECAC57	This study (MRD)
pHERD20T-HA-*mucA*	arabinose inducible wildtype *mucA* with an N-terminus HA tag	MRD6, #89	Damron FH et al. 2009
pHERD20T-*mucP*	arabinose inducible wildtype *mucP*, multicopy	ECAC170	This study
pEXG2 (pARC28)	allelic exchange vector	ECAC42	Rietsch A et al. 2005
pEXG2-*mucA22* (pARC)	*mucA22* allelic replacement vector	ECAC52	Cross AR & Goldberg JB, 2019
pEXGm-Δ*algD*	*algD* clean deletion vector	ECAC127	Jones AK et al. 2010
Primers			
oAC039	ATCGCAACTCTCTACTGTTTCT		Qiu D & Damron FH et al. 2008
oAC040	TGCAAGGCGATTAAGTTGGGT		Qiu D & Damron FH et al. 2008
oAC089	TTCCACACATTATACGAGCCGGAAGCATAAATGTAAAGCAatgagtcgtgaagccctgca		Cross AR & Goldberg JB, 2019
oAC090	CGAGCTCGAGCCCGGGGATCCTCTAGAGTCGACCTGCAGAtcagcggttttccaggctgg		Cross AR & Goldberg JB, 2019
oAC276	GGTACCCGGGGATCCTCTAGAGTCGACCTGCAGGCATGCAatgagtgcgctttacatgat		This study
oAC277	TTTTCCCAGTCACGACGTTGTAAAACGACGGCCAGTGCCActacagacgactcagatcgt		This study

*lowercase nucleotides anneal to plasmid sequence during isothermal assembly

Chapter 5

The alginate biosynthesis operon is autoregulated in *Pseudomonas aeruginosa* through a positive-feedback loop involving the AlgT sigma factor

Ashley R. Cross and Joanna B. Goldberg

unpublished data

ABSTRACT

In *Pseudomonas aeruginosa,* transcription of the alginate biosynthesis operon by the AlgT sigma factor results in a mucoid phenotype. In nonmucoid strains, AlgT is sequestered by the anti-sigma factor MucA and alginate is not produced. Chronic infection isolates, however, often contain frameshift mutations in *mucA* resulting in free AlgT and the unregulated overproduction of alginate. In addition to the alginate biosynthesis operon, AlgT transcribes ~300 additional genes and positively autoregulates itself. Since alginate and AlgT are tightly linked, we hypothesized that disruption of alginate biosynthesis could alter AlgT activity. In this study we deleted *algD* and *algA* in mucoid laboratory strain PAO1 *mucA22*, referred to as PDO300, and observed a significant decrease in *algT* promoter activity. We also found that deletion of *algD*, but not *algA*, disrupts the AlgT positive-feedback loop in PAO1, which contains wildtype MucA. Loss of AlgT promoter activity likewise resulted in diminished expression of the alginate biosynthesis operon. While the mechanism behind this regulation is unclear it is not dependent on alginate production as complementation back to the mucoid phenotype does not restore *algT* promoter activity. This is the first evidence that alginate biosynthesis is autoregulated and that genes within the operon create a positive-feedback loop.

INTRODUCTION

Pseudomonas aeruginosa isolated from chronic lung infections often transition from a nonmucoid to a mucoid phenotype due to the overproduction of the exopolysaccharide alginate (42, 58, 61, 65, 148, 185). Alginate is an exopolysaccharide composed of repeating L-guluronic and D-mannuronic acids and is secreted into the extracellular space to form a capsule around the bacteria (37). Mucoid strains form more robust biofilms, are less likely to be cleared by the immune system, and correlate with a poor patient prognosis (66, 188, 210-212). As a result, alginate regulation and production has been extensively studied for several decades (45, 102, 107, 111, 113, 120, 165).

In nonmucoid strains, the anti-sigma factor MucA sequesters the AlgT sigma factor, which is the master regulator of alginate biosynthesis (47, 48, 114, 169, 191, 194). When AlgT is inactivated, the alginate biosynthesis operon is not transcribed. When free and unregulated, however, AlgT continuously directs transcription of the alginate operon promoter. Overproduction of alginate leads to the mucoid phenotype. AlgT also directs transcription of its own promoter creating a positive-feedback loop (73, 98). Mucoid clinical isolates of *P. aeruginosa* have mutations in *mucA* leading to constitutive alginate production and AlgT expression.

The alginate operon is about 17 kilobases long and is composed of 12 genes; *algD, alg8, alg44, algK, algE, algG, algX, algL, algI, algJ, algF,* and *algA* (72). The enzymes encoded by the first and last genes of the operon, AlgD and AlgA, synthesize the precursors necessary for synthesizing alginate (76, 77). First, the phosphomannose isomerase activity of AlgA converts fructose-6-phosphate into mannose-6-phosphate followed by conversion to mannose-1-phosphate by AlgC, a phosphomannomutase located outside of the alginate biosynthesis operon (80, 81). Next, the GDP-mannose pyrophosphorylase activity of AlgA converts mannose-1-phosphate into

GDP-mannose. Finally, AlgD converts GDP-mannose into GDP-mannuronate. Prior to transport, Alg8 and Alg44 polymerize GDP-mannuronate followed by O-acetylation and epimerization by AlgI, AlgJ, AlgF, AlgX, and AlgG into mature alginate (82-90). The growing alginate chain is then cut and exported by AlgK, AlgE, and AlgL (91-94).

Since AlgT and alginate biosynthesis are tightly linked and highly regulated, we hypothesized that expression of *algT* might be dependent on alginate biosynthesis. In support of our hypothesis we found that *algT* promoter activity in mucoid strain PDO300 is significantly reduced when alginate biosynthesis genes are deleted and this strain is rendered nonmucoid. Therefore, it appears that the alginate biosynthesis operon is autoregulated by a positive-feedback loop containing AlgT. Since AlgT production and the mucoid phenotype contribute to the establishment of chronic infections, understanding how these processes are regulated would provide novel therapeutic targets for this life-threatening bacterium.

RESULTS

Deletion of alginate biosynthesis genes significantly reduces activity of the *algT* promoter. The goal of this study was to determine whether alginate production plays a role in the regulation of AlgT, the sigma factor that directs transcription of the alginate biosynthesis operon. Since AlgT is autoregulated, we created an AlgT reporter by placing the *algT* promoters in front of a promoterless-*lacZ* (P_{algT}-*lacZ)*. Expression of this reporter should be low in nonmucoid strains where *algT* expression is off and high in mucoid strains where AlgT production is high. To confirm this, we inserted P_{algT}-*lacZ* at the single-copy CTX site in isogenic nonmucoid strain PAO1 and isogenic mucoid strain PDO300 and measured LacZ activity. PDO300 is mucoid due to a deletion of a G nucleotide in the anti-sigma factor *mucA*, denoted *mucA22*. MucA22 is not able to sequester AlgT and therefore AlgT constantly directs transcription of itself and the alginate biosynthesis operon. As anticipated, *algT* promoter activity was 7x higher in mucoid PDO300 compared to nonmucoid PAO1 (Fig. 5.1A). Next, we hypothesized that alginate biosynthesis is necessary for *algT* expression. To test this, we deleted biosynthesis genes *algD*, the first gene in the alginate operon, and *algA*, the last gene in the alginate operon. When either *algD* or *algA* were deleted from PDO300 no alginate was produced (Fig. 5.4A). In support of our hypothesis, PDO300 Δ*algD* and PDO300 Δ*algA* had significantly reduced *algT* promoter activity compared to PDO300 (Fig. 5.1A). This result indicates that alginate biosynthesis is required for expression of the *algT* promoter in PDO300.

We were curious if the altered expression of the *algT* promoter in PDO300 Δ*algD* was dependent on the *mucA22* mutation. To test this, we cloned *algT* behind an IPTG-inducible tac promoter (P_{tac}-*algT*) and inserted this construct in single copy at the Tn7 site into PAO1 and PAO1 Δ*algD.* Unlike PDO300*,* PAO1 contains wildtype *mucA*. We can then compare uninduced

and induced *algT* expression on *algT* promoter activity in this normally nonmucoid strain. First, in wildtype PAO1 when *algT* is uninduced, *algT* promoter activity is low, as expected (Fig. 5.1B). When *algT* is induced, however, there is approximately a 2-fold increase in PAO1 *algT* promoter activity (Fig. 5.1B). This is expected since AlgT promotes expression of its own promoter. Induced *algT* expression in PAO1 also resulted in a mucoid phenotype and a significant increase in alginate production (Fig. 5.4B). We hypothesized that *algD* and *algA* are necessary for this AlgT-dependent increase in *algT* promoter activity. To test this, we first induced expression of *algT* in PAO1 Δ*algD* and found no increase in *algT* promoter activity compared to the uninduced control. Therefore, *algD* is required for expression of the *algT* promoter even in the presence of wildtype MucA. Surprisingly, however, when we induced expression of *algT* in PAO1 Δ*algA*, promoter activity was significantly increased to wild type levels. This suggests that *algA* is not required for expression of the *algT* promoter in the presence of wildtype MucA. Both PAO1 Δ*algD* and PAO1 Δ*algA* remain nonmucoid when *algT* is overexpressed (Fig. 5.4B). Therefore, alginate production itself does not restore *algT* promoter activity in the wild type MucA background.

Deletion of alginate biosynthesis genes *algD* and *algA* also alters expression of the alginate operon promoter. Since AlgT has a large regulon, these data imply that disrupting alginate biosynthesis has broad implications in the regulation of many genes. We were particularly interested in knowing if promoter activity of the alginate operon was altered when alginate biosynthesis genes were deleted, since this promoter is directly regulated by AlgT. Because *algT* expression is decreased in PDO300 Δ*algD* and PDO300 Δ*algA* compared to PDO300, we hypothesized that the alginate promoter would also be decreased in expression. To assess this, an alginate operon transcriptional reporter (P_{algD}-*lacZ*) was inserted in single-copy

into each strain and the effects of deleting *algD* or *algA* on promoter activity was measured. Similarly to before, expression of the alginate operon reporter is very low in nonmucoid PAO1 and is significantly increased in mucoid PDO300 (Fig. 5.2A). However, alginate promoter activity of PDO300 is reduced over 3-fold when *algD* or *algA* are deleted (Fig. 5.2A). These data support the hypothesis that decreased *algT* expression in PDO300 Δ*algD* and PDO300 Δ*algA* results in reduced activity of the alginate promoter.

Again, we were also interested in knowing whether *algD* and *algA* are required for robust alginate operon expression in PAO1. We inserted the alginate operon reporter into PAO1, PAO1 Δ*algD*, and PAO1 Δ*algA* strains that each also contained an inducible copy of *algT*. As expected, when *algT* is uninduced alginate promoter activity is low in PAO1 and increased significantly when *algT* is induced (Fig. 5.2B). However, when *algT* is overexpressed in PAO1 Δ*algD*, there is no significant difference in alginate promoter activity. Contrary, when we induced expression of *algT* in PAO1 Δ*algA*, alginate promoter activity was significantly increased almost to wildtype levels. This trend is the same as that observed in Figure 5.1B and indicates that *algD* expression, but not *algA* expression, is required for AlgT-dependent expression of the alginate operon promoter in the presence of wild type MucA. Altogether, we believe these data support a model where the expression of alginate biosynthesis genes drives expression of *algT* and in turn increases expression of the alginate operon.

Complementation increases alginate production, but not *algT* promoter activity. To test specifically that loss of *algD* and *algA* results in loss of *algT* promoter activity we complemented back in trans either *algD* or *algA* on multicopy plasmid pHERD20T (187). We reasoned that restoring the deleted genes, and therefore alginate biosynthesis, would restore *algT* promoter activity. Since PDO300 Δ*algD* and PDO300 Δ*algA* contain clean in-frame deletion we

expected the polar effects of the deletions to be minimal. When *algD* expression is complemented in PDO300 Δ*algD* this strain produced approximately 400 μg/ml of alginate, a significant 4-fold increase compared to when *algD* expression is uninduced (Fig. 5.3A). However, this is still less than the amount of alginate produced by PDO300 (Fig. 5.4A), even though these two strains looked similarly mucoid when streaked on LA. This suggests that the *algD* clean deletion can be complemented in trans, but that deleting the first gene in the alginate operon still has some downstream effects on overall expression and production of alginate. Contrary, when *algA* expression is induced in PDO300 Δ*algA,* alginate production increased 10-fold and was fully restored to wild type levels (Fig. 5.3C). Since *algA* is the last gene in the alginate operon, there are no polar effects of deleted this gene. We then examined whether *algD* or *algA* complementation restored *algT* promoter activity. When we compared uninduced to induced expression of *algD* or *algA* in either PDO300 Δ*algD* or PDO300 Δ*algA*, however, there was no significant difference in *algT* promoter activity (Fig. 5.3B and 5.3D). Therefore, *algT* expression could not be complemented by providing *algD* or *algA* in trans.

Replacing the alginate operon promoter disrupts *algT* promoter activity, independent of alginate production. Next, we hypothesized that loss of alginate production itself regulates *algT* promoter activity, regardless of the *algD* or *algA* mutation. To test this, we replaced the native alginate operon promoter with an arabinose-inducible promoter in PDO300 (188). In this system, when PDO300 is grown without inducer, the arabinose promoter is off, the alginate biosynthesis operon is not expressed, and no alginate is produced. When grown in the presence of arabinose, the alginate operon is transcribed. Therefore, we can compare *algT* promoter activity when alginate production is turned on and off, independent of *algD* or *algA* deletion. When grown without inducer and the alginate operon is turned off, *algT* promoter

activity is significantly reduced and PDO300 is nonmucoid (Fig. 5.5A, 5.5B). However, when the arabinose promoter is induced, even though there is a significant increase in alginate production (Fig. 5.5B), there is no significant increase in *algT* promoter activity (Fig 5.5A). These data suggest that alginate production itself does not regulate *algT* promoter activity.

It is still clear, however, that disrupting the *algD* promoter and/or deleting *algD* or *algA* alters *algT* promoter activity. To address the possibility that deleting *algD* disrupts an unknown trans-acting factor or regulatory element in the promoter/*algD* gene region we wanted to determine if we could complement *algT* promoter activity back in PDO300 Δ*algD* by providing both the *algD* promoter and gene in trans. To do this, a P_{algD}-*algD* fragment containing the alginate promoter and the *algD* gene was inserted into multicopy plasmid pHERD20T. The ability of this fragment to restore *algT* promoter activity in PDO300 Δ*algD* was then assessed. We grew PDO300 Δ*algD* pHERD20T-P_{algD}-*algD* in the presence or absence of inducer and found no significant increase in *algT* promoter activity under either condition and therefore no complementation of *algT* promoter activity (Fig. 5.6). This indicates that providing the alginate promoter and *algD* gene in trans cannot restore *algT* promoter activity.

DISCUSSION AND FUTURE DIRECTIONS

We can now begin to build a model for the regulation of AlgT by alginate biosynthesis in mucoid *P. aeruginosa* (Fig. 5.7). When the anti-sigma factor MucA is degraded as a response to outer membrane stress or truncated due to mutations, such as we see in CF isolates, the sigma factor AlgT is free to initiate transcription of over 300 genes. This includes the 12 genes of the alginate biosynthesis operon. AlgT production is also positively autoregulated with AlgT directing transcription of its own operon. Interestingly, our results seem to indicate that alginate biosynthesis, in some way, isn required for this positive-feedback loop. When *algD*, which encodes a GDP-mannose 6-dehydrogenase, or *algA*, which encodes a dual phosphomannose isomerase/ GDP-mannose pyrophosphorylase, is deleted the positive-feedback loop is disrupted. As a result, the *algT* promoter is reduced in expression and the alginate operon is turned off. This mechanism may be in place to conserve energy and resources when alginate production is compromised. However, this assumes that alginate biosynthesis is the most central and/or costly part of the AlgT regulon and that all of the other genes in the AlgT regulon are dependent on alginate biosynthesis.

While we are closer to understanding this regulation, several questions still remain. Most importantly, what is the mechanism linking alginate biosynthesis and AlgT? It is possible that by deleting *algD* or *algA* there is a buildup of precursors, likely fructose-6-phosphate or GDP-mannose, that triggers down regulation of AlgT. Since GDP-mannose is a shared precursor with LPS biosynthesis, a buildup of GDP-mannose would result in increased production of GDP-rhamnose and therefore increased production of common O antigen. What is the biological relevance of increased common O antigen in the absence of alginate production? Deleting other biosynthetic enzymes outside of the alginate biosynthesis operon, such as *algC*, could test the

precursor hypothesis. However, AlgC is a central bifunctional "check-point" enzyme with phosphomannomutase and phosphoglucomutase activity that generates precursors for a number of *P. aeruginosa* polysaccharides and would likely have off-target effects. Regardless, when *algD* is complemented back in trans (Fig. 5.6) and alginate production is partially restored, the *algT* promoter is still turned off. Likewise, when alginate production is put under control of an inducible promoter and artificially turned on and off, the *algT* promoter remains inactive under both conditions (Fig. 5.3). This suggests that alginate production itself or a buildup of biosynthetic precursors does not control *algT* expression. Since alginate production could not always be restore to wildtype levels, however, we still cannot rule out that this modest decrease in alginate biosynthesis and production could alter *algT* expression and activity.

Furthermore, why does deleting *algA* in PDO300, but not PAO1, disrupt the AlgT positive-feedback loop? This implies a MucA-dependent part to the puzzle since the only difference between PAO1 and PDO300 is the *mucA22* mutation. Although both deletion of *algD* and *algA* result in decreased *algT* promoter activity, the mechanism may be different for each. A pulldown experiment using *algT* promoter DNA and lysates from each strain background could help determine differences in trans acting factors that impact *algT* promoter activity.

Finally, we do not really know if deletion of *algD* and *algA* alter AlgT activity through transcriptional, post-transcriptional, or post-translational regulation of AlgT. The readout of AlgT activity used in these studies is an *algT* or *algD* reporter. We do not know if AlgT activity decreases due to inactivation or repression of the *algT* promoter, degradation of *algT* mRNA, or destabilization of AlgT protein. Additionally, we do not know if all 5 *algT* promoters are being regulated in the same way. Preliminary data generated by Mike Davis, a previous graduate student, found that *algT* mRNA levels are reduced in PDO300 *algD*::FRT (213). The only

difference is that this strain disrupts *algD* with a polar mutation. Future experiments on AlgT, such as RT-qPCR of RNA or western blots of protein, would be required to help tease apart how AlgT is being regulated itself in each strain background and ultimately provide insight into how *algD* and *algA* are impacting its function. Determining if any other genes within the AlgT regulon are impacted by deletion of alginate biosynthesis genes could also provide a clue.

If there is not a clear direct link between alginate biosynthesis and AlgT activity, a more global approach is necessary. A large blue/white transposon screen could be employed to find PDO300 Δ*algD* CTX::P5$_{algT}$-*lacZ* mutants that have restored *algT* promoter expression. Additionally, performing RNA sequencing of PDO300, PDO300 Δ*algD*, and PDO300 Δ*algA* would provide a complementary approach to identify altered genes and pathways. It is clear that regulation of alginate production remains complex. The identification of a novel feedback mechanism linking alginate biosynthesis to alginate promoter expression demonstrates that *P. aeruginosa* continues to be a complex bacterium with many secrets still waiting discovery.

MATERIALS AND METHODS

Bacterial strains and culture conditions. Bacteria were maintained on lysogeny agar (LA) containing 1.5% agar and grown in lysogeny broth (LB). When appropriate, media was supplemented with 10 μg/ml tetracycline, 15 μg/ml gentamycin, or 100 μg/ml carbenicillin for *Escherichia coli* and 100 μg/ml tetracycline, 60 μg/ml gentamycin, or 100 μg/ml carbenicillin for *Pseudomonas aeruginosa*. Vogel-Bonner minimal medium (VBMM) plates supplemented with gentamicin and no salt LB (10 g/l tryptone and 5 g/l yeast extract) containing 15% sucrose were used for allelic exchange (178). Strains were grown at 37°C. Conjugations and sucrose counterselections were performed at 30°C. A list of strains, plasmids, and primers used are available in Table S5.1 and Table S5.2.

Construction of the *algT* reporter. To generate miniCTX1-P5$_{algT}$-optRBS-*lacZ,* 480 bps of the upstream *algT* region starting 20 bps upstream of the start codon, to incorporate the five *algT* promoters but not the native RBS, was amplified using oAC158/oAC159 and inserted into BamHI digest miniCTX1-optRBS-*lacZ* using isothermal assembly (Gibson Assembly Master Mix, New England BioLabs) following the manufacturers protocol. The reactions were transformed into chemically competent DH5α and selected for on tetracycline. Plasmids from single colonies were isolated (Qiagen Miniprep Kit) and screened for the *algT* promoter insertion using oAC32/oAC33.

Construction of pHERD20T-*algA* and pHERD20T-P$_{algD}$-*algD*. To construct pHERD20T-*algA* and pHERD20T-P$_{algD}$-*algD* the *algA* gene or the P$_{algD}$-*algD* were amplified using oAC251/oAC252 or oAC273/oAC274, respectively. Each fragment was ligated into HindIII

digested gel-purified pHERD20T using isothermal assembly (Gibson Assembly Master Mix, New England BioLabs). Plasmids were miniprepped (Qiagen) from carbenicillin resistant colonies and screened for the *algA* or P_{algD}-*algD* insertion using oAC039/oAC040.

Construction of pEXG2-Δ*algA*. To generate pEXG2-Δ*algA* 1000 bps of the upstream region of *algA* was PCR amplified from the PAO1 genomic DNA using oAC245/oAC246 and 1000 bps of downstream region was amplified using oAC247/oAC248. These two fragments were then inserted into HindIII digest pEXG2 using isothermal assembly (Gibson Assembly Master Mix, New England BioLabs) following the manufacturers protocol. The reaction was then transformed by heat-shock into chemically competent DH5a and selected for on gentamicin. Plasmids were extracted (Qiagen Miniprep Kit) from isolated colonies and PCR verified using oAC91/oAC92. Confirmed pEXG2-Δ*algA* was then transformed into chemically competent SM10 in the same way described for DH5α.

Construction of PAO1 Δ*algD* and Δ*algA*. SM10 containing pEXG2-Δ*algA* or pEXGm-Δ*algD* from Matt Wolfgang (214) were conjugated with PAO1 following the puddle-mating protocol described by Hmelo et al. (178). After sucrose counterselection, single colonies were patched onto LA and LA containing gentamicin. Gentamicin sensitive colonies were screened for loss of *algD* or *algA* by single-colony PCR using primers oAC174/oAC175 or oAC249/oAC250, respectively.

Construction of PDO300 Δ*algD* and Δ*algA*. SM10 containing pEXG2-*mucA22* was conjugated with PAO1 Δ*algD* and PAO1 Δ*algA*, following the puddle-mating protocol described by Hmelo

et al. (178). After sucrose counterselection, single colonies were patched onto LA and LA containing gentamicin. Next, *mucA* was amplified, by single colony PCR, from gentamicin sensitive colonies using oAC089/oAC090 and sent to Genewiz for sequencing to identify colonies that contained the *mucA22* mutations.

Generation of reporter strains and *algT* overexpression strains. All plasmids were electroporated into *P. aeruginosa* strains as previously described (177). miniCTX1-P5$_{algT}$-optRBS-*lacZ* and miniCTX1-P$_{algD}$-lacZ (97) were electroporated into PAO1, PAO1 Δ*algD*, PDO300, and PDO300 Δ*algD* and selected for on tetracycline. miniTn7-P$_{tac}$-*algT* was electroporated into PAO1 attCTX::P5$_{algT}$-optRBS-*lacZ*, PAO1 attCTX::P$_{algD}$-lacZ, PAO1 Δ*algD* attCTX::P5$_{algT}$-optRBS-*lacZ*, and PAO1 Δ*algD* attCTX::P$_{algD}$-lacZ and selected for on gentamicin.

ß-galactosidase assay. Assays for promoter activity were performed as described previously (48, 176).

Additional statistical analysis. GraphPad Prism Software (version 6) was used to analyze the data. All data represent biological replicate data with technical replicates. Graphs show mean values and error bars represent standard deviation (SD). *: P<0.05, **: P<0.01, ****: P<0.0001, ns: not significant.

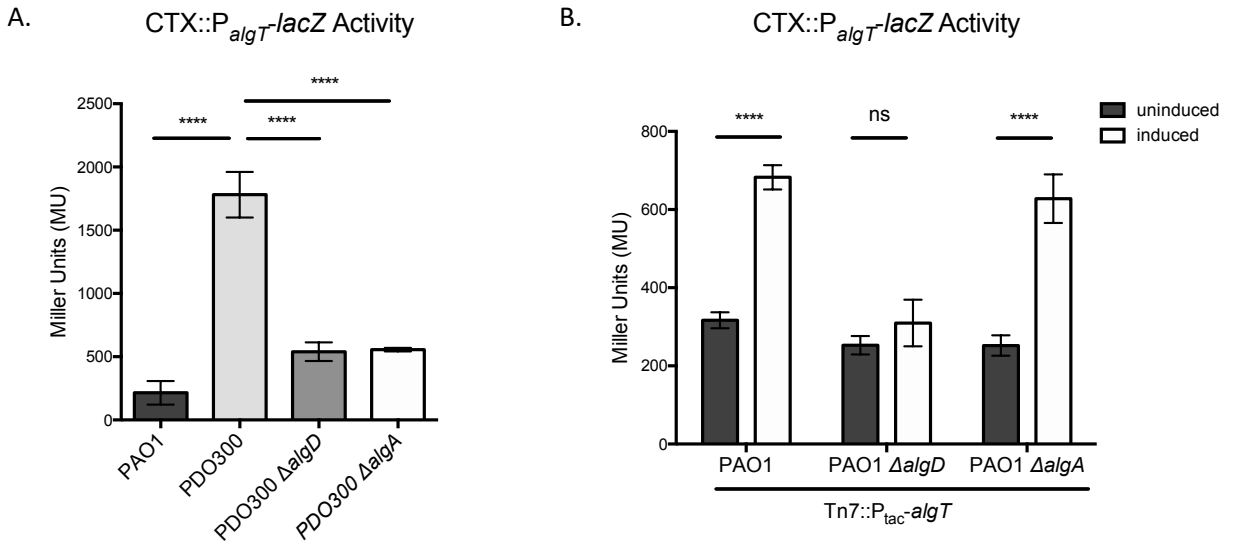

Figure 5.1. Deletion of alginate biosynthesis genes alters activity of the *algT* promoter. The upstream region of *algT* containing all five promoters was transcriptionally fused to a promoterless-*lacZ* and inserted, in single copy, at the CTX site of each strain. ß-galactosidase assays were used to determine promoter activity of the reporter in each strain. A) Nonmucoid PAO1 has low *algT* promoter activity while mucoid strain PDO300 has high activity. This high activity is lost when *algD* is deleted. Significance was determined using a one-way ANOVA with Tukey's multiple comparisons analysis. B) The *algT* coding region was cloned downstream of an inducible tac promoter and inserted, in single copy, at the Tn7 site of each strain. Each strain also contains the *algT* reporter at the CTX site. Significance was determined using a two-way ANOVA with Sidak's multiple comparisons analysis. Error bars represent SD of three biological replicates. ****: $p<0.0001$, ns: not significant.

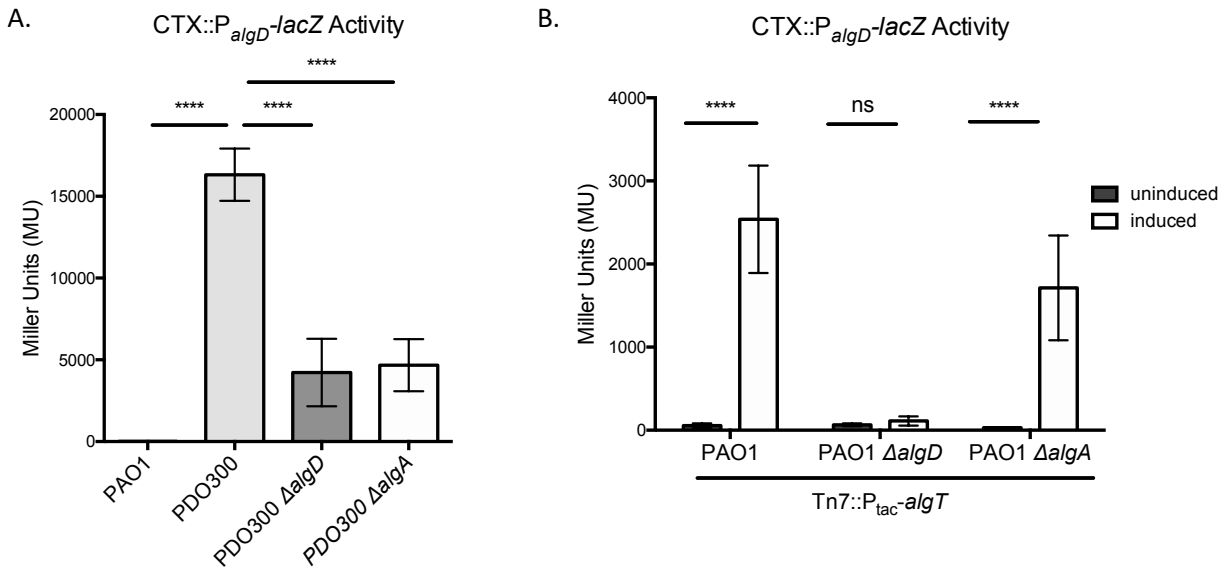

Figure 5.2. Deletion of alginate biosynthesis genes alter expression of the alginate operon promoter. Alginate operon reporter P_{algD}-*lacZ* was inserted at the CTX site of each strain. ß-galactosidase assays were performed and analyzed as described in Figure 4.1. A) *algD* promoter activity of PDO300 is decrease when *algD* or *algA* are deleted. B) Each strain contains the *algD* reporter at the CTX site and P_{tac}-*algT* at the Tn7 site. ****: $p<0.0001$, ns: not significant.

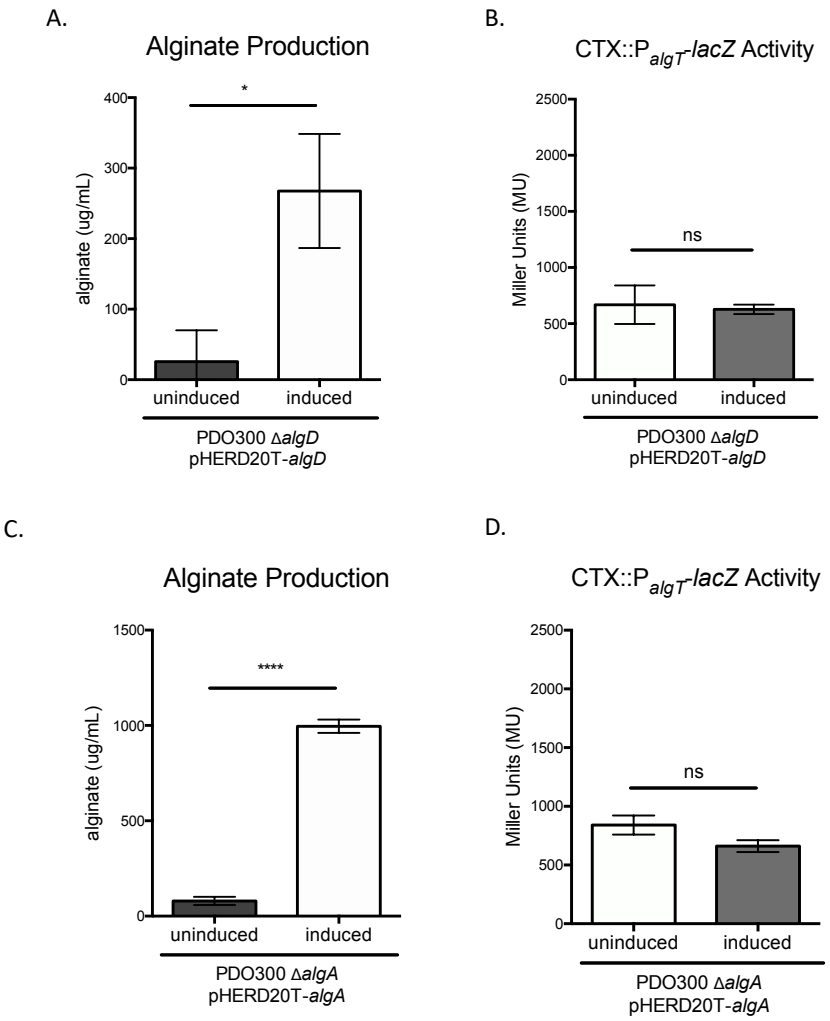

Figure 5.3. PDO300 Δ*algD* and Δ*algA* complementation increases alginate production, but not *algT* promoter activity. PDO300 Δ*algD* was complemented by providing *algD* in trans on multicopy plasmid pHERD20T. Expression was induced by growth in 1% L-arabinose and compared to an uninduced control. A) Alginate was purified from 10 ml of overnight culture and quantified using a carbazole assay. B) ß-galactosidase assays were performed and analyzed as described in Figure 5.1. Significance was determined using an unpaired t-test. Error bars represent SD of three biological replicates. *: $p<0.05$, ****: $p<0.0001$, ns: not significant.

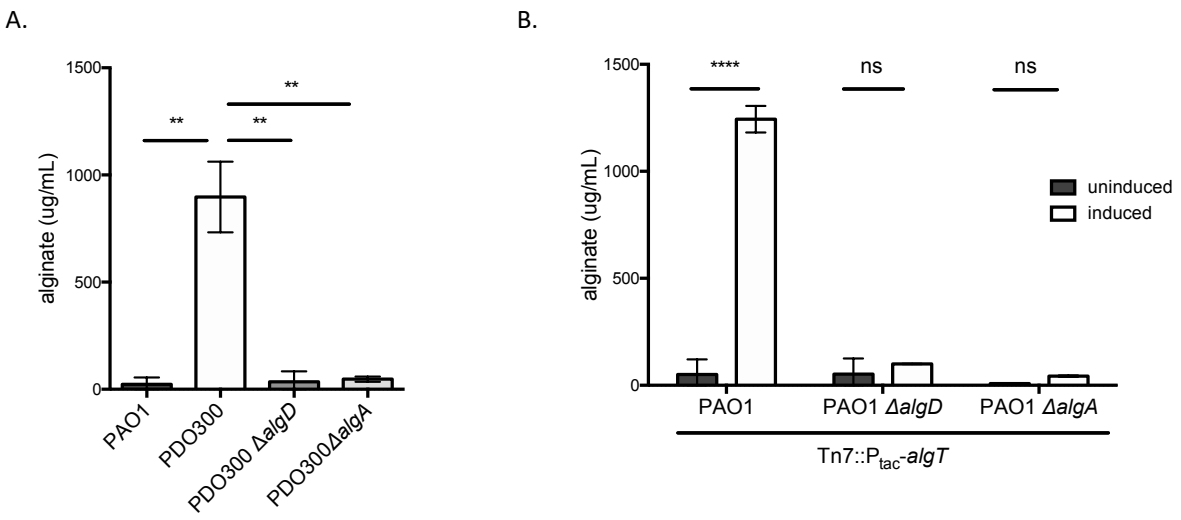

Figure 5.4. Alginate production of PDO300 and PAO1 strains. Alginate was purified from 10 ml of overnight culture and quantified using a carbazole assay. A) PAO1 produces very little alginate while PDO300 produces very high levels of alginate. When *algD*, the first gene in the alginate biosynthesis operon, is deleted no alginate is produced. B) PAO1 Tn7::P_{tac}-*algT*, PAO1 Δ*algD* Tn7::P_{tac}-*algT*, and PAO1 Δ*algA* Tn7::P_{tac}-*algT* contain an IPTG-inducible *algT* inserted in single copy. When PAO1 P_{tac}-*algT* is induced with 1 mM IPTG there is a significant increase in alginate production compared to uninduced conditions. When *algD* or *algA* are deleted, no alginate is detected. **: $p<0.01$, ****: $p<0.0001$, ns: not significant.

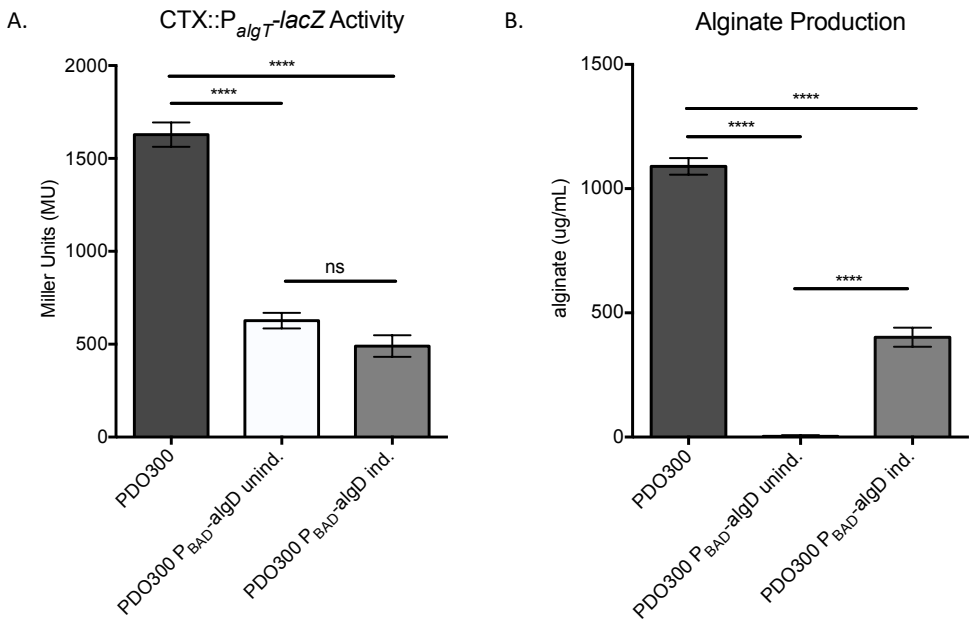

Figure 5.5. Replacing the alginate operon promoter disrupts *algT* promoter activity, independent of alginate production. The native alginate operon promoter was replaced, using homologous recombination, with an arabinose-inducible promoter (P_{BAD}-*algD*). Expression was induced by growth in 1% L-arabinose and compared to wildtype PDO300 or an uninduced control. A) ß-galactosidase assays were performed and analyzed as described in Figure 4.1. Induction of alginate biosynthesis does not restore *algT* promoter activity. B) Alginate was purified from 10 ml of overnight culture and quantified using a carbazole assay. When P_{BAD}-*algD* is induced, alginate levels are increased, but not to wild type levels. Significance was determined using a one-way ANOVA with Tukey's multiple comparisons analysis. Error bars represent SD of three biological replicates. ****: $p<0.0001$, ns: not significant.

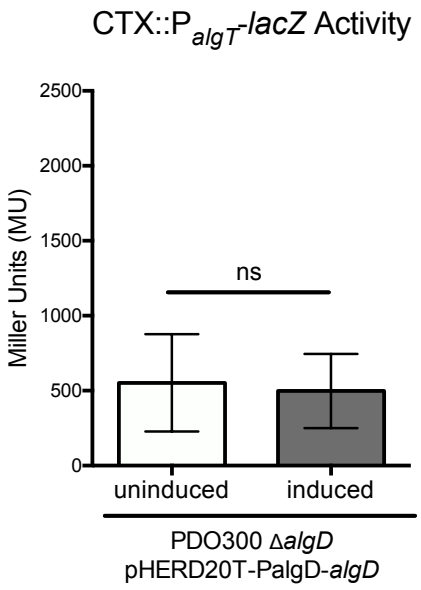

Figure 5.6. Complementation of *algT* activity is not restored when the alginate operon promoter and the *algD* gene are both provided in trans. ß-galactosidase assays were performed and analyzed as described in Figure 5.1. Significance was determined using an unpaired t-test. Error bars represent SD of three biological replicates. ns: not significant.

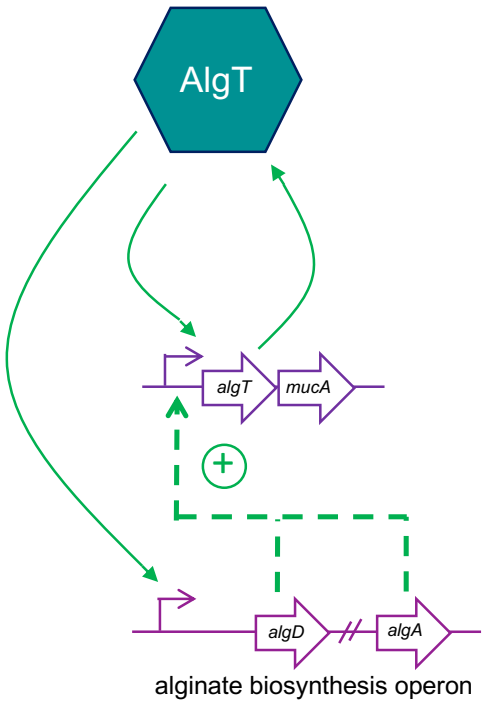

Figure 5.7. Model for the regulation of AlgT in PDO300 by the alginate biosynthesis operon. When the anti-sigma factor MucA is degraded as a response to outer membrane stress or truncated due to mutations, the sigma factor AlgT is free to initiate transcription of over 300 genes. This includes the 12 genes of the alginate biosynthesis operon. AlgT production is also positively autoregulated with AlgT directing transcription of its own operon. When *algD* or *algA* are deleted from PDO300, the *algT* promoter and the alginate operon is turned off.

Table S5.1. Strains and plasmids used in this study.

Name	Description	Location	Reference
P. aeruginosa			
PAO1	nonmucoid laboratory strain		Hancock REW & Carey AM, 1979
PDO300	mucoid PAO1 containing *mucA22* allele	PAC01	Mathee K et al., 1999
PAO1 Δ*algD*	*algD* clean deletion	PAC342	Tseng BS et al. 2013
PDO300 Δ*algD*	*algD* clean deletion	PAC437	This study
PAO1 Δ*algA*	*algA* clean deletion	PAC595	This study
PDO300 Δ*algA*	*algA* clean deletion	PAC597	This study
PAO1 CTX::P5*algT*-optRBS-*lacZ*	*algT* promoter reporter inserted in single-copy	PAC282	This study
PDO300 CTX::P5*algT*-optRBS-*lacZ*	*algT* promoter reporter inserted in single-copy	PAC284	This study
PAO1 CTX::P*algD*-*lacZ*	*algD* promoter reporter inserted in single-copy	PAC99	This study
PDO300 CTX::P*algD*-*lacZ*	*algD* promoter reporter inserted in single-copy	PAC101	This study
PAO1 Δ*algD* CTX::P5*algT*-optRBS-*lacZ*	*algT* promoter reporter inserted in single-copy	PAC488	This study
PDO300 Δ*algD* CTX::P5*algT*-optRBS-*lacZ*	*algT* promoter reporter inserted in single-copy	PAC494	This study
PAO1 Δ*algA* CTX::P5*algT*-optRBS-*lacZ*	*algT* promoter reporter inserted in single-copy	PAC615	This study
PDO300 Δ*algA* CTX::P5*algT*-optRBS-*lacZ*	*algT* promoter reporter inserted in single-copy	PAC619	This study
PAO1 Δ*algD* CTX::P*algD*-*lacZ*	*algD* promoter reporter inserted in single-copy	PAC490	This study
PDO300 Δ*algD* CTX::P*algD*-*lacZ*	*algD* promoter reporter inserted in single-copy	PAC496	This study
PAO1 Δ*algA* CTX::P*algD*-*lacZ*	*algD* promoter reporter inserted in single-copy	PAC617	This study
PDO300 Δ*algA* CTX::P*algD*-*lacZ*	*algD* promoter reporter inserted in single-copy	PAC621	This study
PAO1 CTX::P5*algT*-optRBS-*lacZ* Tn7::Ptac-*algT*	*algT* promoter reporter inserted in single-copy and IPTG inducible *algT* inserted in single-copy	PAC541	This study
PAO1 Δ*algD* CTX::P5*algT*-optRBS-*lacZ* Tn7::Ptac-*algT*	*algT* promoter reporter inserted in single-copy and IPTG inducible *algT* inserted in single-copy	PAC501	This study
PAO1 Δ*algA* CTX::P5*algT*-optRBS-*lacZ* Tn7::Ptac-*algT*	*algT* promoter reporter inserted in single-copy and IPTG inducible *algT* inserted in single-copy	PAC623	This study
PAO1 Δ*algD* CTX::P*algD*-*lacZ* Tn7::Ptac-*algT*	*algD* promoter reporter inserted in single-copy and IPTG inducible *algT* inserted in single-copy	PAC503	This study
PAO1 Δ*algA* CTX::P*algD*-*lacZ* Tn7::Ptac-*algT*	*algD* promoter reporter inserted in single-copy and IPTG inducible *algT* inserted in single-copy	PAC625	This study
PDO300 Δ*algD* pHERD20T-*algD*	contains arabinose inducible *algD* in multicopy	PAC484	This study
PDO300 Δ*algD* CTX::P5*algT*-optRBS-*lacZ* pHERD20T-*algD*	*algT* promoter reporter inserted in single-copy and arabinose inducible *algD* in multicopy	PAC512	This study
PDO300 Δ*algD* CTX::P5*algT*-optRBS-lacZ pHERD20T-PalgD-algD	contains arabinose inducible P*algD*-*algD* in multicopy	PAC682	This study
PDO300 Δ*algA* CTX::P5*algT*-optRBS-*lacZ* pHERD20T-*algA*	*algT* promoter reporter inserted in single-copy and arabinose inducible *algA* in multicopy	PAC627	This study
PDO300 PBAD-*algD*	contains arabinose inducible alginate production	PAC28	This study
PDO300 PBAD-*algD* CTX::P5*algT*-optRBS-*lacZ*	arabinose inducible alginate production and *algT* promoter reporter inserted in single-copy	PAC537	This study
Plasmids (alternative name)		*DH5α*	
miniCTX1-optRBS-*lacZ* (pARC11)	promoterless-*lacZ* reporter with optimized RBS	ECAC16	Cross AR & Goldberg JB, 2019
miniCTX1-P5*algT*-optRBS-*lacZ* (pARC47)	*algT* promoter reporter with optimized RBS	ECAC113	This study
miniCTX1-P*algD*-*lacZ*	*algD* promoter reporter	ECAC61	Damron FH et al. 2009
miniTn7-Gm (pARC41)	Tn7 single copy insertion vector	ECAC87	Meisner J & Goldberg JB. 2016
miniTn7-Gm-Ptac-*algT* (pARC57)	IPTG inducible *algT* in single copy	ECAC141	Cross AR & Goldberg JB, 2019
pHERD20T (pARC06)	arabinose-inducible mutlicopy plasmid	ECAC09	Qiu D & Damron FH et al. 2008
pHERD20T-*algD*	arabinose inducible wildtype algD, multicopy	ECAC57	This study (MRD)
pHERD20T-*algA* (pARC64)	arabinose inducible wildtype algA, multicopy	ECAC162	This study
pHERD20T-P*algD*-*algD* (pARC73)	alginate promoter and *algD* fragement, multicopy	ECAC180	This study
pEXG2 (pARC28)	allelic exchange vector	ECAC42	Rietsch A et al. 2005
pEXG2-*mucA22* (pARC29)	*mucA22* replacement vector	ECAC52	Cross AR & Goldberg JB, 2019
pEXG2-Δ*algA* (pARC63)	*algA* clean deletion vector	ECAC160	This study
pEXGm-Δ*algD*	*algD* clean deletion vector	ECAC127	Jones AK et al. 2010
pEX18Gm-*araC*-ParaBAD-alg (pARC13)	allelic replacement to switch native algD promoter with arabinose inducible promoter	ECAC18	Limoli DH et al. 2017

Table S5.2. Primers used in this study.

Primer Name	Sequence	Reference
oAC032	GACCCACTCTCAGGAGTGAAC	Cross AR & Goldberg JB, 2019
oAC033	CTCTTCGCTATTACGCCAGCTG	Cross AR & Goldberg JB, 2019
oAC039	ATCGCAACTCTCTACTGTTTCT	Qiu D & Damron FH et al. 2008
oAC040	TGCAAGGCGATTAAGTTGGGT	Qiu D & Damron FH et al. 2008
oAC089	TTCCACACATTATACGAGCCGGAAGCATAAATGTAAAGCAatgagtcgtgaagccctgca	Cross AR & Goldberg JB, 2019
oAC090	CGAGCTCGAGCCCGGGGATCCTCTAGAGTCGACCTGCAGAtcagcggttttccaggctgg	Cross AR & Goldberg JB, 2019
oAC091	CCACACATTATACGAGCCGGAAGC	Cross AR & Goldberg JB, 2019
oAC092	GGTACCGAATTCGAGCTCGAGC	Cross AR & Goldberg JB, 2019
oAC158	CTGGAGCTCCACCGCGGTGGCGGCCGCTCTAGAACTAGTGatgcgcaggtgttccggaag	This study
oAC159	AATCATGGTCATAGCTGTTCCTCCTTACTGCAGCCCGGGGgggaggagcttcgagcgtccc	This study
oAC174	TTCCACACATTATACGAGCCGGAAGCATAAATGTAAAGCAagtggccattggcaggcatt	This study
oAC175	CGAGCTCGAGCCCGGGGATCCTCTAGAGTCGACCTGCAGAggtagccgctgtcgatggct	This study
oAC245	TTCCACACATTATACGAGCCGGAAGCATAAATGTAAAGCAcagttcgacgccgactgggt	This study
oAC246	CCCCTGGCGGATCGCTCCGCCAGGGGGCCGGGTCGACGCTgttgtttctccttgaagcga	This study
oAC247	agcgtcgacccggccccctg	This study
oAC248	CGAGCTCGAGCCCGGGGATCCTCTAGAGTCGACCTGCAGAcggcggacccgttcggcgag	This study
oAC249	AGAAGGAGCGCACTGGAGA	This study
oAC250	GTTCATTAATACTCGATGTCCGCTC	This study
oAC251	GGTACCCGGGGATCCTCTAGAGTCGACCTGCAGGCATGCAatgatcccagtaatcctttc	This study
oAC252	TTTTCCCAGTCACGACGTTGTAAAACGACGGCCAGTGCCAtcagcggctgccggcgacca	This study
oAC273	GGTACCCGGGGATCCTCTAGAGTCGACCTGCAGGCATGCAcgccttctggggcgagcgta	This study
oAC274	TTTTCCCAGTCACGACGTTGTAAAACGACGGCCAGTGCCActaccagcagatgccctcgg	This study

*lowercase nucleotides anneal to plasmid sequence during isothermal assembly

Chapter 6

Discussion and future directions for the studies of chronic phenotypes in *Pseudomonas aeruginosa*

Discussion and future studies on chronic *P. aeruginosa* infections.

P. aeruginosa is a robust opportunistic pathogen able to survive and adapt to complex niches. Overproduction of the exopolysaccharide alginate and decreased expression of O antigen are hallmarks of a *P. aeruginosa* chronic lung infection. The regulatory pathways for both alginate and O antigen have been studied extensively for a handful of decades now. However, the studies presented in this dissertation highlight the amount of research that still needs to be completed and the many questions still waiting to be answered. We believe that understanding the regulation of and selection for chronic infection phenotypes will provide novel targets for treating and preventing *P. aeruginosa* from establishing infections within the CF lung.

When identifying likely drug targets for chronic *P. aeruginosa* infections, there are important factors to consider. We must know what processes are essential for adaption and survival in the lung and whether or not these genes, enzymes, or proteins are even expressed. Recent transcriptomics of *P. aeruginosa* sequenced directly from CF sputum found that genes involved in SOS response, long-chain fatty acid catabolism, and efflux pumps are highly expressed. This reflects the continued pressure put on *P. aeruginosa* to adapt, survive, scavenge, and resist antimicrobials within the host. We must also consider whether these processes are variable or different in diverse types of patients.

As mentioned, animal models for studying long-term lung infections have been lacking and therefore hinder our ability to rigorously study *P. aeruginosa* chronic phenotypes as they relate to host-pathogen interactions. It appears that the CF pig will be an ideal animal model for studying chronic bacterial infections. However, infection studies using this model have yet to be performed. Still, once a robust protocol has been developed, it will be paramount to study the adaption of *P. aeruginosa* to the CF pig lungs and the selection for chronic phenotypes. Ideally,

we could use this model to understand what factors select for the overproduction of alginate and the loss of very long O antigen. A long-term *P. aeruginosa* infection model will be crucial to determine the benefits of the co-regulation of alginate and very long O antigen as well as the intermediate steps involved in the establishment of an LPS-rough phenotype.

Discussion and future studies on AlgT.

A large portion of this dissertation focuses on the regulation of *algT* and phenotypes controlled by the AlgT sigma factor. Since AlgT contribute to the establishment of chronic infections, understanding how AlgT and AlgT-dependent phenotypes are regulated will provide novel therapeutic targets. Importantly, for research presented in this dissertation, expression of *algT* was also detected in CF sputum. Therefore, it seems plausible that targeting AlgT could prevent the chronic adaption to the CF lung. However, just preventing activation of AlgT would not necessarily prevent infection. Since AlgT transitions the bacterium from a virulent motile lifestyle to a more sessile lifestyle, deactivating AlgT could actually lead to a more lethal infection. Instead, treating *P. aeruginosa* with a synergistic cocktail containing targeted antibiotics and anti-virulence compounds (such as those that target biofilm formation, siderophore production, quorum sensing, and ultimately AlgT) would likely be necessary to prevent successful adaption of this bacterium to the lung environment in addition to decreasing bacterial load. Further, a chronic animal infection model will be fundamental to testing the plausibility and efficacy of this type of treatment for chronic *P. aeruginosa* infections.

The data presented in Chapter 4 determined that overproduction of the AlgT sigma factor is lethal in mucoid strains and that mutations in the MucP protease protected strains from toxic AlgT production by likely stabilizing MucA. This is surprising since mucoid strains are thought

to inherently overproduce and completely lose regulatory control of AlgT. While we only identified and confirmed one mechanism that ensures survival when AlgT is overexpressed, there may be multiple mechanisms for circumventing AlgT lethality. Since we only sequenced 6 suppressors, it may be worthwhile to sequence many more suppressors in order to identify other likely pathways and even novel pathways involved in regulating AlgT. We are also interested in understanding what is leading to the lethality. We speculate that a certain subset or subsets of genes controlled by AlgT are lethal in high quantities, but since AlgT controls a large quantity of genes it is not obvious which ones this might be. A directed approach could be taken to construct mutants in pathway known to be controlled by AlgT and look for mucoid strains that can survive overproduction of AlgT. Alternatively, a more global approach through transposon mutagenesis could identify a wider range of genes involved in this pathway. In this scenario, you would look for insertions in genes that allow for growth when *algT* is overexpressed.

Further, experiments performed in Chapter 5 present the first evidence that the alginate biosynthesis operon is autoregulated by a feedback loop involving the *algT* operon. Since there is not a clear link between alginate biosynthesis and AlgT activity, a more global approach must be used to identify the pathway linking these two highly regulated operons. First, a large blue/white transposon screen could be employed to find PDO300 Δ*algD* CTX::P5$_{algT}$-*lacZ* mutants that have restored *algT* promoter expression. In this scenario, you would be looking for blue colonies as these are the ones that would have restored *algT* expression. Additionally, performing RNA sequencing of PDO300, PDO300 Δ*algD*, and PDO300 Δ*algA* would provide a complementary approach to identify many genes and pathways affected by loss of alginate biosynthesis. However, this approach would likely provide a lot of hits and not pinpoint an exact direct mechanism.

Discussion and future studies on AlgP.

Since only a small subset of genes were identified in Chapter 2 to be significantly regulated by the histone-like protein AlgP and most of the regulation that we did see was small, we ponder that AlgP might be more involved in fine tuning gene expression rather than regulating genes on or off. This might be typical for histone-like proteins as they are thought to contribute to the overall DNA and nucleoid structure within a cell as a result of their broad DNA binding abilities. Evidence for this stems from the fact that a small purified peptide from the C-terminus of AlgP nonspecifically binds all of the DNA probes that were tested.

Only a little bit is known about AlgP and no biochemical studies have been performed. Future experiments using AlgP to perform chromatin immunoprecipitation sequencing (ChIP-seq) assays could determine if there are any specific sequences bound by AlgP or if, in fact, binding is nonspecific or random. Further, we found that *algP* promoter activity is upregulated during stationary phase. It would be interesting to perform RNA-sequencing in stationary phase cultures to determine if any more genes are significantly regulated by AlgP.

We also have not determined a mechanism for how AlgP, while expressed by both nonmucoid and mucoid strains, can regulate a different subset of genes depending on the strain background. One of our hypotheses is that AlgP requires certain co-factors in order to bind certain regions of DNA. Purifying AlgP and using this in a protein-protein pull-down assay would determine whether this protein has any strain specific co-factors that might be necessary for function by either flowing over supernatants from a nonmucoid strain or mucoid strain.

Discussion and future studies on O antigen.

Appendix 1 and Appendix 2 mainly focuses on identifying factors that regulate the O antigen chain-length control proteins *wzz1* and *wzz2* as well as attempt to determine the physiological and biological relevance of producing two preferred modalities of O antigen. While we are closer to understanding regulation of O antigen in mucoid *P. aeruginosa* (Chapter 3), there may be other factors responsible for regulating chain-length in nonmucoid strains and in other contexts. To begin to understand how O antigen chain length is regulated in response to the environment we focused on building reporters for measuring the expression of the *wzz1* and *wzz2* promoters.

While we extensively mapped the *wzz2* promoter region, this has not been done for *wzz1*. Further, since *wzz1* is serotype specific and the first gene in the serotype specific O antigen biosynthesis operon, the promoter for *wzz1* may be different depending on the strain background. Future studies can determine if there are any common features between the upstream region of these operons. Additionally, since the promoters are likely not all conserved, there may be different transcriptional regulators of *wzz1* dependent on serotype or strain background. For example, as we see in Appendix 2, each serotype strain may behave differently in regards to responses to environmental stimuli, such as human serum.

Experiments ongoing in our laboratory are using the Biolog™ phenotypic microarray plates to discover conditions that impact survival in the absence of very long O antigen. In this system we can quickly compare growth of strains in almost 2,000 different environments. These range from conditions like increasing osmotic pressures, differences in pH, the presence of alternative carbon and nitrogen sources, and chemical stresses such as antibiotics. Once a condition that alters *wzz1* and/or *wzz2* expression is identified using the Biolog™ we can then

more directly assess this using a scaled-up plate assay and collect samples for analyzing O antigen expression by immunoblot or pro-Q glycolipid staining. Also, as previously mentioned, it was shown that high temperatures, low pH, or low concentrations of phosphate or high concentrations of NaCl, $MgCl_2$, glycerol, or sucrose resulted in decreased amounts of the very long high molecular weight O antigen with little effect on the long O antigen lengths. Using the reporters created here we can directly measure the impact of these conditions of *wzz1* and *wzz2* expression. Detailed studies of *wzz1* and *wzz2* expression will provide insight into mechanisms through which *P. aeruginosa* adapts to its environments.

Concluding remarks.

Transition of *P. aeruginosa* from a nonmucoid to a mucoid phenotype correlates with the establishment of a chronic lung infection in people with cystic fibrosis. Understanding how and why the mucoid phenotype emerges will elucidate mechanisms that are selected for during the establishment of a long-term infection and inform us about host-pathogen interactions during chronic infections. Taken together, the data presented in this dissertation contributes to our overall knowledge of how *P. aeruginosa* regulates important chronic infection phenotypes, governed by the AlgT sigma factor. Preventing *P. aeruginosa* from adapting to the CF lung would lead to a better life for people who are infected. A thorough understanding of the multifaceted and complex regulatory systems in *P. aeruginosa* will provide knowledge on how this deadly opportunistic pathogen adapts and persists to cause disease.

Appendix 1

Construction of reporters to test the temperature regulation and single cell dynamics of *wzz1* and *wzz2* in *Pseudomonas aeruginosa*

Adapted from undergraduate research projects designed for

Anika Sinha and Rita Wang

INTRODUCTION

Pseudomonas aeruginosa usually persists in environments associated with human activity and is a prominent opportunistic pathogen, causing life-threatening infections in immunocompromised people (15, 21, 22, 30). The approximately 5,500 genes of the *P. aeruginosa* chromosome are expressed differently depending on which environment the bacterium finds itself (2, 215, 216). It has been long thought that virulence genes are upregulated at higher temperatures so that *P. aeruginosa* can establish an infection in a warm-blooded host (215). However, it is becoming apparent that virulence factors can also be increased in expression at 25°C, i.e. room temperature, compared to 37°C, i.e. human body temperature (217, 218). Understanding how these virulence factors are regulated will aid in developing targeted treatments that can prevent the expression of virulence factors and therefore the establishment of infection.

O antigen, the repeat polysaccharide attached to lipopolysaccharide (LPS), is thought to be thermoregulated (122, 139, 141, 219). The presence of O antigen on the outer membrane aids in resistance to serum as well as for survival and dissemination during an infection (141). *P. aeruginosa* can vary the amount and length of O antigen produced in response to different environmental conditions (143). Previously it was shown that high temperatures, low pH, or low concentrations of phosphate or high concentrations of NaCl, MgCl2, glycerol, or sucrose resulted in decreased amounts of the very long high molecular weight O antigen with little effect on the long O antigen lengths (143). Each O antigen chain length is controlled by a chain-length control protein. Wzz1 controls assembly of long O antigen while Wzz2 controls assembly of very long O antigen (48, 139-141, 220). However, whether any of these conditions affect expression of *wzz1* or *wzz2* was not accessed.

To begin to understand how O antigen chain length is regulated in response to temperature, Erika Kintz, a previous graduate student in our laboratory, studied the effects of *wzz1* and *wzz2* expression in laboratory strain PA103. The *wzz1* gene is located at the beginning of the O antigen biosynthesis operon and the sequence is serotype specific. Contrary, the *wzz2* gene is located elsewhere in the chromosome and conserved among *P. aeruginosa* strains. Kintz found that *wzz2* mRNA, Wzz2 protein production, and very long O antigen are decreased at 37°C compared to 25°C and that *wzz1* expression is unaltered between these two temperatures (219). This is contradictory to *Yersinia enterocolitica* and *Aermonas hydrophilia*, where O antigen is increased in production at the lower temperature (197, 221).

There are 20 different serotypes of *P. aeruginosa*, with each serotype exhibiting a unique O antigen sugar composition and lengths (124). This is in part due to the fact that *wzz1* genes and O antigen loci are serotype specific between each strain (140). However, *wzz2* is located outside of the O antigen operon and is mostly conserved between all *P. aeruginosa* strains (127, 140, 141). Since PA103 is a serotype O11 strain, we were interested in knowing if *wzz1* and *wzz2* temperature regulation is conserved in other serotype backgrounds. Therefore, the *wzz1* and *wzz2* promoters were identified in serotype O5 strain PAO1, fused to a promoterless-*lacZ*, and the effects of temperature on these two reporters was assessed. Additionally, since the regulation of *wzz1* and *wzz2* are typically studied at the population level, using the same promoters we constructed transcriptional fusions to fluorescent proteins in order to assess the expression of both genes at the single cell level using fluorescent microscopy. Unraveling how O antigen is regulated through detailed studies of *wzz1* and *wzz2* expression will provide insight into unique mechanisms of transcriptional regulation through which *P. aeruginosa* adapts to its ever-changing environments.

RESULTS AND DISCUSSION

Promoter activity of different sized fragments from upstream of *wzz2*. In order to better understand the regulation of O antigen we first sought to analyze the *wzz2* promoter in greater detail. Work performed by a previous graduate student Erika Kintz sought to identify the *wzz2* promoter in serotype O11 strain PA103 (219). She found a promoter located ~450 bps upstream of the *wzz2* coding sequence located within the PA0937 gene. Using site directed mutagenesis of this predicted promoter, it was confirmed that there was no other promoter downstream of this promoter. Kintz also found that the PA0937 promoter could drive Wzz2 production. To determine if the location of the *wzz2* promoter in serotype O5 strain PAO1 was the same, 8 different fragments spanning 1000 bps of DNA upstream of the *wzz2* coding region were fused to a promoterless-*lacZ* and inserted in single-copy at the CTX site into the chromosome of PAO1 (Fig. A1.1A).

Promoter activity of each fragment was accesses and compared to a no promoter control (Fig. A1.1B). The 100 bp of *wzz2* upstream DNA fragment had comparable promoter activity to the no promoter control indicating that no promoter exists on this fragment. Conversely, the 200 bp fragment had high promoter activity of ~1500 Miller units (MU) in PAO1 indicating that a promoter is present on this fragment. This is different from PA103 since a promoter driving *wzz2* expression was not identified in this region. The PAO1 500 bp and 1000 bp fragments had similar promoter activities, but slightly reduced activity compared to the 200 bp fragment. This suggests the presence of an additional regulatory region located between 200-500 bp upstream of *wzz2*. Analysis of the 200 bp fragment revealed a predicted AmrZ-binding site (CGATAGCATAATG). AmrZ is a transcription factor that is highly upregulated in mucoid strains. We therefore hypothesized that these fragments would have reduced promoter activity in

mucoid *P. aeruginosa* strain PDO300, which is an isogenic derivative of PAO1. In support of our hypothesis, the 200 bp and 500 bp fragments had activity similar to the no promoter control. The 1000 bp promoter fragment had slightly increased activity, but was still less than the promoter activity of the 1000 bp promoter fragment in PAO1. Therefore, AmrZ binds these fragments in PDO300 and inhibits *wzz2* expression.

To confirm the presence of a promoter at the predicted region, we removed the 200 bp region from the 500 bp promoter fragment (fragment named "500delAmrZ"). This fragment had no promoter activity in either PAO1 or PDO300 (Fig. A1.1B). Therefore, the promoter is contained 100-200 bp upstream of the *wzz2* start codon. Since Kintz identified an alternative promoter ~450 bp upstream of the *wzz2* codon sequence within the PA0937 gene, we also constructed a fragment containing only this region (fragment named "middle"). Likewise, to the previous fragment, no promoter activity in PAO1 or PDO300 was detected from this region. Therefore, unlike in PA103, there is no *wzz2* promoter located within PA0937 in PAO1. This is surprising since the predicted -10 and -35 sequences (TACTACAAT/CTGCCC) are the same in PAO1 and PA103.

We also sought to the activity of the PA0937 promoter in PAO1 and PDO300 since this gene may contribute to the expression of *wzz2*. To test this a fragment containing entire PA0937 gene and promoter (fragment named "middle+PA0937") as well as a fragment containing just the PA0937 promoter (fragment named "PA0937") was accessed. The PA0937 promoter fragment had high promoter activity with the same expression in PAO1 and PDO300 (Fig. A1.1B). Interestingly, the middle+PA0937 fragment still had high promoter activity in PDO300, but had ~-2.5-fold reduced expression in PAO1. This trend is opposite from what we see for the *wzz2* promoter fragments where expression is higher in PAO1.

PA0937 and *wzz2* can be co-transcribed on the same mRNA. As mentioned above, Kintz also found that *wzz2* and PA0937 could be co-transcribed in PA103 (219). Since we found that the PA0937 promoter has very high activity it is therefore likely that this promoter could promote *wzz2* expression. In order to determine if PA0937 and *wzz2* are co-transcribed, we generated cDNA using whole cell RNA from PAO1 and PDO300 and performed PCR using primers located within the coding sequences of PA0937 and *wzz2* (primers F1 + R1). A PCR product should only be amplified if a cDNA sequence contains both genes. As a control, genomic DNA was used in the reaction, which should always amplify a band. When the PCR reactions are separated on a gel, the genomic DNA produced an 800 bp band representing the DNA region connecting PA0937 and *wzz2* (Fig. A1.2). Likewise, PAO1 and PDO300 cDNA samples also produced an 800 bp band, concluding that PA0937 and *wzz2* can be co-transcribed. As a control for no co-transcription, a primer (primer F2) was also designed to bind upstream of the PA0937 promoter. A PCR product should not be produced since an mRNA will not be transcribed from upstream of the promoter. In support of this, PAO1 and PDO300 cDNA samples did not amplify a band using primers F2 + R1 while PAO1 genomic DNA produced ~1250 bp band (Fig. A1.2). A no template control produced no band in either reaction indicating no genomic DNA contamination within the samples.

Altogether these data conclude that PA0937 and *wzz2* can be co-transcribed. Therefore, a portion of the activity from the 1000 bp promoter fragment-*lacZ* reporter in Figure A1.1B could be attributed to the PA0937 promoter. However, since activity of the 1000 bp fragment is more similar to the 500 bp fragment and not as highly expressed as the PA0937 promoter fragment it is likely that the PA0937 promoter does not play a major role in promoting *wzz2* expression.

Identification of the *wzz2* transcription start site in PAO1 and PDO300. We next mapped the transcription start site (TSS) for *wzz2* in both PAO1 and PDO300 using 5'-RACE. In PAO1, we identified a TSS 70 nucleotides upstream of the *wzz2* coding sequence (Fig. A1.3). Based on this result, it is likely that the *wzz2* promoter overlaps with the AmrZ binding site. This makes sense since *wzz2* promoter activity is repressed when AmrZ is overexpressed. It is known that AmrZ can act as a repressor by binding to promoter regions (114). Further, a promoter located in this region validates our promoter assay data that identified a promoter located between nucleotides ~100-200 bps upstream of *wzz2* (Fig. A1.1B). Since *wzz2* promoter activity is repressed in PDO300, we did not expect to identify a *wzz2* TSS in this strain. However, we observed a TSS 246 bps upstream of *wzz2* in PDO300(Fig. A1.3). However, this region does not contain promoter activity (Fig. A1.1B). Therefore, this is likely just background noise.

Temperature alters promoter activity of *wzz1* or *wzz2* in PAO1 in stationary phase. In PA103, Kintz found that the *wzz2* promoter, *wzz2* mRNA, Wzz2 protein production, and very long O antigen are all decreased at 37°C compared to 25°C (219). We hypothesized that the PAO1 *wzz2* promoter would show a similar trend and be decreased in expression at 37°C. First, we grew PAO1 at both 25°C and 37°C to determine at what time point cultures entered exponential and stationary phase at each temperature (Fig. A1.4A). Next, using the 500 bp *wzz2* promoter fragments described above, we accessed whether promoter activity was temperature regulated during exponential and stationary phase growth. During exponential phase, *wzz2* promoter activity had similar levels of expression at both temperatures with no significant differences (Fig. A1.4B). However, at stationary phase, *wzz2* promoter activity was significantly increased at 37°C compared to 25°C (Fig. A1.4B). This is contradictory to what was observed

for strain PA103 where there was an increase *wzz2* promoter activity and protein expression at 25°C compared to 37°C in both exponential and stationary phase.

We were also interested in testing if *wzz1* is temperature regulated. Kintz found a predicted *wzz1* promoter located within the 3'-end of *rpsA* (219). There are two genes located within this region; *orfA* and *himD*. The organization of the *wzz1* promoter region in PAO1 is arranged differently from that of PA103. Analysis of this region revealed an unannotated open reading frame immediately upstream of *wzz1* that shared little similarity to *orfA*. Additionally, the distance between *wzz1* and *rpsA* is 1,180 bps in PAO1 while this distance is 812 bps in PA103. Despite the differences, we constructed a 1250 bp *wzz1* promoter-*lacZ* reporter that extended to contain the 3'-end of *rpsA*. We next assessed whether this fragment had promoter activity and if this activity was different at 25°C compared to 37°C. We observed no difference in *wzz1* promoter activity between 25°C compared to 37°C at exponential phase (Fig. A1.4C). However, at stationary phase we observed a significant increase in *wzz1* promoter activity at 37°C compared to 25°C (Fig. A1.4C). Kintz, however, observed no difference in PA103 *wzz1* promoter activity at either temperature or growth phase. Consequently, it seems that strain background plays an important role in temperature regulation of *wzz1* and *wzz2* in *P. aeruginosa*. Additional experiments are needed to determine if the *wzz1* or *wzz2* promoters as well as production of O antigen are thermoregulated at other temperatures and growth phases. Since *P. aeruginosa* is also a plant pathogen, experiments using lower temperatures could provide insight into plant-pathogen interactions considering the average outdoor temperature in the United States is ~13°C (usclimatedata.com).

The *wzz1* and *wzz2* promoters are both expressed at the single cell level. The ß-galactosidase assays used before give a snapshot of gene expression within a population of cells.

However, we were also interested in knowing if both *wzz1* and *wzz2* are simultaneously expressed at the single cell level or if this expression is heterologous within the population. Since we have identified fragments containing promoter activity for both *wzz1* and *wzz2*, we constructed new fluorescent reporters to test the expression dynamics of each gene at the single cell level using time-lapse fluorescent microscopy. First, the 500 bp *wzz2* promoter fragment was fused to *mCherry* and the 1250 bp *wzz1* promoter fragment was fused to *gfp*. $P_{wzz2(500)}$-*mCherry* was then inserted in single copy at the CTX site and $P_{wzz1(1250)}$-*gfp* was inserted in single copy at the Tn7 site in the chromosome of PAO1. Overnight cultures of this PAO1 CTX::$P_{wzz2(500)}$-*mCherry Tn7::*$P_{wzz1(1250)}$-*gfp* dual reporter strain were serially-diluted to a low optical density, plated onto an agarose pad, and growth of this strain was monitored for 10 hours. The expression of mCherry and GFP was also monitored over time. Analysis of GFP fluorescence as a read out of *wzz1* promoter activity revealed bright green fluorescent single cells at t1 (0 mins). These cells continued to divide and express GFP for the entirety of the experiment (Fig. A1.5). A similar trend was observed for wzz2 promoter activity as a read out of mCherry fluorescence. While this reporter was not as bright as GFP, each individual cell produced red fluorescence throughout the course of the experiment (Fig. A1.5). When overlaid together, the composite image shows each cell with a slight yellow fluorescence indicating that each individual cell is expressing both green and red fluorescence. Taken together we conclude that both *wzz1* and *wzz2* are expressed within each individual cell though out the time points tested. One caveat, however, is that *P. aeruginosa* itself has some autofluorescence and could result in background noise in the experiment. This experiment should be repeated and include wild type PAO1 without any reporters as a control. Secondly, the expression of each of the fluorescent proteins was very low due to low expression of each promoter and the fact that each reporter was inserted in single copy. Future experiments

could optimize this experiment by testing different fluorescent proteins to find a pair where fluorescence can bet better visualize at a low concentration.

Flow cytometry analysis of single PAO1 cells expressing fluorescent reporters for *wzz1* and *wzz2*. A higher throughput method to measure single-cell expression of *wzz1* and *wzz2* is to use flow cytometry. Here, thousands of cells can be quickly and individually analyzed. By using fluorescently labeled cells, we can also analyze the expression of GFP and mCherry within each cell. Wild type PAO1, PAO1 containing either CTX::$P_{wzz2(500)}$-*mCherry* or *Tn7::*$P_{wzz1(1250)}$-*gfp* individually, and the dual reporter strain were all grown overnight, washed, and serially-diluted before being run on the flow cytometer. Wild type PAO1 without any reporters was analyzed first to determine the amount of background fluorescence. This PAO1 strain (orange scatter) had very low fluorescence compared to the other three strains, but still produced a slight green fluorescence and no red fluorescence (Fig. A1.6). Next, PAO1 CTX::$P_{wzz2(500)}$-*mCherry* (red scatter) and PAO1 *Tn7::*$P_{wzz1(1250)}$-*gfp* (green scatter) were individually run through the flow cytometer. PAO1 *Tn7::*$P_{wzz1(1250)}$-*gfp* had an increase in the number of individual cells positive for green fluorescence compared to wild type PAO1 (Fig. A1.6). However, these cells also appeared to be scattering upwards towards the red fluorescent axis of the graph. CTX::$P_{wzz2(500)}$-*mCherry* also had a larger number of cells with positive fluorescence, mostly scattering upwards towards the red axis (Fig. A1.6). When the dual reporter PAO1 CTX::$P_{wzz2(500)}$-*mCherry* or *Tn7::*$P_{wzz1(1250)}$-*gfp* strain (magenta scatter) was compared to the other strains, the scatter mostly overlapped with that of PAO1 CTX::$P_{wzz2(500)}$-*mCherry* (Fig. A1.6). However, a number of cells did exhibit some green fluorescence and had a patter similar to *Tn7::*$P_{wzz1(1250)}$-*gfp*. For all fluorescent strains, each individual cell exhibited different amounts of red or green fluorescence that might be associated with different amounts of expression in each individual cell. Like

mentioned above, it might be necessary to optimize the fluorescent reporters in order to see greater differences between reporters and to also test exponentially growing cells since this could provide a more homogenous fluorescent population with fewer dead cells.

Single cell analysis of PAO1 O antigen mutants using interferometry. While studying *wzz1* and *wzz2* expression reveals insights into the regulation of O antigen chain length, the expression of these genes does not necessarily correlate with amount of long or very long O antigen produced on the surface of each cell. To get around this, we visualized a series of O antigen mutants using interferometry in collaboration with the physics department at the Georgia Institute of Technology. Interferometers shoot electromagnetic waves at a surface and measure the interference produced by the surface. This interference pattern can then be measured and analyzed. While mostly used on large surfaces, we sought to adapt this technique to quantify the differences in the surface of wildtype PAO1 cells that produce both long and very long O antigen as well as a *wzz1* mutant that does not produce long O antigen, a *wzz2* mutant that does not produce very long O antigen and a *galU* mutant that does not produce any O antigen. We hypothesized that the surface roughness would be different between O antigen mutants. We washed overnight cultures of each strain in water, normalized to a low optical density, and spotted this culture on an agarose pad to form a "coffee ring". Images were acquired from the edge of the ring. Next, an image was stitched together encompassing many single cells (Fig. A1.7A-C).

Next, our collaborators developed a machine learning algorithm, based on 100's of single cell images of each mutant, to determine if a computer could discern if a single cell is a wildtype, *wzz1, wzz2,* or a *galU* mutant cell. After feeding the machine many images of each mutant we then gave new images and asked the algorithm to classify the strains as wildtype, *wzz1, wzz2,* or

galU mutants. The results are as follows. If the classifier was given a wild type cell, 50% of the time it was able to discern that it was wildtype, but it would sometimes think the cell was a *wzz2* mutant or a *galU* mutant. However, it would never predict that a wild type cell was a *wzz1* mutant. Next, when fed *galU* mutants, the classifier would guess correctly 80% of the time. 12% of the remaining 20% was incorrectly attributed to wild type cells. Surprisingly, when fed *wzz1* mutants, the classifier 100% of the time distinguish these as *wzz1* mutants. Finally, when given *wzz2* mutants, the classifier determines these to be *wzz2* mutants most of the time. However, it almost as frequently guesses that these are wildtype strains with *galU* mutants not far behind. Ultimately, the most concrete result we can gather from these data is that the *wzz1* mutants have the most different surface from the other three strains. While these data are very preliminary, we might also be able to conclude that wild type cells look very similar to *wzz2* mutants, which do not make very long O antigen. Therefore, it is possible that wild type PAO1 cells mostly contain uncapped LPS or LPS capped with long O antigen with little very long O antigen. Ultimately, this experiment needs to be repeated so that the classifier has more single cell images and biological replicate data in order to produce more robust and rigorous results.

MATERIALS AND METHODS

Construction of *wzz1* and *wzz2* transcriptional *lacZ* reporters. The miniCTX-optRBS-P_{wzz2}-*lacZ* reporters contain either 100 bp (pARC14), 200 bp (pARC25), 500 bp (pARC15), or 1000 bp (pARC16) of the upstream region of the *wzz2* coding sequence, minus the 25 bp immediately upstream of the start codon to avoid the RBS, which were amplified using oAC53/oAC55, oAC53/oAC83, oAC53/oAC54, using oAC52/oAC53, respectively. The 500delAmrZ (pARC49), middle (pARC26), middle+PA0937 (pARC27), and PA0937 (pARC31) promoter fragments were amplified using oAC54/oAC88, oAC54/oAC083, oAC52/oAC083, and oAC52/oAC95, respectively. Each fragment was then inserted into gel purified (Qiagen), BamHI digested miniCTX1-optRBS-*lacZ* using isothermal assembly. miniCTX-optRBS-$P_{wzz1(1250)}$-*lacZ* (pARC32) was constructed by amplifying 1250 bp of the upstream region of the *wzz1* coding sequence, minus the 25 bp immediately upstream of the start codon to avoid the RBS, using oAC98/oAC99. This fragment was then inserted into gel purified (Qiagen), BamHI digested miniCTX1-optRBS-*lacZ* using isothermal assembly. Plasmids were PCR verified using oAC32/33, which amplify across the MCS. PCR verified plasmid was then electroporated into PAO1, as previously described, and selected for on 100 μg/ml tetracycline. Insertion at the CTX site was verified using oAC56/oAC57. A complete list of strains, plasmids, and primers is available in Table A1.1.

RT-PCR. 500 μl of exponential phase culture was added to 1 ml of RNA Protect (Qiagen), incubated at room temperature for 5 mins, and then centrifuged at 5,000 x g for 10 mins. Pellet was air-dried and stored at -80°C. RNA was extracted using the MasterPure RNA Purification Kit (Epicentre) following the manufacturers protocol and DNase treated (TURBO DNase,

Thermo Fisher). Next, 1 μg of total RNA was converted into cDNA using random hexamers using the SuperScript III First-Strand Synthesis System Kit (Invitrogen). Samples were amplified using the following primer pairs: F1; oAC79, F2; oAC87, and R1; oAC78.

5'-RACE. RNA was prepared from 1 ml of exponentially growing cultures (as described above). Next, *wzz2* cDNA was synthesized and 5'-RACE performed using a 5'-RACE System kit (Invitrogen) with modifications for G::C rich DNA fowling the manufacturer's instructions. Briefly, 2.5 μg of RNA was incubated with oAC64 (GSP1) for 10 mins at 70°C and then transferred to a 50°C heat block. At the same time, the PCR master mix (minus the SuperScript II reverse transcriptase) was assembled and incubated at 50°C. Next, the prewarmed reaction mixture and 1 μl of SuperScript II was added to the RNA/primer mixture and continued to be incubated at 50°C for 50 mins. The reaction was then terminated at 70°C for 15 mins and transferred to a 37°C heat block. Once equilibrated, RNase was added and the reaction continued at 37°C for 30 mins. The cDNA was cleaned by adding room temperature binding solution and purified using the provided column and wash buffers and stored at -20°C. Finally, the purified cDNA was tailed with dATP using the terminal transferase enzyme at 37°C for 10 mins which was then heat-inactivated 65°C for 10 minutes. Second strand synthesis was carried out using the 5'-RACE Abridged Anchor primer and again column purified. PCR was performed using oAC66 (GSP2) and the Abridged Universal Amplification (AUAP) primer to amplify the final product. Often, a single PCR was not enough to visualize the reaction on an agarose gel so one or two rounds of nested PCR using oAC80 (GSP3) and AUAP was performed until product could be visualized. The final product, once confirmed by agarose gel electrophoresis, was PCR purified and sequenced by Genewiz using GSP3.

ß-galactosidase assays. Single colonies were used to inoculate LB with no antibiotic. Bacteria were grown at 37°C or 25°C, rolling, for the allotted time indicated by each experiment. LacZ activity and Miller Units were calculated as previously described (48).

Construction of miniTn7-P$_{wzz1}$-*gfp*. The *wzz1* promoter containing an optimized ribosome binding site (RBS) was amplified by PCR using oAC215/oAC216 from pARC32 (described above). *gfp* was amplified by PCR using oAC217/oAC218 from pMRP9-1 (222). Both pieces were then inserted into gel purified (Qiagen), HindIII digested plasmid miniTn7 using Gibson assembly, following the manufacturers protocol. Next, the reaction was transformed into chemically competent DH5α by heat-shock and selected for on gentamicin. Plasmids were PCR verified using oAC215/oAC218. PCR verified plasmid was then electroporated into PAO1, as previously described, and selected for on 60 μg/ml gentamicin.

Construction of miniCTX1-P$_{wzz2}$-*mCherry*. The *wzz2* promoter containing an optimized ribosome binding site (RBS) was amplified by PCR using oAC211/oAC212 from pARC15 (described above). *mCherry* was amplified by PCR using oAC213/oAC214 from pMP7605 (222). Both pieces were then inserted into gel purified (Qiagen), HindIII digested plasmid miniCTX1 using isothermal assembly. The reaction was then transformed into chemically competent DH5α and plasmids were selected for on tetracycline. Plasmids were PCR verified using oAC211/oAC214 (miniCTX1 with no insert was used as a negative control). PCR verified plasmid was then electroporated into PAO1, as previously described, and selected for on 100 μg/ml tetracycline.

Fluorescent microscopy. Cells were grown to exponential phase in LB, back-diluted to an OD_{600} of 0.01 in PBS, and spotted onto 1% agarose pads. Time-lapse images were taken every 40 mins using an inverted fluorescent microscope equipped with a chamber set at 37°C. with the help of Dr. Dai Le in the laboratory of Dr. Minsu Kim. Composite images were compiled and analyzed using ImageJ Fiji software.

Flow cytometry. 1 µl of overnight cultures was diluted in PBS supplemented with 2.5 mM EDTA. Then BacLight was used to stain the cells for 15 mins at room temperature. Next, the suspension was then serially diluted 10-fold in PBS supplemented with 2.5 mM EDTA and then run on a BeckMan Coulter Cytoflex equipped with a SSC-detector off the violet channel (V-SSC) at the Emory flow-cytometry core. The V-SSC allows for better detection of smaller particles than a conventional cytometer. Samples were run at a flow rate of 10 µl/min. Raw fcs files were analyzed using FlowJo 10.4. Since coincident events are possible and cannot be resolved with a typical singlets gate due to the size of the bacteria, event rate and average median fluorescence intensity (MFI) of each sample was calculated. Samples that maintained the same MFI (within 10% of each other) and had an event rate that decreased proportionally with the serial dilutions were analyzed. Sample wells that did not meet these criteria were not analyzed since singlet events could not be separated from coincident events.

Interferometry. A single colony was used to start an overnight culture in LB and grown rolling at 37°C. 1 ml of overnight culture was pelleted and the pellet was washed two times with water. This suspension was then diluted to an OD_{600} of 0.2 and 2 µl was spotted on a very dry agar pad.

100X images were taken using an interferometer (Zygo newview Ametek Ultra Precision Technologies) and stitched together from the “coffee ring”. Small oval shapes ~2-3 μm in length were considered to be single cells. Interferometry was performed and a machine learning algorithm was developed by Ben Kalziqi in Peter Yunker’s lab (Georgia Tech) using hundreds of single cells in order to predict the genotypes of each based on their surface roughness.

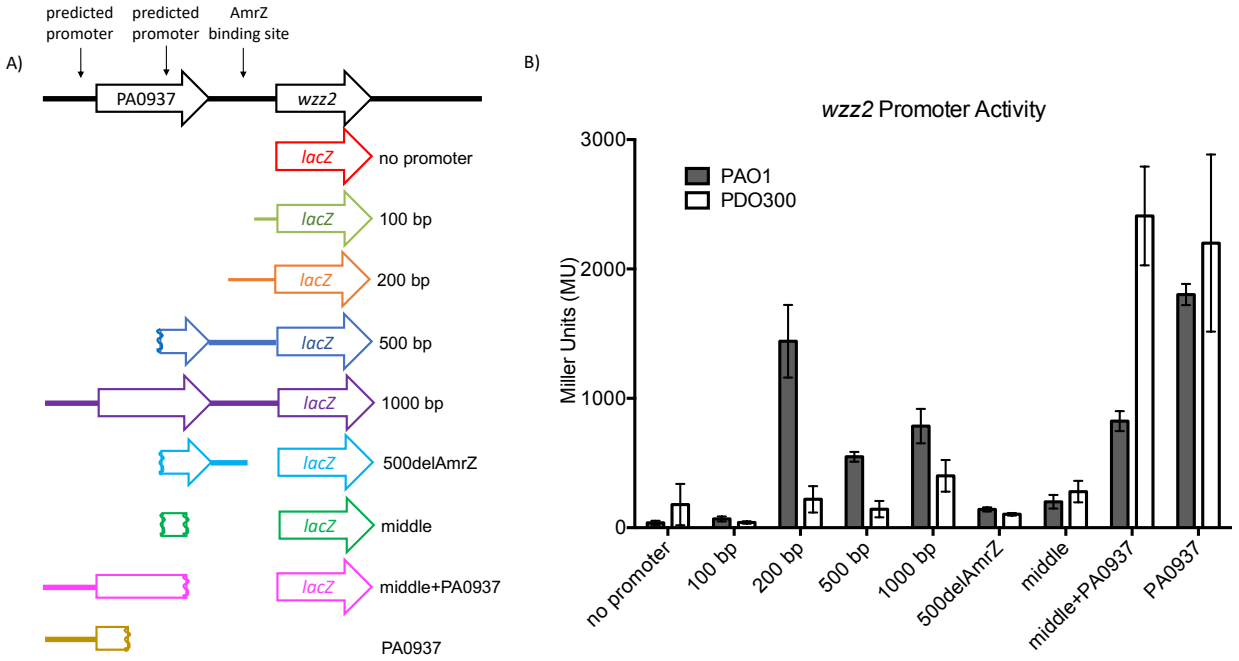

Figure A1.1. Promoter activity of different sized fragments from upstream of *wzz2*. A) Schematic representation of the *wzz2* promoter region in PAO1. The summary of promoter fragments fused to *lacZ* are shown below. B) Each fragment, starting 25 bps upstream of the start codon in order to avoid the ribosome binding site (RBS), was fused to a promoterless-*lacZ* containing an optimized RBS to create transcriptional fusions. Each construct was then inserted, in single copy, into the chromosome of PAO1 and PDO300 at the CTX site. LacZ activity, as a readout of promoter activity, was measured using ß-galactosidase assays. Error bars represent SD.

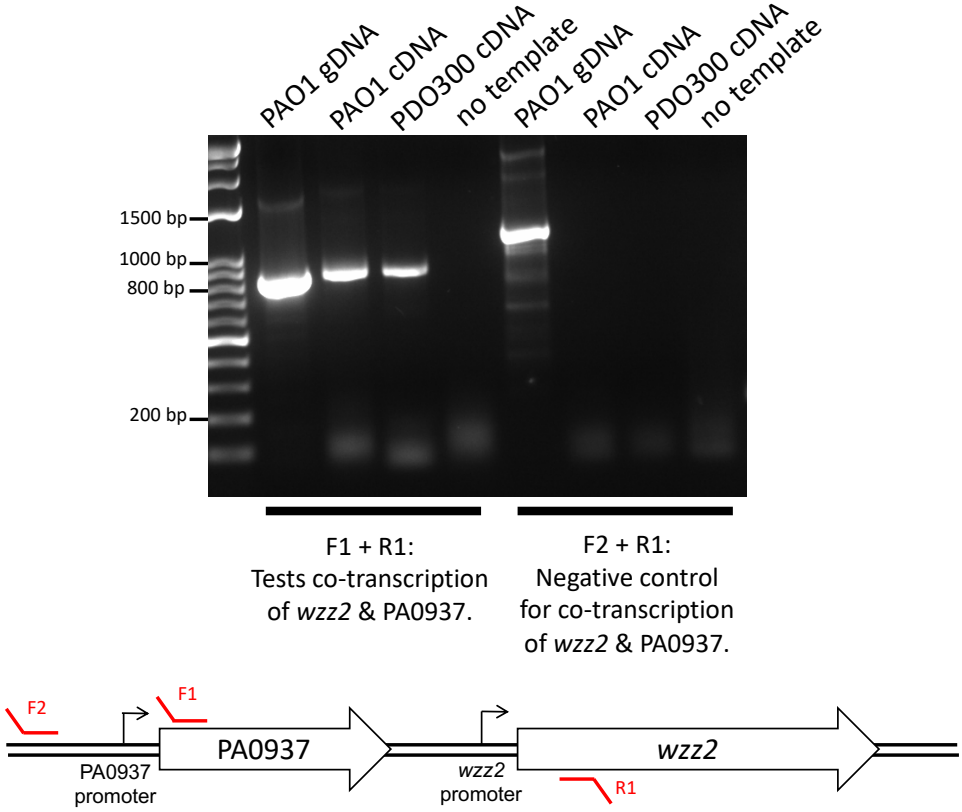

Figure A1.2. PA0937 and *wzz2* can be co-transcribed on the same mRNA. Total RNA was reverse transcribed into cDNA and then amplified by PCR. Top: Agarose gel of PCR reactions. PAO1 genomic DNA (gDNA) is used as a positive control and a no template control was used as a negative control in all three reactions. A band is only amplified in the F1 + R1 cDNA reaction indicating that PA0937 and *wzz2* are co-transcribed. Bottom: Diagram of *wzz2* and PA0937 promoter regions and location of primer binding sites.

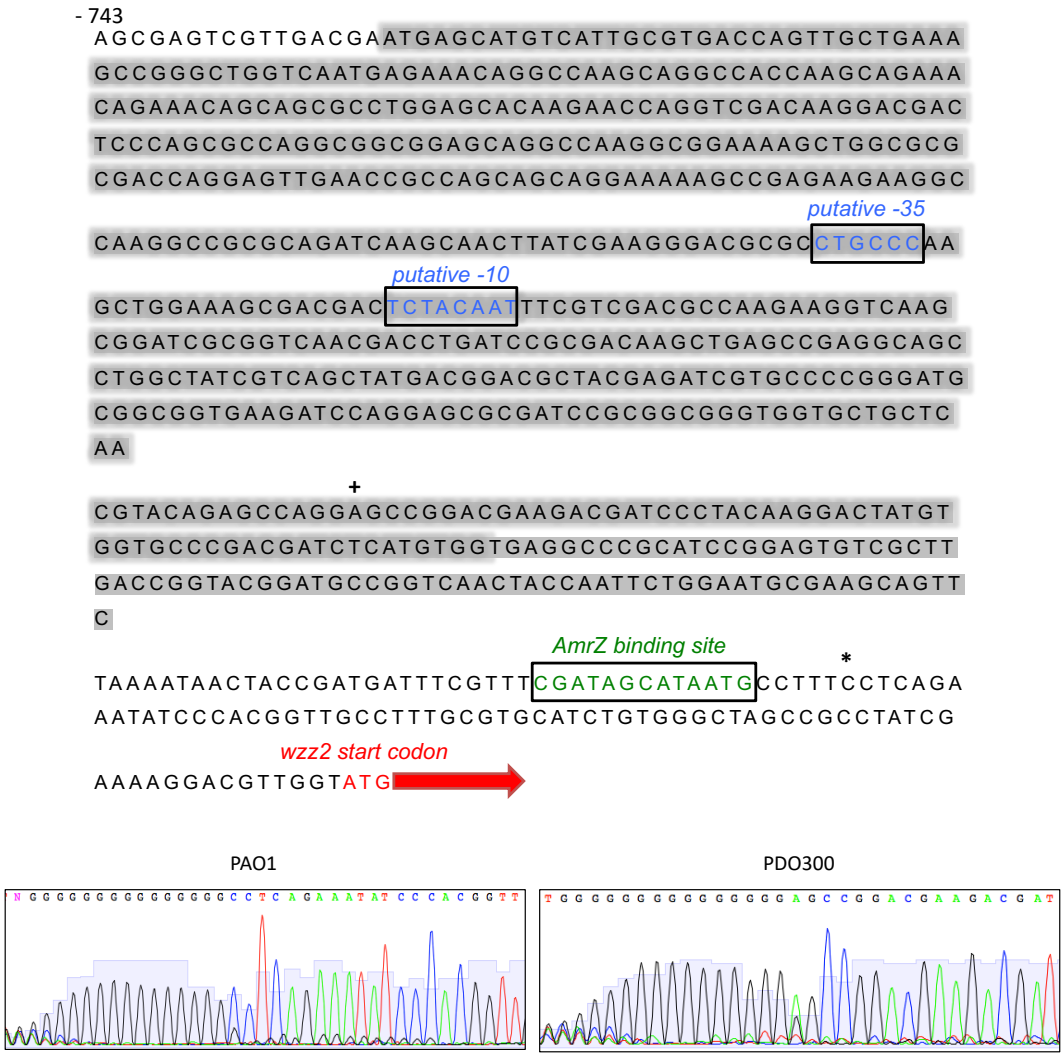

Figure A1.3. Identification of the *wzz2* transcription start site in PAO1 and PDO300. 5'-RACE was performed on *wzz2* cDNA generated from RNA isolated from PAO1 and PDO300 in order to determine the transcription start site (TSS) in each strain. Top: Diagram of important features located in the 743 nucleotides upstream of the *wzz2* coding region Bottom: Raw trace files showing location of each TSS. The start site is preceded by a tail of G nucleotides. Key: *: PAO1 TSS, +: PDO300 TSS, grey highlight: PA0937 coding sequence, green boxed letters: AmrZ binding site, blue boxed letters: Kintz predicted -10 and -35 region.

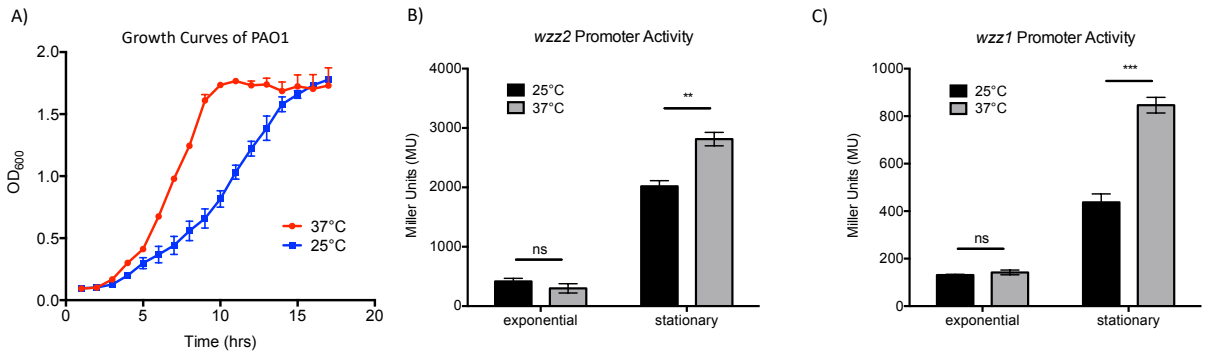

Figure A1.4. Temperature alters promoter activity of *wzz1* or *wzz2* in PAO1 at stationary phase. A) Growth curves for PAO1 grown at 25°C (blue squares) and 37°C (red circles) were performed in 96-well plates in a Synergy-H1 microplate reader. Samples were collected during exponential growth; ~8 hrs for growth at 37°C and ~12 hrs for growth at 25°C. B) Promoter activity of *wzz2* at 25°C and 37°C. C) Promoter activity of *wzz1* promoter at 25°C and 37°C.

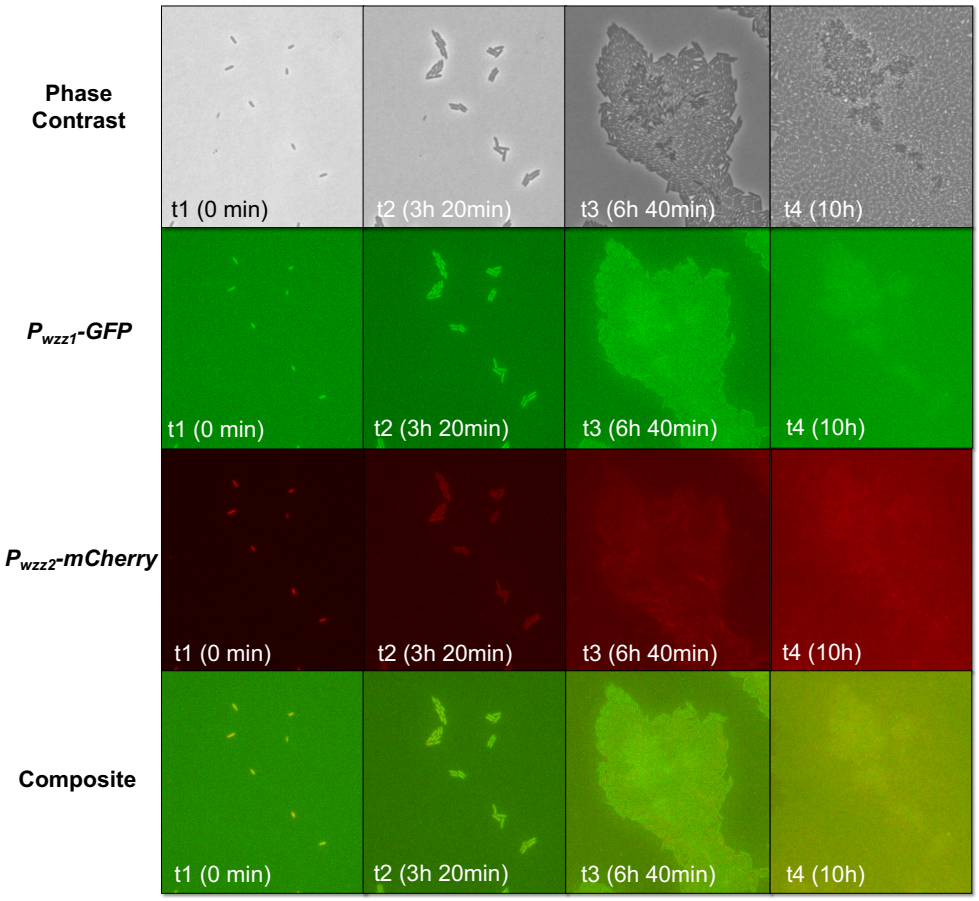

Figure A1.5. The *wzz1* and *wzz2* promoters are both expressed at the single cell level. The growth of PAO1 CTX::P$_{wzz2}$-*mCherry* Tn7::*P$_{wzz1}$-gfp* was monitored over 18 hrs of growth under a confocal fluorescent microscope. Images selected here were taken 200 minutes apart. The brightness of cells reflects the expression level of the *wzz1* and *wzz2* promoters. All individual cells residing in the selected region expressed both *wzz1* and *wzz2* from the beginning of this imaging. The expression of both chain-length regulator genes was sustained as cells proliferated overtime. Photo bleaching occurred around 10 hours into the imaging, which resulted in fading color. Images were compiled and analyzed using ImageJ Fiji software.

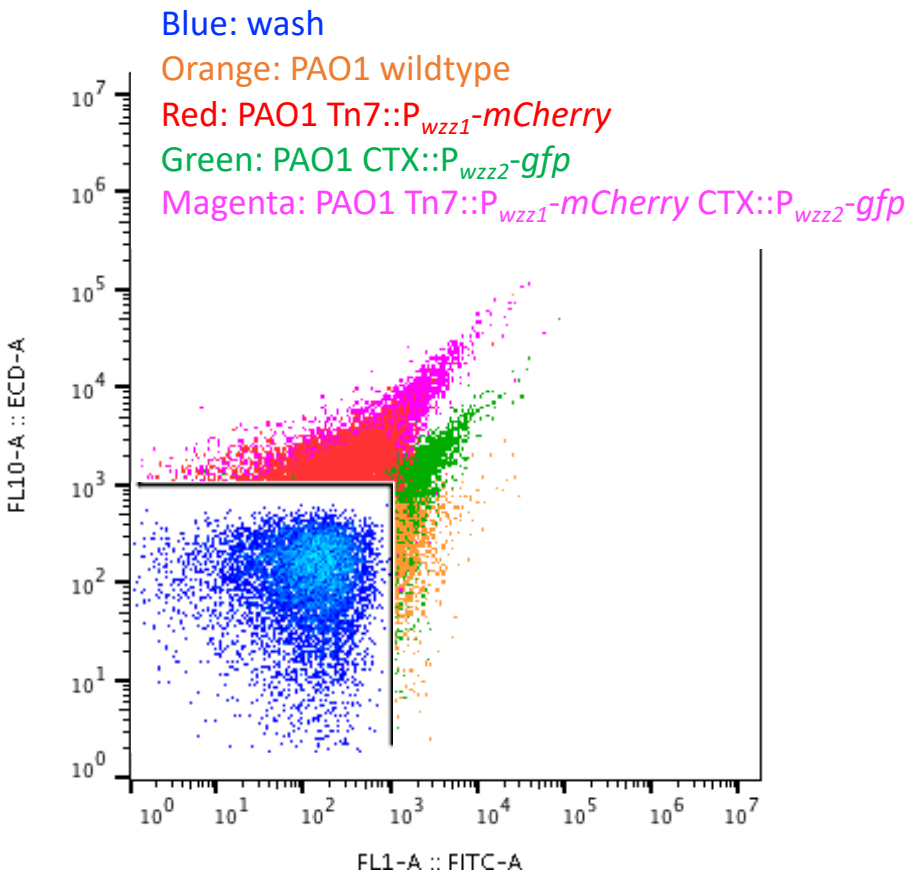

Figure A1.6. Flow cytometry analysis of single PAO1 cells expressing fluorescent reporters for *wzz1* and *wzz2*. Each single dot represents a single cell from an overnight culture grown in LB, no antibiotic. The y-axis represents an increase in red fluorescence while the x-axis represents an increase in green fluorescence. PAO1 wildtype cells have a slight green fluorescence contributing to some background.

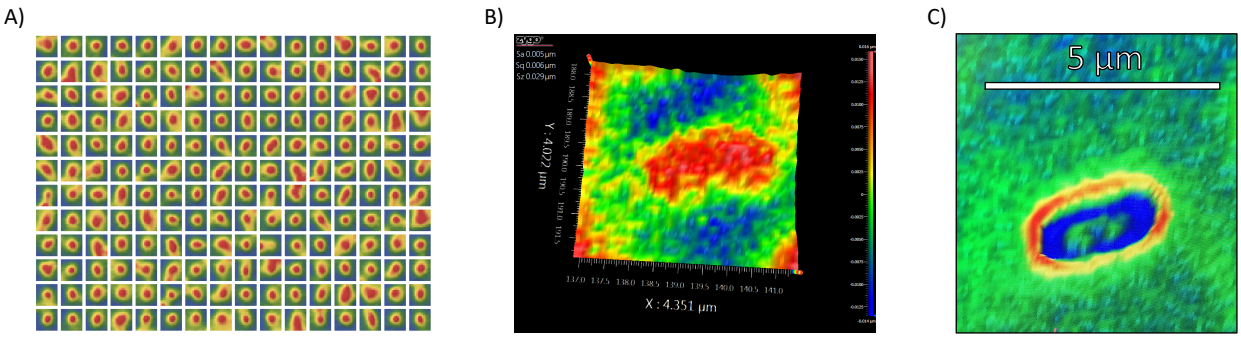

Figure A1.7. Single cell images of PAO1 using interferometry. Overnight cultures were washed and resuspended in water. This suspension was then diluted to an OD_{600} of 0.2 and 2 µl was spotted on a very dry agar pad. 100X images were taken using an interferometer by collaborators at Georgia Tech. A) Representative of 192 single cells of PAO1. B) Zoomed in view of representative PAO1 single cell showing surface roughness. C) Smoothed image of representative PAO1 single cell.

Table A1.1. Strains, plasmids, and primers used in this study.

Name	Description	Location
P. aeruginosa		
PAO1	nonmucoid laboratory strain	
PDO300	mucoid PAO1 *mucA22*	PAC01
PAO1 *wzz1::tet*	*wzz1* transposon mutant PW6291	PAC07
PAO1 *wzz2::tet*	*wzz2* transposon mutant PW2707	PAC03
PAO1 *galU::aacC1*	*galU* mutant disrupted by gentamicin resistant marker	PAC411
PAO1 CTX::optRBS-*lacZ*	no promoter control, single copy	PAC43
PAO1 CTX::P*wzz2*(100)-optRBS-*lacZ*	100 bp *wzz2* promoter fragment reporter, single copy	PAC63
PAO1 CTX::P*wzz2*(200)-optRBS-*lacZ*	200 bp *wzz2* promoter fragment reporter, single copy	PAC45
PAO1 CTX::P*wzz2*(500)-optRBS-*lacZ*	500 bp *wzz2* promoter fragment reporter, single copy	PAC47
PAO1 CTX::P*wzz2*(1000)-optRBS-*lacZ*	1000 bp *wzz2* promoter fragment reporter, single copy	PAC49
PAO1 CTX::P*wzz2*(500delAmrZ)-optRBS-*lacZ*	300 bp *wzz2* promoter fragment reporter missing AmrZ binding stie, single copy	PAC254
PAO1 CTX::P*wzz2*(middle)-optRBS-*lacZ*	predicted *wzz2* promoter fragment within PA0937 reporter, single copy	PAC79
PAO1 CTX::P*wzz2*(middle+PA0937)-optRBS-*lacZ*	PA0937 promoter fragment reporter including PA0937 gene, single copy	PAC81
PAO1 CTX::P*wzz2*(PA0937)-optRBS-*lacZ*	PA0937 promoter fragment reporter, single copy	PAC83
PAO1 CTX::P*wzz1*(1250)-optRBS-*gfp*	1250 bp *wzz1* promoter fragment reporter, single copy	PAC212
PDO300 CTX::optRBS-*lacZ*	no promoter control, single copy	PAC51
PDO300 CTX::P*wzz2*(100)-optRBS-*lacZ*	100 bp *wzz2* promoter fragment reporter, single copy	PAC53
PDO300 CTX::P*wzz2*(200)-optRBS-*lacZ*	200 bp *wzz2* promoter fragment reporter, single copy	PAC65
PDO300 CTX::P*wzz2*(500)-optRBS-*lacZ*	500 bp *wzz2* promoter fragment reporter, single copy	PAC55
PDO300 CTX::P*wzz2*(1000)-optRBS-*lacZ*	1000 bp *wzz2* promoter fragment reporter, single copy	PAC57
PDO300 CTX::P*wzz2*(500delAmrZ)-optRBS-*lacZ*	300 bp *wzz2* promoter fragment reporter missing AmrZ binding stie, single copy	PAC256
PDO300 CTX::P*wzz2*(middle)-optRBS-*lacZ*	predicted *wzz2* promoter fragment within PA0937 reporter, single copy	PAC85
PDO300 CTX::P*wzz2*(middle+PA0937)-optRBS-*lacZ*	PA0937 promoter fragment reporter including PA0937 gene, single copy	PAC87
PDO300 CTX::P*wzz2*(PA0937)-optRBS-*lacZ*	PA0937 promoter fragment reporter, single copy	PAC89
PAO1 CTX::Pwzz2(500)-optRBS-*mCherry*	500 bp *wzz2* promoter fragment red fluorescent reporter, single copy	PAC384
PAO1 Tn7::P*wzz1*(1250)-optRBS-*gfp*	1250 bp *wzz1* promoter fragment green fluorescent reporter, single copy	PAC388
PAO1 CTX::P*wzz2*(500)-optRBS-*mCherry* Tn7::Pwzz1(1250)-optRBS-gfp	dual *wzz2* and *wzz1* fluorescent reporters in single copy	PAC392
Plasmids		*DH5α / SM10*
pARC14	miniCTX-P*wzz2*(100)-optRBS-*lacZ*	ECAC12/32
pARC25	miniCTX-P*wzz2*(200)-optRBS-*lacZ*	ECAC39/41
pARC15	miniCTX-P*wzz2*(500)-optRBS-*lacZ*	ECAC13/33
pARC16	miniCTX-P*wzz2*(1000)-optRBS-*lacZ*	ECAC14/34
pARC49	miniCTX-P*wzz2*(500delAmrZ)-optRBS-*lacZ*	ECAC110/112
pARC26	miniCTX-P*wzz2*(middle)-optRBS-*lacZ*	ECAC46/49
pARC27	miniCTX-P*wzz2*(middle+PA0937)-optRBS-*lacZ*	ECAC47/50
pARC31	miniCTX-P*wzz2*(PA0937)-optRBS-*lacZ*	ECAC48/51
pARC32	miniCTX-P*wzz1*(1250)optRBS-*lacZ*	ECAC98/100
pARC10	miniTn7-P*wzz1*(1250)-optRBS-*gfp*	ECAC147/149
pARC09	miniCTX-P*wzz2*(500)-optRBS-*mCherry*	ECAC144/146
pMRP9-1	contains constitutive *gfp* , multicopy plasmid	ECAC137
pMP7605	contains constitutive *mCherry* , multicopy plasmid	ECAC139
Primers		
oAC32	GACCCACTCTCAGGAGTGAAC	
oAC33	CTCTTCGCTATTACGCCAGCTG	
oAC52	CTGGAGCTCCACCGCGGTGGCGGCCGCTCTAGAACTAGTGccagagtgacttttaccagg	
oAC53	AATCATGGTCATAGCTGTTCCTCCTTACTGCAGCCCGGGGtagcccacagatgcacgcaa	
oAC54	CTGGAGCTCCACCGCGGTGGCGGCCGCTCTAGAACTAGTGcgcgcagatcaagcaactta	
oAC55	CTGGAGCTCCACCGCGGTGGCGGCCGCTCTAGAACTAGTGgcgaagca gttctaaaataa	
oAC56	GACGGCGGAGTTCAGCTGATAT	
oAC57	GTCTGCTGAATCAGGCGCTG	
oAC64	GAAATACTCCAGCCTGCCGG	
oAC66	TCCAGGGCCTTGGTCTGGAT	
oAC78	ATCAGCGCTATCAGCCACTT	
oAC79	CATGTCATTGCGTGACCAGT	
oAC80	CGTAGGCGAGCGCAGC	
oAC83	CTGGAGCTCCACCGCGGTGGCGGCCGCTCTAGAACTAGTGtctcatgtggtgaggcccgc	
oAC87	CACCAGAGTGACTTTTACCAGG	
oAC88	AATCATGGTCATAGCTGTTCCTCCTTACTGCAGCCCGGGGgcgggcctcaccacatgaga	
oAC95	AATCATGGTCATAGCTGTTCCTCCTTACTGCAGCCCGGGGtaagttgcttgatctgcgcg	
oAC98	CTGGAGCTCCACCGCGGTGGCGGCCGCTCTAGAACTAGTGgcaatgaaagaactgcgtaa	
oAC99	AATCATGGTCATAGCTGTTCCTCCTTACTGCAGCCCGGGGcaatcattgaaaaccaatta	
oAC211	AGAACTAGTGGATCCCCCGGGCTGCAGGAATTCGATATCAcgcgcagatcaagcaactta	
oAC212	TGATGATGGCCATGTTATCCTCCTCGCCCTTGCTCACCATagctgttcctccttactgca	
oAC213	atggtgagcaagggcgagga	
oAC214	TTGGGTACCGGGCCCCCCCTCGAGGTCGACGGTATCGATActtgtacagctcgtccatgc	
oAC215	CTCACTAGTGGATCCCCCGGGCTGCAGGAATTCCTCGAGAgcaatgaaagaactgcgtaa	
oAC216	GCACCACCCCGGTGAACAGCTCCTCGCCCTTGCTCACCATagctgttcctccttactgca	
oAC217	atggtgagcaagggcgagga	
oAC218	TCTGGTTGGCCTGCAAGGCCTTCGCGAGGTACCGGGCCCAttacttgtacagctcgtcca	

*lowercase nucleotides anneal to plasmid sequence during isothermal assembly

Appendix 2

Generation and phenotypic analysis of *Pseudomonas aeruginosa wzz* mutants

Adapted from projects designed for

Rita Wang and Christine Knox

INTRODUCTION

Pseudomonas aeruginosa causes acute and chronic lung infections in people with cystic fibrosis (21, 22, 36). O antigen is the repeat polysaccharide attached to the distal end of the lipid-A core LPS molecule that is embedded in the outer membrane (122). It is commonly observed that strains isolated from initial and acute *P. aeruginosa* infections express O antigen, termed LPS-smooth, while strains isolated from chronic infections are LPS-rough, meaning they do not express O antigen (38, 132). *P. aeruginosa* possesses two forms of O antigen; common O antigen (A-band) and specific O antigen (B-band) (39) with specific O antigen defining the 20 different serotypes of *P. aeruginosa* (124). The different serotypes of *P. aeruginosa* characterized by the sugar composition of the specific O antigen molecule (124). Specific O antigen is further divided into two subcategories based on the length of the repeat unit. Long O antigen possesses 12-30 sugar repeats and is controlled by the chain-length control protein Wzz1 while very long O antigen possesses 40-50 sugar repeats (122, 139, 140) and is controlled by the chain-length control protein Wzz2 (140, 141). The *wzz1* sequence is specific to the serotype, while *wzz2* is conserved across serotypes (127, 140).

Chronic *P. aeruginosa* lung infections are a leading cause of morbidity and mortality in these patients (28-30). The most common serotypes infecting people with cystic fibrosis (CF) are serotypes O1, O6, and O7/O8 (223). Upon adaption to the CF lung, *P. aeruginosa* loses expression very long O antigen by repressing expression of *wzz2*, the very long O antigen chain-length regulator (48). Eventually, LPS-rough strains completely lacking O antigen are selected for (186). This suggests that expression and tightly controlled regulation of O antigen is important for the establishment and maintenance of infection.

The physiological relevance of decreased Wzz2 and very long O antigen is not known. Additionally, it is not known whether Wzz2 regulates the very long O antigen chain-lengths in all serotypes. Therefore, we sought to (1) characterize the LPS and O antigen production of each of our 20 serotype strains and their respective *wzz2* mutants and (2) evaluate whether serotype and/or expression of *wzz2* and very long O antigen are critical for resistance to normal human serum, pH, osmolytes, and antibiotics. Overall, we were able to construct a series of *wzz2* mutants and found that some of our mutants did not produce LPS or O antigen as detected by pro-Q staining or western immunoblot suggesting that these strains may be LPS rough due. Finally, when it comes to resistance, loss of *wzz2* does not always result in the same trend (i.e. increased resistance or increases sensitivity) and greatly depends on serotype. Since *wzz2* mutants have not yet been generated for all 20 serotypes, future experiments will continue to create mutants and determine what effects loss of Wzz2 has on O antigen production and resistance to determine if there are any serotype specific phenotypes conferred by Wzz2 or if Wzz2 performs a similar function in all strains.

RESULTS AND DISCUSSION

Pro-Q staining of all serotype strains. Initial LPS characterization of all 20 ATCC serotype strains in our library was performed by Pro-Q staining, which stains the entire LPS molecule. We found that each serotype produced core LPS, but varying amounts and lengths of O antigen (Fig. 2.1). Serotype O7, O12, O14, O15, and O16 strains did not produce detectable quantities of O antigen compared to the other serotypes. O antigen production by serotype O5, O18, and O20 strains were very faint suggesting that these strains do not produce as much O antigen as the other strains.

O antigen immunoblot of all serotype strains. We also visualized the O antigen production of each serotype strain by western immunoblot using specific serotype O antigen antibodies. To do this, we utilized polyvalent polyclonal antibodies grouped based on similarities between the O antigen molecules. Polyvalent group 1 includes serotype O1, O3, O7, O8, O10, O12, O18 strains. Polyvalent group 2 includes O2, O5, O13, O14, O15, O16, O18, and O20 strains. Lastly, polyvalent group 3 is composed of serotype O4, O6, O9, O11, an O17 strains. We grouped these strains based on group and then probed using each polyvalent group antibodies.

Although we originally did not see O antigen produced from some serotype strains using Pro-Q staining, using antibodies specific to each serotype we found that serotype O7, O12, O14, O15, and O16 strains produced large amounts of O antigen (Fig. A2.2). However, O14 still did not produce any O antigen. Interestingly, by immunoblot we were also unable to detect O antigen produced by the serotype O18 strain while serotype O5 and O19 strains produced very low amounts of O antigen, even though the serotype O19 strain produced detectable amounts of O antigen by Pro-Q staining.

Deletion of *wzz2* decreases very long O antigen production in serotype O5 PAO1 and serotype O1 strains. We know that both serotype O5 strain PAO1 and serotype O11 strain PA103 lose production of very long O antigen chain lengths when *wzz2* is deleted (48, 141). We were curious if other serotypes would also have altered production of very long O antigen when *wzz2* is deleted. We started with serotype O1 strain and constructed a *wzz2* deletion mutant. The serotype O1 strain produced less Wzz2, as visualized by western immunoblot, than PAO1 (Fig. A2.3). When *wzz2* was deleted, however, both PAO1 and serotype O1 mutants did not produce detectable Wzz2 (Fig. A2.3). We hypothesized that deletion of *wzz2* would abolish production of very long O antigen. In support of our hypothesis, deletion of *wzz2* in the serotype O1 strain resulted in loss of very long O antigen (Fig. A2.3). Different from that observed for PAO1, however, is that deletion of *wzz2* in the serotype O1 strain also resulted in increased production of shorter O antigen chain lengths (A2.3). Increased production of shorter chain lengths would be expected since more core-LPS molecules are available to by capped by the long O antigen chain length control protein Wzz1. Future experiments will continue to test Wzz2 and very long O antigen production in other serotype strains as these mutants are constructed.

Deletion of *wzz2* does not alter serum resistance in serotype O5 PAO1 or serotype O1 strains. O antigen production is important for resistance to human serum (224). Kintz et al. reported for PA103 that production of the long O antigen, and not very long O antigen, confers this resistance (141). We next wanted to determine if this is the case for PAO1, serotype O1, and serotype O8 strains. First, we confirmed that there was no large growth difference due to deletion of *wzz2* (Fig. A2.4A). We then grew each strain in 20% normal human serum (NHS) and monitored survival after 1 hour and 2 hours of growth. As a control, we also monitored survival

of a PAO1 *galU::aacC1* mutant, which is very sensitive to NHS. Both PAO1 and the serotype O1 strain are very resistant to NHS with survival even increasing between 1 and 2 hours (Fig. A2.4B). PAO1 *galU::aacC1* was sensitive to NHS, with only about 10% of cells surviving after 2 hours. When *wzz2* is deleted from PAO1, this strain is still resistant to NHS (Fig. A2.4B). Contrary, the serotype O1 *wzz2* mutant was very sensitive to NHS with only 2% survival after 1 hour (Fig. A2.4B).

To determine if killing is due to complement proteins contained within the NHS, we also grew each strain in heat-inactivated (HI) serum (Fig. A2.4C). PAO1, PAO1 *wzz2::tet*, and the serotype O1 strain all grew to similar levels in the HI serum as the NHS. PAO1 *galU::aacC1*, which is sensitive to NHS, grew to high levels in HI serum as expected. Surprisingly, the serotype O1 *wzz2* mutant was still quite sensitive to HI serum, but grew a little better than in the NHS. This suggests either 1) the serotype O1 *wzz2* mutant is sensitive to heat-stable components of the NHS or 2) some residual complement proteins are maintained in the HI serum and the serotype O1 *wzz2* mutant is sensitive enough to be affected by this.

Deletion of *wzz1* or *wzz2* does not alter resistance to polymyxin B. The negatively charged LPS barrier of gram-negative bacteria contributes to antibiotic resistance. We were curious if O antigen chain length contributed to the resistance of *P. aeruginosa* to cationic antibiotics gentamicin and polymyxin B. Especially since these antibiotics have also been shown to interact with the outer membrane (225). We chose to compare nonmucoid lab strain PAO1 and isogenic mucoid strain PDO300. PDO300 is mucoid due to overproduction of the exopolysaccharide alginate, which forms a capsule around the cell that might interfere or alter outer membrane targeting molecules.First, we tested resistance to polymyxin B by growing PAO1, PDO300, and each respective *wzz1* and *wzz2* transposon mutants overnight without

selection, normalizing each strain based on optical density, and then plating on increasing concentrations of antibiotic. The PAO1 strains all strains grew on 2 μg/ml polymyxin B with growth beginning to be inhibited on 4 μg/ml concentrations (Fig. A2.5A). Comparably, all PDO300 strains grew to a high density on 4 μg/ml polymyxin B (Fig. A2.5B). Disruption of *wzz1* or *wzz2* did not altered growth of either PAO1 or PDO300 on all concentrations of polymyxin B that were tested.

A PDO300 *wzz2* transposon mutant is more resistant to subinhibitory concentration of gentamicin compared to parent strains and *wzz1* mutants. We also tested resistance of PAO1, PDO300, and each respective *wzz1* and *wzz2* transposon mutants to gentamicin. This time, we also included a strain carrying a gentamicin resistance gene as a positive control, which grew on all concentrations tested. All PAO1 strains only grew to high densities on 2 μg/ml of gentamicin and did not survive on higher concentrations (Fig. A2.6A). Similarly, PDO300 and PDO300 *wzz1::tet* only grew on 2 μg/ml of gentamicin (Fig. A2.6B). Interestingly, PDO300 *wzz2::tet* grew on concentrations of gentamicin up to 8 μg/ml. This is surprising since PDO300 has inherently low expression of *wzz2* (48).

PDO300 *wzz2::tet* grows better in 2 μg/ml concentrations of gentamicin than wild type PDO300 or PAO1 strains. To further validate that PDO300 *wzz2::tet* has increased resistance to gentamicin we grew PAO1, PDO300, and each respective *wzz1* and *wzz2* transposon mutants in increasing concentrations of gentamicin and then quantified survival after 20 hours of growth. Again, all of the PAO1 strains grew similarly, with decreased survival with increasing concentrations of gentamicin with less than 50% of cells surviving at 1 μg/ml gentamicin (Fig. A2.7A). Likewise, PDO300 and PDO300 *wzz1::tet* decreased survival with increasing concentrations of gentamicin (Fig. A2.7B). PDO300 *wzz2::tet*, however, had 90%

survival when grown in 2 μg/ml. Growth in 4 and 8 μg/ml gentamicin was comparable to all of the other strains at these concentrations. Finally, we performed growth curves to monitor the dynamics of all strains when grown in 2 μg/ml gentamicin (Fig. A2.8). These data corroborate our previous findings that PDO300 *wzz2::tet* survives better than all of the other strains throughout the course of the experiment. Still, PDO300 *wzz2::tet* grew at a slower rate and reached an overall lower final optical density than the positive control.

METHODS

Construction of pEXG2-*Δwzz2* deletion plasmid and generation of mutants. To generate pEXG2-Δ*wzz2* 1000 bps of the upstream and downstream regions of *wzz2* was PCR amplified from PAO1 genomic DNA using ck01/ck02 and ck03/ck04, respectively. These two fragments were then inserted into HindIII digest pEXG2 using isothermal assembly (Gibson Assembly Master Mix, New England BioLabs) following the manufacturers protocol. The reaction was then transformed by heat-shock into chemically competent DH5α and selected for on gentamicin. Plasmids were extracted (Qiagen Miniprep Kit) from isolated colonies and PCR verified using oAC91/oAC92. Plasmid pEXG2-Δ*wzz2* was then transformed into chemically competent SM10 by heat-shock. SM10 containing pEXG2-Δ*wzz2* was conjugated with each of the serotype strains following the puddle-mating protocol, in a 3:1 ratio as previously described (178). After sucrose counterselection, single colonies were patched onto LA and LA containing gentamicin. Gentamicin sensitive colonies were screened for loss of *wzz2* by single-colony PCR using primers ck05/ck06. A complete list of strains, plasmids, and primers is available in Table A2.1.

Protein and LPS isolation. Colonies from an overnight LA plate were resupsended in LB and normalized to an OD_{600} of 1.0 and then 1 ml was pelleted. Protein was prepared resuspending the pellet in 50 µl lysis stock buffer (20 mM Tris pH 7.5, 1 mM EDTA, 10 mM $MgCl_2$) containing 10 µg/mL DNase, 10 µg/mL RNase, and 1X ProBlock Protease Inhibitor (Goldbio) and incubated at 37°C for 10 min. Next, 50 µl of 2x Laemmli buffer (Biorad) was added and then the samples were boiled in a water bath for 5 min. Samples were stored at -20°C and then boiled for 5 mins before every use. LPS was prepared by resuspending pelleted bacteria were in 200 µl of

1x Laemmli buffer (Biorad). This suspension was boiled in a water bath for 15 minutes and allowed to cool to room temperature. Next, 10 µl of 10 mg/ml Proteinase K was added to each sample, incubated at 59°C for 3 hours, and then stored at -20°C. After storage, the sample was boiled for 5 mins before every use.

Pro-Q staining. 15 µl of sample was loaded into each well and then separated by SDS-PAGE in a 10% Mini-PROTEAN TGX gel (Bio-Rad) along with CandyCane glycoprotein ladder (Thermo). LPS was then stained using Pro-Q 300 Glycoprotein Stain (Thermo) according to the manufacturer's instructions except that the initial fixation step and each wash step was repeated three times (instead of twice). All steps were performed at room temperature and excess volume of fix and wash solutions were used per gel in each step. In summary, the gel was immediately incubated, rocking in a large glass container, in ~100 ml of fix solution (50% methanol and 5% acetic acid in H_2O) for 45 min. This step was repeated two more times in fresh fix solution. Next, the gel was incubated in ~100 ml wash solution (3% glacial acetic acid in H_2O) for 20 min. This step was repeated two more times in fresh wash solution. Next, the gel was incubated in 25 ml of oxidizing solution (provided with kit) for 30 min and then washed again three times in wash solution as described above. To stain, the Pro-Q Emerald 300 stock solution was diluted 50-fold into Pro-Q Emerald 300 staining buffer (both provided with kit) and the gel was incubated in 25 ml of this stock/buffer solution, rocking in the dark (glass container was wrapped in aluminum foil), for 2 hrs. Finally, the gel was washed once in ~100 ml of wash solution for 20 min. The images were taken with a UV transilluminator.

Western immunoblot. 15 μl of LPS or 10 μl of protein was loaded into each well and then separated by SDS-PAGE in a 10% Mini-PROTEAN TGX gel (Bio-Rad) along with Precision Plus All Blue Protein ladder (Bio-Rad). The protein and LPS were then transferred to a PVDF membrane and blocked for 1 hour, at room temperature, in PBS-T containing 5% milk. Next, specific primary antibody for each serotype or polyvalent group (Table A2.2) was incubated in a 1:5,000 dilution in PBS-T containing 3% BSA overnight at 4°C. Protein was incubated in Wzz2 polyclonal antibody (1:10,000) or EFTu monoclonal antibody (1:10,000) in the same way. Secondary α-rabbit-HRP IgG (Sigma) for O antigen and Wzz2 or α-mouse-HRP IgG for EFTu were incubated in a 1:10,000 dilution in PBS-T containing 3% BSA for 1 hour at room temperature. The blot was visualized using Pierce ECL Western Blotting Substrate (Thermo) according to the manufacturer's instructions.

Serum assay. Single colonies grown overnight in LB were back-diluted 1:20 into fresh LB and grown, rolling at 37ºC, for 2 hours. At the same time, the BacTiter-Glo (Promega) reagent was equilibrated to room temperature and the normal human serum (NHS) and heat-inactivated (HI) serum (inactivated by heating at 56°C for 1 hour) was thawed on ice. After 2 hrs, the subcultured bacteria were spun down (5 min at 4,500 x g) and the pellet was resuspended in 1 ml 1X PBS (filter-sterilized). The OD_{600} was taken of the cell suspension and then normalized to 5 x 10^6 bacteria, assuming that an OD_{600} of 1.0 is equivalent to 1 x 10^9. 80 μl of cell suspension was added to a 96-well V-bottom plate in triplicate. Next, either 20 μl PBS, 20 μl NHS, or 20 μl HI serum was added to each well and mixed gently and incubated at 37ºC for desired time. At each time point (0, 1, and 2 hrs, prepare a replicate plate for each time point being tested), the plate was spun down for 5 mins at 4,000 x g. The supernatant was removed from the plate by turning

the plate upside down over a waste container. Without turning the plate back over, the plate was gently set on a paper towel to remove the rest of the liquid. Next, the pellets in each well were resuspended in 100 µl PBS and mixed by pipetting up and down. 50 µl of each well was then transferred to a black clear-bottom 96-well plate. Finally, 50 µl of BacTiter-Glo reagent was added to each well and was shaken for 5 min at room temperature in the Synergy-H1 microplate reader. Luminescence was then measured to obtain relative fluorescent units (RFUs). Error bars represent standard deviation of three biological replicates. Percent survival was calculated as: [(final RFU in serum - final RFU in PBS) / (initial RFU in PBS)] *100.

Growth curves and survival experiments. Growth curves were performed in 3 ml LB at 37ºC, with continuous shaking, in a 6-well plate using the Synergy-H1 microplate reader. Similarly, growth to determine survival in increasing concentrations of gentamicin (µg/ml) were performed, but in a 96-well plate format. Bar graphs represent OD_{600} after 20 hours of growth. For growth analysis on plates containing increasing concentrations of gentamicin (µg/ml), overnight cultures of each strain grown without antibiotic were normalized to an OD_{600} of 0.5 and serially-diluted (10-fold) onto increasing concentrations of gentamicin. Plates were incubated at 37ºC overnight. Error bars represent standard deviation of three biological replicates.

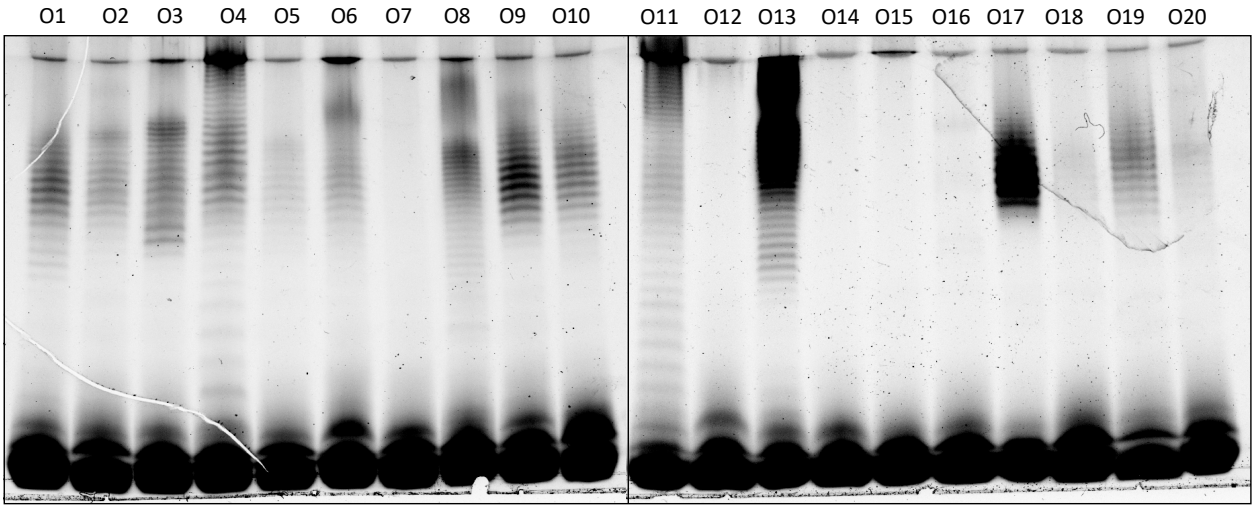

Figure A2.1. Pro-Q staining of all serotype strains. Bacteria were scraped off of a plate, resuspended in PBS, and normalize to the same OD_{600}. Purified LPS was separated by SDS-PAGE in a 10% gel and then stained using Pro-Q 300 Glycoprotein stain. Each serotype is listed above each lane. The dark band at the very bottom of the gel represents the core LPS molecule while each additional band above that represents an addition of an O antigen unit. Banding was visualized using a UV transilluminator.

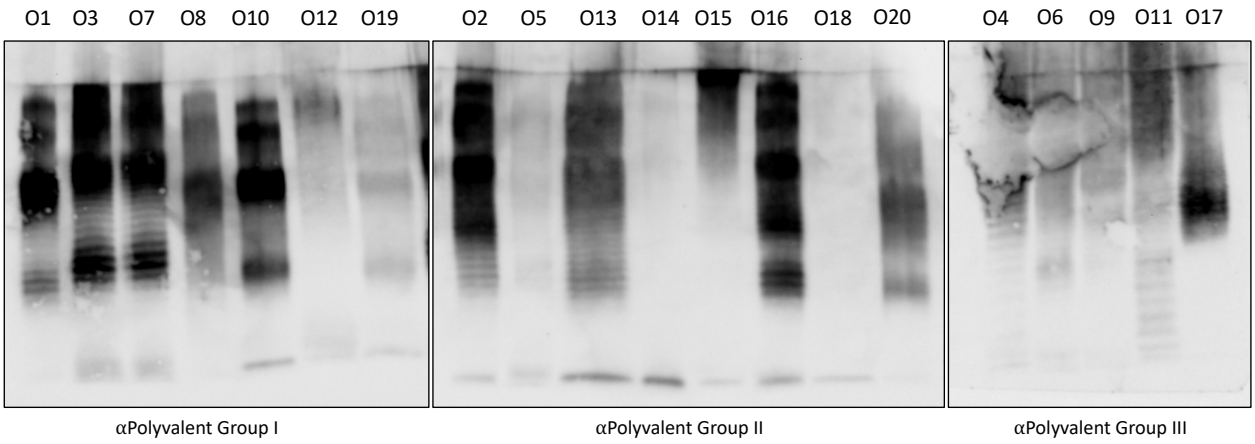

Figure A2.2. O antigen immunoblot of all serotype strains. Samples were prepared and separated by SDS-PAGE as described in Figure A2.1. The LPS was then transferred from the gel to a PVDF membrane blocked, and then incubated with primary antibody specific to each polyvalent group. All samples were then visualized using αrabbit-HRP IgG secondary antibody and chemiluminescence substrate. Each serotype is listed above each lane and each polyvalent group is listed below each membrane. Banding represents the O antigen molecule only.

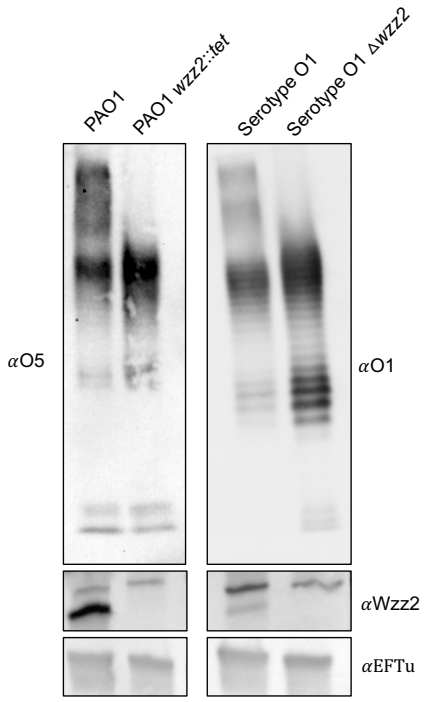

Figure A2.3. Deletion of *wzz2* decreases very long O antigen production in serotype O5 and O1. LPS samples were prepared and western immunoblot was performed as described in Figure A2.2. Serotype specific antibodies used are shown next to each membrane. Protein was prepared and western immunoblot of Wzz2 and EFTu (loading control) are shown. PAO1 and the respective *wzz2::tet* transposon mutant from the PAO1 library were used as a control since this strain lose expression of Wzz2 and very long O antigen when *wzz2* is disrupted. Serotype O1 strain loses expression of very long O antigen and has increased production of the shorter O antigen lengths when *wzz2* is deleted and Wzz2 is not expressed.

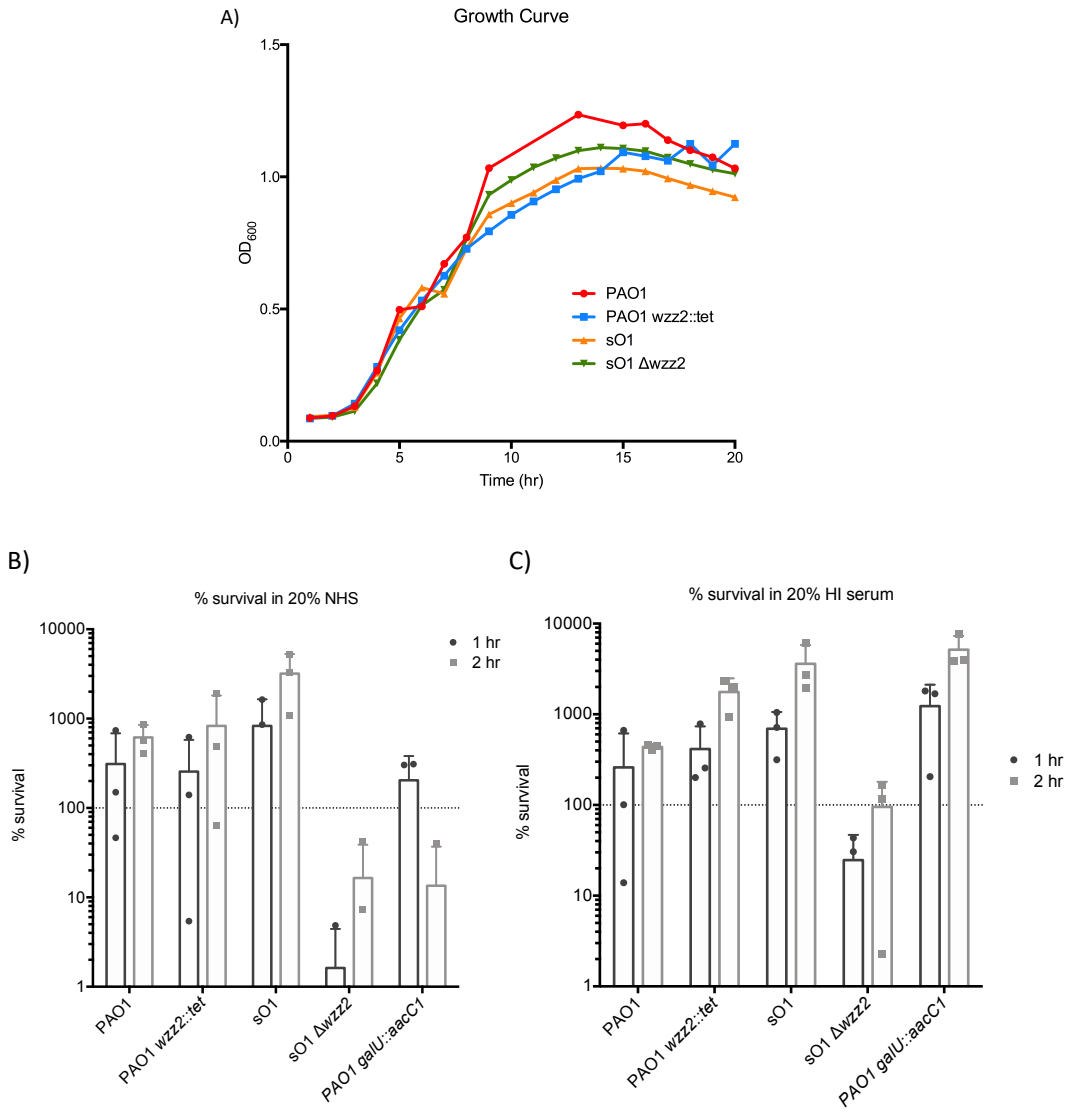

Figure A2.4. Deletion of *wzz2* decreases resistance of serotype O1 to normal human serum, does not alter resistance of serotype O5 PAO1. A) Growth curves of PAO1, serotype O1, and each respective *wzz2* mutant at 37C. Overnight cultures were back-diluted and then allowed to grow for 2 hours in LB. Each culture was normalized and grown for the indicated time in either normal human serum (B) or heat-inactivated serum (C). Cells were then pelleted, supernatants removed, and resuspended in PBS. BacTiter-Glo reagent was then used to measure viability of cells in each reaction following manufacturers protocol. sO1: serotype O1 strain.

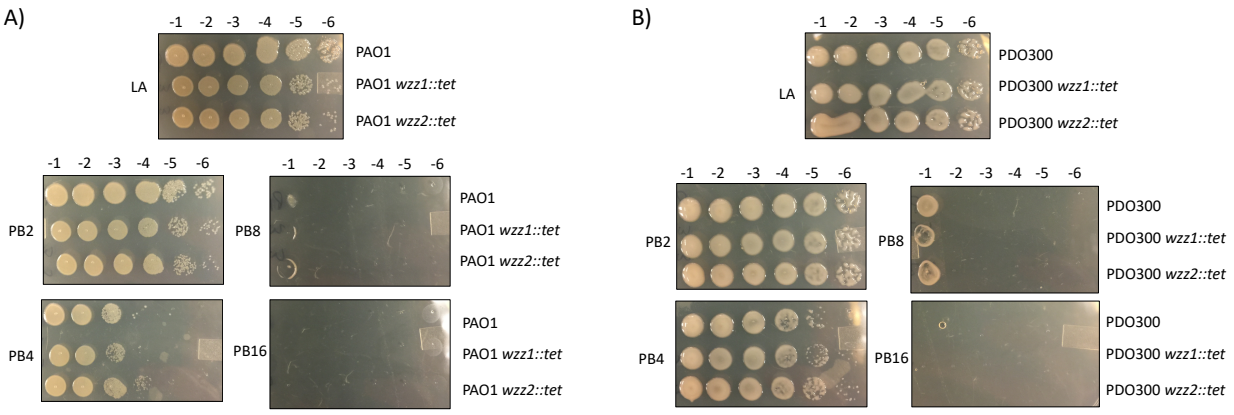

Figure A2.5. Deletion of *wzz1* or *wzz2* does not alter resistance to polymyxin B. A) PAO1 strains. B) PDO300 strains. Overnight cultures of strains grown without antibiotic were normalized to the same OD_{600} and then serially-diluted 10-fold onto increasing concentrations of polymyxin (2, 4, 8, and 16 µg/ml). All images are representative of three biological replicates.

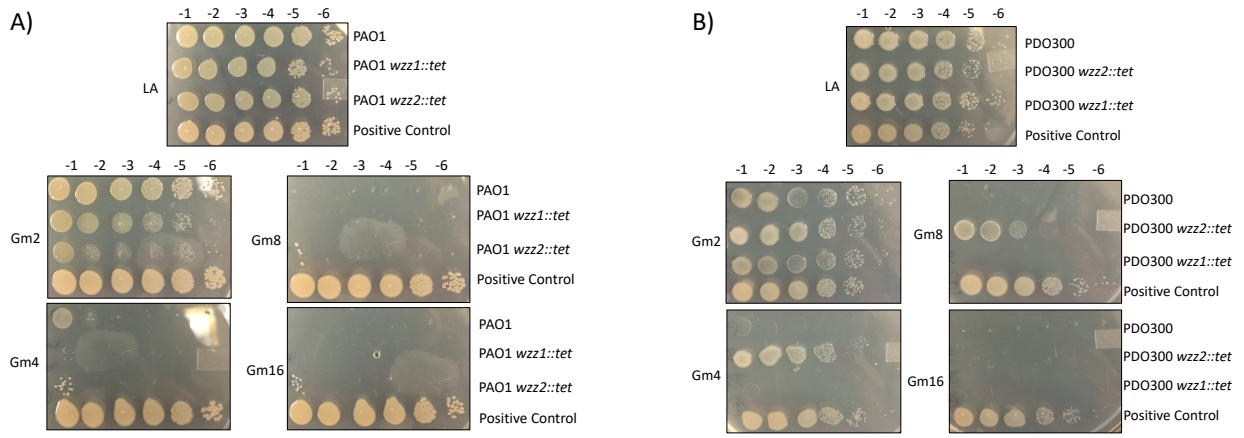

Figure A2.6. A PDO300 *wzz2* transposon mutant is more resistant to subinhibitory concentration of gentamicin compared to parent strains and *wzz1* mutants. A) PAO1 strains. B) PDO300 strains. Overnight cultures of strains grown without antibiotic were normalized to the same OD_{600} and then serially-diluted 10-fold onto increasing concentrations of gentamicin (2, 4, 8, and 16 μg/ml). The positive control strains is PAO1 Tn7::miniTn7-Gm, which contains a gentamicin resistance marker. Note that PDO300 *wzz2::tet* and PDO300 *wzz1::tet* are accidentally plated in reverse order compared to other images. All images are representative of three biological replicates.

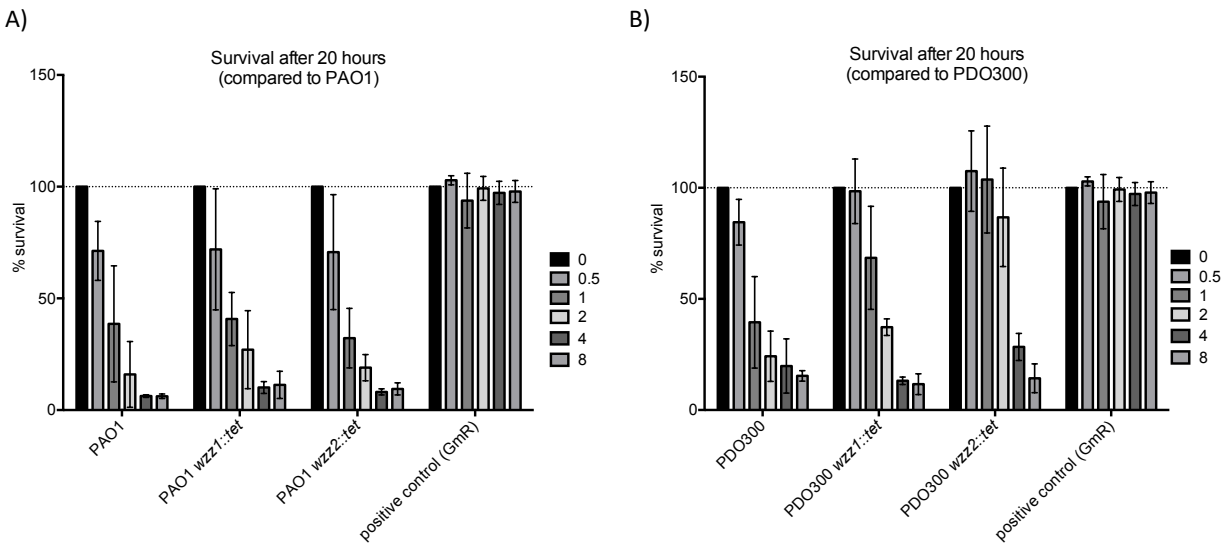

Figure A2.7. PDO300 *wzz2::tet* has increased survival after growth in increasing concentrations of gentamicin. A) PAO1 strains after 20 hrs of growth. B) PDO300 strains after 20 hrs of growth. A 96-well plate was inoculated to the same initial OD_{600} in LB using overnight cultures of each strain. Survival in increasing concentrations of gentamicin (0.5, 1, 2, 4, and 8 μg/ml) was calculated based on OD_{600} after 20 hours of growth and normalized to growth without antibiotic, which was considered 100% survival. The positive control strains is PAO1 Tn7::P_{tac}-*algT*, which contains a gentamicin resistance marker.

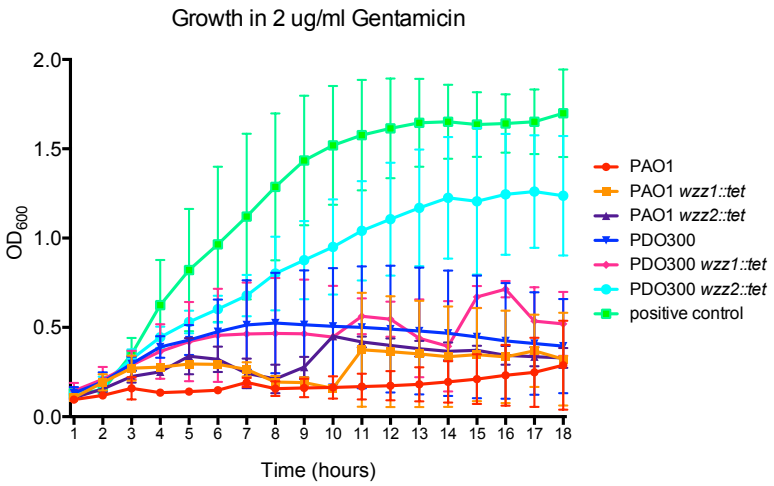

Figure A2.8. PDO300 *wzz2::tet* grows better in 2 μg/ml concentrations of gentamicin than wild type PDO300 or PAO1 strains. A) A 96-well plate was inoculated to the same initial OD_{600} using overnight cultures of each strain and growth in LB containing 2 ug/ml gentamicin was monitored over 20 hours using a Synergy-H1 microplate reader. The positive control strains is PAO1 Tn7::miniTn7-Gm, which contains a gentamicin resistance marker.

Table A2.1. Strains, plasmids, and primers used in this study.

Name	Description	Location
P. aeruginosa		
PAO1		
PAO1 *wzz1::tet*	*wzz1* transposon mutant PW6291	PAC07
PAO1 *wzz2::tet*	*wzz2* transposon mutant PW2707	PAC03
PAO1 *galU::aacC1*	*galU* mutant disrupted by gentamicin resistant marker	PAC411
PDO300	mucoid PAO1 *mucA22*	PAC01
PDO300 *wzz1::tet*	*mucA22* version of PAO1 *wzz1* transposon mutant	PAC376
PDO300 *wzz2::tet*	*mucA22* version of PAO1 *wzz2* transposon mutant	PAC374
Pa. serotype 001	serotype O1 strain	PAC631
Pa. serotype 002	serotype O2 strain	PAC632
Pa. serotype 003	serotype O3 strain	PAC633
Pa. serotype 004	serotype O4 strain	PAC634
Pa. serotype 005	serotype O5 strain	PAC635
Pa. serotype 006	serotype O6 strain	PAC636
Pa. serotype 007	serotype O7 strain	PAC637
Pa. serotype 008	serotype O8 strain	PAC638
Pa. serotype 009	serotype O9 strain	PAC639
Pa. serotype 010	serotype O10 strain	PAC640
Pa. serotype 011	serotype O11 strain	PAC641
Pa. serotype 012	serotype O12 strain	PAC642
Pa. serotype 013	serotype O13 strain	PAC643
Pa. serotype 014	serotype O14 strain	PAC644
Pa. serotype 015	serotype O15 strain	PAC645
Pa. serotype 016	serotype O16 strain	PAC646
Pa. serotype 017	serotype O17 strain	PAC647
Pa. serotype 018	serotype O18 strain	PAC648
Pa. serotype 019	serotype O19 strain	PAC649
Pa. serotype 020	serotype O20 strain	PAC650
Pa. serotype 001 △*wzz2*	serotype O1 strain with *wzz2* deletion	PAC661
PAO1 Tn7::miniTn7-Gm	gentamicin resistant PAO1	PAC322
Plasmids		
pEXG2-△*wzz2*	*wzz2* deletion plasmid	ECAC161
Primers		
ck01	GGAAGCATAAATGTAAAGCAAGGCCCACCAGAGTGACTTTTAC	
ck02	ACCTTTGATCACCAACGTCCTTTTCGATAGG	
ck03	GGACGTTGGTGATCAAAGGTGCGCCCCC	
ck04	AGAGTCGACCTGCAGAAGCTAAGTCGGTTCCTGCCCTG	
ck05	GTGGTGCTGCTCAACGTACA	
ck06	AATAGGCTGGATTTCGGTTG	
oAC091	CCACACATTATACGAGCCGGAAGC	
oAC092	GGTACCGAATTCGAGCTCGAGC	

Table A2.2. Polyvalent and primary antibodies to detect serotype O antigen.

Serotype	Homma scheme	Polyvalent Groups
O1	I	1
O2	B	2
O3	A	1
O4	F	3
O5	B	2
O6	G	3
O7	C	1
O8	C	1
O9	D	3
O10	H	1
O11	E	3
O12	L	1
O13	K	2
O14	K	2
O15	J	2
O16	B	2
O17	N	3
O18	B	2
O19	H	1
O20	B	2
DENKA SEIKEN Key Scientific Products		
Accurate Chemical & Scientific. Westbury, N.Y.		

Appendix 3

Nucleotide duplications in *algT* cause nonmucoid reversion

Adapted from an undergraduate research project

designed for Rita Wang

INTRODUCTION

Chronic *Pseudomonas aeruginosa* isolates are often mucoid due to the overproduction of the exopolysaccharide alginate (42, 148). Alginate production has been shown to protect bacteria from the host immune system and reduce opsonization (212, 226). As a result, isolation of mucoid colonies is associated with poor patient prognosis (61, 65, 185). Mutations in *mucA* are the most common cause of mucoid conversion (42, 51, 120). MucA is an anti-sigma factor responsible for sequestering AlgT, the sigma factor that initiates transcription of the alginate biosynthesis operon (45, 101). In addition to alginate biosynthesis, the AlgT regulon also includes operons for pigment production and motility and ultimately switches the bacteria from a virulent and motile lifestyle to a less virulent and sessile lifestyle (76, 227). This dominant mucoid form of *P. aeruginosa* is difficult to treat. For this reason, AlgT is considered a possible anti-virulence target. Inhibiting AlgT could provide a better outcome for people who suffer from chronic *P. aeruginosa* infections.

AlgT is an extracytoplasmic function (ECF) sigma factor capable of responding to a number of extracellular and periplasmic stresses in order to preserve membrane integrity (104, 107, 108), similar to the *Escherichia coli* stress response sigma factor RpoE. AlgT shares 66% homology to RpoE and activation of both occurs through a conserved regulated intermembrane proteolysis (RIP) cascade (96, 107). Frequently, mucoid strains revert to nonmucoid by acquiring mutations in *algT* (73, 106, 121). Mixtures of nonmucoid, mucoid, and nonmucoid revertants of mucoid strains are likely to coexist during chronic lung infections (199). The aim of this study was to characterize the *algT* sequences from a series of nonmucoid revertants and predict how these reversion mutations affect AlgT function. In doing so we hope to gain a better understanding of how *P. aeruginosa* evolves and adapts during chronic infections and identify opportunities for targeted interventions.

RESULTS AND DISUCUSSION

To identify nonmucoid revertants (NMRs) we grew mucoid strains PDO300, FRD1, CFBR18, and CFBR32 under low aeration, a stressful condition that selects for reversion mutations (106). PDO300 is a laboratory strain originally derived from a nonmucoid burn isolate while strains FRD1, CFBR18, and CFBR32 are all cystic fibrosis (CF) clinical isolates (43, 51). We isolated 18 PDO300 NMRs, 10 FRD1 NMRs, 5 CFBR18 NMRs, and 6 CFBR32 NMRs for a total of 39 NMRs. We then sequenced *algT* from each of the NMRs to determine what proportion had acquired mutations in this gene. For PDO300 and FRD1 about 50% of NMRs had mutations in *algT* (Table A3.1). This percentage was a lower for CFBR18 and CFBR32 strains. Regardless, these data are similar to previous studies that estimated 30-55% of *in vivo* NMRs contain *algT* mutations and upwards of 90% of *in vitro* NMRs containing *algT* mutations (48, 121, 228).

While we observed a number of different types of *algT* mutations, we were especially interested in a 9 bp nucleotide insertion that had occurred in 8 of our NMRs, including 6 of the 18 PDO300 NMRs. This insertion represented a duplication of nucleotides 127-135 (corresponding to amino acids DAQ) or nucleotides 136-144 (corresponding to amino acids EAQ) representing amino acids 43-48 (Fig. A3.1). Several studies have also described a 9 bp insertion in this region (149, 228). While this appears to be a common mechanism of nonmucoid reversion, but how this mutation affects AlgT function is unclear. Sequence alignment of AlgT to *Escherichia coli* RpoE by Sautter et al., predicted that this region is involved in promoter melting (121). We hypothesized that the duplications at this region in *algT* may provide a growth advantage compared to the isogenic mucoid strains and explain why a majority of the NMRs had acquired this mutation. To test this, we calculated the doubling time of PDO300, PDO300 dup1

(DAQ), and PDO300 dup2 (EAQ) cells. We found, however, no significant difference in doubling time or growth rate of these three strains under laboratory conditions (Fig. A3.2).

Next, we used the protein modeling software PyMOL to predict how the duplication of either DAQ or EAQ affects AlgT folding and function. First, we generated a tertiary structure of AlgT based off of known and predicted RpoE structures (Fig. A3.3A). As expected, the protein model of AlgT shows two structured domains attached by a disordered linker. We also generated an electrostatic charge map across AlgT showing positive (blue) and negative (red) charged domains of the protein (Fig. A3.3B). The blue enriched areas at the N-terminus and C-terminus are likely the location of the DNA-binding domains (a -10-promoter binding region and a -35-promoter binding region).

Finally, we mapped the location of the DAQ (pink) and EAQ (green) duplications to the AlgT structure (Fig. A3.4). These amino acids are located in a loop connecting two alpha-helices near the predicted -35-binding region. The duplication of three amino acids at this location did not greatly affect overall protein structure and instead just altered the size of the loop. Therefore, altered protein structure does not seem to be the reason that AlgT is rendered inactive in these nonmucoid revertants. Since aspartate (D) and glutamate (E) are negatively charged amino acids, we instead hypothesize that the addition of negative charges to this primarily positively charged domain alters the affinity of AlgT to DNA and therefore results in loss of DNA-binding and decreased AlgT function.

METHODS

Isolation of nonmucoid revertants. Strains used are listed in Table A3.2. A 1 ml culture of LB was inoculated with a single colony and incubated for 2-5 days with little aeration (vertical shaking) at 37°C. Each day the culture was serially-diluted onto LB and incubated overnight at 37°C. Nonmucoid revertants (NMRs) were picked when the plate still contained both nonmucoid and mucoid colonies and therefore nonmucoid colonies could be compared to the mucoid ones.

AlgT sequencing and modeling. Using single colony PCR, *mucA* and *algT* were amplified using primers oAC89/oAC90 and oAC107/oAC108, respectively. The PCR product was then column purified (Qiagen miniprep kit) and sent for sanger sequencing by Genewiz. AlgT models were built in PyMOL (Molecular Graphics System, Version 2.0 Schrodinger, LLC). Primer sequences are listed in Table A3.2.

Growth curves. Growth curves were performed in 3 ml LB at 37ºC, with continuous shaking for 18 hrs, in a 6-well plate using the Synergy-H1 microplate reader. Doubling time was calculated as 1/slope where slope (OD_{600}/time in minutes) is determined from the linear portion of the logarithmic line.

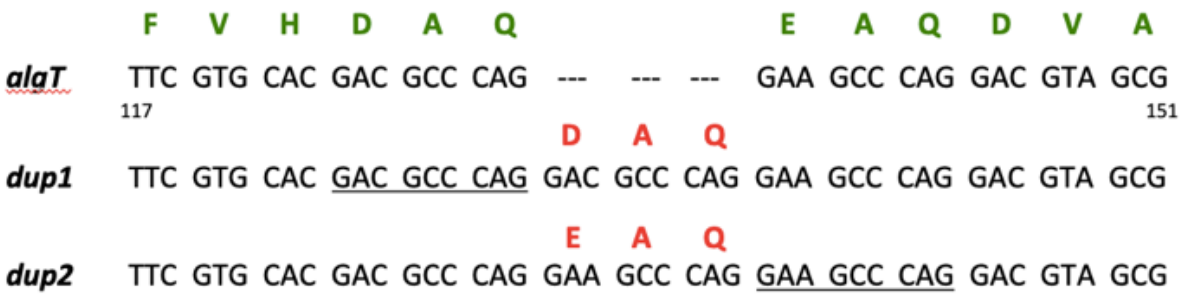

Figure A3.1. AlgT sequence alignment of PDO300 and two nonmucoid revertants. The AlgT amino acid sequence (green) is shown above the 117-151 bp nucleotide sequence (black). Each nonmucoid revertant had an in-frame duplication resulting in the insertion of three amino acids; DAQ (dup1) and EAQ (dup2). The underlined text represents the duplicated amino acids. The insertion of aspartate (D) and glutamate (E) adds a negative charge to AlgT.

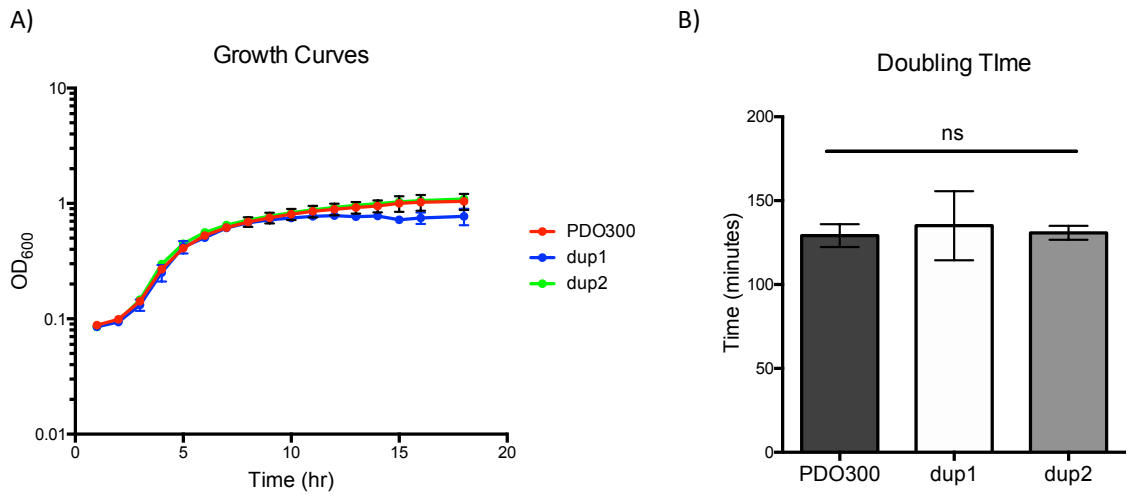

Figure A3.2. Nonmucoid reversion by duplications in AlgT does not result in a growth advantage. Growth curves were performed at 37ºC, with continuous shaking for 18 hrs, in a 6-well plate using the Synergy-H1 microplate reader. Doubling time was calculated between hrs 4 and 7.

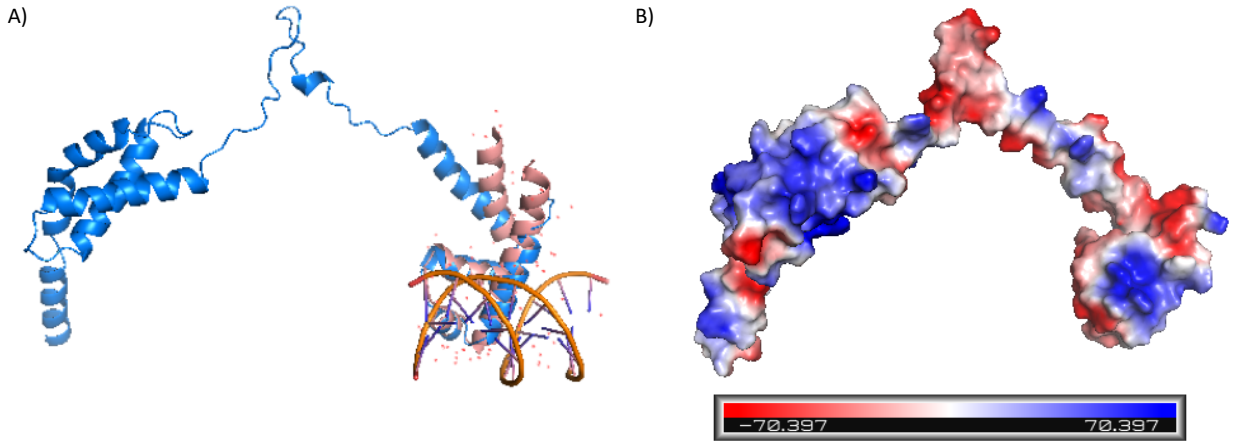

Figure A3.3. Predicted model of AlgT based on *E. coli* RpoE. A) Ribbon model of AlgT (blue) overlaid with the known crystal structure of the RpoE C-terminus (pink). The DNA double helix, representing the -10 promoter binding region, is shown in orange. B) Electrostatic model of AlgT. Blue residues represent positively charged amino acids while red represents negatively charged amino acids.

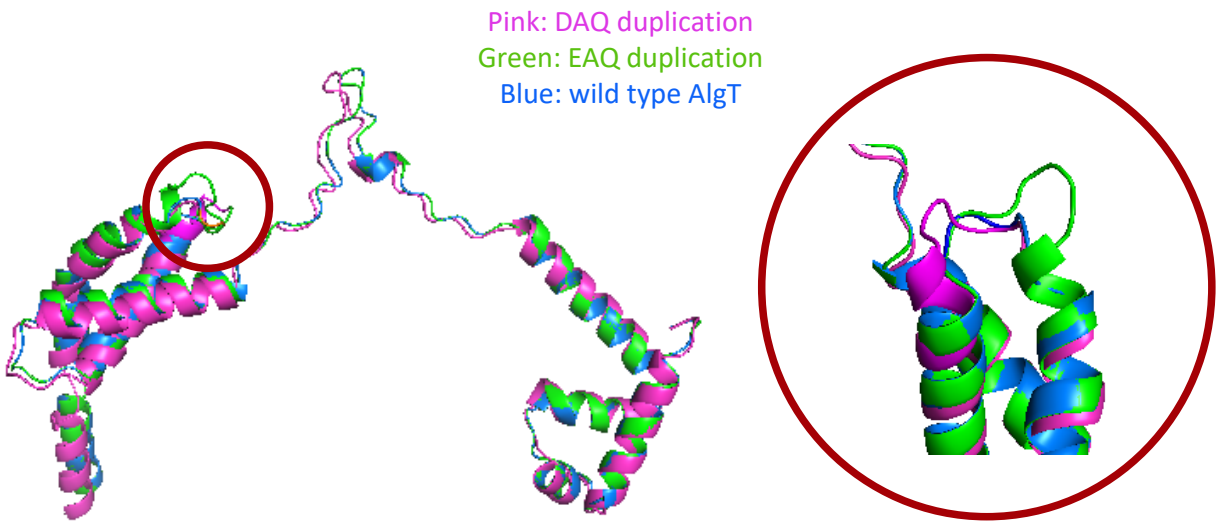

Figure A3.4. Amino acid duplications in AlgT do not dramatically alter predicted protein shape. Overlay of AlgT with predicted structures of AlgT containing duplications (dup1; DAQ and dup2; EAQ). The duplicated amino acids occur in an unstructured loop (enlarged in circle).

Strain	# of NMRs	% *algT* mutations
PDO300	18	56%
FRD1	10	50%
CFBR18	5	40%
CFBR32	6	33%

Table A3.1. Summary of nonmucoid revertants. CFBR18 and CFBR32 are mucoid clinical isolates from the Emory Cystic Fibrosis Biospecimen Repository (CFBR). FRD1 is a mucoid clinical isolate historically used as a lab strain. Overall, 45% of all nonmucoid revertants (NMRs) had mutations in *algT*.

Table A3.2. Strains and primers used in this study.

Name	Description	PAC location
P. aeruginosa		
PDO300	mucoid PAO1 *mucA22*	PAC01
PDO300dup1	contains algT126-134 duplication	PAC273
PDO300dup2	contains algT135-143 duplication	PAC534
FRD1	mucoid CF isolate, lab strain	PAC08
CFBR18	mucoid isolate from Emory CFBR	PAC565
CFBR32	mucoid isolate from Emory CFBR	PAC566
Primers		
oAC089	ATGAGTCGTGAAGCCCTGCA	
oAC090	TCAGCGGTTTTCCAGGCTGG	
oAC107	TGAGCCCGATGCAATCCAT	
oAC108	CAACTGGTAACGCGACCAG	

REFERENCES

1. Diggle SP, Whiteley M. 2019. Microbe Profile: Pseudomonas aeruginosa: opportunistic pathogen and lab rat. Microbiology doi:10.1099/mic.0.000860.
2. Stover C, Pham X, Erwin A, Mizoguchi S, Warrener P, Hickey M, Brinkman F, Hufnagle W, Kowalik D, Lagrou M, Garber R, Goltry L, Tolentino E, Westbrock-Wadman S, Yuan Y, Brody L, Coulter S, Folger K, Kas A, Larbig K, Lim R, Smith K, Spencer D, S. Wong G, Wu Z, Paulsenk I, Reizer J, Saier M, Hancock R, Lory S, Olson M. 2000. Complete genome sequence of Pseudomonas aeruginosa PAO1, an opportunistic pathogen. Nature 406:959-964.
3. Holloway BW. 1955. Genetic Recombination in Pseudomonas aeruginosa. J gen Microbiol 13:572-581.
4. Holloway BW, Morgan AF. 1986. Genome Organization in Pseudomonas. Ann Rev Microbiol 40:79-105.
5. Klockgether J, Munder A, Neugebauer J, Davenport CF, Stanke F, Larbig KD, Heeb S, Schock U, Pohl TM, Wiehlmann L, Tummler B. 2010. Genome diversity of Pseudomonas aeruginosa PAO1 laboratory strains. J Bacteriol 192:1113-21.
6. Preston MJ, Fleiszig S. M. J., Zaidi TS, Goldberg JB, Shortridge JD, Vasil ML, Pier GB. 1995. Rapid and Sensitive Method for Evaluating Pseudomonas aeruginosa Virulence Factors during Corneal Infections in Mice. Infect Immun 63:3497–3501.
7. Chandler CE, Horspool AM, Hill PJ, Wozniak DJ, Schertzer JW, Rasko DA, Ernst RK. 2019. Genomic and Phenotypic Diversity among Ten Laboratory Isolates of Pseudomonas aeruginosa PAO1. J Bacteriol 201.

8. Lee DG, Urbach JM, Wu G, Liberati NT, Feinbaum RL, Miyata S, Diggins LT, He J, Saucier M, Deziel E, Friedman L, Li L, Grills G, Montgomery K, Kucherlapati R, Rahme LG, Ausubel FM. 2006. Genomic analysis reveals that Pseudomonas aeruginosa virulence is combinatorial. Genome Biol 7:R90.

9. Mathee K. 2018. Forensic investigation into the origin of Pseudomonas aeruginosa PA14 - old but not lost. J Med Microbiol 67:1019-1021.

10. Schroth MN, Cho JJ, Green SK, Kominos SD, Microbiology Society P. 2018. Epidemiology of Pseudomonas aeruginosa in agricultural areas. J Med Microbiol 67:1191-1201.

11. Freschi L, Vincent AT, Jeukens J, Emond-Rheault JG, Kukavica-Ibrulj I, Dupont MJ, Charette SJ, Boyle B, Levesque RC. 2019. The Pseudomonas aeruginosa Pan-Genome Provides New Insights on Its Population Structure, Horizontal Gene Transfer, and Pathogenicity. Genome Biol Evol 11:109-120.

12. Poulsen BE, Yang R, Clatworthy AE, White T, Osmulski SJ, Li L, Penaranda C, Lander ES, Shoresh N, Hung DT. 2019. Defining the core essential genome of Pseudomonas aeruginosa. Proc Natl Acad Sci U S A 116:10072-10080.

13. Turner KH, Wessel AK, Palmer GC, Murray JL, Whiteley M. 2015. Essential genome of Pseudomonas aeruginosa in cystic fibrosis sputum. Proc Natl Acad Sci U S A 112:4110-5.

14. Cornforth DM, Dees JL, Ibberson CB, Huse HK, Mathiesen IH, Kirketerp-Moller K, Wolcott RD, Rumbaugh KP, Bjarnsholt T, Whiteley M. 2018. Pseudomonas aeruginosa transcriptome during human infection. Proc Natl Acad Sci U S A 115:E5125-E5134.

15. Crone S, Vives-Florez M, Kvich L, Saunders AM, Malone M, Nicolaisen MH, Martinez-Garcia E, Rojas-Acosta C, Catalina Gomez-Puerto M, Calum H, Whiteley M, Kolter R, Bjarnsholt T. 2019. The environmental occurrence of Pseudomonas aeruginosa. APMIS doi:10.1111/apm.13010.

16. Green SK, Schroth MN, Cho JJ, Kominos SD, B. V-JV. 1974. Agricultural Plants and Soil as a Reservoir for Pseudomonas aeruginosa. Appl Microbiology 28:987-991.

17. Deredjian A, Colinon C, Hien E, Brothier E, Youenou B, Cournoyer B, Dequiedt S, Hartmann A, Jolivet C, Houot S, Ranjard L, Saby NP, Nazaret S. 2014. Low occurrence of Pseudomonas aeruginosa in agricultural soils with and without organic amendment. Front Cell Infect Microbiol 4:53.

18. Ringen LM, Drake CH. 1952. A Study of the Incidence of Pseudomonas aeruginosa from Various Natural Sources. J Bacteriol 64:841-845.

19. Aoi Y, Nakata H, Kida H. 2000. Isolation of Pseudomonas aeruginosa from Ushubetsu River water in Hokkaido, Japan. Japanese Journal of Veterinary Research 48:29-34.

20. Pirnay JP, Matthijs S, Colak H, Chablain P, Bilocq F, Van Eldere J, De Vos D, Zizi M, Triest L, Cornelis P. 2005. Global Pseudomonas aeruginosa biodiversity as reflected in a Belgian river. Environ Microbiol 7:969-80.

21. Bauernfeind A, Bertele RM, Harms BK, Horl G, Jungwirth R, Petermuller C, Przyklenk B, Weisslein-Pfister C. 1987. Qualitative and Quantitative Microbiological Analysis of Sputa of 102 Patients with Cystic Fibrosis. Infection 15.

22. Mearns MB, Hunt GH, Rushworth R. 1972. Bacterial Flora of Respiratory Tract in Patients with Cystic Fibrosis,1950-1971. Archives of Disease in Childhood 47.

23. Quinton PM, Bijman J. 1983. Higher Bioelectric Potentials due to Decreased Chloride Absorbtion in the Sweat Glands of Patients with Cystic Fibrosis. New England Journal of Medicine 308:1185-89.

24. Riordan JR, Romments JM, Kerem B, Alen N, Rozmahel R, Grzelczak Z, Zielenski F, Lok S, Plavsic N, Chou J, Drumm ML, Iannuzzi MC, Collins FS, Tsui L. 1989. Identification of the Cystic Fibrosis Gene: Cloning and Characterization of Complementary DNA. Science 245:1066-1073.

25. Foundation CF. 2018. Patient Registry Annual Data Report.

26. Kreda SM, Davis CW, Rose MC. 2012. CFTR, mucins, and mucus obstruction in cystic fibrosis. Cold Spring Harb Perspect Med 2:a009589.

27. Foundation CF. 2016. Cystic Fibrosis Patient Registry Annual Data Report.

28. Noah TL, Black HR, Cheng P. 1997. Nasal and Bronchoalveolar Lavage Fluid Cytokines in Early Cystic Fibrosis. J Infect Dis 175:638-47.

29. DiMango E, Ratner AJ, Bryan R, Tabibi S, Prince A. 1998. Activation of NF-kB by Adherent Pseudmonas aerugniosa in Normal and Cystic Fibrosis Respiratory Epithelial Cells. J Clin Invest 101:2598-2606.

30. Currie AJ, Speert D, Davidson DJ. 2003. Pseudomonas aeruginosa: Role in the Pathogenesis of the CF Lung Lesion. Seminars in Respiratory and Critical Care Medicine 24.

31. Limoli DH, Yang J, Khansaheb MK, Helfman B, Peng L, Stecenko AA, Goldberg JB. 2016. Staphylococcus aureus and Pseudomonas aeruginosa co-infection is associated with cystic fibrosis-related diabetes and poor clinical outcomes. Eur J Clin Microbiol Infect Dis 35:947-53.

32. Rogers GB, Hart CA, Mason JR, Hughes M, Walshaw MJ, Bruce KD. 2003. Bacterial diversity in cases of lung infection in cystic fibrosis patients: 16S ribosomal DNA (rDNA) length heterogeneity PCR and 16S rDNA terminal restriction fragment length polymorphism profiling. J Clin Microbiol 41:3548-58.

33. Zhao J, Schloss PD, Kalikin LM, Carmody LA, Foster BK, Petrosino JF, Cavalcoli JD, VanDevanter DR, Murray S, Li JZ, Young VB, LiPuma JJ. 2012. Decade-long bacterial community dynamics in cystic fibrosis airways. Proc Natl Acad Sci U S A 109:5809-14.

34. Huang NN, Van Loon EL, Sheng KT. 1961. The flora of the respiratory tract of patients with cystic fibrosis of the pancreas. The Jounral of Pediatrics 59:512-521.

35. Flynn JM, Niccum D, Dunitz JM, Hunter RC. 2016. Evidence and Role for Bacterial Mucin Degradation in Cystic Fibrosis Airway Disease. PLoS Pathog 12:e1005846.

36. Deretic V, Schurr MJ, Hongwei Y. 1995. Pseudomonas aeruginosa, mucoidy and the chronic infection phenotype in cystic fibrosis. Trends in Microbiol 3:351-356.

37. Evans LR, Linker A. 1973. Production and Characterization of the Slime Polysaccharide of Pseudomonas aeruginosa. J Bacteriol:915-924.

38. Hancock REW, Mutharia LM, Chan L, Darveau RP, Speert DP, Pier GB. 1983. Pseudmonas aeruginosa isolates from Patients with Cystic Fibrosis: A Class of Serum-Sensitive, Nontypable Strains Deficient in Lipopolysaccharide O Side Chains. Infect Immun 42:170-177.

39. Rivera M, Bryan LE, Hancock REW, McGroarty EJ. 1988. Heterogeneity of Lipopolysaccharides from Pseudomonas aeruginosa: Analysis of Lipopolysaccharide Chain Length. J Bacteriol 170:512-521.

40. Mahenthiralingam E, Campbell ME, Speert DP. 1994. Nonmotility and Phagocytic Resistance of Pseudomonas aeruginosa Isolates from Chronically Colonized Patients with Cystic Fibrosis. Infect Immun 62:596-605.

41. Luzar MA, Thomassen MJ, Montie TC. 1985. Flagella and Motility Alterations in Pseudomonas aeruginosa Strains from Patients with Cystic Fibrosis: Relationship to Patient Clinical Condition. Infect Immun 50:577-582.

42. Boucher JC, Yu H, Mudd MH, Deretic V. 1997. Mucoid Pseudomonas aeruginosa in Cystic Fibrosis: Characterization of muc Mutations in Clinical Isolates and Analysis of Clearance in a Mouse Model of Respiratory Infection. Infect Immun 65:3838-3846.

43. Ohman DE, Chakrabarty AM. 1981. Genetic Mapping of Chromosomal Determinants for the Production of the Exopolysaccharide Alginate in a Pseudomonas aeruginosa Cystic Fibrosis Isolate. Infect Immun 33:142-148.

44. Flynn JL, Ohman DE. 1988. Cloning of Genes from Mucoid Pseudomonas aeruginosa Which Control Spontaneous Conversion to the Alginate Production Phenotype. J Bacteriol 170:1452-1460.

45. Mathee K. MCJ, Ohman D. E. 1997. Posttranslational Control of the algT (algU)-Encoded sigma22 for Expression of the Alginate Regulon in Pseudomonas aeruginosa and Localization of Its Antagonist Proteins MucA and MucB (AlgN). J Bacteriol 179:3711-3720.

46. Garrett ES, Demetra P, Wozniak DJ. 1999. Negative Control of Flagellum Synthesis in Pseudomonas aeruginosa Is Modulated by the Alternative Sigma Factor AlgT (AlgU). J Bacteriol 181:7401–7404.

47. Tart AH, Wolfgang MC, Wozniak DJ. 2005. The alternative sigma factor AlgT represses Pseudomonas aeruginosa flagellum biosynthesis by inhibiting expression of fleQ. J Bacteriol 187:7955-62.

48. Cross AR, Goldberg JB. 2019. Remodeling of O Antigen in Mucoid Pseudomonas aeruginosa via Transcriptional Repression of wzz2. mBio 10.

49. McAvoy MJ, Newton V, Paull A, Morgan J, Gacesa P, Russell NJ. 1983. Isolation of mucoid strains of Pseudomonas aeruginosa from non-cystic-fibrosis patients and characterisation of the structure of their secreted alginate. J Med Microbiol 28:183-189.

50. Murphy TF, Brauer AL, Eschberger K, Lobbins P, Grove L, Cai X, Sethi S. 2008. Pseudomonas aeruginosa in chronic obstructive pulmonary disease. Am J Respir Crit Care Med 177:853-60.

51. Mathee K, Ciofu O, Sternbrg C, Lindum PW, Campbell JIA, Jensen P, Johnsten AH, Givskov M, Ohman DE, Molin S, Hoiby N, Kharazmi A. 1999. Mucoid conversion of Pseudmonas aeruginosa by hydrogen peroxide: a mechanism for virulence activation in the cystic fibrosis lung. Microbiology 145:1349-1357.

52. DeVault JD, Kimbara K, Chakrabarty AM. 1990. Pulmonary dehydration and infection in cystic fibrosis: evidence that ethanol activates alginate gene expression and induction of mucoidy in Pseudomonas aeruginosa. Mol Microbiol 4:737-745.

53. Berry A, DeVault JD, Chakrabarty AM. 1989. High Osmolarity Is a Signal for Enhanced algD Transcription in Mucoid and Nonmucoid Pseudomonas aeruginosa Strains. J Bacteriol 171:2312-2317.

54. Hassett DJ. 1996. Anaerobic Production of Alginate by Pseudomonas aeruginosa: Alginate Restricts Diffusion of Oxygen. J Bacteriol:7322-7325.

55. Semaniakou A, Croll RP, Chappe V. 2018. Animal Models in the Pathophysiology of Cystic Fibrosis. Front Pharmacol 9:1475.

56. McCarron A, Donnelley M, Parsons D. 2018. Airway disease phenotypes in animal models of cystic fibrosis. Respir Res 19:54.

57. Woods DE, Sokol PA, Bryan LE, Storey DG, Mattingly SJ, J. VH, Ceri H. 1991. In vivo Regulation of Virulence in Pseudomonas aeruginosa Associated with GeneticRearrangement. J Infect Dis 163:63:143-.

58. Doggett RG, Harrison GM, Wallis ES. 1964. Comparison of some properties of Pseudomonas aeruginosa isolated from infections in persons with and without Cystic Fibrosis. J Bacteriol 82:427-431.

59. Doggett RG, Harrison GM, Carter Jr RE. 1971. Mucoid Pseudomonas aeruginosa in Patients with Chronic Illnesses. The Lancet.

60. Phillips I. 1969. Identification of Pseudomonas aeruginosa in the Clinical Laboratory. J Med Microbiol 2:9-16.

61. Lam J, Chan R, Lam K, Costerton JW. 1980. Production of Mucoid Microcolonies by Pseudomonas aeruginosa Within Infected Lungs in Cystic Fibrosis. Infect Immun 28:546-556.

62. Doggett RG, Harrison GM, Stillwell RN, Wallis ES. 1966. An atypical Pseudomonas aeruginosa associated with cystic fibrosis of the pancreas. The Jounral of Pediatrics 68:215-221.

63. Linker A, Jones RS. 1966. A New Polysaccharide Resembling Alginic Acid Isolated from Pseudomonads. J Biol Chem 241:3845-3851.

64. Linker A, Jones RS. 1964. A Polysaccharide resembling Alginic Acid from a Pseudomonas Microorganism. Nature 204:187-188.

65. Govan JRW, Deretic V. 1996. Microbial Pathogenesis in Cystic Fibrosis: Mucoid Pseudomonas aeruginosa and Burkholderia cepacia. Microbiologicial Reviews 60:539-574.

66. Malhotra S, Hayes D, Jr., Wozniak DJ. 2019. Mucoid Pseudomonas aeruginosa and regional inflammation in the cystic fibrosis lung. J Cyst Fibros doi:10.1016/j.jcf.2019.04.009.

67. Price CE, Brown DG, Limoli DH, Phelan VV, O'Toole GA. 2019. Exogenous alginate protects Staphylococcus aureus from killing by Pseudomonas aeruginosa. J Bacteriol doi:10.1128/JB.00559-19.

68. Fyfe JAM, Govan JRW. 1980. Alginate Synthesis in Mucoid Pseudomonas aeruginosa : a Chromosomal Locus Involved in Control. J Gen Microbiol 119:443-450.

69. Goldberg JB, Ohman DE. 1984. Cloning and Expression in Pseudomonas aeruginosa of a Gene Involved in the Production of Alginate. J Bacteriol 158:1115-1121.

70. Darzins A, Chakrabarty AM. 1984. Cloning of Genes Controlling Alginate Biosynthesis from a Mucoid Cystic Fibrosis Isolate of Pseudomonas aeruginosa. J Bacteriol 159:9-18.

71. Darzins A, Wang SK, Vanags RI, Chakrabarty AM. 1985. Clustering of Mutations Affecting Alginic Acid Biosynthesis in Mucoid Pseudomonas aeruginosa. J Bacteriol 164:516-524.

72. Chitnis CE, Ohman DE. 1993. Genetic analysis of the alginate biosynthetic gene cluster of Pseudomonas aeruginosa shows evidence of an operonic structure. Mol Microbiol.

73. DeVries CA, Ohman DE. 1994. Mucoid-to-Nonmucoid Conversion in Alginate-Producing Pseudomonas aeruginosa Often Results from Spontaneous Mutations in algT, Encoding a Putative Alternate Sigma Factor, and Shows Evidence for Autoregulation. J Bacteriol 176:6677-6687.

74. MacGeorge J, Korolik V, Morgan AF, Asche V, Holloway BW. 1986. Transfer of a chromosomal locus responsible for mucoid colony morphology in Pseudomonas aeruginosa isolated from cystic fibrosis patients to P. aeruginosa PAO. J Med Microbiol 21:331-336.

75. Wang I, Sa-Correia I, Darzins A, Chakrabarty AM. 1987. Characterization of the Pseudomonas aeruginosa Alginate (alg) Gene Region II. J Gen Microbiol 133:2303-2314.

76. Deretic V. GJF, Chakrabarty A. M. 1987. Gene algD Coding for GDPmannose Dehydrogenase Is Transcriptionally Activated in Mucoid Pseudomonas aeruginosa. J Bacteriol 169:351-358.

77. Shinabarger D, Berry A, May TB, Rothmely R, Fialholl A, Chakrabarty. A. M. 1991. Purification and Characterization of Phosphomannose Isomerase-Guanosine Diphospho-D-mannose Pyrophosphorylase - A Bifunctional Enzyme in the Alginate Biosymthetic Pathway of Pseudomonas aeruginosa. J Biol Chem.

78. Gill JF, Deretic V, Chakrabarty AM. 1987. Overproduction and Assay of Pseudomonas aeruginosa Phosphomannose Isomerase. J Bacteriol 167:611-615.

79. Sa-Correia I, Darzins A, Wang S, Berry A, Chakrabarty AM. 1987. Alginate Biosynthetic Enzymes in Mucoid and Nonmucoid Pseudomonas aeruginosa: Overproduction of Phosphomannose Isomerase, Phosphomannomutase, and GDP-

Mannose Pyrophosphorylase by Overexpression of the Phosphomannose Isomerase (pmi) Gene. J Bacteriol 169:3224-3231.

80. Olvera C. Goldberg J. B. SR, Soberon-Chavez G. 1999. The Pseudomonas aeruginosa algC gene product participates in rhamnolipid biosynthesis. FEMS Microbiology Letters 179:85-90.

81. Coyne J, M. J.,, Russell KS, Coyle CL, Goldberg JB. 1994. The Pseudomonas aeruginosa algC Gene Encodes Phosphoglucomutase, Required for the Synthesis of a Complete Lipopolysaccharide Core. J Bacteriol 176:3500-3507.

82. Maharaj R, May TB, Wang S, Chakrabarty AM. 1993. Sequence of the alg8 and alg44 genes involved in the synthesis of alginate by Pseudomonas aeruginosa. Gene:267-269.

83. Remminghorst U, Rehm BH. 2006. Alg44, a unique protein required for alginate biosynthesis in Pseudomonas aeruginosa. FEBS Lett 580:3883-8.

84. Shinabarger D, May TB, Boyd A, Ghosh M, Chakrabarty AM. 1993. Nucleotide sequence and expression of the Pseudomonas aeruginosa algF gene controlling acetylation of alginate. Mol Microbiol 9:1027-1035.

85. Franklin MJ, Ohman DE. 1996. Identification of algI and algJ in the Pseudomonas aeruginosa Alginate Biosynthetic Gene Cluster Which Are Required for Alginate O Acetylation. J Bacteriol 178:2186–2195.

86. Hay D. I. SO, Filitcheva J., Rehm B.H.A. 2012. Identification of a periplasmic AlgK–AlgX–MucD multiprotein complex in Pseudomonas aeruginosa involved in biosynthesis and regulation of alginate. Appl Microbiol Biotechnol 93:215-227.

87. Gutsche J, Remminghorst U, Rehm BH. 2006. Biochemical analysis of alginate biosynthesis protein AlgX from Pseudomonas aeruginosa: purification of an AlgX-MucD (AlgY) protein complex. Biochimie 88:245-51.

88. Robles-Price A, Wong TY, Sletta H, Valla S, Schiller NL. 2004. AlgX is a periplasmic protein required for alginate biosynthesis in Pseudomonas aeruginosa. J Bacteriol 186:7369-77.

89. Weadge JT, Yip PP, Robinson H, Arnett K, Tipton PA, Howell PL. 2010. Expression, purification, crystallization and preliminary X-ray analysis of Pseudomonas aeruginosa AlgX. Acta Crystallogr Sect F Struct Biol Cryst Commun 66:588-91.

90. Franklin MJ, Chitnis CE, Gacesa P, Sonesson A, White C, Ohman DE. 1994. Pseudomonas aeruginosa AlgG Is a Polymer Level Alginate C5-Mannuronan Epimerase. J Bacteriol 176:1821-1830.

91. Aarons SJ, Sutherland IW, Chakrabarty AM, Gallagher MP. 1997. A novel gene, algK, from the alginate biosynthetic cluster of Pseudornonas aeruginosa. Microbiology 143:641-652.

92. Jain S, Ohman DE. 1998. Deletion of algK in Mucoid Pseudomonas aeruginosa Blocks Alginate Polymer Formation and Results in Uronic Acid Secretion. J Bacteriol 180:634–641.

93. Monday SR, Schiller NL. 1996. Alginate Synthesis in Pseudomonas aeruginosa: the Role of AlgL (Alginate Lyase) and AlgX. J Bacteriol 178:625-632.

94. Chu L, May TB, Chakrabarty. A. M., Misra TK. 1991. Nucleotide sequence and expression of the algE gene involved in alginate biosynthesis by Pseudomonas aeruginosa. Gene 107:1-10.

95. Jain S, Ohman DE. 2005. Role of an alginate lyase for alginate transport in mucoid Pseudomonas aeruginosa. Infect Immun 73:6429-36.

96. Damron FH, Goldberg JB. 2012. Proteolytic regulation of alginate overproduction in Pseudomonas aeruginosa. Mol Microbiol 84:595-607.

97. Damron FH, Qiu D, Yu HD. 2009. The Pseudomonas aeruginosa sensor kinase KinB negatively controls alginate production through AlgW-dependent MucA proteolysis. J Bacteriol 191:2285-95.

98. Schurr MJ, Yu H, Boucher JC, Hibler NS, Deretic V. 1995. Multiple Promoters and Induction by Heat Shock of the Gene Encoding the Alternative Sigma Factor AlgU (sigmaE) Which Controls Mucoidy in Cystic Fibrosis Isolates of Pseudomonas aeruginosa. J Bacteriol 177.

99. Xie Z, Hershberger CD, Shankar S, Ye RW, Chakrabarty AM. 1996. Sigma Factor–Anti-Sigma Factor Interaction in Alginate Synthesis: Inhibition of AlgT by Muc. J Bacteriol 178:4990–4996.

100. Hershberger CD, Ye RW, Parsek MR, Xie Z, Chakrabarty AM. 1995. The algT (algU) gene of Pseudomonas aeruginosa, a key regulator involved in alginate biosynthesis, encodes an alternative sigma-factor (sigmaE). PNAS 92:7941-7945.

101. Schurr M. J. YH, Martinez-Salazar J. M., Boucher J. C., Deretic V. 1996. Control of AlgU, a Member of the sigmaE-Like Family of Stress Sigma Factors, by the Negative Regulators MucA and MucB and Pseudomonas aeruginosa Conversion toMucoidy in Cystic Fibrosis. J Bacteriol 178:4997-5004.

102. Goldberg JB, Gorman WL, Flynn JL, Ohman DE. 1993. A Mutation in algN Permits trans Activation of Alginate Production by algT in Pseudomonas Species. J Bacteriol 175:1303-1308.

103. Li S, Lou X, Xu Y, Teng X, Liu R, Zhang Q, Wu W, Wang Y, Bartlam M. 2019. Structural basis for the recognition of MucA by MucB and AlgU in Pseudomonas aeruginosa. FEBS J doi:10.1111/febs.14995.

104. Wood LF, Ohman DE. 2009. Use of cell wall stress to characterize sigma 22 (AlgT/U) activation by regulated proteolysis and its regulon in Pseudomonas aeruginosa. Mol Microbiol 72:183-201.

105. Damron FH, Yu HD. 2011. Pseudomonas aeruginosa MucD regulates the alginate pathway through activation of MucA degradation via MucP proteolytic activity. J Bacteriol 193:286-91.

106. Delgado C, Florez L, Lollett I, Lopez C, Kangeyan S, Kumari H, Stylianou M, Smiddy RJ, Schneper L, Sautter RT, Szatmari G, Mathee K. 2018. Pseudomonas aeruginosa Regulated Intramembrane Proteolysis (RIP): Protease MucP can Overcome Mutations in the AlgO Periplasmic Protease to Restore Alginate Production in Nonmucoid Revertants. J Bacteriol doi:10.1128/JB.00215-18.

107. Wood LF, Leech AJ, Ohman DE. 2006. Cell wall-inhibitory antibiotics activate the alginate biosynthesis operon in Pseudomonas aeruginosa: Roles of sigma (AlgT) and the AlgW and Prc proteases. Mol Microbiol 62:412-26.

108. Wood LF, Ohman DE. 2012. Identification of genes in the sigma(22) regulon of Pseudomonas aeruginosa required for cell envelope homeostasis in either the planktonic or the sessile mode of growth. mBio 3.

109. Deretic V, Gill JF, Chakrabarty AM. 1987. Pseudomonas aeruginosa infection in cystic ribrosis: nucleotide sequence and transcriptional regulation of the algD gene. Nucleic Acids Res 15:4567-4581.

110. Goldberg JB, Ohman DE. 1987. Construction and Characterization of Pseudomonas aeruginosa algB Mutants: Role of algB in High-Level Production of Alginate. J Bacteriol 169:1593-1602.

111. Wozniak DJ, Ohman DE. 1991. Pseudomonas aeruginosa AlgB, a Two-Component Response Regulator of the NtrC Family, Is Required for algD Transcription. J Bacteriol 173:1406-1413.

112. Baynham PJ, Wozniak DJ. 1996. Identification and characterization of AlgZ, an AlgT-dependent DNA-binding protein required for Pseudomonas aeruginosa algD transcription. Mol Microbiol 22:97-108.

113. Wozniak DJ, Ohman DE. 1994. Transcriptional Analysis of the Pseudomonas aeruginosa Genes algR, algB, and algD Reveals a Hierarchy of Alginate Gene Expression Which Is Modulated by algT. J Bacteriol 176:6007-6014.

114. Jones CJ, Newsom D, Kelly B, Irie Y, Jennings LK, Xu B, Limoli DH, Harrison JJ, Parsek MR, White P, Wozniak DJ. 2014. ChIP-Seq and RNA-Seq reveal an AmrZ-mediated mechanism for cyclic di-GMP synthesis and biofilm development by Pseudomonas aeruginosa. PLoS Pathog 10.

115. Kong W, Zhao J, Kang H, Zhu M, Zhou T, Deng X, Liang H. 2015. ChIP-seq reveals the global regulator AlgR mediating cyclic di-GMP synthesis in Pseudomonas aeruginosa. Nucleic Acids Res 43:8268-82.

116. Leech AJ, Sprinkle A, Wood L, Wozniak DJ, Ohman DE. 2008. The NtrC family regulator AlgB, which controls alginate biosynthesis in mucoid Pseudomonas aeruginosa, binds directly to the algD promoter. J Bacteriol 190:581-9.

117. Deretic V, Govan JRW, Konyecsni WM, Martin DW. 1990. Mucoid Pseudomonas aeruginosa in cystic fibrosis: mutations in the muc loci affect transcription of the algR and algD genes in response to environmental stimuli. Mol Microbiol 4:189-196.

118. Wang D, Hildebrand F, Ye L, Wei Q, Maa LZ. 2015. Genome Sequence of Mucoid Pseudomonas aeruginosa Strain FRD1. Genome Announc 3:e00376-15.

119. Varga JJ, Barbier M, Mulet X, Bielecki P, Bartell JA, Owings JP, Martinez-Ramos I, Hittle LE, Davis MR, Jr., Damron FH, Liechti GW, Puchalka J, dos Santos VA, Ernst RK, Papin JA, Alberti S, Oliver A, Goldberg JB. 2015. Genotypic and phenotypic analyses of a Pseudomonas aeruginosa chronic bronchiectasis isolate reveal differences from cystic fibrosis and laboratory strains. BMC Genomics 16:883.

120. Martin DW, Schurr MJ, Mudd MH, Govan JRW, Holloway BW, Deretic V. 1993. Mechanism of conversion to mucoidy in Pseudmonas aeruginosa infecting cystic fibrosis patients. Proc Natl Acad Sci U S A 90:8377-8381.

121. Sautter R, Ramos D, Schneper L, Ciofu O, Wassermann T, Koh CL, Heydorn A, Hentzer M, Hoiby N, Kharazmi A, Molin S, Devries CA, Ohman DE, Mathee K. 2012. A complex multilevel attack on Pseudomonas aeruginosa algT/U expression and algT/U activity results in the loss of alginate production. Gene 498:242-53.

122. Rocchetta HL, Burrows LL, Lam JS. 1999. Genetics of O-Antigen Biosynthesis in Pseudomonas aeruginosa. Microbiol Mol Biol Rev:523-553.

123. King JD, Kocincova D, Westman EL, Lam JS. 2009. Lipopolysaccharide biosynthesis in Pseudomonas aeruginosa. Innate Immunity 15:261-312.

124. Liu PV, Matsumoto H, Kusama H, Bergan T. 1983. Survey of Heat-Stable, Major Somatic Antigens of Pseudomonas aeruginosa. International Journal of Systematic Bacteriology 33:256-264.

125. Liu PV, Wang S. 1990. Three New Major Somatic Antigens of Pseudomonas aeruginosa. J Clin Micro 28:922-925.

126. Hancock REW, Leive LL, Makela PH, Rietschel ET, Strittmatter W, Morrison DC. 1986. Lipopolysaccharide Nomenclature-Past, Present, and Future. J Bacteriol 166:699-705.

127. Islam ST, Lam JS. 2014. Synthesis of bacterial polysaccharides via the Wzx/Wzy-dependent pathway. Can J Microbiol 60:697-716.

128. Raymond CK, Sims EH, Kas A, Spencer DH, Kutyavin TV, Ivey RG, Zhou Y, Kaul R, Clendenning JB, Olson MV. 2002. Genetic Variation at the O-Antigen Biosynthetic Locus in Pseudomonas aeruginosa. J Bacteriol 184:3614-3622.

129. Burrows LL, Charter DF, Lam JS. 1996. Molecular charaterization of the Pseudmonas aeruginosa serotype O5 (PAO1) B-band lipopolysaccharide gene cluster. Mol Microbiol 22:481-495.

130. Lightfoot J, Lam JS. 1993. Chromosomal mapping, expression and synthesis of lipopoiysaccharide In Pseudomonas aeruginosa: a roie for guanosine diphospho (GDP)-D-mannose. Mol Microbiol 8:771-782.

131. Whitfield C. 1995. Biosynthesis of lipopolysaccharide O antigens. Trends in Micro 3:178-185.

132. Chester IR, Meadow PM, Pitt TL. 1973. The Relationship between the O-antigenic Lipopolysaccharides and Serological Specificity in Strains of Pseudomonas aeruginosa of different O-serotypes. Journal of General Microbiology 78:305-318.

133. Ojeniyi B, Baek L, Hoiby N. 1985. Polyagglutinability Due to Loss of O-Antigenic Determinants in Pseudomonas aeruginosa Strains Isolated from Cystic Fibrosis Patients. Acta Path Microbiol Immunol Scand B 93:7-13.

134. Penketh A, Pitt T, Roberts D, Hodson ME, Batten JC. 1983. The Relationship of Phenotype Changes in Pseudomonas aeruginosa to the Clinical Condiition of Patients with Cystic Fibrosis. Am Rev Respir Dis 127:605-608.

135. Evans DJ, Pier GB, Coyne Jr MJ, Goidberg JB. 1994. The rfb locus from Pseudomonas aeruginosa strain PA103 promotes the expression of O antigen by both LPS-rough and LPS-smooth isolates from cystic fibrosis patients. Mol Microbiol 13:427-434.

136. Davis MR, Muszynski A, Lollett IV, Pritchett CL, RW C, Goldberg JB. 2012. Identification of the Mutation Responsible for the Temperature- Sensitive Lipopolysaccharide O-Antigen Defect in the Pseudomonas aeruginosa Cystic Fibrosis Isolate 2192. J Bacteriol 195:1504-1514.

137. Kelly NM, MacDonald MH, Martin N, Nicas T, Hancock REW. 1990. Comparison of the Outer Membrane Protein and Lipopolysaccharide Profiles of Mucoid and Nonmucoid Pseudomonas aeruginosa. J Clin Microbiol 28: 2017-2021.

138. Ma L, Wang J, Wang S, Anderson EM, Lam JS, Parsek MR, Wozniak DJ. 2012. Synthesis of multiple Pseudomonas aeruginosa biofilm matrix exopolysaccharides is post-transcriptionally regulated. Environ Microbiol 14:1995-2005.

139. Burrows LL, Chow D, Lam JS. 1997. Pseudomonas aeruginosa B-Band O-Antigen Chain Length Is Modulated by Wzz (Rol). J Bacteriol 179:1482-1489.

140. Daniels C, Griffiths C, Cowles B, Lam JS. 2002. Pseudomonas aeruginosa O-antigen chain length is determined before ligation to lipid A core. Environ Microbiol 4:883-897.

141. Kintz E, Scarff JM, DiGiandomenico A, Goldberg JB. 2008. Lipopolysaccharide O-antigen chain length regulation in Pseudomonas aeruginosa serogroup O11 strain PA103. J Bacteriol 190:2709-16.

142. Lam JS, Taylor VL, Islam ST, Hao Y, Kocincova D. 2011. Genetic and Functional Diversity of Pseudomonas aeruginosa Lipopolysaccharide. Front Microbiol 2:118.

143. McGroarty EJ, Rivera M. 1990. Growth-Dependent Alterations in Production of Serotype-Specific and Common Antigen Lipopolysaccharides in Pseudomonas aeruginosa PAO1. Infect Immun 58:1030-1037.

144. Potvin E, Sanschagrin F, Levesque RC. 2008. Sigma factors in Pseudomonas aeruginosa. FEMS Microbiol Rev 32:38-55.

145. Lee J, Zhang L. 2015. The hierarchy quorum sensing network in Pseudomonas aeruginosa. Protein Cell 6:26-41.

146. Whiteley M, Diggle SP, Greenberg EP. 2017. Progress in and promise of bacterial quorum sensing research. Nature 551:313-320.

147. Quinton PM. 2008. Cystic fibrosis: impaired bicarbonate secretion and mucoviscidosis. Lancet 372:415-417.

148. Doggett RG, Harrison GM, Carter Jr. RE. 1971. Mucoid Pseudomonas aeruginosa in Patients with Chronic Illness. The Lancet:236-237.

149. Candido Cacador N, Paulino da Costa Capizzani C, Gomes Monteiro Marin Torres LA, Galetti R, Ciofu O, da Costa Darini AL, Hoiby N. 2018. Adaptation of Pseudomonas aeruginosa to the chronic phenotype by mutations in the algTmucABD operon in isolates from Brazilian cystic fibrosis patients. PLoS One 13:e0208013.

150. Diggle S, Winzer K, A.; L, P.; W, M.; C. 2002. Advancing the quorum in Pseudomonas aeruginosa: MvaT and the regulation of N-acylhomoserine lactone production and virulence gene expression. J Bacteriol 184:2576-86.

151. Vallet I, Diggle SP, Stacey RE, Camara M, Ventre I, Lory S, Lazdunski A, Williams P, Filloux A. 2004. Biofilm formation in Pseudomonas aeruginosa: fimbrial cup gene clusters are controlled by the transcriptional regulator MvaT. J Bacteriol 186:2880-90.

152. Toussaint B, Delic-Attree I, Vignais P. 1993. Pseudomonas aeruginosa contains an IHF-like Protein That Binds to the algD Promoter. Biochem Biophys Res Commun 196:416-421.

153. Kato J, Misra T K, Chakrabarty A M. 1990. AlgR3, a protein resembling eukaryotic histone H1, regulates alginate synthesis in Pseudomonas aeruginosa. Proc Natl Acad Sci U S A 87:2887-2891.

154. Konyecsni WM, Deretic V. 1990. DNA Sequence and Expression Analysis of algP and algQ, Components of the Multigene System Transcriptionally Regulating Mucoidy in Pseudomonas aeruginosa: algP Contains Multiple Direct Repeats. J Bacteriol 172:2511-2520.

155. Deretic V, Hibler NS, Holt SC. 1992. Immunocytochemical Analysis of A1gP(Hpl),a Histone like Element Participating in Control of Mucoidy in Pseudomonas aeruginosa. J Bacteriol 174: 824-831.

156. Deretic V, Konyescni WM. 1990. A Procaryotic Regulatory Factor with a Histone HI-Like Carboxy-Terminal Domain: Clonal Variation of Repeats within algP, a Gene Involved in Regulation of Mucoidy inPseudomonas aeruginosa. J Bacteriol 172:5544-5554.

157. Pier GB, Matthews WJ Jr., DD E. 1983. Immunochemical Characterization of the Mucoid Exopolysaccharide of Pseudomonas aeruginosa. J Infect Dis 147.

158. Yoon SS, Karabulut AC, Lipscomb JD, Hennigan RF, Lymar SV, Groce SL, Herr AB, Howell ML, Kiley PJ, Schurr MJ, Gaston B, Choi KH, Schweizer HP, Hassett DJ. 2007. Two-pronged survival strategy for the major cystic fibrosis pathogen, Pseudomonas aeruginosa, lacking the capacity to degrade nitric oxide during anaerobic respiration. EMBO J 26:3662-72.

159. Babin BM, Atangcho L, van Eldijk MB, Sweredoski MJ, Moradian A, Hess S, Tolker-Nielsen T, Newman DK, DA. T. 2017. Selective Proteomic Analysis of Antibiotic-Tolerant Cellular Subpopulations in Pseudomonas aeruginosa Biofilms. mBio doi:10.1128/mBio.01593-17.

160. Schuster M, Hawkins AC, Harwood CS, Greenberg EP. 2004. The Pseudomonas aeruginosa RpoS regulon and its relationship to quorum sensing. Mol Microbiol 51:973-985.

161. Whiteley M, Parsek M, P. GE. 2000. Regulation of Quorum Sensing by RpoS in Pseudomonas aeruginosa. J Bacteriol 182:4356–4360.

162. Savli H, Karadenizli A, Kolayli F, Gundes S, Ozbek U, Vahaboglu H. 2003. Expression stability of six housekeeping genes: a proposal for resistance gene quantification studies

of Pseudomonas aeruginosa by real-time quantitative RT-PCR. Journal of Medical Microbiology 52:403-408.

163. Held K, Ramage E, Jacobs M, Gallagher L, Manoil C. 2012. Sequence-verified two-allele transposon mutant library for Pseudomonas aeruginosa PAO1. J Bacteriol 194:6387-9.

164. Jacobs MA, Alwood A, Thaipisuttikul I, Spencer D, Haugen E, Ernst S, Will O, Kaul R, Raymond C, Levy R, Chun-Rong L, Guenthner D, Bovee D, Olson MV, Manoil C. 2003. Comprehensive transposon mutant library of Pseudomonas aeruginosa. Proc Natl Acad Sci U S A 100:14339-44.

165. Baynham PJ, Wozniak DJ. 1996. Identification and characterization of AlgZ, an AlgT-dependent DNA-binding protein required for Pseudomonas aeruginosa algD transcription. Mol Microbiol 22:97-108.

166. Onteniente L, Brisse S, Tassios PT, Vergnaud G. 2003. Evaluation of the Polymorphisms Associated with Tandem Repeats for Pseudomonas aeruginosa Strain Typing. Journal of Clinical Microbiology 41:4991-4997.

167. Chung JC, Becq J, Fraser L, Schulz-Trieglaff O, Bond NJ, Foweraker J, Bruce KD, Smith GP, Welch M. 2012. Genomic variation among contemporary Pseudomonas aeruginosa isolates from chronically infected cystic fibrosis patients. J Bacteriol 194:4857-66.

168. Lucchetti-Miganeh C, Redelberger D, Chambonnier G, Rechenmann F, Elsen S, Bordi C, Jeannot K, Attrée I, Plésiat P, de Bentzmann S. 2014. Pseudomonas aeruginosa Genome Evolution in Patients and under the Hospital Environment. Pathogens 3:309-340.

169. Firoved AM, Deretic V. 2003. Microarray Analysis of Global Gene Expression in Mucoid Pseudomonas aeruginosa. J Bacteriol 185:1071-1081.

170. Tunney MM, Field TR, Moriarty TF, Patrick S, Doering G, Muhlebach MS, Wolfgang MC, Boucher R, Gilpin DF, McDowell A, Elborn JS. 2008. Detection of anaerobic bacteria in high numbers in sputum from patients with cystic fibrosis. Am J Respir Crit Care Med 177:995-1001.

171. Dieter Worlitzsch RT, Martina Ulrich, Ute Schwab, Aynur Cekici, Keith C. Meyer, Peter Birrer, Gabriel Bellon, Jürgen Berger, Tilo Weiss, Konrad Botzenhart, James R. Yankaskas, Scott Randell, Richard C. Boucher, and Gerd Döring. 2002. Effects of reduced mucus oxygen concentration in airway Pseudomonas infections of cystic fibrosis patients. Journal of Clinical Investigation 109:317-325.

172. Weinging Z, Cross AR, Crowe-McAuliffe C, Weigert-Munoz A, Csatary EE, Solinski AE, Krysiak J, Goldberg J, Wilson DN, Medina E, Wuest WM, Sieber SA. 2019. The Natural Product Elegaphenone Potentiates Antibiotic Effects Against Pseudomonas aeruginosa. Angew Chem Int Ed 58:1-5.

173. Schulz S, Eckweiler D, Bielecka A, Nicolai T, Franke R, Dotsch A, Hornischer K, Bruchmann S, Duvel J, Haussler S. 2015. Elucidation of sigma factor-associated networks in Pseudomonas aeruginosa reveals a modular architecture with limited and function-specific crosstalk. PLoS Pathog 11:e1004744.

174. Palmer KL, Mashburn LM, Singh PK, Whiteley M. 2005. Cystic fibrosis sputum supports growth and cues key aspects of Pseudomonas aeruginosa physiology. J Bacteriol 187:5267-77.

175. Knutson CA, Jeanes A. 1968. A New Modification of the Carbazole Analysis: Applications to Heteropolysaccharides. Analytical Biochemistry 24:470-481.

176. Miller JH. 1973. Experiments in Molecular Genetics. Cold Spring Harbor Laboratory, Cold Spring Harbor, New York:466.

177. Choi KH, Kumar A, Schweizer HP. 2006. A 10-min method for preparation of highly electrocompetent Pseudomonas aeruginosa cells: application for DNA fragment transfer between chromosomes and plasmid transformation. J Microbiol Methods 64:391-7.

178. Hmelo LR, Borlee BR, Almblad H, Love ME, Randall TE, Tseng BS, Lin C, Irie Y, Storek KM, Yang JJ, Siehnel RJ, Howell PL, Singh PK, Tolker-Nielsen T, Parsek MR, Schweizer HP, Harrison JJ. 2015. Precision-engineering the Pseudomonas aeruginosa genome with two-step allelic exchange. Nat Protoc 10:1820-41.

179. Bailey J, Manoil C. 2002. Genome-wide internal tagging of bacterial exported proteins. Nat Biotechnol 20:839-842.

180. Martin M. 2011. Cutadapt removes adapter sequences from high-throughput sequencing reads. EMBnetJournal, 17.

181. Langmead B, Salzberg SL. 2012. Fast gapped-read alignment with Bowtie 2. Nat Methods 9:357-9.

182. Anders S, Pyl PT, Huber W. 2014. HTSeq--a Python framework to work with high-throughput sequencing data. Bioinformatics 31:166-169.

183. Love MI, Huber W, Anders S. 2014. Moderated estimation of fold change and dispersion for RNA-seq data with DESeq2. Genome Biol 15:550.

184. Strateva T, Yordanov D. 2009. Pseudomonas aeruginosa - a phenomenon of bacterial resistance. J Med Microbiol 58:1133-48.

185. Gilligan PH. 1991. Microbiology of Airway Disease in Patients with Cystic Fibrosis. Clinical Microbiology Reviews 4:35-51.

186. Hancock R. E. W. MLM, Chan L. Darveau R. P., Speert D. P. and Pier G. B. 1983. Pseudomonas aeruginosa Isolates from Patients with Cystic Fibrosis: A Class of Serum-Sensitive, Nontypable Strains Deficient in Lipopolysaccharide 0 Side Chains. Infect Immun 42:170-177.

187. Qiu D, Damron FH, Mima T, Schweizer HP, Yu HD. 2008. PBAD-based shuttle vectors for functional analysis of toxic and highly regulated genes in Pseudomonas and Burkholderia spp. and other bacteria. Appl Environ Microbiol 74:7422-6.

188. Limoli DH, Whitfield GB, Kitao T, Ivey ML, Davis Jr. MR, Grahl N, Hogan DA, Rahme LG, Howell PL, O'Toole GA, J.B G. 2017. Pseudomonas aeruginosa Alginate Overproduction Promotes Coexistence with Staphylococcus aureus in a Model of Cystic Fibrosis Respiratory Infection. mBio 8.

189. Yu H, Mudd M, Boucher JC, Schurr MJ, Deretic V. 1997. Identification of the algZ Gene Upstream of the Response Regulator algR and Its Participation in Control of Alginate Production in Pseudomonas aeruginosa. J Bacteriol 179:187-193.

190. Baynham PJ, Ramsey DM, Gvozdyev BV, Cordonnier EM, Wozniak DJ. 2006. The Pseudomonas aeruginosa ribbon-helix-helix DNA-binding protein AlgZ (AmrZ) controls twitching motility and biogenesis of type IV pili. J Bacteriol 188:132-40.

191. Lizewski SE, Schurr JR, Jackson DW, Frisk A, Carterson AJ, Schurr MJ. 2004. Identification of AlgR-regulated genes in Pseudomonas aeruginosa by use of microarray analysis. J Bacteriol 186:5672-84.

192. Morici LA, Carterson AJ, Wagner VE, Frisk A, Schurr JR, Honer zu Bentrup K, Hassett DJ, Iglewski BH, Sauer K, Schurr MJ. 2007. Pseudomonas aeruginosa AlgR represses the Rhl quorum-sensing system in a biofilm-specific manner. J Bacteriol 189:7752-64.

193. Ramsey DM, Baynham PJ, Wozniak DJ. 2005. Binding of Pseudomonas aeruginosa AlgZ to sites upstream of the algZ promoter leads to repression of transcription. J Bacteriol 187:4430-43.

194. Tart AH, Blanks MJ, Wozniak DJ. 2006. The AlgT-dependent transcriptional regulator AmrZ (AlgZ) inhibits flagellum biosynthesis in mucoid, nonmotile Pseudomonas aeruginosa cystic fibrosis isolates. J Bacteriol 188:6483-9.

195. Jones C. J. RCR, Mann E. E., Wozniak D. J. 2013. AmrZ Modulates Pseudmonas aeruginosa Biofilm Architecture by Directly Repressing Transcription of the psl Operon. J Bacteriol 195:1637-1644.

196. Baynham PJ, Brown A.L., Hall L.L, and Wozniak D.J. 1999. Pseudomonas aeruginosa AlgZ, a ribbon-helix-helix DNA-binding protein, is essential for alginate synthesis and algD transcriptional activation. Mol Microbiol 33:1069-1080.

197. Bengoechea J.A. ZL, Toivanen P., and Skurnik M. 2002. Regulatory network of lipopolysaccharide O-antigen biosynthesis in Yersinia enterocolitica includes cell envelope-dependent signals. Mol Microbiol 44:1045-1062.

198. Pescaretti Mde L, Lopez FE, Morero RD, Delgado MA. 2011. The PmrA/PmrB regulatory system controls the expression of the wzzfepE gene involved in the O-antigen synthesis of Salmonella enterica serovar Typhimurium. Microbiology 157:2515-21.

199. Malhotra S, Limoli DH, English AE, Parsek MR, Wozniak DJ. 2018. Mixed Communities of Mucoid and Nonmucoid Pseudomonas aeruginosa Exhibit Enhanced Resistance to Host Antimicrobials. mBio doi:10.1128/mBio.

200. Bragonzi ADW, Gerald B. Pier, Petra Timpert, Martina Ulrich, Morten Hentzer, Jens Bo Andersen, Michael Givskov, Massimo Conese, and Gerd Do¨ring. 2005. Nonmucoid

Pseudomonas aeruginosa Expresses Alginate in the Lungs of Patients with Cystic Fibrosis and in a Mouse Model. JID 192:410-419.

201. Choi KH, Schweizer HP. 2006. mini-Tn7 insertion in bacteria with single attTn7 sites: example Pseudomonas aeruginosa. Nat Protoc 1:153-61.

202. Choi KH, Mima T, Casart Y, Rholl D, Kumar A, Beacham IR, Schweizer HP. 2008. Genetic tools for select-agent-compliant manipulation of Burkholderia pseudomallei. Appl Environ Microbiol 74:1064-75.

203. Davis MR, Goldberg JB. 2012. Purification and visualization of lipopolysaccharide from Gram-negative bacteria by hot aqueous-phenol extraction. J Vis Exp doi:10.3791/3916.

204. Meisner J, Goldberg JB. 2016. The Escherichia coli rhaSR-PrhaBAD Inducible Promoter System Allows Tightly Controlled Gene Expression over a Wide Range in Pseudomonas aeruginosa. Appl Environ Microbiol 82:6715-6727.

205. Damron FH, Davis MR, Jr., Withers TR, Ernst RK, Goldberg JB, Yu G, Yu HD. 2011. Vanadate and triclosan synergistically induce alginate production by Pseudomonas aeruginosa strain PAO1. Mol Microbiol 81:554-70.

206. Yu H. S, M. J., Deretic V. 1995. Fuctional Equivalence of Escherichia coli sigmaE and Pseudomonas aeruginosa AlgU: E. coli rpoE Restores Mucoidy and Reduces Sensitivity to Reactive Oxygen Intermediates in algU Mutants of P. aeruginosa. J Bacteriol 117:3259-3268.

207. Qiu D, Eisinger VM, Rowen DW, Yu HD. 2007. Regulated proteolysis controls mucoid conversion in Pseudomonas aeruginosa. Proc Natl Acad Sci U S A 104:8107-12.

208. Delgado MA, Mouslim C, Groisman EA. 2006. The PmrA/PmrB and RcsC/YojN/RcsB systems control expression of the Salmonella O-antigen chain length determinant. Mol Microbiol 60:39-50.

209. Bankevich A, Nurk S, Antipov D, Gurevich AA, Dvorkin M, Kulikov AS, Lesin VM, Nikolenko SI, Pham S, Prjibelski AD, Pyshkin AV, Sirotkin AV, Vyahhi N, Tesler G, Alekseyev MA, Pevzner PA. 2012. SPAdes: a new genome assembly algorithm and its applications to single-cell sequencing. J Comput Biol 19:455-77.

210. Gloag ES, Marshall CW, Snyder D, Lewin GR, Harris JS, Santos-Lopez A, Chaney SB, Whiteley M, Cooper VS, Wozniak DJ. 2019. Pseudomonas aeruginosa Interstrain Dynamics and Selection of Hyperbiofilm Mutants during a Chronic Infection. MBio 10.

211. Jones CJ, Wozniak DJ. 2017. Psl Produced by Mucoid Pseudomonas aeruginosa Contributes to the Establishment of Biofilms and Immune Evasion. mBio 8.

212. M. BRSaM. 1980. Immunologic Investigations of Mucoid Strains of Pseudomonas aeruginosa: Comparison of Susceptibility to Opsonic Antibody in Mucoid and Nonmucoid Strains. Journal of Infectious Diseases 141.

213. Davis M. 2013. Dissertation- Lipopolysaccharide and Alginate in Mucoid Pseudomonas aeruginosa.

214. Jones AK, Fulcher NB, Balzer GJ, Urbanowski ML, Pritchett CL, Schurr MJ, Yahr TL, Wolfgang MC. 2010. Activation of the Pseudomonas aeruginosa AlgU regulon through mucA mutation inhibits cyclic AMP/Vfr signaling. J Bacteriol 192:5709-17.

215. Wurtzel O, Yoder-Himes DR, Han K, Dandekar AA, Edelheit S, Greenberg EP, Sorek R, Lory S. 2012. The single-nucleotide resolution transcriptome of Pseudomonas aeruginosa grown in body temperature. PLoS Pathog 8:e1002945.

216. Barbier M, Damron FH, Bielecki P, Suarez-Diez M, Puchalka J, Alberti S, Dos Santos VM, Goldberg JB. 2014. From the environment to the host: re-wiring of the transcriptome of Pseudomonas aeruginosa from 22 degrees C to 37 degrees C. PLoS One 9:e89941.

217. Prezioso S. 2018. Dissertation- Thermoregulation of Two Pseudomona aeruginosa Virulence Factors.

218. Owings JP, Kuiper EG, Prezioso SM, Meisner J, Varga JJ, Zelinskaya N, Dammer EB, Duong DM, Seyfried NT, Alberti S, Conn GL, Goldberg JB. 2016. Pseudomonas aeruginosa EftM Is a Thermoregulated Methyltransferase. J Biol Chem 291:3280-90.

219. Kintz E. 2011. Dissertation- Regulation of O antigen Chain Length in Pseudomonas aeruginosa.

220. Roccetta HL, Burrows LL, Lam JS. 1999. Genetics of O-Antigen Biosynthesis in Pseudomonas aeruginosa. Microbiology and Molecular Biology Reviews 63:523-553.

221. Jimenez N, Canals R, Salo MT, Vilches S, Merino S, Tomas JM. 2008. The Aeromonas hydrophila wb*O34 gene cluster: genetics and temperature regulation. J Bacteriol 190:4198-209.

222. Darch SE, Simoska O, Fitzpatrick M, Barraza JP, Stevenson KJ, Bonnecaze RT, Shear JB, Whiteley M. 2018. Spatial determinants of quorum signaling in a Pseudomonas aeruginosa infection model. Proc Natl Acad Sci U S A 115:4779-4784.

223. Thrane SW, Taylor VL, Lund O, Lam JS, Jelsbak L. 2016. Application of Whole-Genome Sequencing Data for O-Specific Antigen Analysis and In Silico Serotyping of Pseudomonas aeruginosa Isolates. J Clin Microbiol 54:1782-1788.

224. Priebe GP, Dean CR, Zaidi T, Meluleni GJ, Coleman FT, Coutinho YS, Noto MJ, Urban TA, Pier GB, Goldberg JB. 2004. The galU Gene of Pseudomonas aeruginosa is required for corneal infection and efficient systemic spread following pneumonia but not for infection confined to the lung. Infect Immun 72:4224-32.

225. Rivera M, Hancock R, Sawyer J, Haug A, McGroarty E. 1988. Enhanced Binding of Polycationic Antibiotics to Lipopolysaccharide from an Aminoglycoside-Supersusceptible, tolA Mutant Strain of Pseudomonas aeruginosa. 32:649-655.

226. Pier G. B. SJM, Ames Pl, Edwards M., Auerbach H., Goldfarb J., Speert D., Hurwitch S. 1987. Opsonophagocytic killing antibody to Pseudomonas aeruginosa mucoid exopolysaccharide in older noncolonized patients with Cystic Fibrosis. New England Journal of Medicine 317.

227. Garrett E. S. PD, Wozniak D. J. 1999. Negative control of Flagellum synthesis in Pseudomonas aeruginosa is modulated by the alternative sigma factor AlgT (AlgU). J Bacteriol 181:7401-7404.

228. Ciofu O, Lee B, Johannesson M, Hermansen NO, Meyer P, Hoiby N, Scandinavian Cystic Fibrosis Study C. 2008. Investigation of the algT operon sequence in mucoid and non-mucoid Pseudomonas aeruginosa isolates from 115 Scandinavian patients with cystic fibrosis and in 88 in vitro non-mucoid revertants. Microbiology 154:103-13.